Modeling Population Dynamics: a Graphical Approach

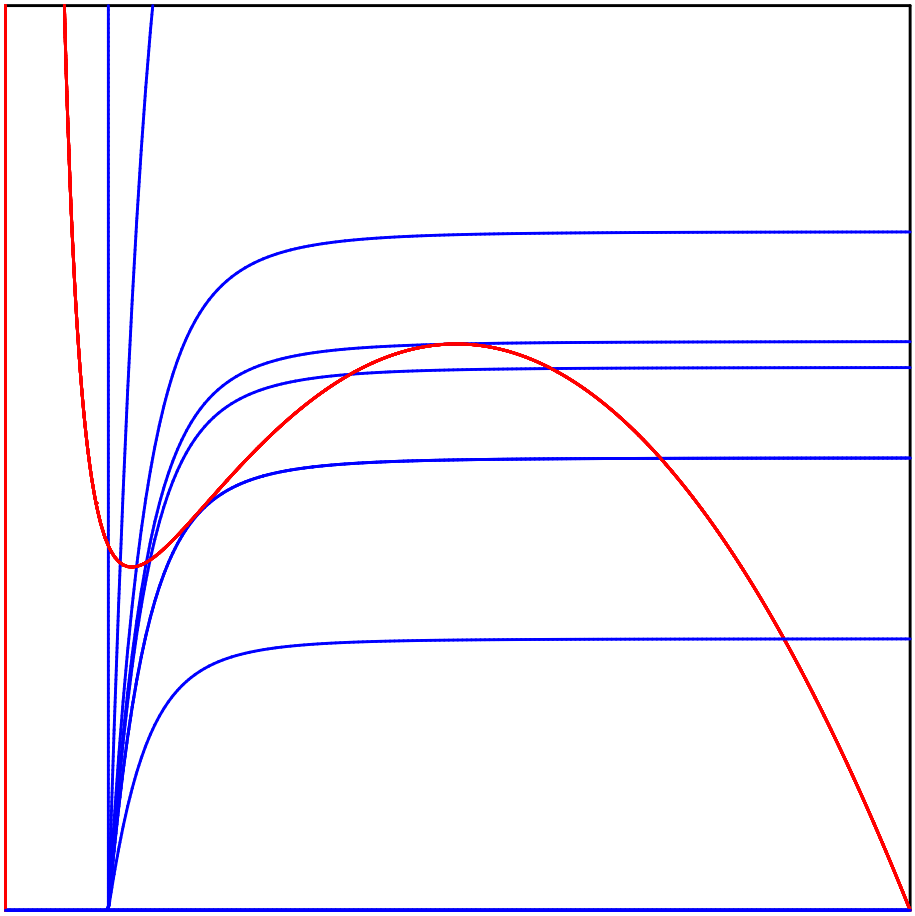

Rob J. de Boer

Theoretical Biology & Bioinformatics

Utrecht University

Ebook publically available at: http://tbb.bio.uu.nl/rdb/books/

Contents

Chapter 1

Preface

This book is an introduction into modeling population dynamics in ecology. Because there are several good textbooks on this subject, the book needs a novel "niche" to justify its existence. Unique features of the book are: (1) an emphasis on "parameter free" phase plane analysis, (2) the usage of the epidemiological concept of an R_0 (or fitness) to simplify parameter conditions, and (3) a strong emphasis on model development. The last point is the most important, and makes this book somewhat anti-historical in places. Rather than just explaining the famous classical models, we will first attempt to derive each model ourselves by translating biological processes, like birth, death, and predation, into intuitive graphs. These graphs are subsequently translated into simple mathematical functions. Collecting all functions in systems of differential equations we obtain mathematical models that are typically similar, but often not identical, to the classical models covered in other textbooks.

What is the reason for this rather laborious procedure for explaining models to students? I think it is important that biologists can identify each term in a mathematical model with a biological process for which they have some knowledge, or at least some intuition. For example, one often needs biological insight to know how, or even whether, birth and death rates depend on the population size. Since, the models we develop by our procedure ultimately resemble the classical models in theoretical ecology, we do obtain a proper mechanistic understanding of the classical model. Sometimes we end up with models with quite different properties, however. These cases are even more important because we learn to be critical of mathematical models, and definitely be critical of the conventional procedure of just employing a classical model for any new ecological problem at hand.

The phrase "a graphical approach" in the title has two connotations. First, we will sketch graphs for the effects of the population density on biological processes like the *per capita* birth rate and the *per capita* death rate. Second, most models will be analyzed by sketching nullclines in phase space. Both have the advantage that we can keep the mathematics that is required for analyzing models at a level that should be understandable for motivated students in biology. Most pictures in this book are made with GRIND, which is a computer program that is good at drawing nullclines and phase space analysis. During the course you will work with a version of GRIND in R (see Chapter 15).

Because the parameter values of biological models are typically not known, there is a strong emphasis in this course on analyzing models with free parameters. This has the enormous advantage that the results will be general, and that we do not run the risk of ignoring possibilities

that may occur for different parameter settings. Most pictures in this book therefore have no numbers along the axes (except for zero and one); rather they have parameter expressions for most of the points of interest. Additionally, we will employ the epidemiological concept of an R_0, and the critical resource density R^*, to simplify several parameter conditions.

This course only covers simple caricature models that are designed to capture the essentials of the biological problem at hand. Such simple models can be completely understood and therefore give good insight and new ideas about the biological problem (May, 2004). Another area of theoretical ecology is about large scale simulation models that are designed to summarize the existing knowledge about a particular ecosystem, and to predict what could happen if the circumstances change. Although such models are not covered in this book, the book should nevertheless also be useful for students interested in developing large scale models. First, the small components of large models should be developed by the same mechanistic process that we here use for simple models. Second, it is a sobering lesson to let oneself be surprised by the unexpected behavior of the simple models that are covered in this course, and such a lesson seems essential for developing the required scientific scrutinizing attitude toward large scale models.

The expected audience of this book is students of biology and ecology. Too many biologists treat a mathematical model as a "black box" that is too difficult to understand. A main objective of this course is to open the black box and show students in biology how to develop simple mathematical models themselves. This allows for a much better understanding, and for a healthy critical attitude toward the existing models in the field. Readers are expected to be familiar with phase space analysis, i.e., should know how to sketch nullclines and derive a Jacobi matrix. The first section of the Appendix provides a short summary on these prerequisites. A complete tutorial on deriving Jacobi matrices is provided in accompanying ebook that can also be downloaded from `http://tbb.bio.uu.nl/rdb/books/`.

Finally, this book originated from a theoretical ecology course given decades ago by Paulien Hogeweg at Utrecht University to biology students. She taught me the strength of phase plane analysis and simple caricature models. Some of the most interesting exercises in this book stem from that course. After I started teaching this course its contents and presentation have evolved, and have adapted to the behavior, the questions, and the comments from numerous students having attended this course.

Chapter 2

Introduction

This course is an introduction into Theoretical Biology for biology students. We will teach you how to read mathematical models, and how to analyze them, with the ultimate aim that you can critically judge the assumptions and the contributions of such models whenever you encounter them in your future biological research. Mathematical models are used in all areas of biology. Most models in this course are formulated in ordinary differential equations (ODEs). These will be analyzed by computing steady states, and by sketching nullclines. We will develop the differential equations by ourselves following a simple graphical procedure, depicting each biological process separately. Experience with an approach for writing models will help you to evaluate models proposed by others.

This first chapter introduces some basic concepts underlying modeling with differential equations. To keep models general they typically have free parameters, i.e., parameters are letters instead of numbers. You will become familiar with the notion of a "solution", "steady state", "half life", and the "expected life span". Concepts like solution and steady state are important because a differential equation describes the *change* of the population size, rather than its *actual size*. We will start with utterly simple models that are only convenient to introduce these concepts. The later models in the course are more challenging and much more interesting.

2.1 The simplest possible model

A truly simple mathematical model is the following

$$\frac{\mathrm{d}M}{\mathrm{d}t} = k \ , \tag{2.1}$$

which says that the variable M increases at a rate k per time unit. For instance, this could describe the amount of pesticide in your body when you eat the same amount of fruit sprayed with pesticide every day. Another example is to say that M is the amount of money in your bank account, and that k is the amount of Euros that are deposited in this account on a daily basis. In the latter case the "dimension" of the parameter k is "Euros per day". The ODE formalism assumes that the changes in your bank account are continuous. Although this is evidently wrong, because money is typically deposited on a monthly basis, this makes little difference when one considers time scales longer than one month.

This equation is so simple that one can derive its *solution*

$$M(t) = M(0) + kt \ , \tag{2.2}$$

where $M(0)$ is the initial value (e.g., the amount of money that was deposited when the account was opened). Plotting $M(t)$ in time therefore gives a straight line with slope k intersecting the vertical axis at $M(0)$. The slope of this line is k, which is the derivative defined by Eq. (2.1). Thus, the differential equation Eq. (2.1) gives the "rate of change" and the solution of Eq. (2.2) gives the "population size at time t". Typically, differential equations are too complicated for solving them explicitly, and their solutions are not available. In this course we will not consider the integration methods required for obtaining those solutions. However, having a solution, one can easily check it by taking the derivative with respect to time. For example, the derivative of Eq. (2.2) with respect to time is $\partial_t[M(0) + kt] = k$, which is indeed the right hand side of Eq. (2.1). Summarizing, the solution in Eq. (2.2) gives the amount of money at time t, and Eq. (2.1) gives the daily rate of change.

As yet, the model assumes that you spend no money from the account. Suppose now that you on average spend s Euros per day. The model then becomes $\mathrm{d}M/\mathrm{d}t = k - s$ Euros per day. Mathematically this remains the same as Eq. (2.1), and one obtains exactly the same results as above by just replacing k with $k - s$. If $k < s$, i.e., if you spend more than you receive, the bank account will decrease and ultimately become negative. The time to bankruptcy can be solved from the solution of Eq. (2.2): from $0 = M(0) + (k - s)t$ one obtains $t = -M(0)/(k - s)$. Although our model has free parameters, i.e., although we do not know the value of k or s, it is perfectly possible to do these calculations.

This all becomes a little less trivial when one makes the more realistic assumption that your spending is proportional to the amount of money you have. Suppose that you spend a fixed fraction, d, of your money per day. The model now becomes

$$\frac{\mathrm{d}M}{\mathrm{d}t} = k - dM \ , \tag{2.3}$$

where the parameter d is a "rate" and here has the dimension "per day". This can be checked from the whole term dM, which should have the same dimension as k, i.e., "Euros per day". Biological examples of Eq. (2.3) are red blood cells produced by bone marrow, shrimps being washed onto a beach, daily intake of vitamins, and so on. The k parameter then defines the inflow, or production, and the d parameter is a death rate. Although this seems a very simple extension of Eq. (2.1), it is much more difficult to obtain the solution

$$M(t) = \frac{k}{d}\left(1 - \mathrm{e}^{-dt}\right) + M(0)\mathrm{e}^{-dt} \ , \tag{2.4}$$

which is depicted in Fig. 2.1a. The term on the right gives the exponential loss of the initial value of the bank account. The term on the left is more complicated, but when evaluated at long time scales, e.g., for $t \to \infty$, the term $(1 - \mathrm{e}^{-dt})$ will approach one, and one obtains the "steady state" $\bar{M} = k/d$. We conclude that the solution of Eq. (2.4) ultimately approaches the steady state $M = k/d$, which is the ratio of your daily income and daily spending. Note that this is true for any value of the initial condition $M(0)$.

Fortunately, we do not always need a solution to understand the behavior of a model. The same steady state can also directly be obtained from the differential equation. Since a steady state means that the rate of change of the population is zero we set

$$\frac{\mathrm{d}M}{\mathrm{d}t} = k - dM = 0 \quad \text{to obtain} \quad \bar{M} = \frac{k}{d} \ , \tag{2.5}$$

which is the same value as obtained above from the solution for $t \to \infty$. Note that a steady state also gives the population size. This steady state provides some insight in the behavior of the model, and therefore in the way people spend their money. Suppose that rich people spend the same *fraction* of their money as poor people do, and that rich people just have a higher daily income k. This means that both rich and poor people approach a steady state where their spending balances their income. Basically, this model says that people with a 2-fold higher income spend 2-fold more money, and have 2-fold more money in the bank. This is not completely trivial: if you were asked what would happen with your bank account if both your income and spending increases n-fold you might have given a different answer.

2.2 Exponential growth and decay

Consider the unfortunate case that your daily income dries up, i.e., having a certain amount of money $M(0)$ at time zero, one sets $k = 0$ and is left with $\mathrm{d}M/\mathrm{d}t = -dM$. This is the famous equation for exponential decay of radioactive particles, with the almost equally famous solution $M(t) = M(0)\mathrm{e}^{-dt}$. Ultimately, i.e., for $t \to \infty$, the population size will approach zero. Plotting the natural logarithm of $M(t)$ as a function of time would give a straight line with slope $-d$ per day. This equation allows us to introduce two important concepts: the half life and the expected life span. The half life is defined as the time it takes to lose half of the population size, and is found from the solution of the ODE. From

$$\frac{M(0)}{2} = M(0)\mathrm{e}^{-dt} \quad \text{one obtains} \quad \ln\frac{1}{2} = -dt \quad \text{or} \quad t = \frac{\ln 2}{d} \; . \tag{2.6}$$

Since $\ln 2 \simeq 0.69$ the half life is approximately $0.69/d$ days. Note that the dimension is correct: a half life indeed has dimension time because we have argued above that d is a rate with dimension day^{-1}. The other concept is expected life span: if radioactive particles or biological individuals have a probability d to die per unit of time, their expected life span is $1/d$ time units. This is like throwing a die. If the probability to throw a four is $1/6$, the expected waiting time to get a four is six trials. Finally, note that this model has only one steady state, $\bar{M} = 0$, and that this state is stable because it is approached at infinite time. A steady state with a population size of zero is often called a "trivial" steady state.

The opposite of exponential decay is exponential growth

$$\frac{\mathrm{d}N}{\mathrm{d}t} = rN \quad \text{with the solution} \quad N(t) = N(0)\mathrm{e}^{rt} \; , \tag{2.7}$$

where the parameter r is known as the "natural rate of increase". The solution can easily be checked: the derivative of $N(0)\mathrm{e}^{rt}$ with respect to t is $rN(0)\mathrm{e}^{rt} = rN(t)$. Biological examples of this equation are the growth of mankind, the exponential growth of a pathogen in a host, the growth of a tumor, and so on. Similar to the half life defined above, one can define a doubling time for populations that are growing exponentially:

$$2N(0) = N(0)\mathrm{e}^{rt} \quad \text{gives} \quad \ln 2 = rt \quad \text{or} \quad t = \ln[2]/r \; . \tag{2.8}$$

This model also has only one steady state, $\bar{N} = 0$, which is unstable because any small perturbation above $N = 0$ will initiate unlimited growth of the population. To obtain a non-trivial (or non-zero) steady state population size in populations maintaining themselves by reproduction one needs density dependent birth or death rates. This is the subject of the next chapter.

In biological populations, this natural rate of increase of $\mathrm{d}N/\mathrm{d}t = rN$ should obviously be a composite of birth and death rates. A more natural model for a biological population that grows exponentially therefore is

$$\frac{\mathrm{d}N}{\mathrm{d}t} = (b-d)N \quad \text{with solution} \quad N(t) = N(0)\mathrm{e}^{(b-d)t} \ , \tag{2.9}$$

where b is a birth rate with dimension t^{-1}, and d is the death rate with the same dimension. Writing the model with explicit birth and death rates has the advantage that the parameters of the model are strictly positive (which will be true for all parameters in this course). Moreover, one now knows that the "generation time" or "expected life span" is $1/d$ time units. Since every individual has a birth rate of b new individuals per unit of time, and has an expected life span of $1/d$ time units, the expected number of offspring of an individual over its entire life-span is $R_0 = b/d$ (see Chapter 16). We will use this R_0 as the maximum "fitness" of an individual, i.e., the life-time number of offspring expected under the best possible circumstances. In epidemiology the R_0 is used for predicting the spread of an infectious disease: whenever $R_0 < 1$ a disease will not be able to spread in a population because a single infected host is expected to be replaced by less than one newly infected host (Anderson & May, 1991); see Chapter 16.

Biological examples of Eq. (2.9) are mankind, the exponential growth of algae in a lake, and so on. Similarly, the natural rate of increase $r = b - d$ yields a "doubling time" solved from $2N(0) = N(0)\mathrm{e}^{rt}$ giving $t = \ln[2]/r$ time units. A famous example of the latter is the data from Malthus (1798) who investigated the birth records of a parish in the United Kingdom and found that the local population had a doubling time of 30 years. Solving the natural rate of increase r per year from $30 = \ln[2]/r$ yields $r = \ln[2]/30 = 0.0231$ per year, which is sometimes expressed as a growth rate of 2.31% per year. More than 200 years later the global human growth rate is still approximately 2% per year. Simple exponential growth therefore seems a fairly realistic model to describe the growth of the quite complicated human population over a period of several centuries.

In this book we will give solutions of differential equations whenever they are known, but for most interesting models the solution is not known. We will not explain how these solutions are obtained. The textbook by Adler (1997) gives an overview of methods of integration. You can also use software like Mathematica to find the explicit solution of some of the differential equations used here. Solutions are typically difficult to obtain, but much more easy to check. For instance the solution $N(t) = N(0)\mathrm{e}^{(b-d)t}$ of $\mathrm{d}N/\mathrm{d}t = (b-d)N$, can easily be checked: by the chain rule the derivative of $N(0)\mathrm{e}^{(b-d)t}$ with respect to t is $N(0)(b-d)\mathrm{e}^{(b-d)t} = (b-d)N(t)$.

2.3 Summary

An ordinary differential equation (ODE) describes the rate of change of a population. The actual population size is given by the solution of the ODE, which is generally not available. To find the population size one can compute the steady state(s) of the model (the ODE), and/or solve the ODEs numerically on a computer, which gives the model behavior. Steady states are derived by setting the rate of change to zero, and solving for the actual population size. Doubling times and half-lives are solved from the solution of the exponential growth (or decay) equation $N(t) = N(0)\mathrm{e}^{rt}$. The fitness, R_0, of a population is the expected number of offspring of one individual over one generation, under the best possible circumstances.

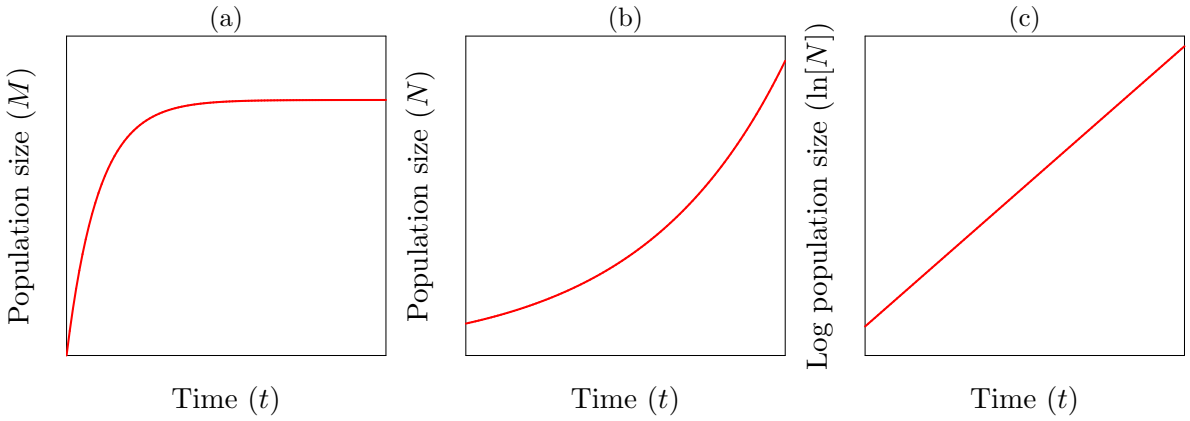

Figure 2.1: Population growth. Panel (a) depicts the solution of Eq. (2.4). Panels (b) and (c) depict exponential growth on a linear and a logarithmic vertical axis, respectively. A differential equation describes the slope of the solution for each value of the variable(s): $\mathrm{d}N/\mathrm{d}t$ is the slope of the $N(t) = N(0)\mathrm{e}^{rt}$ curve for each value of $N(t)$.

2.4 Exercises

Question 2.0. Read the chapter

a. What is the difference between a parameter and a variable?
b. What is the difference between the solution of an ODE and its steady state?
c. Why is the ODE $\mathrm{d}x/\mathrm{d}t$ not telling you how much x there is at time t?
d. What is the dimension of d in $\mathrm{d}x/\mathrm{d}t = -dx$?
e. What is a half-life and a doubling time?
f. What is the difference between a half-life and an expected life span?
g. What is a steady state? When is a steady state called 'trivial'?

Question 2.1. Red blood cells

Red blood cells are produced in the bone marrow at a rate of m cells per day. They have a density independent death rate of d per day.

a. Which differential equation from this chapter would be a correct model for the population dynamics of red blood cells?
b. Suppose you donate blood. Sketch your red blood cell count predicted by this model in a time plot.
c. Suppose a sportsman increases his red blood cell count by receiving blood. Sketch a time plot of his red blood cell count.

Question 2.2. Pesticide on apples

During their growth season apples are frequently sprayed with pesticide to prevent damage by insects. By eating apples you accumulate this pesticide in your body. An important factor determining the concentration of pesticide is their half life in the human body. An appropriate mathematical model is

$$\frac{\mathrm{d}P}{\mathrm{d}t} = \sigma - \delta P \ ,$$

where σ is the daily intake of pesticide, i.e., $\sigma = \alpha A$ where A is the number of apples that you eat per day and α is the amount of pesticide per apple, and δ is the daily rate at which the pesticide decays in human tissues.

a. Sketch the amount of pesticide in your body, $P(t)$, as a function of your age, assuming you

eat the same number of apples throughout your life.

b. How much pesticide do you ultimately accumulate after eating apples for decades?

c. Suppose you have been eating apples for decades and stop because you are concerned about the unhealthy effects of the pesticide. How long does it take to reduce your pesticide level by 50%?

d. Suppose you start eating two apples per day instead of just one. How will that change the model, and what is the new steady state? How long will it now take to reduce pesticide levels by 50% if you stop eating apples?

e. What is the decay rate if the half-life is 50 days?

Question 2.3. Bacterial growth

Every time you brush your teeth, bacteria enter your blood circulation. Since this a nutritious environment for them they immediately start to grow exponentially. Fortunately, we have neutrophils in our blood that readily kill bacteria upon encountering them. A simple model would be:

$$\frac{\mathrm{d}B}{\mathrm{d}t} = rB - kNB \ ,$$

where B and N are the number of bacteria and neutrophils per ml of blood, r is the growth rate of the bacteria (per hour), and k is the rate at which bacteria are killed by neutrophils.

a. What is the doubling time of the bacteria in the absence of neutrophils?

b. Neutrophils are short-lived cells produced in the bone marrow, and chemotherapy can markedly reduce the neutrophil counts in the peripheral blood. What is the critical number of neutrophils that is required to prevent rampant bacterial infections after chemotherapy?

c. What is the dimension of the parameters r and k?

d. The kBN term is called a mass-action term because it is proportional to both the bacterial and the neutrophil densities. A disadvantage of such a term is that each neutrophil is assumed to kill an infinite number of bacteria per hour if the bacterial density $B \to \infty$ (please check this). Later in the course we will use saturation functions to allow for maximum killing rates per killer cell. An example of such a model would be $\mathrm{d}B/\mathrm{d}t = rB - kNB/(h+B)$ where the total number of bacteria killed per hour approaches kN when $B \to \infty$ (please check this). What is now the dimension of k?

e. What is now the critical number of neutrophils that is required to prevent bacterial infections after chemotherapy? Can you sketch this?

f. What is the dimension of h, and how would you interpret that parameter?

Question 2.4. Injecting anesthesia

Before you undergo a minor operation a certain amount of anesthesia is injected in the muscle of your upper arm. From there it slowly flows into the blood where it exerts its sedating effect. From the blood it is picked up by the liver, where it is ultimately degraded. We write the following model for the amount of anesthesia in the muscle M, blood B and liver L:

$$\frac{\mathrm{d}M}{\mathrm{d}t} = -eM \ , \quad \frac{\mathrm{d}B}{\mathrm{d}t} = eM - cB \quad \text{and} \quad \frac{\mathrm{d}L}{\mathrm{d}t} = cB - \delta L \ ,$$

where the parameter e is the efflux from the muscle, c is the clearance from the blood, and δ is the degradation in the liver. All parameters are rates per hour. We assume that the degradation in the muscle and blood is negligible. The initial amount of anesthesia injected is $M(0)$: the amount in the muscle at time zero.

a. Sketch the amounts of anesthesia in the muscle, $M(t)$, in the blood, $B(t)$, and in the liver, $L(t)$, as a function of time.

b. How long does it take before half of the injected amount has flown from the muscle to the blood?

c. Is this the right time to do the operation?

d. Suppose the degradation rate is slow, i.e., let $\delta \to 0$, how much anesthesia will ultimately end up in the liver?

Question 2.5. SARS
Consider a deadly infectious disease, e.g., SARS, and write the following model for the spread of the disease:

$$\frac{\mathrm{d}I}{\mathrm{d}t} = \beta I - \delta I \ ,$$

where I is the number of human individuals infected with SARS, β is the number of new cases each infected individual causes per day, and $1/\delta$ is the number of days an infected individual survives before he/she dies of SARS. Epidemiologists define the R_0 of a disease as the maximum number of new cases expected per infected individual. Since an infected individual here is expected to live for $1/\delta$ days, and is expected to cause β new cases per day, the R_0 of this disease is β/δ.

a. It has been estimated that on average a SARS patient causes $R_0 = 3$ new cases, during a typical disease period of two weeks (Lipsitch *et al.*, 2003). Most patients die at the end of these two weeks. How long does it take with these parameters to reach the point where 3×10^9 individuals (i.e., half of the world population) are infected? Note that at this time point the healthy uninfected pool is less than half of the world population because many people will have died (i.e., your simple estimate is a worst case estimate).

b. Do you think this is a realistic estimate? How would you extend the model to make it more realistic?

Question 2.6. Physics (Extra exercise for cool students)
The linear ODEs used in this chapter should be familiar to those of you who studied the famous equations for velocity and acceleration. One typically writes:

$$\frac{\mathrm{d}x}{\mathrm{d}t} = v \quad \text{and} \quad \frac{\mathrm{d}v}{\mathrm{d}t} = a \ ,$$

where x is the total distance covered, v is the velocity, and a is the time derivative of the velocity, which is defined as the "acceleration". Integrating $\mathrm{d}v/\mathrm{d}t$ gives $v(t) = at + v(0)$, where the integration constant $v(0)$ is the velocity at time zero, and integrating $\mathrm{d}x/\mathrm{d}t = at + v(0)$ gives $x(t) = \frac{1}{2}at^2 + v(0)t$.

a. Check the dimensions of v and a.

b. Check these solutions.

Chapter 3

Population growth: replication

Populations change by migration, birth and death processes. In Chapter 2 we saw that one can write simple differential equations for populations that maintain themselves by immigration, and by replication (i.e., birth). We will here study similar models with explicit birth and death processes, and will add functions to describe how these processes may depend on the population size. There are always many different models for each particular situation, and rather than taking well-known equations for granted, we will introduce an approach for "how to develop a mathematical model". Models will be analyzed by computing steady states, and by sketching nullclines. It is important to realize that all models introduced here require a number of "unrealistic assumptions": (1) all individuals are equal, (2) the population is well-mixed, (3) the population size N is large, and (4) the parameters are constants. Nevertheless such "unrealistic" models will help us to think clearly about the biology described by the model (May, 2004).

We have seen in Chapter 2 that a non-replicating population which is maintained by an external influx, and has a density independent death rate, e.g., Eq. (2.3), will ultimately approach a steady state where the influx balances the death. This is not so for a model with density independent *per capita* birth and death rates: the only equilibrium of Eq. (2.9) is $N = 0$. If $b > d$, i.e., if the fitness $R_0 > 1$, this equilibrium is unstable because introducing the smallest number of individuals into the $N = 0$ state leads to exponential growth (see Chapter 16). If $R_0 < 1$ this equilibrium is stable because every population will ultimately go extinct (i.e., for $t \to \infty$ the solution $N(0)\mathrm{e}^{(b-d)t} \to 0$ when $d > b$). Note that one could argue that Eq. (2.9) also has a steady state when $b = d$. However, this is a rare and strange condition because the birth rate and the death rate would have to stay exactly the same over long time scales.

Birth and death rates are typically not fixed because the processes of birth and death can depend on the population size. Due to competition at high population densities birth rates may become lower and death rates higher when the population size increases (see Fig. 3.1). This is called density dependence. We here wish to develop models that are realistic in the sense that we understand which biological process is mechanistically responsible for the regulation of the population size. A good procedure for developing such models is to determine beforehand which process, i.e., birth or death, has the strongest density-dependent effect. The next step is to sketch a natural functional relationship between the biological process and the population density.

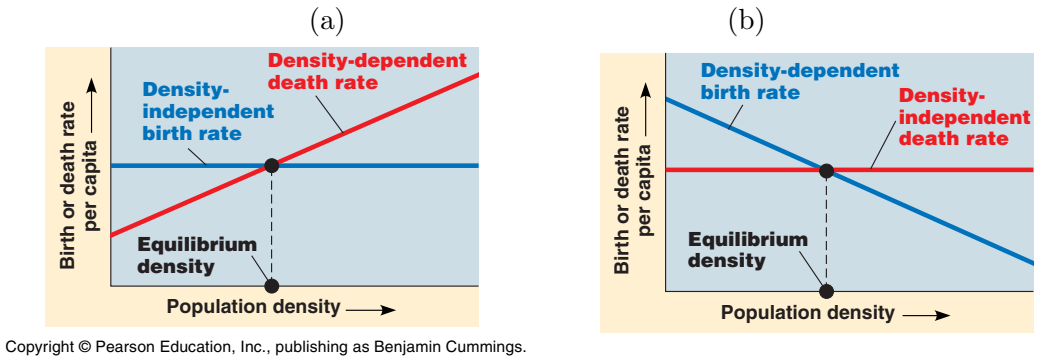

Figure 3.1: Graphs of the *per capita* birth and death rates. Equilibrium points correspond to the intersection points where the birth rate equals the death rate. From: Campbell & Reece (2008).

3.1 Density dependent death

If the death rate increases with the population size one could, for example, propose a simple linear increase of the *per capita* death rate with the population size (see Fig. 3.1a). This linear increase need not be realistic, but would certainly be a natural first extension of Eq. (2.9). Since we already have a normal death rate d in Eq. (2.9), a simple mathematical function for the graph in Fig. 3.1a is $f(N) = d + cN$, where d is the normal death rate that is approached when the population size is small, and where c is the slope with which the death rate increases with N. To incorporate the death rate of Fig. 3.1a into our model one can multiply the death rate parameter d in the $\mathrm{d}N/\mathrm{d}t = (b-d)N$ of Eq. (2.9) with a non-dimensional function like $f(N) = (1 + N/k)$, where the dimension of the parameter k is biomass, or individuals, and its exact interpretation is that the death rate has doubled when $N = k$. Because $f(N) = 1$ when $N \to 0$ the minimum *per capita* death rate (or maximum generation time) remains exactly the same. The full model becomes

$$\frac{\mathrm{d}N}{\mathrm{d}t} = [b - d(1 + N/k)]N \ . \tag{3.1}$$

At low population sizes the expected life span of the individuals remains $1/d$ time units, and they always have a birth rate b per time unit. Since the R_0 is a maximum fitness, it is computed for an individual under optimal conditions, which here means $N \to 0$. The fitness of individuals obeying Eq. (3.1) therefore equals $R_0 = b/d$.

To search for steady states of Eq. (3.1) one sets $\mathrm{d}N/\mathrm{d}t = 0$, cancels the trivial $N = 0$ solution, and solves from the remainder

$$b - d = dN/k \quad \text{that} \quad \bar{N} = k\frac{b-d}{d} = k(R_0 - 1) \tag{3.2}$$

is the non-trivial steady state population size. In ecology such a steady state is called the "carrying capacity". A simple linear density dependent death rate is therefore sufficient to deliver a carrying capacity. Here, the carrying capacity depends strongly on the fitness of the population, i.e., doubling $(R_0 - 1)$ doubles the steady state population size.

To test whether these steady states are stable one could study the solution of Eq. (3.1) to see what happens when $t \to \infty$. Although this solution is known (see below), we prefer to introduce a graphical method for determining the stability of a steady state. Fig. 3.1a sketches the *per capita* birth and death rates as a function of the population size in one graph. When these lines intersect the birth and death rates are equal and the population is at steady state. To check the

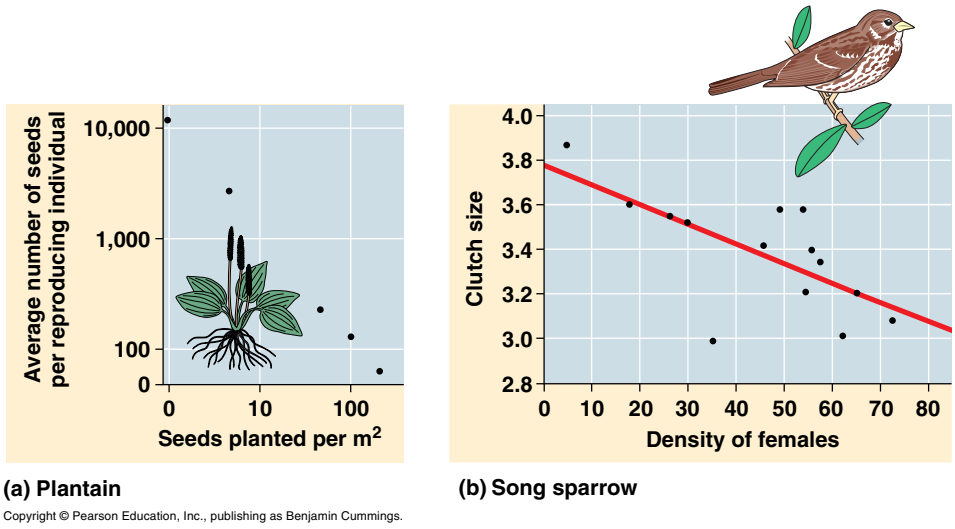

Figure 3.2: Panels (a) and (b) show for a plant species and a bird species that the *per capita* reproduction rate depends on the population size. From: Campbell & Reece (2002).

stability of the non-trivial steady state, one can study what happens when the population size is somewhat increased. Increasing N from the equilibrium density $\bar{N}$ makes $\mathrm{d}N/\mathrm{d}t < 0$ because the death rate exceeds the birth rate. This forces the population back to its steady state value. Similarly, decreasing N makes $\mathrm{d}N/\mathrm{d}t > 0$ which pushes the population back to the steady state. We conclude that the non-trivial steady state is stable. The instability of the trivial steady state $N = 0$ can also be checked from Fig. 3.1a: increasing N from $\bar{N} = 0$ makes $\mathrm{d}N/\mathrm{d}t > 0$ whenever $b > d$, i.e., whenever the fitness $R_0 > 1$.

3.2 Density dependent birth

Alternatively, one may argue that the *per capita* birth rate b should decrease with the population size. Experimental evidence supporting a decreasing birth rate in two natural populations is shown in Fig. 3.2. The simplest functional relationship between the *per capita* birth rate and the population size is again a linear one (see Fig. 3.1b), and a simple mathematical description is $f(N) = b - cN$, where b is the birth rate at low population densities. Since we already have a maximum birth rate in the $\mathrm{d}N/\mathrm{d}t = (b-d)N$ of Eq. (2.9), we multiply the birth rate parameter, b, by the linear non-dimensional function, $f(N) = (1 - N/k)$, such that the model becomes

$$\frac{\mathrm{d}N}{\mathrm{d}t} = [b(1 - N/k) - d]N \ . \tag{3.3}$$

The dimension of the parameter k is again biomass, or individuals, and its exact interpretation now is that the birth rate becomes zero when $N = k$. The advantage of using this non-dimensional function, $f(N) \leq 1$, that approaches one when $N \to 0$, is that the interpretation of the maximum birth rate remains the same. At low population sizes the fitness of individuals obeying Eq. (3.3) therefore remains $R_0 = b/d$, which is natural because at a sufficiently low population size there should be no difference between the two models. The steady states now are $N = 0$ and solving

$$b - d = b\frac{N}{k} \quad \text{yields} \quad \bar{N} = k(1 - d/b) = k(1 - 1/R_0) \ . \tag{3.4}$$

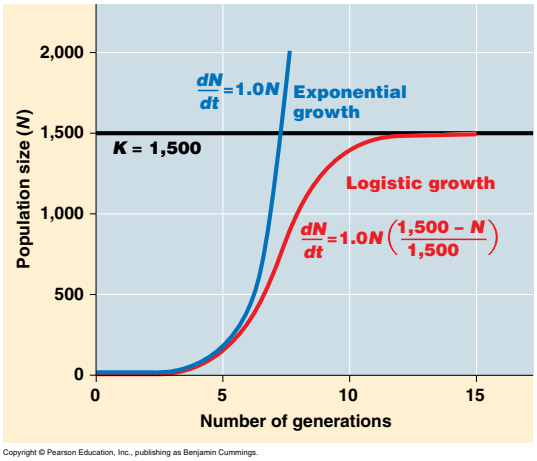

Figure 3.3: Logistic growth. From: Campbell & Reece (2008).

A simple linear density dependent birth term therefore also allows for a carrying capacity. When $R_0 \gg 1$, this carrying capacity approaches the value of k, and becomes fairly independent of the fitness. By the same procedure as illustrated above one can test graphically from Fig. 3.1b that the carrying capacity is stable, and that $N = 0$ is unstable.

3.3 Logistic growth

Since the model with density dependent death and the one with density dependent birth are both of the form $\mathrm{d}N/\mathrm{d}t = \alpha N - \beta N^2$, where α and β are arbitrary parameters, one can rewrite both models into the classical "logistic equation":

$$\frac{\mathrm{d}N}{\mathrm{d}t} = rN(1 - N/K) \ , \quad \text{with solution} \quad N(t) = \frac{KN(0)}{N(0) + \mathrm{e}^{-rt}(K - N(0))} \ , \tag{3.5}$$

with a natural rate of increase of $r = b - d$, and where K is the carrying capacity of the population. The behavior of the three models is therefore the same: starting from a small initial population the growth is first exponential, and later approaches zero when the population size approaches the carrying capacity (see Fig. 3.3). Starting from a large initial population, i.e., from $N(0) > K$, the population size will decline until the carrying capacity is approached. Because Eq. (3.5) has no explicit death rate, the R_0 is not defined.

3.4 Non-replicating populations

In non-replicating populations one can also define density dependent production

$$\frac{\mathrm{d}N}{\mathrm{d}t} = s[1 - N/k] - dN \tag{3.6}$$

where the rate of successful immigrations decreases with N. The steady state obtained from solving $\mathrm{d}N/\mathrm{d}t = 0$ is $\bar{N} = sk/(dk + s)$, which is a saturation function of the source s. Since this model has no *per capita* growth rate, one has to determine the stability of the steady state

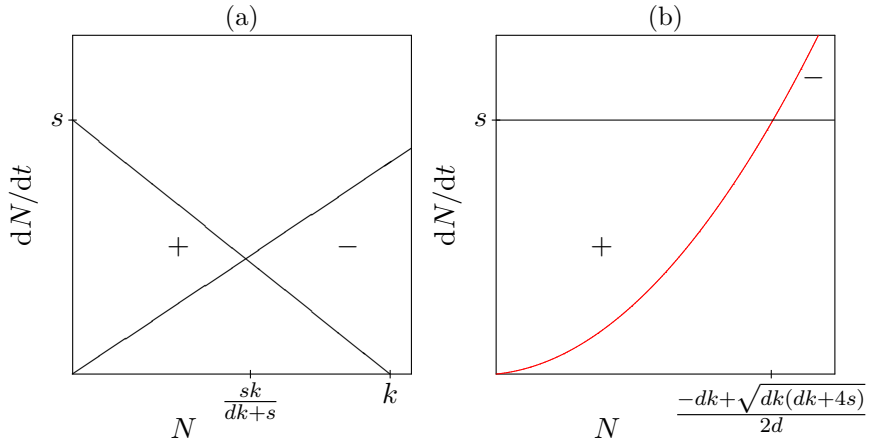

Figure 3.4: Graphical analysis of growth functions by plotting the total population growth and death as a function of N for Eq. (3.6) (a) and Eq. (3.7) (b). The intersects correspond to steady states.

by plotting the population growth and the population death rate in one graph (see Fig. 3.4a). The steady state is stable because increasing $\bar{N}$ results in a reduction of the population size, i.e., $\mathrm{d}N/\mathrm{d}t < 0$, and decreasing $\bar{N}$ results in population growth.

Similarly, one can allow for density dependent death, e.g.,

$$\frac{\mathrm{d}N}{\mathrm{d}t} = s - dN[1 + N/k] \;, \tag{3.7}$$

with steady states $N = \frac{-dk \pm \sqrt{dk(dk+4s)}}{2d}$. Because the square root term is positive and larger than dk, the positive root of this quadratic equation corresponds to a meaningful steady state, and the negative root has to be ignored. Plotting the population growth, s, and the total death, $dN[1 + N/k]$ in one graph again reveals that this steady state is stable (see Fig. 3.4b).

3.5 Stability and return time

The steady state $N = 0$ in Fig. 3.1 is not stable because small perturbations increasing N makes $\mathrm{d}N/\mathrm{d}t > 0$, which further increases N. The non-trivial steady states in Fig. 3.1 and Fig. 3.4 are stable because increasing N makes $\mathrm{d}N/\mathrm{d}t < 0$. It appears that steady states are stable when $\partial_N[\mathrm{d}N/\mathrm{d}t] < 0$, and unstable when this slope is positive (see Fig. 3.5). Note that ∂_N means the derivative with respect to N, i.e., $\partial_x\, x^2 = 2x$ and $\partial_t N = \mathrm{d}N/\mathrm{d}t$ (which is also written as N').

Mathematically one can linearize any continuous function $f(x)$ around any particular value, e.g., $\bar{x}$, by its local derivative $\partial_x\, f(\bar{x})$ in that point:

$$f(x) \simeq f(\bar{x}) + \partial_x\, f(\bar{x})\,(x - \bar{x}) \;, \tag{3.8}$$

where $h = x - \bar{x}$ is a small distance in the x-direction, and $f' = \partial_x\, f(\bar{x})$ is the derivative of $f(x)$ with respect to x at the value $x = \bar{x}$ (see Fig. 18.4 in the Appendix, and the accompanying Ebook (Panfilov *et al.*, 2016)). To apply this to our stability analysis one rewrites $f(N)$ into $f(\bar{N} + h)$ where $\bar{N}$ is the steady state population size and h is considered to be a small disturbance of the population density from the steady state, i.e., $h = N - \bar{N}$. Following Eq. (3.8) one rewrites $\mathrm{d}N/\mathrm{d}t$ into

$$\frac{\mathrm{d}N}{\mathrm{d}t} = f(N) \simeq f(\bar{N}) + \partial_N f(\bar{N})\,(N - \bar{N}) = 0 + \lambda h \;, \tag{3.9}$$

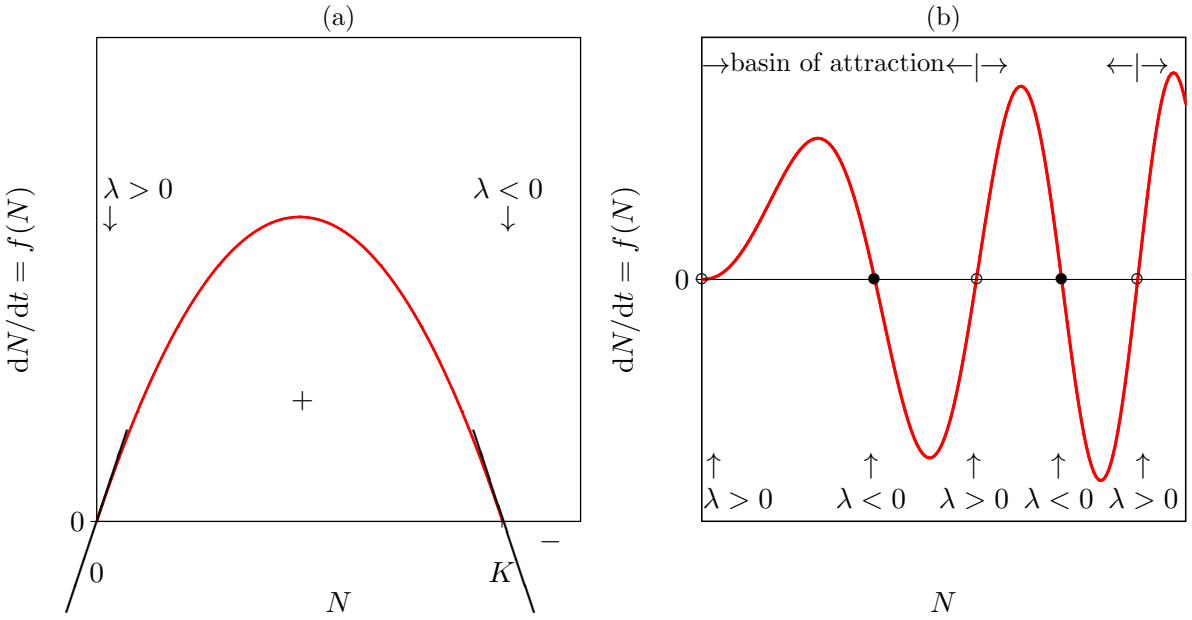

Figure 3.5: The stability of a steady state is determined by the local derivative (slope) of the growth function at the steady state. Panel (a) depicts the logistic growth function $f(N) = rN(1 - N/K)$ and Panel (b) depicts an arbitrary growth function.

because $f(\bar{N}) = 0$, and where we have defined $\lambda = \partial_N f(\bar{N})$ as the local derivative of $f(N)$ at $N = \bar{N}$, and $h = N - \bar{N}$ as the distance to the steady state. Because the sum of two derivatives is the derivative of the sum, and $\mathrm{d}\bar{N}/\mathrm{d}t = 0$, we can apply the following trick

$$\frac{\mathrm{d}N}{\mathrm{d}t} = \frac{\mathrm{d}N}{\mathrm{d}t} - \frac{\mathrm{d}\bar{N}}{\mathrm{d}t} = \frac{\mathrm{d}(N - \bar{N})}{\mathrm{d}t} = \frac{\mathrm{d}h}{\mathrm{d}t} \ , \tag{3.10}$$

to obtain

$$\frac{\mathrm{d}h}{\mathrm{d}t} = \lambda h \quad \text{with solution} \quad h(t) = h(0)\mathrm{e}^{\lambda t} \ , \tag{3.11}$$

for the behavior of the distance, h, to the steady state. Thus, whenever the local tangent λ at the equilibrium point is positive, small disturbances, h, grow. Whenever $\lambda < 0$ they decline, and the equilibrium point is stable. For an arbitrary growth function this dependence on the slope λ is illustrated in Fig. 3.5b. This figure shows that the unstable steady states, here saddle points, separate the basins of attraction of the stable steady states.

For example, for the logistic equation, $f(N) = rN(1 - N/K)$, one obtains $\lambda = r - 2rN/K$. At the carrying capacity of the logistic equation, i.e., at $N = K$, the local tangent is $\lambda = -r$, and at $N = 0$ we obtain $\lambda = r$ (see Fig. 3.5a), arguing that $N = K$ is a stable steady state, and $N = 0$ is an unstable steady state.

The stability of a steady state can be expressed as a "Return time"

$$T_R = -\frac{1}{\lambda} \ , \tag{3.12}$$

i.e., the more negative λ the faster perturbations die out. For example, consider the return time of the logistic growth equation around its carrying capacity. Above we derived that at $\bar{N} = K$ the tangent $\lambda = -r$. This means that $T_R = 1/r$, i.e., the larger r the shorter the return time. Populations that grow fast are therefore more resistant to perturbations. The paradigm of r-selected and K-selected species in ecology is built upon this theory. Finally, note that

the dimensions are correct: because r is a rate with dimension "time^{-1}", T_R indeed has the dimension "time".

3.6 Summary

A stable non-trivial population size is called a carrying capacity. Replicating populations will only have a carrying capacity when the *per capita* birth and/or death rate depend on the population density. For non-replicating populations this is not the case because they approach a stable steady state without any population regulation (i.e., without density dependence [or homeostasis]). A steady state is stable if the local derivative of the growth function is negative. The steeper this derivative, the shorter the return time.

3.7 Exercises

Question 3.1. Seed bank
Write a simple population growth model for an annual vegetation growing from seeds that are buried in the soil (i.e., a seed bank). Consider a large seed bank, and let the contribution of the current vegetation to the seed bank be negligible, i.e., assume that the number of seeds remains constant.

Question 3.2. Carrying capacity
What do you expect for the individual well-being in a population that is approaching its carrying capacity:
a. Do you expect the individual birth rate to be small or large?
b. Do you expect the individual death rate to be small or large?
c. In which population would you prefer to live: a small expanding population, or in one that is approaching carrying capacity?
d. Optimists like Julian Simon advise the American government by saying that "every human being represents hands to work, and not just another mouth to feed" (Cohen, 1995). We can investigate this proposal by arguing that the carrying capacity K in Eq. (3.5) increases with the population size. Test a simple example, e.g., $K = k\sqrt{N}$, and see how this influences the result. Do you still expect a carrying capacity where the individual well-being is at its minimum?

Question 3.3. Assumptions
Differential equation models for population dynamics are based upon a number of rather unrealistic assumptions.
a. Give a number of these assumptions.
b. How can models still be reasonable and helpful in biological research?

Question 3.4. Fishing herring
Let us assume that the dynamics of the herring population in the North Sea is more or less following the logistic growth, i.e., use Eq. (3.5).
a. Sketch the population growth $\mathrm{d}N/\mathrm{d}t = f(N)$ as a function of the population size N.
b. What is the maximum of the function $f(N)$?

c. What is the long-term optimal population size for the fisher men, and what would then be the maximum harvest (i.e., the maximum number of fish captured per unit of time)?
d. Include this maximum harvest explicitly in the model.
e. Sketch the growth of the population as a function of its size for this new situation, and show that this quota is too large.
f. What would be a more durable quota for fishing herring?

Question 3.5. Owls
There is an owl species that exclusively uses tree hollows for breeding. The growth of this owl population is limited by the availability of breeding places. Assume that the owls can easily find an unoccupied tree, and implement that very strictly into your model.
a. Draw a graph of the number of offspring per year as a function of the population size.
b. Make a model for the population size of the owls.
c. Draw a graph of the expected number of offspring per individual as a function of population size. This graph should be in agreement with the previous one.
d. Assume there is no mortality, and sketch the population density as a function of time.
e. Now sketch the population density as a function of time, assuming density independent mortality.

Question 3.6. Patches
Consider an environment with K patches. Each patch can be occupied by exactly one individual of a species. For simplicity, assume a density independent mortality, and assume that the *per capita* birth rate is limited by the availability of patches.
a. Define a model for population growth, assuming that the birth rate depends linearly on the number of empty patches.
b. What is the fitness R_0? Compute the steady states, and express these in terms of the fitness.
c. Is K the carrying capacity of the population?
d. Draw the curves for the *per capita* birth and death rates as a function of the population size. Use these to determine the stability of steady states.
e. Now define a model for population growth, assuming that the relation between the *per capita* birth and the number of empty patches is described by a saturation function (instead of a linear function). Use a simple Hill function (see Page 139).
f. Draw the curve for the *per capita* birth rate and death rate as a function of the population size.
g. Is K the carrying capacity of the population?

Question 3.7. Return time
Compute the return time of:
a. the non-trivial steady state of the density dependent death model $\mathrm{d}N/\mathrm{d}t = bN - dN[1+N/k]$.
b. the steady state of the non-replicating population $\mathrm{d}N/\mathrm{d}t = s - dN$.

Question 3.8. Regulation of birth rates
An alternative for the logistic growth equation with a density dependent birth rate is the equation

$$\frac{\mathrm{d}N}{\mathrm{d}t} = \frac{bN}{1+N} - dN \ ,$$

with the parameters b for the maximum birth rate, and d for the mortality. The population is normalized such that the growth is half maximal at $N = 1$. Because this model makes a clear distinction between birth and mortality it seems preferable for biological reasons.
a. Check that b indeed is the maximum growth rate per individual.
b. What is the fitness, R_0?
c. Compute the steady states and give their stability. Hint: Remember the quotient rule of

differentiation given in Eq. (18.34).

d. What is the return time? Consider a population with a high fitness; what is the most important factor defining the return time?

e. At what population density does the total population growth reach a maximum value?

f. How would you compute this maximum population growth rate?

Chapter 4

Non-linear density dependence

From the previous chapter we have learned that a general procedure to develop a mathematical model is to enumerate the various processes contributing to the change of the population size, and to sketch how each of these processes should depend on the population size(s). Typically, it was most convenient to describe a process in terms of the change "per individual". For instance, we sketched how the *per capita* birth and death rates depend on the population size. The simple models developed in the previous chapter above assumed that the birth and/or death rates were linear functions of the population density. This is obviously not generally the case. Intuitively, one would expect that competition only kicks in at high population densities.

In the appendix we let you become familiar with a few families of convenient functions, e.g., Hill-functions and exponential functions

$$f(x) = \frac{x^n}{h^n + x^n} \quad \text{and} \quad f(x) = 1 - \mathrm{e}^{-\ln[2]x/h} \ , \tag{4.1}$$

respectively (see Page 139). Both can be used to formulate positive and negative effects of populations onto each other. Hill-functions and exponential functions define two families of functions $f(x)$ that increase with x, that are zero when $x = 0$, are half-maximal when $x = h$, and that approach a maximum $f(x) = 1$ when $x \to \infty$. Because these functions are dimensionless and remain bounded between zero and one, i.e., $0 \leq f(x) < 1$, one can easily multiply any term in a model (corresponding to some biological process) with such a function. The maximum $f(x) \to 1$ yields the maximum positive effect of the populations onto each other, and $f(x) = 0$ the minimum effect (whenever one would need a different maximum in the model, one simply multiplies $f(x)$ with a parameter). Having increasing functions $0 \leq f(x) < 1$, one can easily define decreasing functions by taking $g(x) = 1 - f(x)$ (see Page 139).

4.1 Density dependent birth

For a replicating population with density dependent growth one would write

$$\frac{\mathrm{d}N}{\mathrm{d}t} = (bf(N) - d)N \ , \tag{4.2}$$

and one could use several candidates of the decreasing density dependent function $f(N)$ like

$$f(N) = 1 - \frac{N}{2k} \ , \quad f(N) = \frac{1}{1 + N/k} \ , \quad f(N) = \frac{1}{1 + [N/k]^2} \quad \text{and} \quad f(N) = \mathrm{e}^{-\ln[2]N/k} \ , \tag{4.3}$$

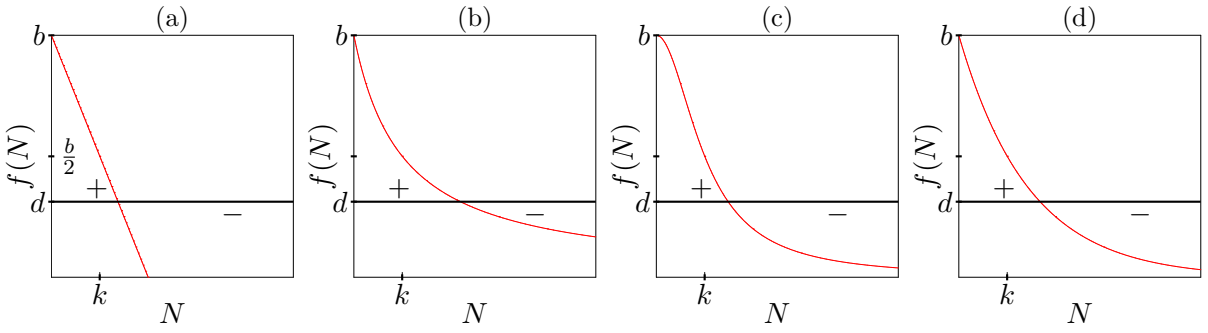

Figure 4.1: Density dependent birth rates defined by Eq. (4.3). The declining curves in Panels (a)–(d) correspond to *per capita* birth rate, $bf(N)$, where the density dependence is defined by one of the four functions in Eq. (4.3). The horizontal lines depict the density independent *per capita* death rate of Eq. (4.2). The intersects therefore correspond to steady states.

Function	$f(0)$	$f(k)$	$f(\infty)$	R_0	Carrying capacity
$f(N) = \max(0, 1 - N/[2k])$	1	0.5	0	b/d	$\bar{N} = 2k(1 - 1/R_0)$
$f(N) = 1/(1 + N/k)$	1	0.5	0	b/d	$\bar{N} = k(R_0 - 1)$
$f(N) = 1/(1 + [N/k]^2)$	1	0.5	0	b/d	$\bar{N} = k\sqrt{R_0 - 1}$
$f(N) = \mathrm{e}^{-\ln[2]N/k}$	1	0.5	0	b/d	$\bar{N} = (k/\ln[2])\ln[R_0]$

Table 4.1: Different properties of several functions for density dependent growth in $\mathrm{d}N/\mathrm{d}t = (bf(N) - d)N$.

which are depicted in Fig. 4.1. Data supporting density dependent growth functions are depicted in Fig. 3.2. Because the birth rate should probably remain close to maximal as long as the population size is sufficiently small, and is only expected to decrease when competition kicks in, the sigmoid function of Eq. (4.3)c seems most realistic. Note that Campbell & Reece (2002, 2005) draw a straight line through the Song sparrow data depicted in Fig. 3.2b, i.e., they suggest the linear function of Eq. (4.3)a, but one could also argue that the clutch size remains approximately 3.5 per female until the density exceeds 50 females, and then drops steeply. The Plantain (*Plantago*) data in Fig. 3.2a basically argue that the number of seeds per plant, y, obeys $y \simeq 10^4/x$ (check the values at $x = 1, 10$ and 100). This is similar to a "birth" rate $b/(1 + N)$. Each of the four models has a single non-trivial steady state (see Table 4.1) and this steady state is always stable (see Fig. 4.1). At the steady state $\mathrm{d}N/\mathrm{d}t = 0$, and increasing the population size to a value slightly above its steady state value brings the model in a region where $\mathrm{d}N/\mathrm{d}t < 0$ (as indicated by the $-$ signs in Fig. 4.1), whereas decreasing the population to a value slightly below the steady state value increases $\mathrm{d}N/\mathrm{d}t$ (see the $+$ signs).

Since all these functions are bounded between zero and one, i.e., $0 \leq f(N) < 1$, the fitness in these models is always $R_0 = b/d$. Although the different functions may reflect quite a different biology, the models that result from incorporating them have a very similar behavior. For instance, starting with a small population the population size plotted in time will always look like a sigmoid function. In other words, finding a population with a sigmoid population growth tells us very little about its underlying density dependent regulation. Table 4.1 shows the models differ in how the carrying capacity depends on the fitness R_0. In the exercises you will study the differences in the dynamics of these models using `grind.R`.

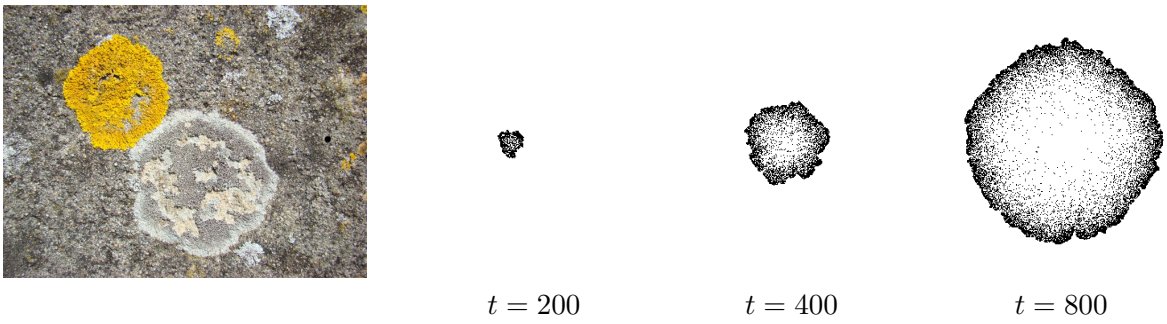

Figure 4.2: Lichens growing as an expanding disk. The three panels on the right show three snapshots of a computer simulation, with time proceeding from left to right. In this Cellular Automaton fresh empty pixels that are surrounded neighboring live pixels can become alive, dead pixels remain dead (exhausted) forever, and all live pixels die with some probability.

4.2 Density dependent death

A general model for density dependent death rates would be

$$\frac{\mathrm{d}N}{\mathrm{d}t} = (b - d[1 + (N/k)^m])N \tag{4.4}$$

which has a linear increase in the death rate when $m = 1$, and a faster than linear increase when $m > 1$. The interpretation of k remains the same, i.e., when $N = k$ the death rate has doubled. Having a fitness $R_0 = b/d$ the steady state is $\bar{N} = k\sqrt[m]{R_0 - 1}$. For $m = 1$ Fig. 3.1a shows that this steady state is stable. Confirm for yourself that this is true for all values of m by sketching the same picture for $m = 1/2$ and $m = 2$.

4.3 Summary

Density dependent processes are probably not linear, and are typically expected to become significant only at a large population size. Hill functions and/or exponential functions are convenient for defining any preferred dependence on the population size. How the carrying capacity depends on the R_0 depends strongly on the choice of the function used for defining the density dependence. A sigmoid density dependence seems most realistic, but is also the most cumbersome function to handle algebraically.

4.4 Exercises

Question 4.1. Lichens
Lichens grow in a thin crust. Assume the shape of the crust to be a perfect circle. Further, assume that reproduction can only take place at the edge of this circular crust, whereas the mortality is uniform. A first approximation would be that the total biomass is proportional to the area of this circle, i.e., $A = c\pi r^2$, where r is its radius and c is a constant scaling from area to biomass. Since reproduction takes place at the border, realize that the circumference of the circle is given by $2\pi r$.

a. Solve the radius from the biomass expression and make an ODE for the biomass of such a lichen.
b. What is the steady state of the total biomass?
c. Draw the curve for the growth per unit of biomass as a function of the total biomass.
d. How will the biomass change over time (sketch the curve)?
e. A problem of this model is the infinite *per capita* growth at small densities. How would you repair that?
f. Another problem is that after some time a growing lichen will be thin in the middle and ticker at the edge, because the area in the middle is older and has had more time to die. To study this one would need to make a spatial model (see Fig. 4.2). Cool students could try to see what happens if the lichen grows as a ring with a certain width, while reproduction still occurs at the border.

Question 4.2. Life stages
Consider an insect population consisting of larvae (L) and adults (A). Assume that adults give birth to larvae (asexual), and that these larvae become adults. Adults have a density independent mortality. Larvae compete with adults and have a mortality that is dependent on the density of adults (and use a simple term for this).
a. Make a model for the growth of such a population, using two ODEs.
b. Draw nullclines and determine the stability of all steady states.
c. Assume that the dynamics of the larvae is much faster than that of adults, i.e. make a "quasi steady state" assumption for the larvae.
d. Give the new adult equation. Does this equation look familiar to you?
e. What model would you get if one makes the quasi steady state assumption for the adults, rather than the larvae?
f. Which of the two assumptions do you think is most realistic?

Question 4.3. Allee effect
The Allee effect is famous for modeling populations of whales. It has been argued that at low population densities the whales have difficulties finding mates. Develop a model for the females in a whale population, incorporating an Allee effect by assuming that at low (female) population densities the birth rate decreases due to limited availability of males. To have a carrying capacity you will also have to allow for density dependent birth or death.

Question 4.4. Nullcline
Sketch the nullcline of

$$\frac{\mathrm{d}R}{\mathrm{d}t} = \frac{bR}{1+R/h} - dR - cRN$$

in a phase space of N versus R.

Chapter 5

Consumption

Having developed a number of models for population growth with density dependent growth and/or death terms, the time seems ripe to develop models for a consumer feeding on some kind of resource. Examples are herbivores grazing on a vegetation, raptors foraging for rodents, and bacteria consuming macromolecules. Because the amount of resource diminishes by consumption, one should automatically have competition between the consumers, which delivers density dependent effects that will ultimately limit the total population size. In the previous chapter we developed a strategy to sketch a simple graph for each biological process at hand, and then translate such a graph into a mathematical function for the model. Like we did above, we will again think in terms of individuals, and sketch their *per capita* birth rates and death rates, to develop a resource consumer, or predator prey, model.

First consider the resource. This could be a replicating population maintained by birth and death processes, or a population with a source and a death term. An example of the latter would be shrimps that are washed onto a beach from the sea, forming a resource on which seagulls are feeding. An example of the former is a population of green algae that form the resource of zooplankton (e.g., *Daphnia*). Starting with a replicating population we consider a population with a density dependent birth rate, and a density independent death rate (see Fig. 5.1a & b). In the previous chapter we have modeled such a population with

$$\frac{\mathrm{d}R}{\mathrm{d}t} = \left[\frac{b}{1+(R/k)^2} - d\right] R \,, \tag{5.1}$$

which has an $R_0 = b/d$ and a carrying capacity $\bar{R} = K = k\sqrt{R_0 - 1}$.

Suppose that one has measured the feeding rate of zooplankton as a function of the density of the algae, and that for a realistic range of algal densities one has found the simple linear relationship depicted in Fig. 5.1c for the *per capita* zooplankton feeding efficiency. (It could well be that at densities, R, much higher than the carrying capacity, K, the *per capita* consumption rate increases slower than linear, but that this would not be of interest because one never expects the algae density to exceed its carrying capacity). The simple linear relationship in Fig. 5.1c obviously translates into the function $f = cR$ where f is the number of prey caught per predator per unit of time. To know the total impact of predation on the prey population one simply multiplies f with the actual number of predators, and arrives at cRN for the predation term. Adding this to Eq. (5.1) yields

$$\frac{\mathrm{d}R}{\mathrm{d}t} = \left[\frac{b}{1+(R/k)^2} - d - cN\right] R \,. \tag{5.2}$$

The nullcline of this equation can be sketched in a 2-dimensional phase space of predators and prey. First, one cancels the $R = 0$ solution from $\mathrm{d}R/\mathrm{d}t = 0$ (which is a nullcline corresponding to the predator axis). Next, the simplest approach is to write N as function of R, i.e.,

$$N = \frac{b/c}{1 + (R/k)^2} - d/c \ , \tag{5.3}$$

which is the sigmoid declining Hill function depicted in Fig. 5.2. We know that $R = k\sqrt{R_0 - 1}$ when $N = 0$, and one can see that $N = (b-d)/c$ when $R = 0$, and that $N \to -d/c$ for $R \to \infty$. The area below the R-nullcline is the area where $\mathrm{d}R/\mathrm{d}t > 0$. Above the nullcline $\mathrm{d}R/\mathrm{d}t < 0$, because the predator density and/or the prey density is too high. Note that the shape of the prey nullcline reflects the *per capita* growth rate of the prey. This is a natural result because the nullcline equation is of the form $cN = [\mathrm{d}R/\mathrm{d}t]/R$ (see below).

The next mission is to add the predator equation. One needs to know how the *per capita* predator birth rate depends on their consumption of resource (i.e., $f = cR$). The birth rate should increase with this *per capita* consumption, but one expects that at a certain level of consumption the birth rate slows down due to "diminishing returns". Such a relationship, e.g., a *per capita* birth rate of

$$g(f) = \beta \frac{cR}{H + cR} = \beta \frac{R}{h + R} \ , \tag{5.4}$$

where β is the maximum birth rate and $h = H/c$, is depicted in Fig. 5.1d. Assuming that the predators have a simple density independent death (see Fig. 5.1e) one obtains

$$\frac{\mathrm{d}N}{\mathrm{d}t} = \left[\frac{\beta R}{h + R} - \delta \right] N \ , \tag{5.5}$$

with $R_0' = \beta/\delta$.

The nullcline of the predators is much more simple. Canceling $N = 0$ from $\mathrm{d}N/\mathrm{d}t = 0$ delivers the prey axis as one part of the nullcline and solving

$$\frac{\beta R}{h + R} - \delta = 0 \quad \text{yields} \quad R = \frac{h}{R_0' - 1} \ , \tag{5.6}$$

where $R_0' = \beta/\delta$. This corresponds to a vertical line in the predator prey phase space (see Fig. 5.2a). On the left of this nullcline, i.e., when $R < h/(R_0' - 1)$, the predator population declines because there is not enough food, on the right one finds that $\mathrm{d}N/\mathrm{d}t > 0$. The critical prey density $R^* = h/(R_0' - 1)$ therefore corresponds to the food density that the predator requires for maintaining itself (Tilman, 1980, 1982).

The two nullclines will intersect whenever $R^* < K$ (see Fig. 5.2a). When the nullclines intersect the model has three steady states. The first, $(\bar{R}, \bar{N}) = (0, 0)$, is unstable because the local vector field has the unstable direction $\mathrm{d}R/\mathrm{d}t > 0$. The second, $(\bar{R}, \bar{N}) = (K, 0)$ is also unstable because the local vector field has the unstable direction $\mathrm{d}N/\mathrm{d}t > 0$. Both are saddle points. The third, non-trivial (i.e., non-zero), steady state is located at $(\bar{R}, \bar{N}) = (R^*, \bar{N})$. Thus, the larger the fitness, R_0', of the predator the stronger the depletion of the prey. To determine the stability of the non-trivial steady state one has to resort to linearization and compute the Jacobian of the equilibrium point. Chapter 18 explains how to derive a "graphical Jacobian" from the phase space. For the trace of the matrix we check the effect of the population on itself. For the off-diagonal elements we take the effect of the variables on each other:

$$J = \begin{pmatrix} -\alpha & -\beta \\ \gamma & 0 \end{pmatrix} \quad \text{which implies that} \quad \mathrm{tr} = -\alpha < 0 \quad \text{and} \quad \det = \beta\gamma > 0 \ . \tag{5.7}$$

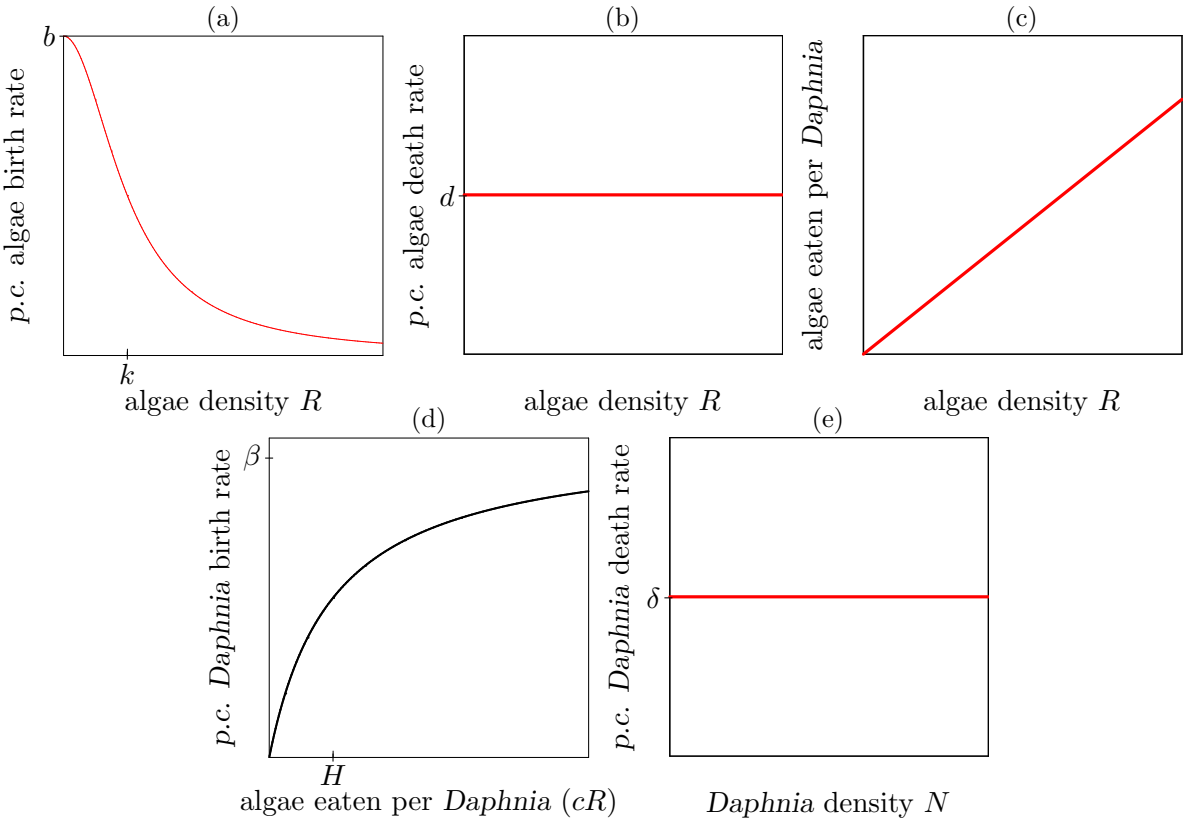

Figure 5.1: Population dynamical characteristics of a population of algae, R, and a population of *Daphnia*, N. The *p.c.* in the figure means *per capita*.

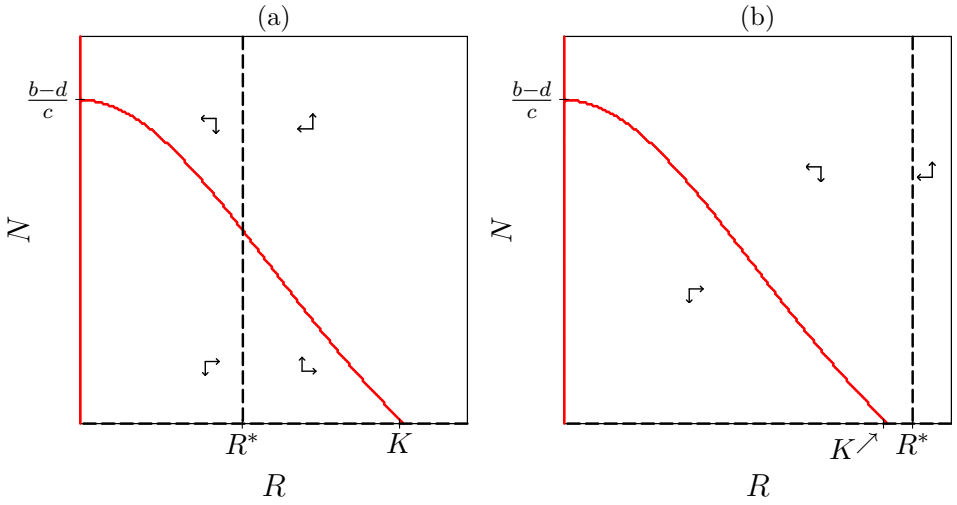

Figure 5.2: The nullclines of the predator prey model defined by Eqs. (5.2) & (5.5). The intersect of the sigmoid nullcline with the horizontal axis defines the carrying capacity of the prey, which is defined in the text as $K = k\sqrt{R_0 - 1}$. The predator nullcline is located at the critical prey density $R^* = \frac{h}{R_0' - 1}$.

The steady state is therefore always stable. If it is located near the carrying capacity, i.e., if $R^* \simeq K$, the steady state is a stable node. Otherwise it is a stable spiral point, and the behavior of the model is a dampened oscillation.

The case where the nullclines fail to intersect has the biological interpretation that the critical

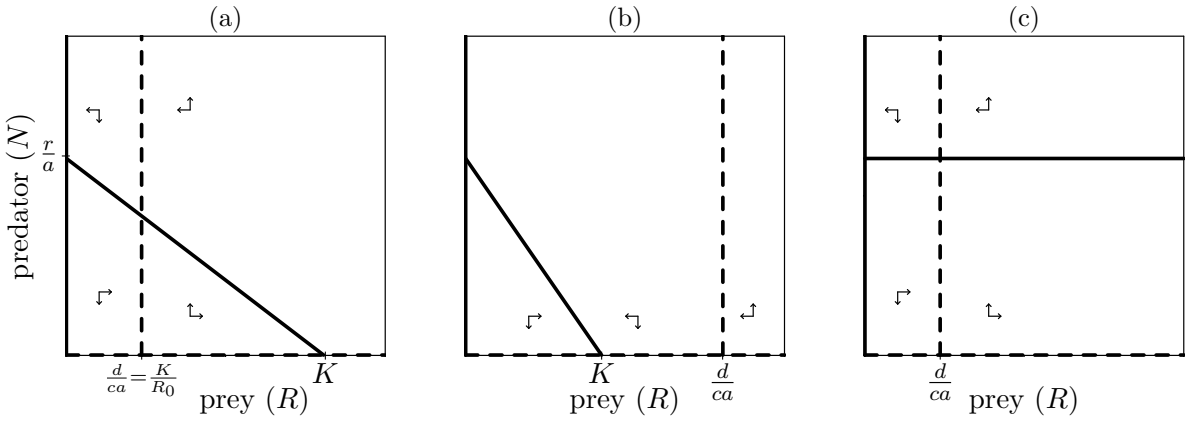

Figure 5.3: The phase space of the "robust" Lotka Volterra model (a,b) and that of the Lotka Volterra model without a carrying capacity of the prey (c). The predator nullcline is located at the critical prey density $R^* = \frac{d}{ca} = \frac{K}{R_0}$.

food density required by the predator is larger than the carrying capacity of the prey (see Fig. 5.2b). In that case one can see from the local vector field that the steady state $(\bar{R}, \bar{N}) = (K, 0)$ is a stable node. In terms of algae and zooplankton this would correspond to a lake that has so few nutrients that the maximum algae density of the lake is too small to maintain a zooplankton population.

Finally, for the situation of a non-replicating resource, e.g., shrimps being washed onto a beach, one would rewrite Eq. (5.2) into the simple

$$\frac{\mathrm{d}R}{\mathrm{d}t} = s - dR - cRN \ , \tag{5.8}$$

where d is the rate at which shrimps die or are washed back into the sea. It is a good exercise to sketch the nullclines of this model with Eq. (5.5) for the predator population.

5.1 Lotka Volterra model

The oldest and most famous predator prey model is the Lotka Volterra model proposed independently by Lotka (1913) and Volterra (1926). The model is much simpler than the model developed above because (a) it lumps prey birth and death rates into one logistic growth term, and (b) it assumes that the predator birth rate remains a linear function of their *per capita* consumption. Thus, the equations are

$$\frac{\mathrm{d}R}{\mathrm{d}t} = rR(1 - R/K) - aRN \ , \quad \frac{\mathrm{d}N}{\mathrm{d}t} = caRN - dN \ . \tag{5.9}$$

The $\mathrm{d}N/\mathrm{d}t = 0$ isocline is given by $N = 0$ and $R = d/(ca)$, and the $\mathrm{d}R/\mathrm{d}t = 0$ isocline is $R = 0$ and $N = (r/a)(1 - R/K)$, which again reflects the shape of the *per capita* growth function. Depicted in a phase space with N on the vertical axis and R on the horizontal axis, the predator nullcline is a vertical line at the critical resource density $R^* = d/(ca)$. The prey nullcine is a declining straight line, intersecting the vertical axis at $N = r/a$ and the horizontal axis at $R = K$ (see Fig. 5.3a). The model has three steady states: $(0, 0)$, $(K, 0)$ and $(d/(ca), (r/a)[1 - d/(caK)])$. The latter non-trivial equilibrium will only exist if $d/(ca) < K$; if it exists the two (trivial) equilibria on the axes are saddle points.

The R_0 of the prey is not defined because the logistic growth term collapses birth and death into a net growth term. Since $\mathrm{d}N/\mathrm{d}t$ has separate birth and death terms, one can calculate an R_0 for the predator. Since the *per capita* predator birth rate, caR, depends on the prey density, we substitute the maximum prey density $R = K$ in the birth rate, caR, because the R_0 is calculated for the best possible circumstances (see Chapter 16). Doing so one arrives at $R_0 = caK/d$. $R_0 = 1$ can indeed be used as an invasion criterion: the predator can only grow when $caK > d$. Expressed in terms of the R_0, the predator nullcline is located at $R = K/R_0$, which says that the degree by which a predator depletes its prey population is completely determined by its R_0. A predator with an $R_0 = 10$ decreases the equilibrium prey density to 10% of its carrying capacity. Note that this is only true when the predator birth rate increases linearly with the prey density: above we found that the depletion of the prey was determined by the ratio of the saturation constant, h, and the R_0.

The location of the predator nullcline again has the interpretation of the minimum prey density the predator requires for its maintenance: whenever $R < K/R_0$ one can see from the phase space in Fig. 5.3, and from Eq. (5.9), that $\mathrm{d}N/\mathrm{d}t < 0$. The non-trivial steady state is located at $(\bar{R}, \bar{N}) = (K/R_0, r/a[1 - 1/R_0])$. For predators with a high fitness, i.e., predators having an $R_0 \gg 1$, the steady state is located approximately at $(\bar{R}, \bar{N}) = (K/R_0, r/a)$.

The Jacobian of the non-trivial steady state can be calculated explicitly (see Chapter 18). From the phase space in Fig. 5.3 one can also read the graphical Jacobian

$$J = \begin{pmatrix} -\alpha & -\beta \\ \gamma & 0 \end{pmatrix} \quad \text{with} \quad \mathrm{tr} = -\alpha < 0 \quad \text{and} \quad \det = \beta\gamma > 0 \; . \tag{5.10}$$

Thus, the non-trivial steady state is always stable. If it is located close to the carrying capacity it is a stable node. Otherwise, i.e., if $R_0 \gg 1$, it is a stable spiral point.

The Lotka Volterra model is sometimes written in a structurally unstable form with $K \to \infty$, i.e., without a carrying capacity of the prey:

$$\frac{\mathrm{d}R}{\mathrm{d}t} = rR - aRN \; , \quad \frac{\mathrm{d}N}{\mathrm{d}t} = caRN - dN \; . \tag{5.11}$$

This model is mathematically elegant but has limited biological relevance. The reason is that any small change of the model will lead to a qualitatively different type of behavior. The model is said to be "structurally unstable". Therefore one should not use it in biological research; mathematicians use the model in teaching examples because the model is so elegantly simple. The non-trivial $\mathrm{d}R/\mathrm{d}t = 0$ isocline is $N = r/a$ and the non-zero $\mathrm{d}N/\mathrm{d}t = 0$ isocline is $R = d/(ca)$. These nullclines immediately yield the non-trivial steady state at $(\bar{R}, \bar{N}) = (d/(ca), r/a)$. The Jacobian of this steady state is

$$J = \begin{pmatrix} r - a\bar{N} & -a\bar{R} \\ ca\bar{N} & ca\bar{R} - d \end{pmatrix} \quad = \quad \begin{pmatrix} 0 & -d/c \\ cr & 0 \end{pmatrix} \; . \tag{5.12}$$

Because $\mathrm{tr}(J) = 0$ the steady state has a "neutral" stability. The eigenvalues of this matrix are

$$\lambda_\pm \quad = \quad \pm\sqrt{-dr} \quad = \quad \pm \mathrm{i}\sqrt{dr} \; ; \tag{5.13}$$

see Page 144. Because the eigenvalues have no real part the system is not structurally stable: any small change of the system will either make the equilibrium stable or unstable. The behavior of the model are cycles of neutral stability: any perturbation of the predator or prey densities leads to a new cycle.

5.2 Generalization

Qualitatively the model of Equations (5.2 & 5.5) is very similar to the standard Lotka Volterra model. The prey nullcline is a monotonically decreasing line, the predator nullcline is a vertical line, and the non-trivial steady state is always stable. For which class of models should one expect this "Lotka Volterra" like phase space?

A vertical predator nullcline is obtained whenever one can cancel the predator from the predator equation. Rewriting Eq. (5.5) in a more general form like

$$\frac{\mathrm{d}N}{\mathrm{d}t} = [\beta f(R) - \delta]\, N \ , \tag{5.14}$$

one indeed obtains a vertical predator nullcline for any function $f(R)$. The nullcline will no longer be vertical whenever the predator N is present in the term between the square brackets. This will be the case when the functional response is predator dependent, i.e., when one replaces $f(R)$ by $f(R, N)$, or when the death rate is density dependent, e.g., when δ is replaced by $\delta(1+\epsilon N^m)$. In both cases the predator nullcline will typically be slanted to the right, which changes the effect of the predator on itself from zero to negative. The Jacobian then becomes

$$J = \begin{pmatrix} -p & -q \\ r & -s \end{pmatrix} \quad \text{with} \quad \mathrm{tr} = -p - s < 0 \quad \text{and} \quad \det = ps + qr > 0 \ . \tag{5.15}$$

The steady state therefore remains stable, and most of the conclusions drawn in this chapter seem robust to allowing for direct competition among the predators.

Above we have already seen that the prey nullcline has the shape of the *per capita* prey growth. Even for the more general form of Eq. (5.2)

$$\frac{\mathrm{d}R}{\mathrm{d}t} = [g(R) - cN]\, R \ , \tag{5.16}$$

where $g(R)$ is an arbitrary function defining the *per capita* growth of R, one obtains that the shape of the prey nullcline reflects the shape of the *per capita* growth function $g(R)$, because the nullcline can be written as $N = g(R)/c$. Thus, whatever the *per capita* growth of the prey, the nullcline will be the same monotonically decreasing function delivering a "Lotka Volterra like" phase space, whenever one can cancel the prey from the consumption term, here cNR. Otherwise the nullcline expression is more complicated. Summarizing, a "Lotka Volterra like" phase space requires a "mass action" type consumption term (mass action means the product of the concentrations, here the product of the population sizes).

5.3 Summary

Lotka Volterra type nullclines are obtained when the prey variable can be canceled from the predation term in the prey equation. In such models the shape of the prey nullcline reflects the *per capita* growth of the prey. Because the predator nullcline is typically vertical, the non-trivial steady state prey density is completely determined by the parameters of the predator.

5.4 Exercises

Question 5.1. Desert
Consider the following model for a vegetation V in a desert. The growth of the vegetation is limited in the amount of water W in the soil:

$$\frac{\mathrm{d}W}{\mathrm{d}t} = a - bWV - cW \quad \text{and} \quad \frac{\mathrm{d}V}{\mathrm{d}t} = dWV - eV \ ,$$

where a is the rainfall dependent water uptake in the soil,
b is the extra water uptake and evaporation by the vegetation,
c is the normal evaporation,
d is the water dependent growth of the vegetation,
and e is the death rate of the vegetation.
For this exercise consider steady state situations.

a. How much water does the soil contain if there is no vegetation?
b. Suppose the rainfall increases two-fold because of a change in climate. How much water would the soil contain if there is still no vegetation?
c. How much water would the soil contain if there is a vegetation?
d. How much water would the soil contain if the rainfall increases two-fold in the presence of a vegetation?
e. Draw the nullclines, and determine the stability of the steady states.
f. How would the increased rainfall change these nullclines?

Question 5.2. Monkeys
Consider a certain area within a tropical rain forest, and ignore all seasonality. Two monkey species in this area eat the fruits from a particular fig species. One of the monkey species eats the fruits when they are unripe, and the other prefers these fruits when they are ripe. Study this system over a relatively short time period, during which the number of fig trees remains constant. Additionally, the two monkey populations are changing by immigration and emigration only, and not through birth and death. Assume that the emigration rate depends on the availability of fruit.

a. Devise a simple model in terms of differential equations for the two monkey populations and for the ripe and unripe fruits (i.e., write four ODEs).
b. What extra assumptions were required for your model?
c. Draw the nullclines of the unripe and ripe fruits in absence of the two monkey populations.
d. Since migration of monkeys is a much faster process than the ripening of the fruits (i.e., a time scale of days versus weeks), we can make a quasi steady state assumption (QSS) for the two monkey populations. Write the QSS equations, and combine parameter combinations into new parameters if this simplifies the new ODEs.
e. Draw the nullclines of the unripe and ripe fruit in the quasi steady state model, and analyze the steady states.
f. How can one derive the densities of the monkeys from this phase portrait?
g. Draw in a single figure the fruit nullclines for the model without monkeys and for the QSS model.

Question 5.3. Return time (Extra exercise for cool students)
Compute the return time of the non-trivial steady state of the Lotka Volterra model and study how this depends on the mechanism of the density dependence of the prey. For reasons of simplicity it is convenient to assume the typical case where the non-trivial steady state is a stable spiral point (and not a stable node), and to first compute the return time of a general form of the Lotka Volterra model, e.g.,

$$\frac{\mathrm{d}R}{\mathrm{d}t} = rR - \gamma R^2 - aRN \quad \text{and} \quad \frac{\mathrm{d}N}{\mathrm{d}t} = caRN - \delta N \ .$$

a. Compute the return time of this general form.

b. What is the return time when we explicitly make the birth rate density dependent (e.g., replace $rR - \gamma R^2$ with $bR[1 - R/k] - dR$)? Is the birth or the death rate determining the return time?
c. Address the same questions for a Lotka Volterra model with a density dependent death rate of the prey.
d. Interpret your results.

Chapter 6

Functional response

The previous chapter suggested that one may obtain a qualitatively new phase space, and therefore possibly new behavior, when the prey cannot be canceled from the consumption term in the prey equation. When the consumption of a single predator does not linearly depend on the prey density, like it did in the $f(R) = cR$ in Fig. 5.1c, the prey nullcline is no longer expected to reflect the monotonically declining *per capita* growth of the prey.

The function describing how the total consumption of an individual predator depends on the prey density is called the "functional response". Above we have used the so-called "linear" functional response. Holling (1959) defined three non-linear responses

$$f(R) = a\min(1, \frac{R}{2h}) \ , \quad f(R) = a\frac{R}{h+R} \quad \text{and} \quad f(R) = a\frac{R^2}{h^2+R^2} \ , \tag{6.1}$$

which are called the type I, II, and III, respectively (see Fig. 6.1). All three functions approach a maximum corresponding to the maximum number of prey a predator can catch within a certain time unit. Holling's motivation for this maximum was the "handling time": even at an infinite prey density the predator cannot consume the prey infinitely fast because of the time required to handle, eat, and digest the prey. The Holling type II and type III responses are conventional Hill functions. Thus, we know that a is the maximum consumption rate, and that h is the prey density at which the *per capita* consumption is half maximal. Synonyms of the type II and III

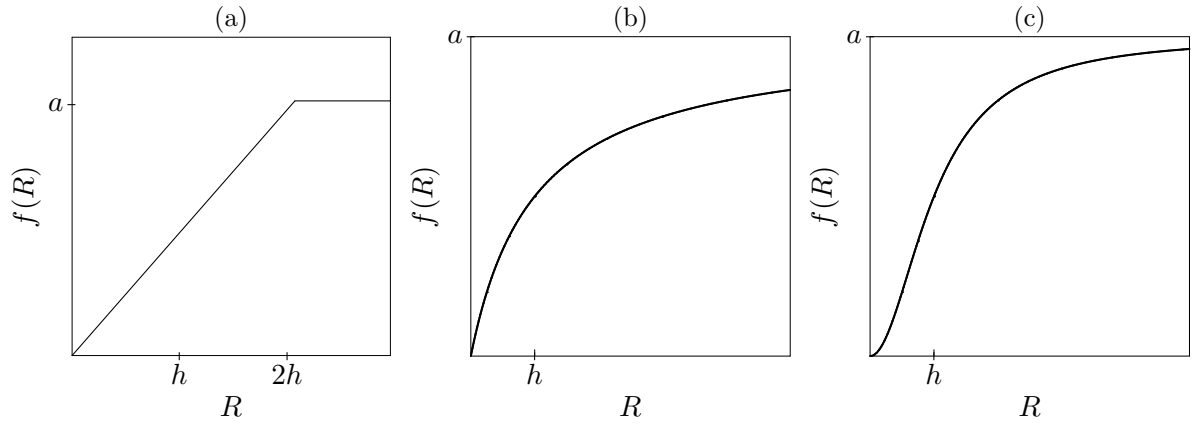

Figure 6.1: The Holling type I functional response (a), the Monod (Holling type II) functional response (b), and the sigmoid (Holling type III) functional response (c).

responses are the "Monod saturation" and the "sigmoid" functional response, respectively. Both will be discussed at length in this chapter. The type I response is linear until the *per capita* consumption rate equals the maximum of a prey per time unit, and will be discussed in Section 6.3.

6.1 Monod functional response

The previous chapter showed that one obtains qualitatively similar nullclines for the prey for any *per capita* growth function that monotonically declines with the prey density. To simplify the algebra we therefore replace the more complicated growth term with explicit birth and death rates in Eq. (5.1) with a simple logistic growth term. The price that we pay is that the R_0 of the prey is no longer defined. Considering the Monod saturated *per capita* consumption of the predator of Eq. (6.1)b, one immediately arrives at

$$\frac{\mathrm{d}R}{\mathrm{d}t} = rR(1-R/K) - \frac{aRN}{h+R} \ , \tag{6.2}$$

where the new parameter a is the maximum number of prey a single predator can catch per time unit, and the parameter h is the prey density at which the predator catch rate is $a/2$ prey per unit of time. The $\mathrm{d}R/\mathrm{d}t = 0$ isocline can be found by setting Eq. (6.2) to zero and solving

$$R = 0 \quad \text{and} \quad N = (r/a)(1-R/K)(h+R) \ , \tag{6.3}$$

where the latter is a parabola crossing $N = 0$ at $R = K$ and $R = -h$, and having its maximum value at $R = (K-h)/2$. In Fig. 6.2 this parabola is depicted for positive population densities. Note that we have indeed lost the general property of the previous models that the prey nullcline is a monotonically declining function of the prey density R.

For the predator it is typically assumed that the *per capita* birth rate is proportional to the *per capita* consumption, but we will here do the more general case of Fig. 5.1d where the predator birth rate, β, is a conventional saturation function of its consumption. Since the *per capita* consumption equals $aR/(h+R)$, one obtains for the *per capita* birth rate of a predator

$$g(R) = \frac{c\frac{aR}{h+R}}{H + \frac{aR}{h+R}} = \frac{caR}{H(h+R)+aR} = \frac{\beta R}{h'+R} \tag{6.4}$$

where $\beta = ca/(H+a)$ and $h' = hH/(H+a) < h$. Assuming a simple density independent death rate for the predator one obtains

$$\frac{\mathrm{d}N}{\mathrm{d}t} = \frac{\beta RN}{h'+R} - dN \ , \tag{6.5}$$

where h' is the prey density where the predator birth rate is half maximal, i.e., $\beta/2$. Note that $h' < h$, i.e., that the predator birth rate saturates at lower prey densities than the predator consumption rate (which actually confirms the unconventional choice made in Eq. (5.5) of having no saturation in the consumption term, while allowing for saturation in the birth rate of the predator). Since most authors typically assume that the predator's birth rate is proportional to its consumption, they typically set $h' = h$. The maximum fitness of the predator is $R_0 = c/d$, and the $\mathrm{d}N/\mathrm{d}t = 0$ isocline is located at $R^* = dh'/(c-d) = h'/(R_0-1)$, and therefore remains a vertical line. This nullcline again corresponds to the minimal prey density the predator requires for its maintenance. Since most authors typically assume that the predator's birth rate is

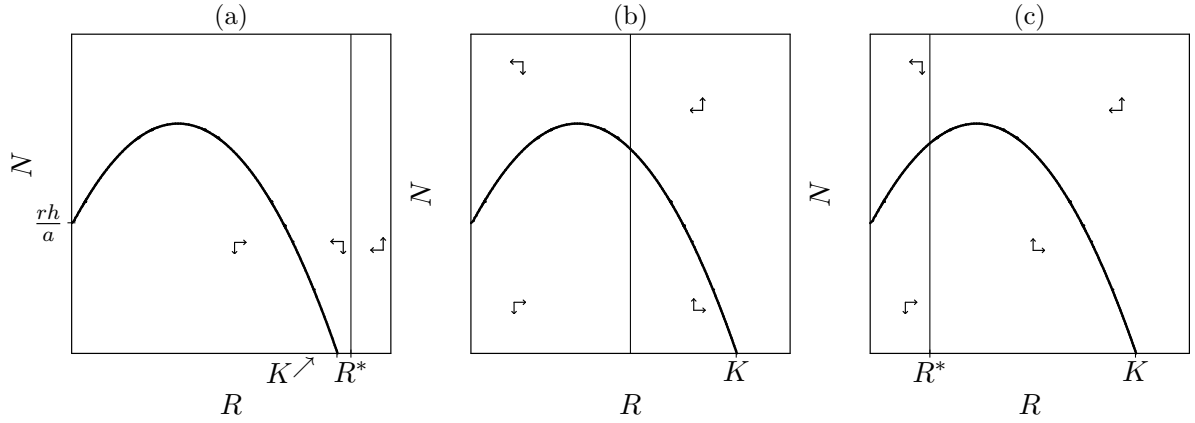

Figure 6.2: The three qualitatively different phase spaces of the Monod model. The parabola is the prey nullcline intersecting the horizontal axis at $R = K$ and the vertical axis at $N = rh/a$. The vertical predator nullcline is located at $R^* = h'/(R_0 - 1)$.

proportional to its consumption, they typically set $h' = h$. Check for yourself how the nullclines change when the birth rate, $\beta = caR/(h + R)$, and $h' = h$.

The model has maximally three steady states: two trivial states $(\bar{R}, \bar{N}) = (0, 0)$, $(K, 0)$, and the non-trivial co-existence state when $R^* < K$, i.e., when the minimal prey density required for predator growth is smaller than the carrying capacity of the prey. Fig. 6.2 depicts the three qualitatively different phase spaces of the Monod model. In Fig. 6.2a the predator cannot maintain itself because $R_0 - 1 < h'/K$, i.e., even the maximum prey density K is insufficient for predator growth. As a consequence $(\bar{R}, \bar{N}) = (K, 0)$ is a stable steady state (see the vector field in Fig. 6.2a). One interpretation is a situation with a poor availability of nutrients such that the resource R has a low carrying capacity. The maximum prey density is too low for another trophic layer in the food chain.

Fig. 6.2b depicts the situation where the predator nullcline is located at the right side of the top of the parabolic prey nullcline, i.e., where $(K - h)/2 < R^*$. The local vector field is identical to that of the Lotka Volterra model (or that in Fig. 5.2a):

$$J = \begin{pmatrix} -\alpha & -\beta \\ \gamma & 0 \end{pmatrix} \quad \text{with} \quad \text{tr} = -\alpha < 0 \quad \text{and} \quad \det = \beta\gamma > 0 \ . \tag{6.6}$$

Thus, the non-trivial steady state will be stable whenever the predator nullcline intersects the prey nullcline at the right hand side of the maximum of the parabola. In Fig. 6.2c the nullclines intersect at the left hand side of the maximum of the parabola because $(K - h)/2 > R^*$. From the local vector field one now reads that the graphical Jacobian

$$J = \begin{pmatrix} \alpha & -\beta \\ \gamma & 0 \end{pmatrix} \quad \text{with} \quad \text{tr} = \alpha > 0 \ . \tag{6.7}$$

The steady state is unstable because the local feedback of the prey on itself is positive: increasing the number of prey increases the growth of the prey. The reason for this positive feedback is the saturated functional response. Increasing the prey density will decrease the *per capita* killing rate of the prey. The behavior of the model in this situation is a stable limit cycle (see Fig. 6.3). One can indeed check that none of the trivial steady states, i.e., $(\bar{R}, \bar{N}) = (0, 0)$ or $(K, 0)$, is an attractor of the system. The predator therefore cannot go extinct, and the stable limit cycle has to be the global attractor of the system.

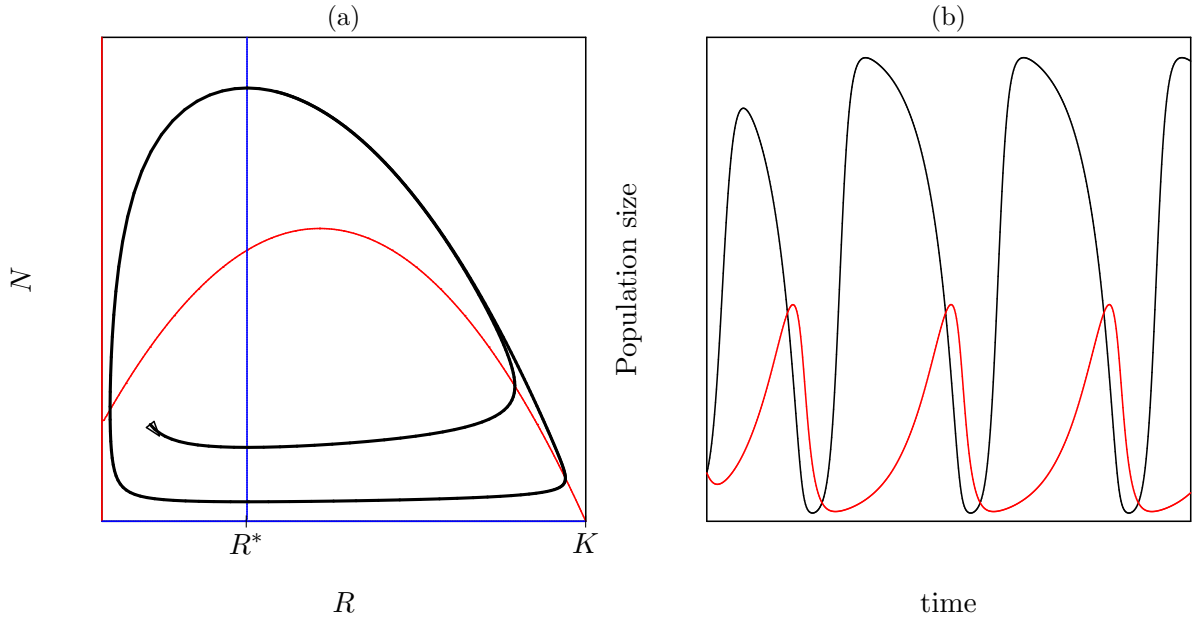

Figure 6.3: Limit cycle behavior in the Monod model. Panel (a) displays a trajectory approaching a stable limit cycle in phase space, and Panel (b) shows the same trajectory in time. The population varying with the largest amplitude is the prey.

Predator prey models with the "humped" prey nullcline of Fig. 6.2 have been used for the famous Paradox of Enrichment (Rosenzweig, 1971). Rosenzweig studied euthrophication (enrichment) of lakes with algae and zooplankton, and showed that increasing the carrying capacity of the algae failed to increase the density of the algae. The enrichment with nutrients for the algae rather increased the zooplankton density, and could lead to a destabilization of the steady state (Rosenzweig, 1971). From Fig. 6.2 one can indeed see that increasing the carrying capacity K:

1. increases the density of the algae in Panel (a) where there is no zooplankton
2. leaves the density of the algae at $R^* = h'/(R_0 - 1)$ and increases the zooplankton density in Panel (b)
3. destabilizes the system by a Hopf-bifurcation (see Chapter 14), leading to oscillations around an average density of the algae of $R^* = h'/(R_0 - 1)$ in Panel (c).
4. could even drive the zooplankton to extinction if at high values of K the limit cycles have such a large amplitude that they approach the $N = 0$ axis (Rosenzweig, 1971).

Note that enrichment of an oligotrophic system first increases the diversity of the system when the predator starts to maintain itself, but that ultimately it would decrease the diversity, and leads to a green lake with a large density of algae. These predictions have been confirmed in bacterial food chains by Kaunzinger & Morin (1998); see Chapter 8.

Limit cycle behavior

When the non-trivial steady state is unstable the model displays oscillatory behavior and approaches a stable limit cycle (Fig. 6.3). On the limit cycle the predator and prey densities oscillate out of phase because predator densities increase only after the prey has increased (see Fig. 6.3b). Oscillatory behavior is frequently observed in ecological populations. The most famous example is the oscillatory behavior of lynx and hare populations in Canada, that were discovered in the records of the furs brought in by hunters in the last century. Surprisingly, the hare and lynx cycles are not always out of phase, and ecologists are performing experiments

to understand the precise mechanism underlying this famous oscillation (Stenseth *et al.*, 1999). Another famous example of predator prey oscillations are the cycles of algae and zooplankton in the spring (McCauley *et al.*, 1999; Fussmann *et al.*, 2000; Murdoch *et al.*, 2002; Yoshida *et al.*, 2003). Periodic behavior is easily obtained in mathematical models and is frequently observed in nature. Note that these oscillations are autonomous: there is no periodic forcing from outside driving this. The periodic behavior arose by the destabilization of the non-trivial steady state, i.e., at a Hopf bifurcation (see Chapter 14).

6.2 Sigmoid functional response

For large herbivores one often uses a sigmoid functional response because these animals hardly graze if the vegetation is too poor. Alternatively, one can use a sigmoid functional response for prey species that can hide efficiently in "refugia". At low prey densities most prey individuals will be hard to find for the predator because they are all hidden in these refugia. When at higher prey densities all refugia are filled the *per capita* consumption by the predator will increase rapidly. Although one could write a "shifted" Monod saturated functional response, i.e., $f(R) = (R-k)/(h+R-k)$, where k is the number of refugia, one typically writes a sigmoid functional response for prey with refugia.

Adopting simple logistic growth for the prey the ODE, for the prey becomes

$$\frac{\mathrm{d}R}{\mathrm{d}t} = rR(1 - R/K) - \frac{aR^2N}{h^2 + R^2} \ , \tag{6.8}$$

and if the predator birth rate is the same saturation function of its consumption as we used in Eq. (6.4) one obtains

$$\frac{\mathrm{d}N}{\mathrm{d}t} = \frac{cR^2N}{h'^2 + R^2} - dN \ , \tag{6.9}$$

where $c = a\alpha/(H + \alpha)$ and $h' = h\sqrt{H/(H + a)} < h$. If the predator birth rate can be assumed to be proportional to its consumption one can easily check that $h' = h$. The R_0 of this predator remains $R_0 = c/d$ and the $\mathrm{d}N/\mathrm{d}t = 0$ nullcline is located at $R^* = h'/\sqrt{R_0 - 1}$, which remains a vertical line in Fig. 6.5. Thus, very little has changed for the predator nullcline. Its intersection with the horizontal prey axis remains to have the interpretation of the minimum prey density required for predator growth.

In order to find the prey nullcline, one sets Eq. (6.8) to zero and cancels the $R = 0$ solution, to obtain

$$N = \frac{r(h^2 + R^2)}{aR} \left(1 - \frac{R}{K}\right) \ , \tag{6.10}$$

which has a vertical asymptote at $R = 0$ and is zero when $R = K$. One can take the derivative of this function to find its minima and maxima (see Section 18.6 in the appendix), but because this all becomes rather complicated, one typically constructs the nullcline graphically (Noy-Meir, 1975). The procedure is to separate Eq. (6.8) into its positive logistic growth term, and its negative sigmoid predation term. Both one can sketch as a function of the prey density R (see Fig. 6.4a). The positive term is a parabola intersecting the horizontal axis at $R = 0$ and $R = K$. The predation term is a sigmoid function with a maximum depending on the predator N. Thus, one has to sketch a family of functions for various values of N (see Fig. 6.4a).

To know when and where in Fig. 6.4a the curves intersect it is crucial to know their slopes around the origin, and the maximum values they can obtain. For the slope at the origin one

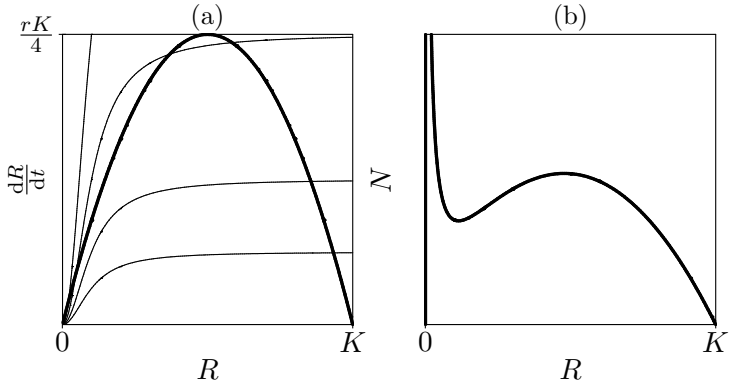

Figure 6.4: The prey nullcline of Eq. (6.8) is constructed by sketching its positive and negative part in one diagram (a) for various values of N. The intersects in (a) deliver the $\mathrm{d}R/\mathrm{d}t = 0$ nullcline in (b).

takes the derivative with respect to the horizontal variable, which here is the prey R. For the logistic growth part in Eq. (6.8),

$$\partial_R \, rR(1 - R/K) = r - 2rR/K \quad \text{which for } R = 0 \text{ equals} \quad r \ , \tag{6.11}$$

showing that the local slope of the parabola in the origin is r. For the grazing terms in Eq. (6.8),

$$\partial_R \, \frac{aR^2N}{h^2 + R^2} = \frac{2aRN}{h^2 + R^2} - \frac{2aR^3N}{(h^2 + R^2)^2} \quad \text{which for } R = 0 \text{ yields} \quad 0 \ , \tag{6.12}$$

implying that the grazing curves leave the origin with slope zero. The sigmoid curves therefore always start below the parabola, whatever the predator density N. At infinite prey density the maximum of the predation term is aN, which for sufficiently large predator densities will always exceed the maximum of the parabola $rK/4$ (see Fig. 6.4a). Whenever the positive growth term and the negative predation term intersect, they cancel each other and $\mathrm{d}R/\mathrm{d}t = 0$. For various values of the predator density N one finds the intersects and plots these into the phase space of N versus R (see Fig. 6.4b). When h is sufficiently small this leads to a $\mathrm{d}R/\mathrm{d}t = 0$ nullcline with a minimum and a maximum, when h is too large the nullcline declines monotonically. In Section 18.6 in the appendix we derive that the nullcline is non-monotonic when $h < K/(3\sqrt{3}) \simeq K/5$. Whatever the precise situation the model has maximally three steady states: $(0, 0)$, $(K, 0)$, and a non-trivial equilibrium when $R^* < K$, i.e., when the minimal prey density required for predator growth is smaller than the carrying capacity of the prey.

Because the predator nullcline can be located anywhere on the horizontal prey axis, there are maximally four qualitatively different phase spaces (see Fig. 6.5). Basically, this extends the three possibilities of the Monod saturated model with the stable case of Fig. 6.5d, where the intersect with the vertical predator nullcline falls left of the minimum of the prey nullcline. The graphical Jabobian of this new steady state is

$$J = \begin{pmatrix} -\alpha & -\beta \\ \gamma & 0 \end{pmatrix} \quad \text{with} \quad \mathrm{tr}J < 0 \quad \text{and} \quad \det J > 0 \ , \tag{6.13}$$

which therefore is a stable point. The three other cases are similar to those of the Monod saturated model.

By enrichment, i.e., by increasing K, one will proceed through the same situations as one does in the Monod saturated model, i.e., from a prey population increasing with the carrying capacity in Fig. 6.5(a), to a stable co-existence in (b), to stable limit cycles in (c). One main difference

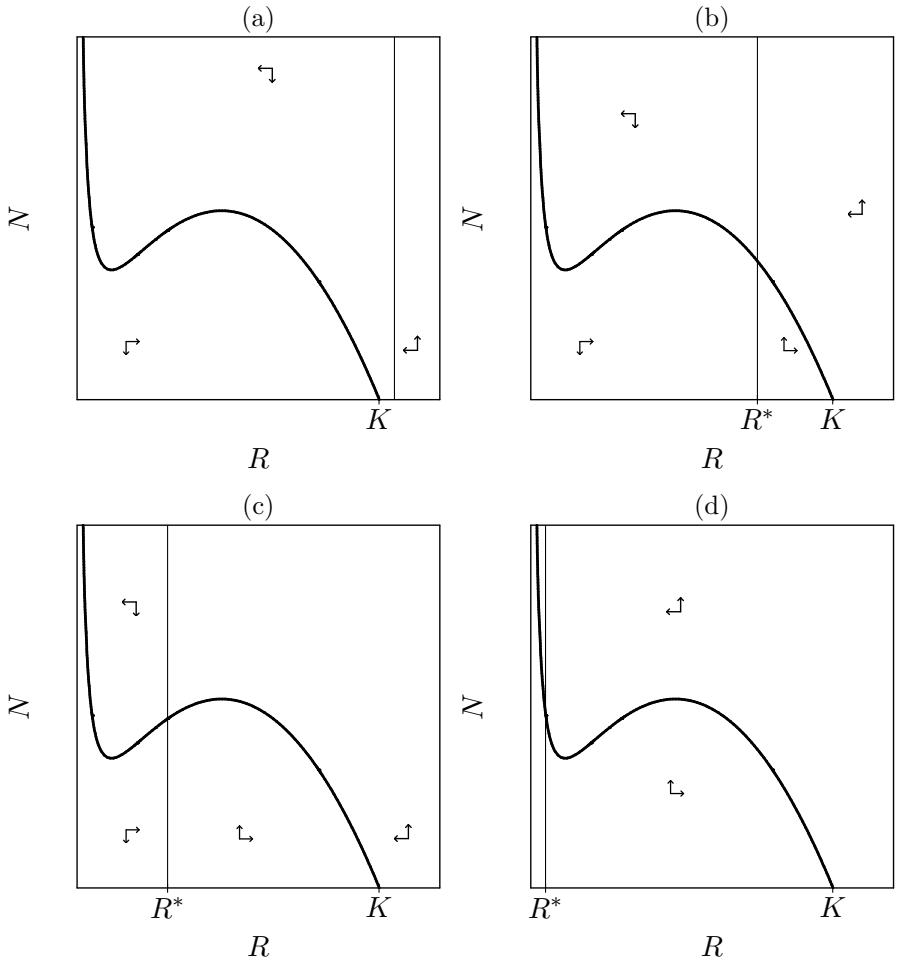

Figure 6.5: The four qualitatively different phase spaces of the sigmoid (Holling type III) predator prey model. The vertical line is the predator nullcline located at $R^* = \frac{h'}{\sqrt{R_0 - 1}}$. Section 18.6 in the appendix shows that the prey nullcline will only have this non-monotonic shape when the h parameter is small compared to the carrying capacity K. If $h > K/3\sqrt{3}$ the prey nullcline declines monotonically, and the phase spaces will resemble those of the Lotka Volterra like models discussed in Chapter 5.

is that the amplitude of the limit cycles remains smaller because they shrink in amplitude when the stable situation of panel (d) is approached. The other main difference is that the oscillatory behavior dies at high values of the carrying capacity. For the algae-zooplankton systems the effect of the functional response on the amplitude of the limit cycles is quite important because the oscillations that are observed in nature are much milder than those of the Monod saturated model for realistic parameter values (McCauley *et al.*, 1999; Murdoch *et al.*, 2002; Scheffer & De Boer, 1995). Measurements of the functional response of zooplankton grazing on algae strongly support a Holling type II response, however.

6.3 A Holling type I/II functional response

It is widely recognized that the complicated prey nullcline of Fig. 6.5 requires a shifted or a sigmoid functional response. This is not generally true, however. There are functional responses that look very similar to the Monod saturated function, and nevertheless deliver a prey nullcline with a minimum and a maximum. These response functions can be constructed from the general

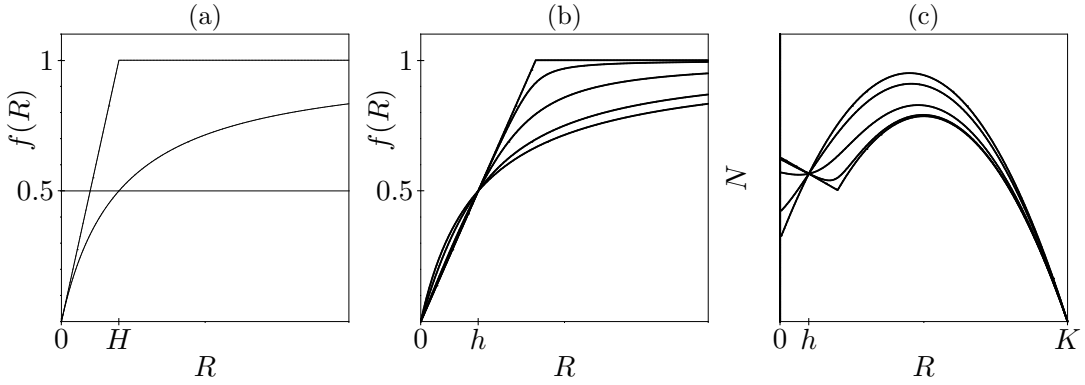

Figure 6.6: The hyperbolic function of Eq. (6.14). Panel (a) depicts $f(R)$ defined by Eq. (6.14) for a curvature parameter, $\gamma = 0$ (curved line), and for $\gamma = 1$ (discontinuous line). The former is equal to the Monod function $f(R) = R/(H + R)$, with $f(R) = \frac{1}{2}$ at $R = H$, and the latter is equal to the type I functional response $f(R) = \min(1, R/H)$, which becomes horizontal at $R = H$. Panel (b) depicts the same function for $\gamma = 0, 0.5, 0.9, 0.99$ and $\gamma = 1$, where we have defined $H = h/(1 - \gamma/2)$ to give the functions an "equivalent" half-maximal value, $f(R) = \frac{1}{2}$ when $R = h$. Panel (c) depicts the prey nullcline of Eq. (6.15) for this functional response, and for the same five values of γ. The parabola depicts the Holling type II response ($\gamma = 0$), the discontinuous line the Holling type I functional response ($\gamma = 1$); the nullclines in between are novel.

definition of hyperbolic functions and can be written as

$$f(R) = \frac{2R}{H + R + \sqrt{(H + R)^2 - 4\gamma HR}} \ . \tag{6.14}$$

When one sets the "curvature parameter" $\gamma = 0$, this becomes equal to the Holling type II function, $f(R) = R/(H + R)$, Setting the curvature to $\gamma = 1$ delivers the discontinuous Holling type I function, $f(R) = \min(1, R/H)$, depicted in Fig. 6.6a; which is not so easy to check analytically. Both functions have the same slope, $\partial_R f = 1/H$ at $R = 0$, but at $R = H$ the function $f(R) = 1/2$ for $\gamma = 0$, and it is at its maximum $f(R) = 1$ for $\gamma = 1$ (see Fig. 6.6a). To make the functions equivalent at their half-maximal values, one solves R from $f(R) = 1/2$ in Eq. (6.14) to find that the half maximal values occur at $R = H(1-\gamma/2)$. Thus, defining h as the prey density where $f(R)$ is half maximal, i.e., $h = H(1 - \gamma/2)$, one can define $H = h/(1 - \gamma/2)$ to obtain a function that is half-maximal at $R = h$ for any value of γ (see Fig. 6.6b).

For $\gamma > 0$ this new functional response is not as rounded as the Monod response, and this delivers qualitatively different nullclines (Fig. 6.6c). Consider the conventional predator prey model

$$\frac{\mathrm{d}R}{\mathrm{d}t} = rR(1 - R/K) - aNf(R) \quad \text{and} \quad \frac{\mathrm{d}N}{\mathrm{d}t} = caNf(R) - dN \ , \tag{6.15}$$

with $R_0 = ca/d$, and a functional response defined by Eq. (6.14) with $H = h/(1 - \gamma/2)$, with the convenient property that $f(R) = 1/2$ when $R = h$. The fact that the prey nullcline of the Monod saturated model with $\gamma = 0$ can differ so much from a relatively similar functional responses obtained with $\gamma > 0$, is disturbing because we prefer results that are more generic, and do not depend crucially on the curvature of the saturation function chosen to describe the functional response.

The predator nullcline also deserves some attention. At prey densities much higher than the saturation constant, h, the functional response function, $f(R)$, equals one for the type I response ($\gamma = 1$), and $f(R) \simeq 1$ for the response functions with $\gamma \to 1$. Whenever this is the case the

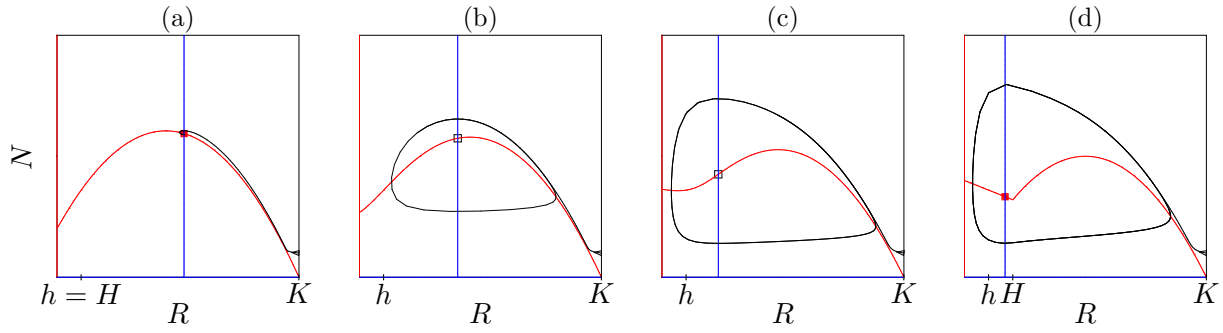

Figure 6.7: The nullclines of the Holling type I/II functional response for the curvature parameter $\gamma = 0$ [and $h = H$] (a), $\gamma = 0.5$ (b), $\gamma = 0.9$ (c), and $\gamma = 1$ [and $H = 2h$] (d). The predator nullcline is always located at $f(R) = d/(ca)$ (see Eq. (6.15)). Solid squares mark stable steady states, open squares unstable points. Parameter values ($r = K = 1$, $a = 0.5$, $d = 0.42$, $c = 1$ and $h = 0.1$).

predator ODE approaches

$$\frac{\mathrm{d}N}{\mathrm{d}t} \simeq [ca - d]N \ , \tag{6.16}$$

which is only zero for the particular parameter condition $ca = d$ (i.e., $R_0 = 1$). This means that the predator nullcline in the Holling type I model can only be located at a sufficiently low prey density, i.e., in the region where $R < 2h$, where the nullcline approaches the "Lotka Volterra" like straight line. The non-trivial steady state of a model with a Holling type I functional response can therefore only be stable (see Fig. 6.7d).

Similar restrictions apply when $\gamma \to 1$. The prey nullcline only has its non-monotonic shape when $h \ll K$; otherwise it is monotonically declining (which is also true for a model based upon a sigmoid functional response; see Section 18.6 in the appendix). Because $f(R) \simeq 1$ when $R \gg h$, the predator nullcline can only be located in regions where $R < 2h$ (see Eq. (6.16)). For large values of the curvature, it is therefore difficult to have a predator-prey model that has a stable steady state located at the right side of the top of the prey nullcline in Fig. 6.7c. This means that for large γ the model either has a stable steady state in the declining part of the prey nullcline (Fig. 6.7d), or an unstable equilibrium point located in the rising part of the prey nullcline, which is surrounded by a stable limit cycle (Fig. 6.7c). Interestingly, for large γ the stable steady state can co-exist with a similar stable limit cycle (see Fig. 6.7d). The seperatrix between these two attractors is formed by an invisible unstable limit cycle (see Chapter 14) that is also surrounding the steady state.

6.4 Formal derivation of a functional response

The Monod functional response can be derived in the same way as the conventional Michaelis-Menten enzyme expression is derived. To this end one splits the predators, N, into a subpopulation C that is actually handling the prey, and a free subpopulation, F, that is trying to catch the prey R. By conservation one knows that $N = F + C$. To describe the predators catching and handling prey one could write

$$\frac{\mathrm{d}C}{\mathrm{d}t} = kRF - hC \quad \text{or} \quad \frac{\mathrm{d}C}{\mathrm{d}t} = kR(N - C) - hC \ , \tag{6.17}$$

where k is a rate at which the free predators catch prey, and $1/h$ is the time they require to handle the prey. Since the time scale of handling prey is much more rapid than the time scale

at which the prey and predators reproduce, one can make a quasi steady state assumption for the complex, $\mathrm{d}C/\mathrm{d}t = 0$, and obtain that

$$C = \frac{kNR}{h + kR} = \frac{NR}{h' + R} \ , \tag{6.18}$$

where $h' = h/k$ is the prey density at which half of the predators are expected to be handling prey.

To see how this ends up in the prey population one could add $\mathrm{d}C/\mathrm{d}t = kRF - hC = 0$ to the ODE for the prey, i.e., $\mathrm{d}R/\mathrm{d}t = rR(1 - R/K) - kRF$, giving

$$\frac{\mathrm{d}R}{\mathrm{d}t} = rR(1 - R/K) - hC = rR(1 - R/K) - \frac{hNR}{h' + R} \ , \tag{6.19}$$

which is a normal Holling type II functional response. For the predators one could argue that the birth rate should be proportional to the number of predators that are handling and consuming prey, and write that

$$\frac{\mathrm{d}N}{\mathrm{d}t} = cC - dN = \frac{cNR}{h' + R} - dN \ , \tag{6.20}$$

which again delivers the Monod saturated predator prey model.

One can also use this analysis for writing the ODEs for a predator consuming several species of prey. Let k_i be the catch rate for species R_i and assume for simplicity that all prey species require the same handling time. By the k_i parameter, the predator can have different preferences for the different prey species. The conservation equation now becomes $N = F + \sum_i C_i$ and for each complex one writes $\mathrm{d}C_i/\mathrm{d}t = k_i R_i F - hC_i = 0$. Summing all $\mathrm{d}C_i/\mathrm{d}t$ equations yields

$$\sum_i \frac{\mathrm{d}C_i}{\mathrm{d}t} = \sum_i k_i R_i F - h \sum_i C_i = \sum_i k_i R_i \Big(N - \sum_j C_j \Big) - h \sum_i C_i = 0 \ , \tag{6.21}$$

which can be rewritten into

$$\sum_i C_i = \frac{N \sum_i k_i R_i}{h + \sum_j k_j R_j} \quad \text{and, hence,} \quad C_i = \frac{N k_i R_i}{h + \sum_j k_j R_j} \ . \tag{6.22}$$

For each prey species i one can again add $\mathrm{d}C_i/\mathrm{d}t = k_i R_i F - hC_i = 0$ to

$$\frac{\mathrm{d}R_i}{\mathrm{d}t} = rR_i(1 - R_i/K_i) - k_i R_i F \quad \text{giving} \quad \frac{\mathrm{d}R_i}{\mathrm{d}t} = rR_i(1 - R_i/K_i) - \frac{hk_i R_i N}{h + \sum_j k_j R_j} \ . \tag{6.23}$$

For the predators one would argue that their reproduction is proportional to all predators in complex with prey, and write that

$$\frac{\mathrm{d}N}{\mathrm{d}t} = c \sum_i C_i - dN = \frac{cN \sum_i k_i R_i}{h + \sum_j k_j R_j} - dN \ . \tag{6.24}$$

Although this all works out quite nicely, this does not imply that saturated functional responses are actually due to the handling time derived here. One could also argue that the saturation is simply due to satiation of the predators at high prey densities.

6.5 Summary

The Holling type II and III functional responses explain periodic behavior in predator prey models. Enrichment of a predator prey system by increasing the carrying capacity of the prey can easily lead to destabilization (by a Hopf bifurcation) and oscillatory behavior. Unfortunately, the nullclines depend rather critically on the precise form of the functions used for the functional response.

6.6 Exercises

Question 6.1. Parameters
A simple resource consumer model based on a saturated functional response is:

$$\frac{\mathrm{d}R}{\mathrm{d}t} = a_1 R(1 - R/K) - b_1 N \frac{R}{c_1 + R}$$

$$\frac{\mathrm{d}N}{\mathrm{d}t} = -a_2 N + b_2 N \frac{R}{c_2 + R}$$

a. Give a biological interpretation and the dimension of all parameters.
b. Is it biologically reasonable to choose $b_1 = b_2$?
c. Give an interpretation for the following parameter choices $c_1 = c_2$, $c_1 > c_2$ and $c_1 < c_2$.

Question 6.2. Eutrophication: 2D
Consider an algae zooplankton system based upon a sigmoid functional response, and assume direct competition between zooplankton at high densities. Study the effect of eutrophication.
a. Make a model of the system described above, and sketch the nullclines.
b. What parameter varies with the nutrient concentration?
c. What are the possible effects of eutrophication, given either a strong or a weak intraspecific competition in the zooplankton? Draw the qualitatively different nullcline situations.
d. What do you learn from this about the usage of models to predict environmental effects?

Question 6.3. Luckinbill
Fig. 6.8 depicts the data of Luckinbill (1973). The horizontal axis gives the time in either hours (Panel A) or days (Panels B & C). The vertical axis is population density in numbers per ml. The solid line depicts the prey *Paramecium* and the dotted line the predator *Didinium*. Panel A: *Paramecium* and *Didinium* in normal medium. Panel B: *Paramecium* and *Didinium* in a medium with methyl-cellulose, which increases the viscosity of the medium. At day 17 *Didinium* dies out. Panel C: as Panel B after halving the concentration of food for the prey *Paramecium*. In Panels B and C the fat line at the top gives the density of *Paramecium* in the same medium in the absence of the predator.
a. Write a simple consumer resource model to explain these data.
b. Identify the differences between the experiments with differences in parameter values of the model.
c. Draw for each of the three situations the nullclines of the model, and a trajectory corresponding to the data.
d. Does your model provide a good interpretation of the data?
e. What are the most important differences between the model and the data?

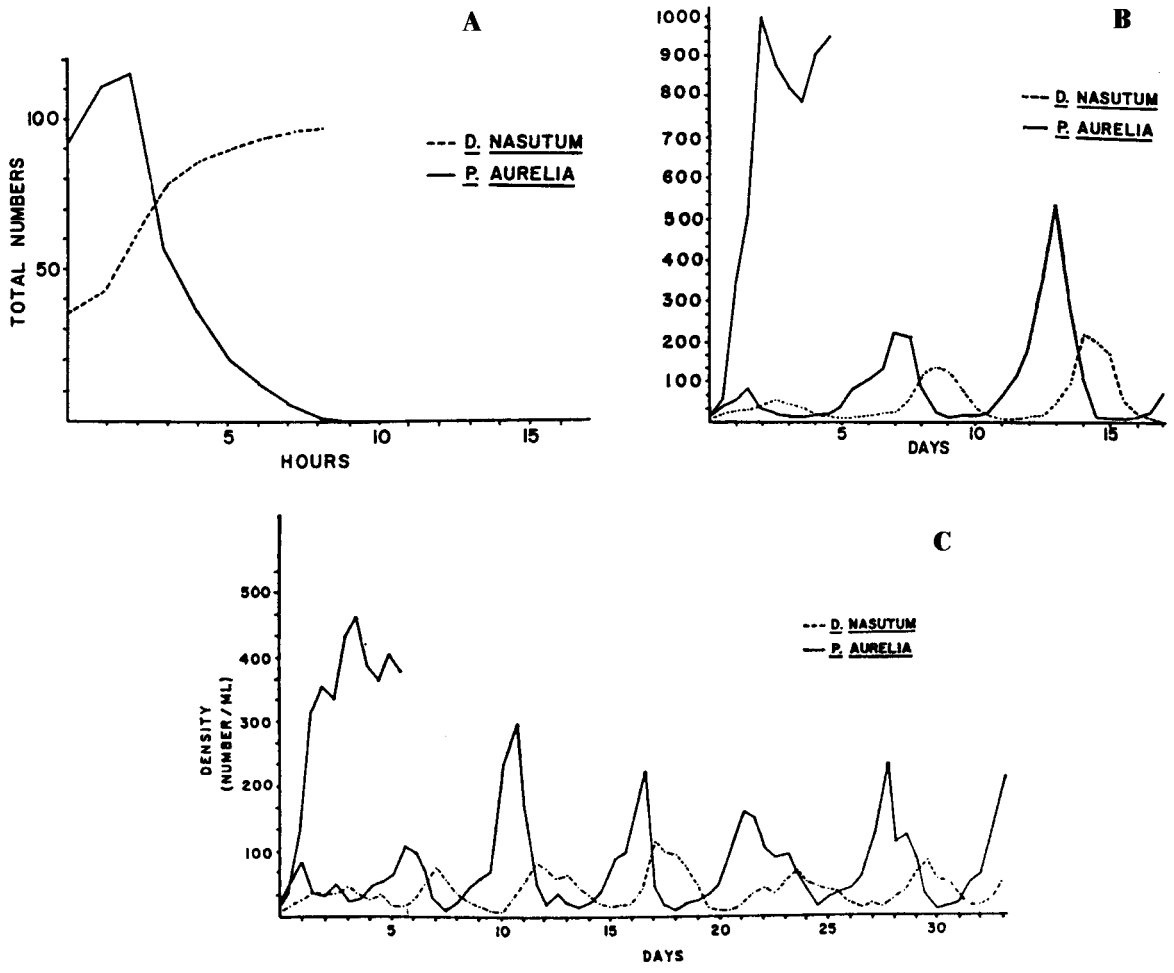

Figure 6.8: The data from Luckinbill (1973). The horizontal axis gives the time in either hours or days, and the vertical axis the population density in numbers per ml. The solid line is the prey *Paramecium* and the dotted line the predator *Didinium*. Panel A: *Paramecium* and *Didinium* in normal medium. Panel B: *Paramecium* and *Didinium* in a medium with methyl-cellulose, which increases the viscosity of the medium, which decreases the food intake of *Didinium*. Panel C: as Panel B but with half the amount of food for *Paramecium*. In Panels B and C the fat line at the top represents the population density of *Paramecium* in the absence of the predator.

Question 6.4. Filter feeders

Copepods are filter feeders. The organ they use for filtering is also used for respiration, and filtering is continued even in the presence of large amounts of food. Excess food is killed and excreted. The phytoplankton on its own grows exponentially until it approaches its carrying capacity. Assume a mass action predation term.

a. Make a model describing the interaction between copepods and phytoplankton.

b. Analyze the model using nullclines.

c. How does the return time of this model differ from the return time of a standard model without saturation of the predator consumption?

d. How does the behavior of this model differ from the model without saturation of the predator consumption?

e. Mussels are filter feeders that can separate respiration and food uptake. In the presence of large amounts of food, respiration continues whereas food uptake saturates. Analyse this new system using nullclines and draw a trajectory in phase space.

Question 6.5. Exponential function response
Predator prey models with a saturated functional response are not always written with a Hill function. An equally simple saturation function is the exponential function:

$$\frac{\mathrm{d}R}{\mathrm{d}t} = rR(1-R/K) - aN(1-\mathrm{e}^{-\ln[2]R/h}) \quad \text{with} \quad \frac{\mathrm{d}N}{\mathrm{d}t} = caN(1-\mathrm{e}^{-\ln[2]R/h}) - dN \ .$$

Solving $1/2 = \mathrm{e}^{-\ln[2]x/h}$ delivers $x = h$, which means that the functional response remains half maximal at $R = h$.

a. What is the meaning of the parameter a?

b. We have seen that replacing the simple Monod function with the hyperbolic function of Eq. (6.14) had a large impact on the phase space of this model. Check with `grind.R` whether the same is true for the exponential functional response (see the file `exp.R`).

Chapter 7

Predator-dependent functional responses

All functional responses considered hitherto depend on the prey density only, and can hence be written as functions $f(R)$. If there is direct competition between predators for catching prey one would have a situation where the *per capita* consumption efficiency declines with the predator density, i.e., a functional response $f(R, N)$ for which $\partial_N f() < 0$. Predators that increase their feeding efficiency by hunting in groups also require a "predator-dependent functional response" but with the property that $\partial_N f() > 0$.

7.1 Ratio-dependent predation

Arditi & Ginzburg (1989) and Ginzburg & Akçakaya (1992) criticized the predator prey models discussed above because these models "predict" that feeding the prey fails to increase the prey density at steady state (see also their book (Arditi & Ginzburg, 2012)). Indeed we have seen that all enrichment ends up in the predator density. Moreover, when the reasonable Holling type II functional response with reasonable parameters is used for modeling algae-zooplankton systems, euthrophication typically leads to oscillatory behavior with an amplitude that is typically not observed in nature (Arditi & Ginzburg, 1989; Ginzburg & Akçakaya, 1992; McCauley *et al.*, 1999; Murdoch *et al.*, 2002; Scheffer & De Boer, 1995). Although a simple density dependent death term of the zooplankton already helps to solve these problems, this remains an active area of research.

Arditi & Ginzburg (1989) and Ginzburg & Akçakaya (1992) argued that one can improve predator prey models by making the predation dependent of the number of prey per predator, i.e., by using "ratio-dependent predation". They argued that a predator will never interact with all of the individuals of the whole prey population, but only with the prey in its own neighborhood (or territory). For territorial predators it is obvious that the predator can only catch those prey individuals that are located in the territory, and, if the prey are uniformly distributed over the territories, one can use the number of prey per predator, i.e., the ratio R/N, for the number of prey available for each predator.

Arditi & Ginzberg assumed that a predator can only see $\hat{R} = R/N$ prey, and that the feeding

efficiency on this subpopulation of the prey obeys a Holling type II functional response, i.e.,

$$f(\hat{R},N)=\frac{a\hat{R}}{h+\hat{R}} \quad \text{or} \quad f(R,N)=\frac{aR/N}{h+R/N}=\frac{aR}{hN+R}\ , \tag{7.1}$$

which defines the ratio-dependent predator prey model

$$\begin{aligned}\frac{\mathrm{d}R}{\mathrm{d}t} &= rR(1-R/K)-\frac{aRN}{hN+R}\\ \frac{\mathrm{d}N}{\mathrm{d}t} &= \frac{caRN}{hN+R}-dN\ ,\end{aligned} \tag{7.2}$$

when one assumes that the predator birth rate is proportional to its consumption. To study the dimensions of the parameters we test the functional response for a large prey population:

$$\lim_{R\to\infty}\ \frac{aR}{hN+R}=\lim_{R\to\infty}\ \frac{a}{hN/R+1}=a\ , \tag{7.3}$$

which demonstrates that the parameter a has the simple interpretation of the maximum number of prey consumed per predator. One can therefore define the fitness as $R_0=ca/d$.

The predator nullcline is computed by setting $\mathrm{d}N/\mathrm{d}t=0$

$$N=0 \quad \text{or} \quad N=\frac{ca-d}{dh}\ R=\frac{R_0-1}{h}\ R\ , \tag{7.4}$$

which shows that the predator nullcline is a diagonal line through the origin with slope $(R_0-1)/h$. Note that it is strange because small predator populations start to grow at infinitely small prey densities (i.e., $R^*=0$). For the prey nullcline one can employ the graphical construction method, by sketching the growth and predation terms as a function of the prey density R (see Fig. 7.1). The logistic growth term delivers the same parabola as before (with derivative r in the origin). The predation term is a family of functions, $aRN/(hN+R)$, depending on both N and R. For the slope around $R=0$ one computes

$$\partial_R\ \frac{aRN}{hN+R}=\frac{aN}{hN+R}-\frac{aRN}{(hN+R)^2} \quad \text{which for } R=0 \text{ yields} \quad \partial_R=\frac{a}{h}\ . \tag{7.5}$$

To compute the maximum of the predation terms one takes

$$\lim_{N\to\infty}\ \frac{aNR}{hN+R} \quad = \quad \frac{a}{h}\ R\ , \tag{7.6}$$

and observes that for large numbers of predators the predation terms approach a diagonal line through the origin, that has the same slope as the predation terms with lower numbers of predators have in the origin. Because the predator terms have a maximum slope a/h there are two possibilities:

1. $a/h<r$ for which the predation curves start below the parabolic growth curve, and therefore can intersect only once (see Fig. 7.1a), and
2. $a/h>r$ which means that the predation terms start above the parabola, and thanks to their saturated form, can intersect twice (see Fig. 7.1b).

Since the total consumption increases with a/h, the first case is called the "limited predation" case. For large predator densities in the limited predation situation, the predation curves intersect the parabola at approximately the same prey density. This prey density therefore defines a vertical asymptote in the nullcline of the prey (see Fig. 7.2a). Note that the position of the asymptote can easily be computed from $(a/h)R=rR(1-R/K)$. By constructing the graphical Jacobian from the local vector field one can see that the non-trivial steady state is always stable:

$$J=\begin{pmatrix}-\alpha & -\beta\\ \gamma & -\delta\end{pmatrix} \quad \text{with} \quad \mathrm{tr}J=-\alpha-\delta<0 \quad \text{and} \quad \det J=\alpha\delta+\beta\gamma>0\ . \tag{7.7}$$

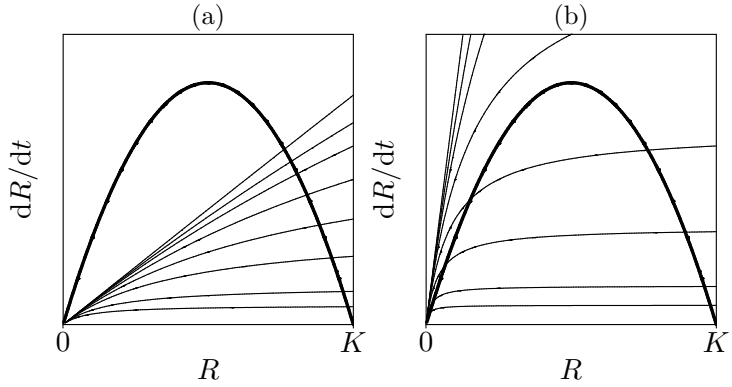

Figure 7.1: The nullcline construction for the ratio dependent model of Eq. (7.2).

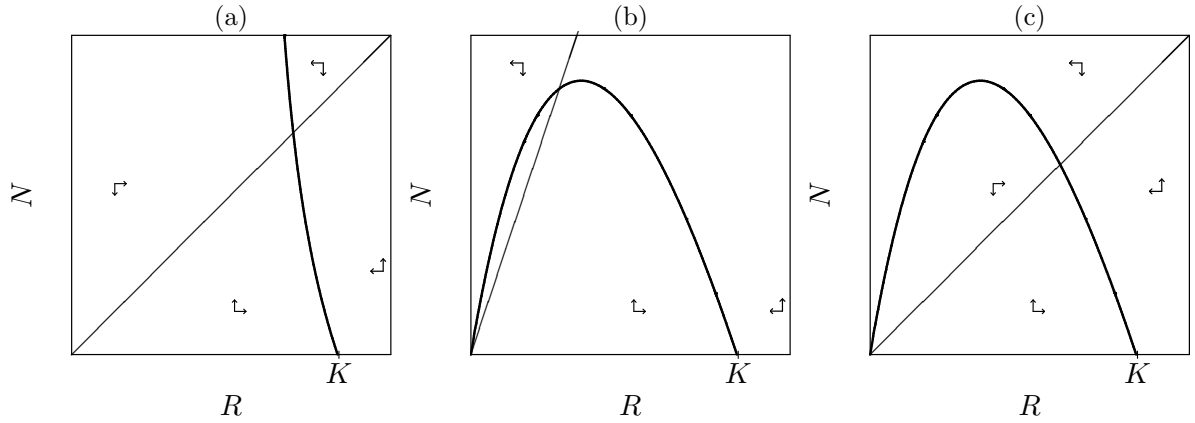

Figure 7.2: The three qualitatively different phase spaces of the ratio-dependent predator prey model.

In the second case a parabolic shape emerges when the prey nullcline is constructed (see Fig. 7.2b & c). The diagonal predator nullcline can intersect on the left or on the right of the top. When the intersection is on the right side of the top the graphical Jacobian is the same as above for the limited predation case:

$$J = \begin{pmatrix} -\alpha & -\beta \\ \gamma & -\delta \end{pmatrix} \quad \text{with} \quad \mathrm{tr}(J) = -\alpha - \delta < 0 \quad \text{and} \quad \det(J) = \alpha\delta + \beta\gamma > 0 \ . \tag{7.8}$$

which implies that the steady state is stable. Left of the top the graphical Jacobian is

$$J = \begin{pmatrix} \alpha & -\beta \\ \gamma & -\delta \end{pmatrix} \quad \text{with} \quad \mathrm{tr}J = \alpha - \delta \ . \tag{7.9}$$

The sign of the trace remains unestablished, and one cannot tell if the state is stable. Numerical analysis has shown that the steady state can be unstable, and, if so, that the behavior is a stable limit cycle.

A feature of the ratio-dependent model is that the steady state densities of both the prey and the predator increase with enrichment (i.e., when K is increased). This is a simple consequence of the diagonal prey nullcline. Additionally, enrichment does not lead to oscillations because in the limited predation case, the steady state is always stable, whatever the value of K. Indeed, one cannot leave the limited predation case by just increasing K (i.e., K is not part of the $a/h < r$ condition). For the other case, where oscillations are theoretically possible (Fig. 7.2c), it has been shown that one also cannot destabilize the stable steady state in Fig. 7.2c by merely increasing the carrying capacity (Huisman & De Boer, 1997).

Although the model seems elegantly simple it has its problems. This was already indicated by the predator nullcline that runs through the origin: the model has no minimum prey density required for predator growth. The reason is that at low predator densities the ratio R/N will become infinite, which indeed allows small predator populations to grow on very small prey populations. This is not only biologically unreasonable, but can also lead to very strange limit cycle behavior (Abrams, 1994).

7.2 Developing a better model

To learn what went wrong with the ratio-dependent model we will start all over again and derive a model ourselves for the situation where the prey population is distributed uniformly over the territories of the predators. Visualize a large habitat that by far exceeds the maximum territory size of a single predator. Let the total prey and predator population sizes in this habitat be defined by R and N, respectively. When the predator density is high, the total area is equally divided into relatively small territories, leading to the ratio-dependent model where the number of available prey per predator is $\hat{R} = R/N$. When the predator density is low, each predator occupies a preferred territory of some maximum size. Letting this size be the fraction α of the total area, each predator is expected to have $\hat{R} = \alpha R$ prey in its territory. Combining the two, the actual number of available prey per predator can be written as $\hat{R} = \min(\alpha R, R/N) = R\min(\alpha, 1/N)$ which has a discontinuity at $N = 1/\alpha$ where the preferred territory size equals the size obtained by a fair sharing of the total area.

Knowing the number of prey that each predator can feed upon, one can rewrite the normal Monod saturated predator prey model as

$$\begin{aligned} \frac{\mathrm{d}R}{\mathrm{d}t} &= rR(1-R/K) - \frac{a\hat{R}N}{h+\hat{R}} \\ \frac{\mathrm{d}N}{\mathrm{d}t} &= \frac{ca\hat{R}N}{h+\hat{R}} - dN \ , \end{aligned} \tag{7.10}$$

where $\hat{R} = R\,\min(\alpha, 1/N)$. Because the model is discontinuous when $N = 1/\alpha$, one studies the model separately for the two cases. For low numbers of predators, i.e., when $N \leq 1/\alpha$, the territory size is at its maximum, and the number of prey per territory is $\hat{R} = \alpha R$. Since this remains proportional to the global prey density, R, and one obtains the normal Holling type II model:

$$\begin{aligned} \frac{\mathrm{d}R}{\mathrm{d}t} &= rR(1-R/K) - \frac{aRN}{h'+R} \\ \frac{\mathrm{d}N}{\mathrm{d}t} &= \frac{caRN}{h'+R} - dN \ , \end{aligned} \tag{7.11}$$

where $h' = h/\alpha$. This implies that one expects the normal nullclines of Fig. 6.2 whenever $N \leq 1/\alpha$. For high predator densities, each predator is expected to have $\hat{R} = R/N$ prey in its territory. This corresponds to the ratio-dependent model, and one obtains Eq. (7.2), which means that for $N > 1/\alpha$ one also expects the nullclines of Fig. 7.2.

At the line $N = 1/\alpha$ in the phase space the models have to be identical. On this line the nullclines have to merge, and they switch from one case into the other (see Fig. 7.3). The main difference between our own model and the ratio-dependent model is that the predator nullcline now defines a "minimum prey density" that a predator requires for survival. Our own model

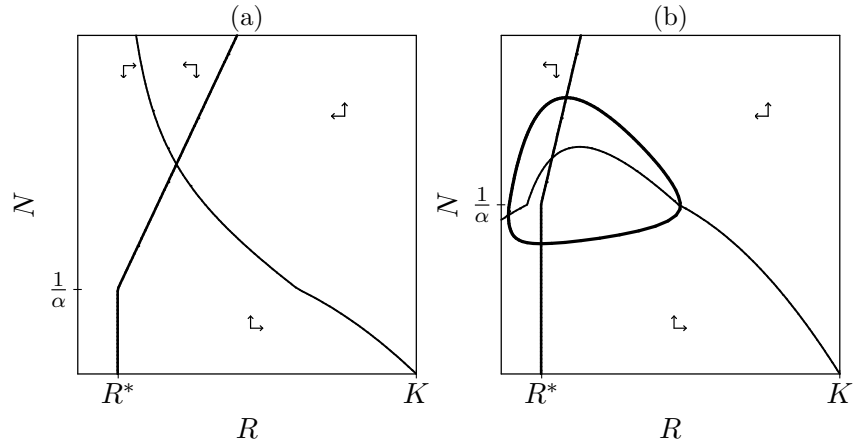

Figure 7.3: The two different phase spaces of a territorial predator prey model. Panel (a) reflects a limited predation situation and Panel (b) the case with more intense predation. In both Panels $R^* = \frac{h'}{R_0 - 1}$.

therefore no longer suffers from the artificial properties of the ratio-dependent model (Abrams, 1994), and we have learned that these problems were all due to the simplifying assumption that all prey are shared equally by the predators even if there are only very few predators.

7.3 Beddington functional response

The ratio-dependent functional response is just one example of the more general predator dependent functional responses (Abrams, 1994). For cases where predators compete directly for catching prey one can phenomenologically extend a saturated functional response with a term by which the predators increase the saturation constant, e.g.,

$$f(R, N) = \frac{aR}{h + eN + R} \ , \tag{7.12}$$

which is known as the Beddington (1975) functional response, and which for $e = 0$ is identical to the Monod saturated functional response. The parameter e defines the strength of the competition between the predators (note that setting $e < 0$ would deliver a function where predators help each other in catching prey). For a large prey population the Beddington function approaches

$$\lim_{R \to \infty} \ \frac{aR}{h + eN + R} = a \ , \tag{7.13}$$

which shows that the interpretation of a remains the maximum number of prey a predator can eat per unit of time. The corresponding Beddington model is written as

$$\begin{aligned} \frac{\mathrm{d}R}{\mathrm{d}t} &= rR(1 - R/K) - \frac{aRN}{h + eN + R} \\ \frac{\mathrm{d}N}{\mathrm{d}t} &= \frac{caRN}{h + eN + R} - dN \ . \end{aligned} \tag{7.14}$$

The predator nullcline is obtained by setting $\mathrm{d}N/\mathrm{d}t = 0$ and finding the solutions

$$N = 0 \quad \text{and} \quad N = \frac{ca - d}{de} \ R - \frac{h}{e} = \frac{R_0 - 1}{e} \ R - \frac{h}{e} \ . \tag{7.15}$$

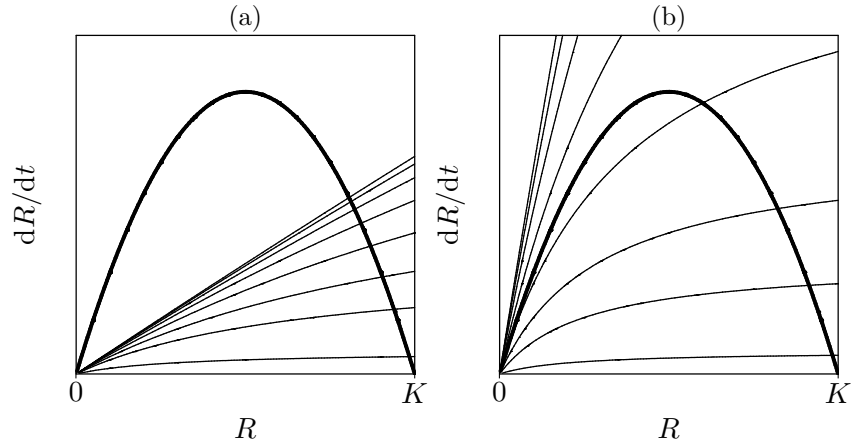

Figure 7.4: The two qualitatively different nullcline constructions of the Beddington predator prey model. In Panel (a) we have set $a/e < r$ and in (b) we consider $r < a/c$

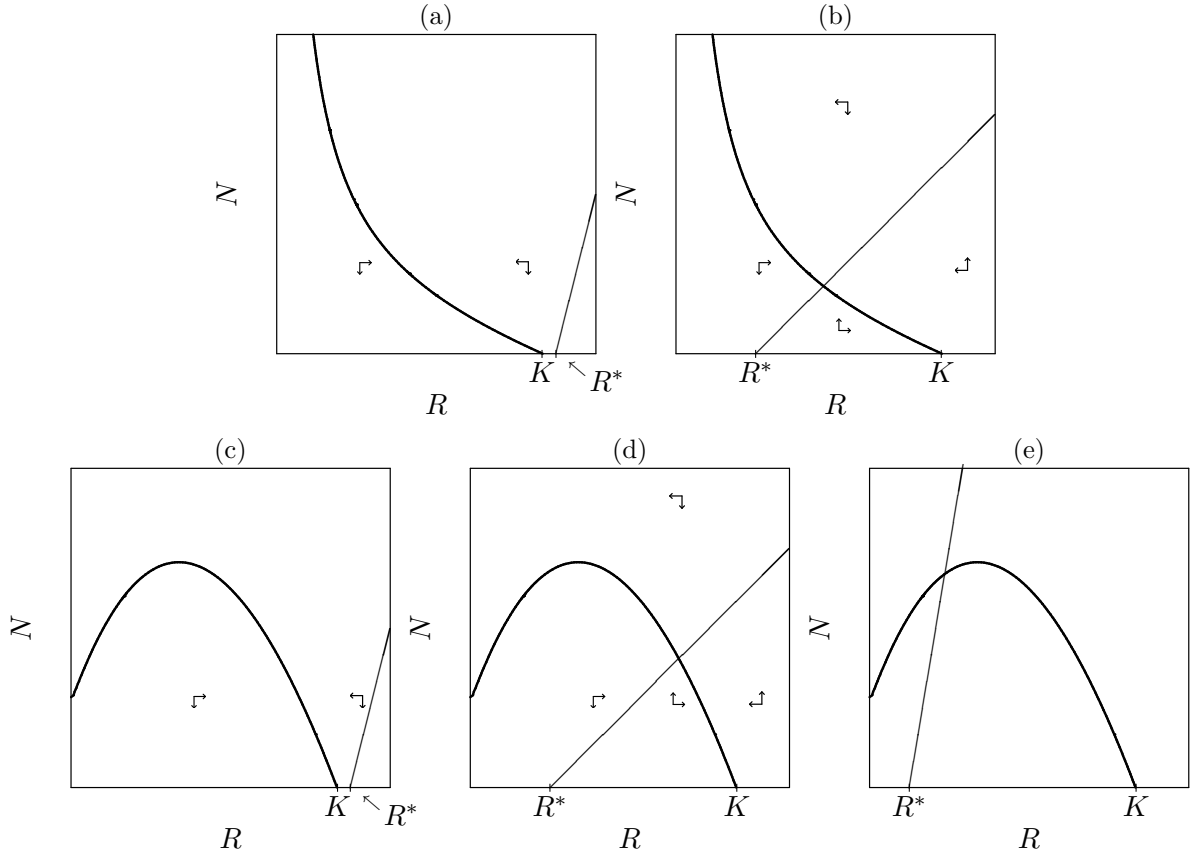

Figure 7.5: The five qualitatively different phase spaces of the Beddington predator prey model, where the critical prey density for net predator growth, $R^* = \frac{h}{R_0 - 1}$.

The last expression defines a line with slope $(R_0 - 1)/e$ that intersects the horizontal axis at $R = h/(R_0 - 1)$. The predator nullcline is therefore a slanted line with the same minimal prey density $R^* = h/(R_0 - 1)$ as the Monod saturated model.

The prey nullcline can again be found by graphical construction. Plotting the predation term $aRN/(h + eN + R)$ as a function of R defines a family of curves depending on the predator density N. The slope of these functions in the origin is found from the derivative with respect

to R:

$$\partial_R \frac{aRN}{h+eN+R} = \frac{aN}{h+eN+R} - \frac{aRN}{(h+eN+R)^2} \quad \text{which for } R=0 \text{ yields} \quad \frac{aN}{h+eN} . \quad (7.16)$$

The slope in the origin therefore increases with the predator density. For large numbers of predators the predation term approaches

$$\lim_{N\to\infty} \frac{aRN}{h+eN+R} \quad = \quad \frac{a}{e} R . \quad (7.17)$$

Because the predation functions approach the slanted asymptote with slope a/e, one again has to consider two cases. If $a/e < r$ the predation functions will intersect the logistic parabola only once. One therefore obtains a prey nullcline with a vertical asymptote (see Fig. 7.4 and Fig. 7.5), which is the limited predation situation. When $a/e \simeq r$, this vertical asymptote can disappear allowing the prey nullcline to intersect the vertical axis (not shown). If $a/e > r$ there will be one intersection point at low predator densities, two intersections at intermediate numbers, and no intersection points at high predator numbers. This yields a truncated "parabola" similar to that of the Monod saturated model. Because the predator nullcline can intersect either on the left of the maximum, or on the right side, one obtains two qualitatively different phases spaces (see Fig. 7.5d & e).

The Beddington model therefore has the two limited predation situations depicted in the top row of Fig. 7.5. The stability of the steady states is similar to those of the ratio dependent model, i.e., the steady state is always stable in Fig. 7.5b. The bottom row of the figure depicts the three $a/e > r$ situations. When the predator nullcline intersects at the right side of the maximum of the prey nullcline the equilibrium is stable. The sign of the trace in Fig. 7.5e cannot be determined from the vector field, but the nullclines do intersect unstable section of the prey nullcline. Numerical analysis confirms that the steady state can be unstable, and that the model behavior approaches a stable limit cycle in this situation. Increasing the carrying capacity to study enrichment, one can destabilize the system by moving from a phase depicted in panel (d) to the one depicted in (e). This was not possible in the ratio dependent model (Huisman & De Boer, 1997). Because the Beddington model has a minimum prey density of $R^* = h/(R_0 - 1)$, one also has the two "poor" situations of Panels (a) and (c), where the predator cannot be maintained (because $K < R^*$). These were also absent from the ratio dependent model.

7.4 Summary

Predator dependent functional responses forces one to also consider limited predation phase spaces with a steady state that is necessarily stable. Oscillations and a Paradox of Enrichment are easily recovered in the non-limited predation situations. The ratio dependent model is just one, somewhat unfortunate, example of a predator dependent response (Abrams, 1994).

7.5 Exercises

Question 7.1. Wolves
Wolves hunt in packs and help each other catch prey (this is also true for several other predator species, e.g., spoonbills).

a. Write a model for this situation using a functional response with $\partial_N f(R, N) > 0$.
b. Study the model by phase plane analysis. (You will probably require `grind.R`).

Question 7.2. Saturation in predators
Sometimes there is a maximum rate at which prey can be killed by the predators. An example is susceptible hosts that are infected by infected individuals. One would then write something like

$$\frac{\mathrm{d}R}{\mathrm{d}t} = rR(1 - R/K) - aRf(N) \quad \text{where} \quad f(N) = \frac{N}{h + N} \ , \tag{7.18}$$

and where a is the maximum death rate of the prey R when there is an infinite predator population.
a. Sketch the nullclines of this model.
b. Verify these with `grind.R`.

Chapter 8

Food chain models

Ecological food webs typically contain several layers where the consumers eating from the bottom resource layer are the prey of another predator. The predator prey models discussed above can easily be extended with a "top predator" that lives off the predator population N. Doing so one obtains a food chain model of three species. Strangely, the steady states of such a food chain depend strongly on its length. The steady state properties of food chains with an even length are very different from those with an odd length (Arditi & Ginzburg, 1989; Abrams, 1994). Although this seems strange, there are experimental data from bacterial food chains confirming these predictions from the models (Kaunzinger & Morin, 1998).

8.1 A 3-dimensional food chain

Extending the Lotka Volterra predator prey model with a top-predator T is straightforward, e.g.,

$$\frac{\mathrm{d}R}{\mathrm{d}t} = [r(1-R/K) - bN]R \ , \ \frac{\mathrm{d}N}{\mathrm{d}t} = [bR - d - cT]N \quad \text{and} \quad \frac{\mathrm{d}T}{\mathrm{d}t} = [cN - e]T \ . \qquad (8.1\text{a,b,c})$$

This simple model has several steady states, and we will study what happens when the carrying capacity, K, of the resource is increased. When the prey is alone, i.e., when $N = T = 0$, one obtains $\bar{R} = K$ from Eq. (8.1)a. This carrying capacity is a measure of the total amount of nutrients available in the ecosystem. At low values of the carrying capacity, there are not enough nutrients to maintain the predator (i.e., $R^* = d/b > K$), and the predator can only exist if its $R_0 > 1$, which means that $bK/d > 1$. If, after increasing K, the predator has successfully invaded, the new steady state (with still $T = 0$) is

$$\bar{R} = \frac{d}{b} \quad \text{and} \quad \bar{N} = \frac{r}{b}\left(1 - \frac{d}{bK}\right) = \frac{r}{b}\left(1 - \frac{1}{R_0}\right) \ . \qquad (8.2)$$

Note that the previous state $(\bar{R}, \bar{N}, \bar{T}) = (K, 0, 0)$ still exists, but has become unstable because $\mathrm{d}N/\mathrm{d}t > 0$ in the neighborhood of that state.

Similarly, the top-predator can only invade when $R_0' = c\bar{N}/e > 1$. Because $\bar{N}$ increases as a function of K, and approaches a maximum $\bar{N} = r/b$, the fitness of the top-predator can be defined as $R_0' = \frac{cr}{be}$. The top-predator can only invade when the carrying capacity K is

sufficiently large, and $R_0' > 1$. When $T > 0$ the steady state of the prey and predator is

$$\bar{N} = \frac{e}{c} \quad \text{and} \quad \bar{R} = K\left(1 - \frac{be}{rc}\right) , \tag{8.3}$$

where we re-observe the parameter condition $R_0' = \frac{cr}{be} > 1$.

Summarizing, we observe that when the carrying capacity is increased the resource is first proportional to K, it is independent of K when the food chain has an even length, and becomes proportional to K again when the food chain has an odd length of three species.

8.2 Summary

Whether the resource density increases with its carrying capacity depends on the length of the food chain. This is because the whole food chain determines from which equation one solves the steady state densities.

8.3 Exercises

Question 8.1. Nullclines
Sketch the 3-dimensional nullclines of Eq. (8.1) for the three situations considered above.

Question 8.2. Kaunzinger
Read the paper by Kaunzinger & Morin (1998).

a. Compute the steady state of the top-predator of Eq. (8.1) to study whether it depends on the carrying capacity.

b. Sketch how in the Lotka Volterra model of this chapter the prey and the two predators increase with the carrying capacity of the prey (i.e., their productivity).

c. Compare that to their Fig. 1: are the figures exactly the same? How important are these differences?

d. The authors claim that the prey increases somewhat with the productivity in the 2-dimensional food chain. How would you change the model to account for that result?

Question 8.3. Chaos
A simple system of a prey species R eaten by a predator N, eaten by a top-predator T can have a chaotic attractor (Hogeweg & Hesper, 1978; Hastings & Powell, 1991). Consider the following system with two Holling type II functional response functions

$$\frac{\mathrm{d}R}{\mathrm{d}t} = R(1-R) - c_1 N f(R) ,$$

$$\frac{\mathrm{d}N}{\mathrm{d}t} = -a_N N + c_1 N f(R) - c_2 T g(N) ,$$

$$\frac{\mathrm{d}T}{\mathrm{d}t} = -a_T T + c_2 T g(N) ,$$

where

$$f(R) = \frac{R}{1 + b_1 R} \quad \text{and} \quad g(N) = \frac{N}{1 + b_2 N} .$$

Hastings & Powell (1991) studied this system for the parameters $2 \leq b_1 \leq 6.2$, $c_1 = 5$, $c_2 = 0.1$, $b_2 = 2$, $a_N = 0.4$, en $a_T = 0.01$. For biological reasons the time scale of the interaction between N and T was made slower than that between R and N, i.e., $a_N \gg a_T$. This model is available as the file `chaos.R`.

a. Sketch with pencil and paper the phase space of R and N. Do you expect oscillations for their parameters in the absence of the top-predator T?

b. Compute the expression of the $\mathrm{d}T/\mathrm{d}t = 0$ nullcline, and sketch that line in the phase space of **a**. Do you expect T to invade?

c. Sketch the nullclines with `grind.R` and see how they match those sketched with pencil and paper.

d. Vary the parameter b_1 to observe how the model behavior changes (see the file `chaos.R`).

e. Do this with and without noise on one of the parameters.

Question 8.4. Detritus

In a closed ecosystem nutrients should cycle through a food chain and become available again when prey, predators, and top-predators die and decompose. One could write that the total amount of "free" nutrients is given by $F = K - R - N - T$, where K is the total amount of nutrients in the system. Study how in this system with recycling nutrients the nullclines, and the behavior of the system, change when the amount of nutrients, K, is increased.

Chapter 9

Resource competition

Competition for resources like nutrients, food, light, and/or space is the most obvious form of competition in ecosystems. In this chapter we derive resource competition models from the predator prey models developed in the previous chapters. We have already seen that the population size of predators feeding on some resource is naturally limited by the depletion of the prey population. The consumption of the resource therefore delivers an indirect form of specific competition between the predators. When studying two populations that are feeding on a resource that is not taken into account, one is bound to find interspecific competition between the consumer populations.

Following the basic theme of this book we will develop models for resource competition ourselves from the predator prey models that we have learned to understand in previous chapters. In most cases we will not end up with the "classical" Lotka Volterra competition equations, that are based upon simple mass action interaction terms between the competitors. We will derive that two species using the same resource cannot coexist, and derive conditions determining which species will outcompete the other (and learn that this need not be the species with the largest carrying capacity). This illustrates the importance of deriving models, rather than copying them from the textbooks.

First, consider the following model for two consumers N_1 and N_2 of a resource R

$$\frac{\mathrm{d}R}{\mathrm{d}t} = s - dR - c_1RN_1 - c_2RN_2 \ , \tag{9.1}$$

$$\frac{\mathrm{d}N_1}{\mathrm{d}t} = \Big(\frac{\beta_1 c_1 R}{h_1 + c_1 R} - \delta_1\Big)N_1 = \Big(\frac{\beta_1 R}{H_1 + R} - \delta_1\Big)N_1 \ , \tag{9.2}$$

$$\frac{\mathrm{d}N_2}{\mathrm{d}t} = \Big(\frac{\beta_2 c_2 R}{h_2 + c_2 R} - \delta_2\Big)N_2 = \Big(\frac{\beta_2 R}{H_2 + R} - \delta_2\Big)N_2 \ , \tag{9.3}$$

where $H_i = h_i/c_i$, and the c_iR terms reflect the amount of resource eaten per consumer per unit of time (say per day), and where this consumption translates into a consumer birth rate by a saturation function (β_i is the maximum birth rate, and the birth rate is half maximal when $c_iR = h_i$).

The carrying capacity of the resource is found by setting $N_1 = N_2 = 0$ and solving $\mathrm{d}R/\mathrm{d}t = 0$ to obtain that $\bar{R} = s/d$. Since the birth rates are saturation functions of the consumption rate we can define the fitness of both consumers as $R_{0_i} = \beta_i/\delta_i$, and we can define R_i^* as the minimal resource density required required for growth of the consumers (Tilman, 1980, 1982), by solving

$\mathrm{d}N_i/\mathrm{d}t = 0$ for R, i.e.,

$$R_i^* = \frac{h_i}{c_i(R_{0_i} - 1)} = \frac{H_i}{R_{0_i} - 1} \ . \tag{9.4}$$

The consumer requiring the lowest resource density, R_i^*, is expected to win the competition because the other consumer can not maintain itself at this density (Tilman, 1980, 1982). Importantly, this simple criterion for competitive exclusion is independent of the form of the resource equation. From the R_i^* expression in Eq. (9.4) we read that species with the highest R_{0_i}, and the lowest ratio, H_i, of resource requirements over consumption, is expected to exclude the other species.

To study how resource competition shapes the interaction between the two competitors, one can make a quasi steady state (QSS) assumption for the resource, i.e.,

$$\frac{\mathrm{d}R}{\mathrm{d}t} = 0 \quad \text{giving} \quad \hat{R} = \frac{s}{d + c_1N_1 + c_2N_2} \ . \tag{9.5}$$

Substitution of $\hat{R}$ into the consumer equations gives

$$\frac{\mathrm{d}N_i}{\mathrm{d}t} = N_i\Big(\frac{\beta_i s}{s + H_i(d + c_iN_i + c_jN_j)} - \delta_i\Big) = N_i\Big(\frac{b_i}{1 + N_i/k_i + N_j/k_j} - \delta_i\Big) \ , \tag{9.6}$$

where $H_i = h_i/c_i$, $i, j \in \{1, 2\}$, and b_i, k_i, and k_j are complicated combinations of many parameters (i.e., $b_i = \beta_i c_i s/(c_i s + h_i d)$ and $k_i = c_i h_i/(c_i s + h_i d)$). The latter simplified form in Eq. (9.6) reveals that this is an extension of one of the density dependent birth models in Chapter 4, with an inverse Hill function $f(N) = 1/(1 + N/k)$ describing the effect of the population density on the *per capita* birth rate. The "carrying capacity", K_i, of each consumer can be found by setting $N_j = 0$ and solving $\mathrm{d}N_i/\mathrm{d}t = 0$ from Eq. (9.6)

$$K_i = \frac{s}{h_i}\Big(R_{0_i} - 1\Big) - \frac{d}{c_i} = \frac{s}{c_i R_i^*} - \frac{d}{c_i} \ , \tag{9.7}$$

i.e., the best competitor with the lowest R_i^* tends to have the highest carrying capacity.

To sketch the $\mathrm{d}N_1/\mathrm{d}t = 0$ nullcline one solves N_2 from $\mathrm{d}N_1/\mathrm{d}t = 0$ in Eq. (9.6), to obtain that $N_1 = 0$ and

$$N_2 = \frac{s}{h_1}\frac{c_1}{c_2}\ (R_{0_1} - 1) - \frac{d}{c_2} - \frac{c_1}{c_2}N_1 = \frac{s}{c_2 R_1^*} - \frac{d}{c_2} - \frac{c_1}{c_2}N_1 \ , \tag{9.8}$$

which is a diagonal line with slope $-c_1/c_2$ intersecting the vertical axis at $N_2 = \frac{s}{c_2 R_1^*} - \frac{d}{c_2}$; see Fig. 9.1a. Similarly, for the $\mathrm{d}N_2/\mathrm{d}t = 0$ nullcline one solves N_2 from $\mathrm{d}N_2/\mathrm{d}t = 0$ in Eq. (9.6), and will obtain that $N_2 = 0$ and

$$N_2 = \frac{s}{h_2}\ (R_{0_2} - 1) - \frac{d}{c_2} - \frac{c_1}{c_2}N_1 = \frac{s}{c_2 R_2^*} - \frac{d}{c_2} - \frac{c_1}{c_2}N_1 \ , \tag{9.9}$$

which intersects the vertical axis at the carrying capacity of N_2, and the horizontal axis at $N_1 = \frac{s}{c_1 R_2^*} - \frac{d}{c_1}$; see Fig. 9.1a.

Thus, the nullclines are two parallel lines differing in the consumption, c_i, requirement, h_i, and R_0 parameters. From intersections with the axes in Fig. 9.1a one can see that the heavy $\mathrm{d}N_1/\mathrm{d}t = 0$ nullcline is located at the top just because $R_1^* < R_2^*$, which indeed was the criterion for N_1 being the best competitor. Although by Eq. (9.7) the carrying capacity decreases with R_i^*, the best competitor need not be the species with the largest carrying capacity because the carrying capacity is also inversely related to the consumption rate, c_i (see the exercises).

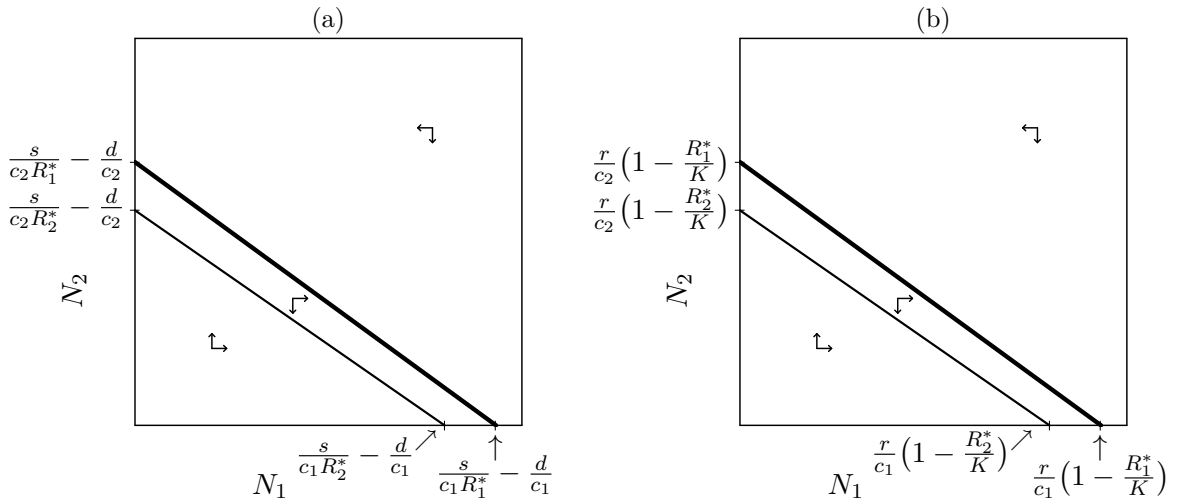

Figure 9.1: The 2-dimensional QSS nullclines of Eqs. (9.1) to (9.3) (a), and those of Eq. (9.10) with Eqs. (9.2) and (9.3) (b). In both Panels the heavy line is the $\mathrm{d}N_1/\mathrm{d}t = 0$ nullcline, because we chose $R_1^* < R_2^*$.

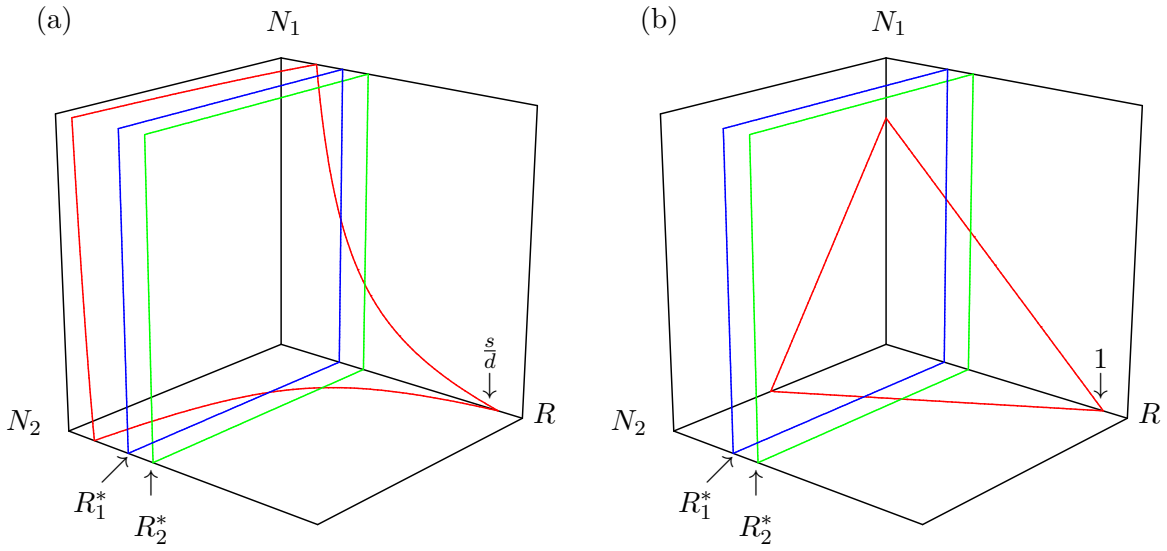

Figure 9.2: The 3-dimensional nullclines for two consumers on a non-replicating resource (a) and on a replicating resource (b).

We conclude that there cannot be an equilibrium in which the two species co-exist. This is the principle of "competitive exclusion": two consumers using the same resource exclude each other. This also defines the concept on an "ecological niche": species can only co-exist when they occupy different niches. Although the nullclines resemble the straight lines of a Lotka-Volterra competition model (see below), the underlying model that we have derived differs from the classical Lotka-Volterra competition model because the interaction terms are based upon declining Hill functions, rather than on mass action terms.

One can also consider the full 3-dimensional model by sketching its 3-dimensional nullclines (see Fig. 9.2a). The two nullclines of the consumers are easy to sketch because we have already computed that they are located at the critical resource densities R_i^*; see Fig. 9.2a. The consumer planes therefore again run parallel to each other, and cannot intersect in an equilibrium where

$dN_1/dt = dN_2/dt = 0$. This reconfirms the competitive exclusion result. The 3-dimensional nullcline of the resource can be drawn by separately considering the R versus N_1 plane for $N_2 = 0$, and the R versus N_2 plane for $N_1 = 0$ (see Fig. 9.2a). When both N_1 and N_2 are zero the resource population has the carrying capacity $\bar{R} = s/d$, which is the intersection point on the R-axis. When $N_2 = 0$ one obtains from Eq. (9.1) that $N_1 = s/(c_1R) - d/c_1$. This has a vertical asymptote $R = 0$, and a horizontal asymptote $N_1 = -d/c_1$ which is approached for $R \to \infty$. The $dR/dt = 0$ nullcline for $N_2 = 0$ therefore has the hyperbolic shape depicted in Fig. 9.2a. Since the same arguments apply for the plane where $N_1 = 0$, one finds a similar hyperbolic nullcline in the bottom plane of the phase space in Fig. 9.2a.

To test the stability of the steady states of a 3-dimensional phase space one has to resort to an invasion criterion. First consider the vector fields: $dR/dt > 0$ below its carrying capacity, and hence below the hyperbolic $dR/dt = 0$ nullcline. The vertical consumer nullclines correspond to the minimum resource density for predator growth. At the right side of the N_1-nullcline $dN_1/dt > 0$, and at the right side of the N_2-nullcline $dN_2/dt > 0$. The carrying capacity point of the resource is unstable in Fig. 9.2a because it is located above the consumer planes, i.e., both $dN_1/dt > 0$ and $dN_2/dt > 0$ when $R = s/d$. The intersection point of the N_2 and the R-nullcline is unstable because it is located on the right side of the N_1-nullcline, i.e., if N_1 were introduced in this 2-dimensional steady state it would grow and invade. Conversely, N_2 cannot invade in the R with N_1 equilibrium because locally $dN_2/dt < 0$. Since the 2-dimensional equilibrium of R with N_1 is stable, we conclude that N_1 excludes N_2 because its nullcline is located at a lower prey density. Because the resource is depleted to this minimal density this is sometimes called the pessimization principle (Mylius & Diekmann, 1995).

Finally, remain aware that this remains an equilibrium result. We have only shown that the two consumers cannot coexist in an equilibrium. Non-equilibrium co-existence is possible, and in one of the exercises you will study two consumers on one resource that co-exist thanks to their periodic or chaotic behavior (see Fig. 11.2).

9.1 Two consumers on a replicating resource

The previous section demonstrated that two consumers on a non-replicating resource are not expected to co-exist. Now consider the same two consumers on a resource replicating by logistic growth,

$$\frac{dR}{dt} = rR(1 - R/K) - c_1RN_1 - c_2RN_2 \ , \tag{9.10}$$

and use the same equations for the consumers (Eqs. 9.2 and 9.3). As we have not changed the consumer equations we know that the definitions of the critical resource density, R_i^*, and the fitness, R_{0_i}, remain the same, and that the species with the lowest resource requirement should be the winner. Because the two dN_i/dt equations have remained the same as those in the first model (see Eqs. 9.2 & 9.3), the predator nullclines in the 3-dimensional phase space remain the same two parallel planes (see Fig. 9.2b). This immediately reconfirms the competitive exclusion. To sketch the 3-dimensional nullcline of the resource, one derives that for $N_2 = 0$ the nullcline of the resource is a simple straight line, $N_1 = (r/c_1)[1 - R]$, that we know from the Lotka Volterra model. Similarly, for $N_1 = 0$ one obtains a straight line from $N_2 = r/c_2$ when $R = 0$ to $R = 1$ when $N_2 = 0$. The invasion criterion can be used in exactly the same way as in Fig. 9.2a to show that the species with the lowest resource requirement, R_i^*, wins.

To compare this model with the classical Lotka-Volterra competition model, we again make a

quasi steady state assumption for the resource, i.e.,

$$\hat{R} = 0 \quad \text{and} \quad \hat{R} = K - \frac{c_1 K}{r} N_1 - \frac{c_2 K}{r} N_2 \ , \tag{9.11}$$

and substituting the latter into Eqs. (9.2) and (9.3) yields

$$\frac{\mathrm{d}N_i}{\mathrm{d}t} = N_i \Big(\frac{\beta_i (r - c_i N_i - c_j N_j)}{r + r H_i / K - c_i N_i - c_i N_j} - \delta_i \Big) \ , \tag{9.12}$$

where $H_i = h_i / c_i$ and $i, j \in \{1, 2\}$. This is again not based upon the simple mass action interaction terms of classical Lotka-Volterra competition model (see Section 9.2). One may recognize the mass action terms of the Lotka-Volterra in the numerator, implying that this will resemble the Lotka-Volterra competition model when $r + r H_i / K \gg c_i N_i + c_i N_j$. The carrying capacity of the consumers is found by setting $N_j = 0$ and solving N_i from $\mathrm{d}N_i/\mathrm{d}t = 0$ in Eq. (9.12), i.e.,

$$\bar{N}_i = \frac{r}{c_i} \Big(1 - \frac{R_i^*}{K} \Big)$$

and the $\mathrm{d}N_1/\mathrm{d}t = 0$ nullcline is obtained by solving N_2 from Eq. (9.12)

$$N_2 = \frac{r}{c_2} \Big(1 - \frac{R_1^*}{K} \Big) - \frac{c_1}{c_2} N_1 \ ,$$

which is again a straight line with slope $-c_1/c_2$. Since the $\mathrm{d}N_2/\mathrm{d}t = 0$ nullcline has the same slope (not shown) we again find the (expected) parallel consumer nullclines of two consumers using the same resource (see Fig. 9.1b). Summarizing, we again find competition equations with interaction terms that are more complicated than mass action terms, but having linear nullclines resembling those of the Lotka-Volterra competition model. Note that we could have used a non-linear functional response for the consumption of resource in both models, and that this would have complicated the algebra, but that this would not have altered the conclusions on competitive exclusion as the R^* criterion is based upon the consumer equations only. A saturated function response can give rise to oscillations, however, and these may allow for non-equilibrium co-existence (see Chapter 11).

9.2 The Lotka-Volterra competiton model

The Lotka-Volterra competiton model is typically written as

$$\frac{\mathrm{d}N_1}{\mathrm{d}t} = r_1 N_1 \Big(1 - \frac{N_1}{K_1} - \frac{N_2}{C_1} \Big) \quad \text{and} \quad \frac{\mathrm{d}N_2}{\mathrm{d}t} = r_2 N_2 \Big(1 - \frac{N_1}{C_2} - \frac{N_2}{K_2} \Big) \ , \tag{9.13}$$

which basically extends the logistic growth model with a mass action competition term. To sketch the nullclines one solves N_2 from $\mathrm{d}N_i/\mathrm{d}t = 0$ in Eq. (9.13), i.e.,

$$N_2 = C_1 \Big(1 - \frac{N_1}{K_1} \Big) \quad \text{and} \quad N_2 = K_2 \Big(1 - \frac{N_1}{C_2} \Big) \ , \tag{9.14}$$

forming the classical straight nullclines running from $N_2 = C_1$ on the vertical axis to $N_1 = K_1$ on the horizontal axis for $\mathrm{d}N_1/\mathrm{d}t = 0$, and for $\mathrm{d}N_2/\mathrm{d}t = 0$ from $N_2 = K_2$ to $N_1 = C_2$. Since during resource competition the niche overlap with members of another species should be lower than that with conspecifics, two consumers on a single resource should require that $C_1 > K_1$ and $C_2 > K_2$. After scaling the carrying capacities to $K_1 = K_2 = 1$ one can see this means that the nullclines should not intersect (see below).

Note that we would obtained the mass action terms of the Lotka-Volterra model if we had written the consumer model of Eq. (9.2) and Eq. (9.3) as

$$\frac{\mathrm{d}N_1}{\mathrm{d}t} = \Big(\frac{c_1}{h_1}R - \delta_1\Big)N_1 \quad \text{and} \quad \frac{\mathrm{d}N_2}{\mathrm{d}t} = \Big(\frac{c_2}{h_2}R - \delta_2\Big)N_2 \ , \tag{9.15}$$

where the h_i constants define conversion rates, and had substituted the QSS of the replicating resource (Eq. (9.11)). In this simplified model the fitness is defined as $R_{0_i} = \frac{c_1 K}{h_1 \delta_1}$, and the critical resource density is defined as $R_i^* = \frac{h_1 \delta_1}{c_1}$, which is K/R_{0_i} (see Chapter 5). Hence we would have found that the winner with the lowest resource requirements necessarily has the largest fitness. However, since this simplified model is not easily extendable into competition for several resources, as one would obtain several independent "birth rates" in Eq. (9.15), e.g.,

$$\frac{\mathrm{d}N_1}{\mathrm{d}t} = \Big(\frac{c_{11}}{h_{11}}R_1 + \frac{c_{12}}{h_{12}}R_2 - \delta_1\Big)N_1 \ .$$

We therefore return to the saturated birth rates of Eq. (9.2) and Eq. (9.3) in the next section.

9.3 Two consumers on two resources

The previous two sections demonstrated that two consumers on one resource are expected to have a phase space with two parallel nullclines. However, in a phase space of two consumers on two resources, it should be possible to have intersecting nullclines. For instance, when each consumer specializes on one resource, there is no competition between the consumers, and the nullclines should be independent of each other, intersecting orthogonally in a stable co-existence point. Here we will again derive competition models from a consumer resource models to study under which conditions this steady state is expected to be stable.

Studying consumers using several resources one has to decide whether or not these resources are "essential", meaning that they cannot replace each other, or "substitutable", meaning that they can be added up into a total intake (Tilman, 1980, 1982). Let us first extend the model of Eq. (9.1) to Eq. (9.3) into a situation of two consumers sharing two substitutable resources, by defining birth rates depending on the summed resource intake,

$$\frac{\mathrm{d}R_1}{\mathrm{d}t} = s_1 - d_1 R_1 - c_{11} N_1 R_1 - c_{21} N_2 R_1 \ , \tag{9.16}$$

$$\frac{\mathrm{d}R_2}{\mathrm{d}t} = s_2 - d_2 R_2 - c_{12} N_1 R_2 - c_{22} N_2 R_2 \ , \tag{9.17}$$

$$\frac{\mathrm{d}N_1}{\mathrm{d}t} = \Big(\beta_1 \ \frac{c_{11}R_1 + c_{12}R_2}{h_1 + c_{11}R_1 + c_{12}R_2} - \delta_1\Big)N_1 \ , \tag{9.18}$$

$$\frac{\mathrm{d}N_2}{\mathrm{d}t} = \Big(\beta_2 \ \frac{c_{21}R_1 + c_{22}R_2}{h_2 + c_{21}R_1 + c_{22}R_2} - \delta_2\Big)N_2 \ , \tag{9.19}$$

where the $c_{ij}R_j$ terms are the *per capita* consumption rates, and the consumed resources contribute equally to the birth rate of each consumer. The saturation constants, h_i, define the density of consumed resources at which the birth rate is half-maximal. Since at low consumption rates the saturation functions approach $(c_{11}R_1 + c_{12}R_2)/h_1$ and $(c_{21}R_1 + c_{22}R_2)/h_2$, the saturation constants, h_1 and h_2, also play the role of a conversion factor from the resource to the consumer level.

Since the *per capita* birth and death rates of the consumers in Eqs. (9.18) and (9.19) only depend on the resource densities one can draw the $\mathrm{d}N_1/\mathrm{d}t = 0$ and the $\mathrm{d}N_2/\mathrm{d}t = 0$ nullclines in a phase

space defined by the two resources (see Fig. 9.3a). Such a picture is called a Tilman diagram (Tilman, 1980, 1982). These nullclines define the minimum amount of resources, (R_1^*, R_2^*), the consumers need to grow, and in Fig. 9.3(a) and (b), $\mathrm{d}N_1/\mathrm{d}t > 0$ or $\mathrm{d}N_2/\mathrm{d}t > 0$ above their nullclines. If, and only if, these nullclines intersect, there is a steady state resource density, (R_1, R_2), at which $\mathrm{d}N_1/\mathrm{d}t = \mathrm{d}N_2/\mathrm{d}t = 0$. To sketch the nullclines in the Tilman diagram we solve $\mathrm{d}N_1/\mathrm{d}t = 0$ and $\mathrm{d}N_2/\mathrm{d}t = 0$ for R_2, which gives the following expressions for the two consumer nullclines

$$R_2 = \frac{h_1}{c_{12}(R_{0_1} - 1)} - \frac{c_{11}}{c_{12}} R_1 \quad \text{and} \quad R_2 = \frac{h_2}{c_{22}(R_{0_2} - 1)} - \frac{c_{21}}{c_{22}} R_1 \ , \tag{9.20}$$

where $R_{0_i} = \beta_i/\delta_i$. Using the definition of the critical resource density, $R_{ij}^* = \frac{h_i}{c_{ij}(R_{0_i}-1)}$, we can simplify these consumer nullclines into $R_2 = R_{12}^* - \frac{c_{11}}{c_{12}} R_1$ and $R_2 = R_{22}^* - \frac{c_{21}}{c_{22}} R_1$, which defines two straight lines that may intersect when their slopes are unequal, i.e., when $\frac{c_{11}}{c_{12}} \neq \frac{c_{21}}{c_{22}}$, and when their four intersects with the axes, i.e., $R_2 = R_{12}^*, R_1 = R_{11}^*, R_2 = R_{22}^*$, and $R_1 = R_{21}^*$, respectively, also allow the nullclines to cross (see Fig. 9.3b).

When the species have the same diet, $c_{11} = c_{21}$ and $c_{12} = c_{22}$, the slopes of the nullclines will be two parallel lines, and the species will exclude each other. The species with the lowest resource requirements, R_{ij}^*, will have the lowest nullcline, and be the best competitor. Requiring low amounts of consumed resources, i.e., having a low h_i parameter, consuming a lot, i.e., having high c_{ij} parameters, and having a high R_0, all contribute to have low R_{ij}^*s and becoming the best competitor. Finally, when the species perfectly specialize on one resource, i.e., $c_{21} = c_{12} = 0$, the Tilman diagram will simplify to two perpendicular lines located at $R_1 = R_{11}^*$ and $R_2 = R_{22}^*$.

Finding an intersection between the consumer nullclines in a Tilman diagram does not guarantee that the consumers can co-exist because this is not necessarily a 4-dimensional steady state (as we have not required $\mathrm{d}R_1/\mathrm{d}t = \mathrm{d}R_2/\mathrm{d}t = 0$), and even if the intersection point corresponds to a steady state, the equilibrium could be unstable. To study the existence of the steady state we can again make a quasi steady state assumption for the resources and (numerically) plot the consumer nullclines in a conventional phase space defined by the consumer densities (see Fig. 9.3c and d). The QSSA consumer nullclines are complicated expressions that intersect the horizontal and vertical axis in the carrying capacities. For the stability analysis we formally have to consider the 4-dimensional Jacobian of the model (see below), but if the QSSA is realistic we can use the vector field in Fig. 9.3d to see that the steady state is expected to be stable.

For two consumers on two substitutable resources one can show by an intuitive argument that this state, if it exists, is indeed expected to be stable. Consider Fig. 9.3c where the nullclines fail to intersect and diminish the niche overlap by decreasing c_{12} and c_{21}. This will turn the upper $\mathrm{d}N_1/\mathrm{d}t = 0$ nullcline more vertical, and the lower $\mathrm{d}N_2/\mathrm{d}t = 0$ isocline more horizontal, as we know that when $c_{12} = c_{21} = 0$, they are perfectly vertical and horizontal lines at $N_1 = K_1$ and $N_2 = K_2$. At some value of the decreasing consumption rates the nullclines will intersect in the carrying capacity, K_1, of the winning species. This is a bifurcation point because for even lower values of c_{12} and c_{21} the nullclines intersect in a non-trivial steady state (see Fig. 9.3d), which is a stable node. Thus, two consumers on two substitutable resources can always coexist if their niche overlap is sufficiently small, as their non-trivial steady state is always expected to be stable. This will change when we consider essential resources, however.

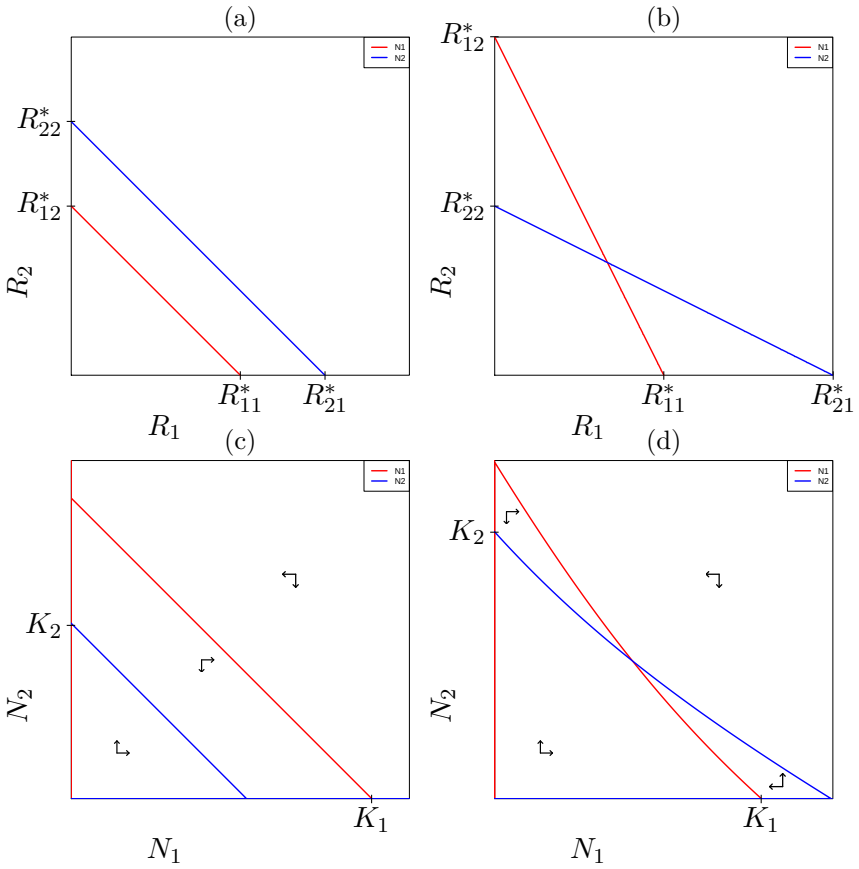

Figure 9.3: Consumer nullclines for a situation with two substitutable resources that are maintained by a source. Panels (a) and (b) at the top depict the nullclines of Eqs. (9.18) and (9.19) as function of the resource densities (these are Tilman diagrams), and Panels (c) and (d) at the bottom depict the consumer nullclines after making a QSSA, $\mathrm{d}R_1/\mathrm{d}t = \mathrm{d}R_2/\mathrm{d}t = 0$, for the resources. When the consumers have the same diet (Panels (a) and (c)) the nullclines fail to intersect, and giving N_1 an advantage by setting $h_1 < h_2$ (or, alternatively, $R_{0_1} > R_{0_2}$), the $\mathrm{d}N_1/\mathrm{d}t = 0$ nullcline is located at lower resource densities in Panel (a) and at higher consumer densities in Panel (c). When the consumers have a different diet (Panels (b) and (d), where $c_{12} < c_{11}$, $c_{21} < c_{22}$ and $h_1 = h_2$), the nullclines may intersect. The (curved) QSSA nullclines in Panel (d) suggest that this intersection point corresponds to a stable steady state (see the vector field). This figure was made with the model `additiveS.R`

9.4 Two Essential Resources

For "essential" resources that cannot be substituted for one another, one would write a model like

$$\frac{\mathrm{d}N_1}{\mathrm{d}t} = \left(\beta_1 \frac{c_{11}R_1}{h_{11}+c_{11}R_1} \frac{c_{12}R_2}{h_{12}+c_{12}R_2} - \delta_1\right)N_1 \ , \tag{9.21}$$

$$\frac{\mathrm{d}N_2}{\mathrm{d}t} = \left(\beta_2 \frac{c_{21}R_1}{h_{21}+c_{21}R_1} \frac{c_{22}R_2}{h_{22}+c_{22}R_2} - \delta_2\right)N_2 \ , \tag{9.22}$$

where by the multiplication of two saturation functions we require that both resources should be consumed in sufficient amounts. Fig. 9.4(a) and (b) depicts Tilman diagrams for this model. Note that we could again define ratios, $H_{ij} = h_{ij}/c_{ij}$, to illustrate that the consumer equations

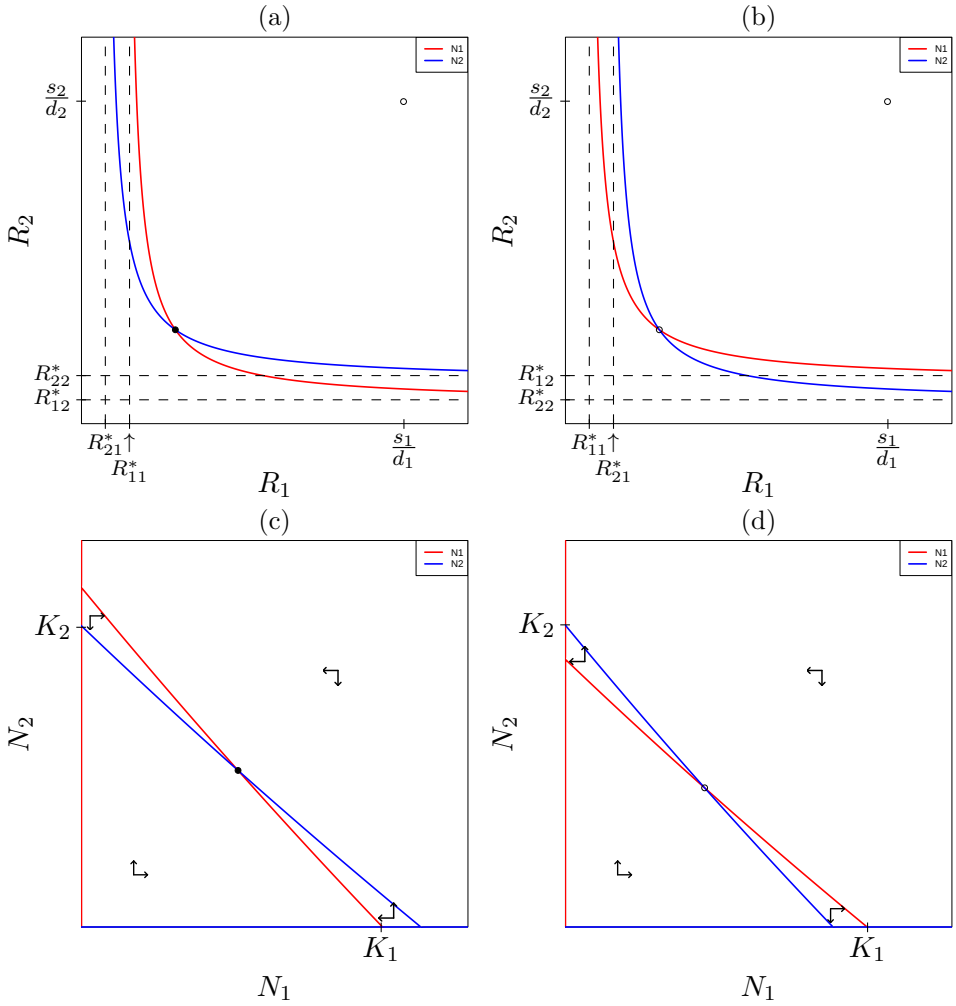

Figure 9.4: Consumer nullclines for a situation with two essential resources (that are maintained by a source) for a stable steady state (Panels (a) and (c)) and for an unstable steady state (Panels (b) and (d)). The panels at the top depict the nullclines of Eqs. (9.21) and (9.22) as function of the resource densities (these are Tilman diagrams). The dashed lines are asymptotes. The circle in the upper corners depicts the (unstable) steady state of the resources in the absence of consumers. The other bullets and circles reflects a stability of steady state with consumers. The panels at the bottom provide the nullclines of Eqs. (9.21) and (9.22) after making a QSSA for the resources (i.e., Eqs. (9.16) and (9.17)). This figure was made with the model `essentialS.R`.

only depend on the ratio of the requirement over the consumption, i.e.,

$$\frac{\mathrm{d}N_1}{\mathrm{d}t} = \Big(\beta_1 \frac{R_1}{H_{11}+R_1}\frac{R_2}{H_{12}+R_2} - \delta_1\Big)N_1 \quad \text{and} \quad \frac{\mathrm{d}N_2}{\mathrm{d}t} = \Big(\beta_2 \frac{R_1}{H_{21}+R_1}\frac{R_2}{H_{22}+R_2} - \delta_2\Big)N_2 \ .$$

The consumer nullclines in a phase spanned up by the two resources are hyperbolic functions with asymptotes defining the minimal resource densities these consumers require. These asymptotes can be found by setting $\mathrm{d}N_i/\mathrm{d}t = 0$ for $R_1 \to \infty$ or $R_2 \to \infty$, i.e., $R_1 = R^*_{11}, R_2 = R^*_{12}, R_1 = R^*_{21}$, and $R_2 = R^*_{22}$, respectively (see Fig. 9.4a and b). Whether or not the nullclines will intersect therefore depends on the R^*s, and the species with the lowest requirements, h_{ij}, the highest consumption rates, c_{ij}, and highest R_0 will have the lowest nullcline, and be the winner whenever the nullclines fail to intersect.

In all panels of Fig. 9.4 we have set $c_{11} > c_{12}$ and $c_{22} > c_{21}$, i.e., consumer one specializes

on resource one, and consumer two on resource two, and in Fig. 9.4(c) and (d) we have used resources that are maintained by a source (i.e., Eqs. (9.16) and (9.17)). In the stable situation of Fig. 9.4a and c we accordingly set $h_{11} > h_{12}$ and $h_{22} > h_{21}$, to let each species eat most of the resource it requires most (which would be "optimal" in an evolutionary sense (see the chapter by Tilman in (McLean & May, 2007))). We have made the unstable situation of Fig. 9.4(b) and (d) by setting $h_{11} = h_{12} = h_{21} = h_{22}$, which means that the first consumer competes more strongly with the second consumer that with itself because the second consumer eats more of resource two than consumer one. Apparently, the latter leads to an unstable steady state, and a situation where only one of the consumers survives. The initial condition will determine who persists, and hence this is called a "founder controlled" situation. Since the Tilman diagrams in Fig. 9.4(a) and (b) are much simpler than the QSSA nullclines in Panels (c) and (d), it would be much more efficient if one can read the stability of the steady state from the relative location of the consumer nullclines in the Tilman diagram. The next section will show how that can be done.

9.5 4-dimensional Jacobian

To formally study the stability of the steady state of these models one should study the Jacobian of the 4-dimensional system. Fortunately, this is feasible because this Jacobi matrix contains many zero elements. For instance, the Jacobian of the model with substitutable resource, i.e., Eqs. (9.16) to (9.19), can be written as

$$J = \begin{pmatrix} \partial_{R_1} R_1' & \dots & \partial_{N_2} R_1' \\ \vdots & \ddots & \\ \partial_{R_1} N_2' & \dots & \partial_{N_2} N_2' \end{pmatrix} = \begin{pmatrix} -d_1 - c_{11}\bar{N}_1 - c_{21}\bar{N}_2 & 0 & -c_{11}\bar{R}_1 & -c_{21}\bar{R}_1 \\ 0 & -d_2 - c_{12}\bar{N}_1 - c_{22}\bar{N}_2 & -c_{12}\bar{R}_2 & -c_{22}\bar{R}_2 \\ \Phi_1 c_{11} & \Phi_1 c_{12} & 0 & 0 \\ \Phi_2 c_{21} & \Phi_2 c_{22} & 0 & 0 \end{pmatrix} \tag{9.23}$$

where

$$\Phi_1 = \frac{\beta_1 h_1 \bar{N}_1}{(h_1 + c_{11}\bar{R}_1 + c_{12}\bar{R}_2)^2} \quad \text{and} \quad \Phi_2 = \frac{\beta_2 h_2 \bar{N}_2}{(h_2 + c_{21}\bar{R}_1 + c_{22}\bar{R}_2)^2}$$

Note that the two $\partial_{N_i} N_i'$ elements are zero because $\partial_{N_i} N_i'$ is the *per capita* growth rate, which is zero at steady state. The two $\partial_{N_j} N_i'$ elements are zero because the consumer equations do not contain the other consumer, and the two $\partial_{R_j} R_i'$ elements are zero because the resource equations do not contain the other resource. This Jacobian can be simplified into a matrix with the same structure of signs and zeros,

$$J = \begin{pmatrix} -\rho_1 & 0 & -\gamma_{11} & -\gamma_{21} \\ 0 & -\rho_2 & -\gamma_{12} & -\gamma_{22} \\ \phi_{11} & \phi_{12} & 0 & 0 \\ \phi_{21} & \phi_{22} & 0 & 0 \end{pmatrix} , \tag{9.24}$$

where ρ_i elements define the feedback of the resources onto themselves, the γ_{ij} elements define the *per capita* amounts of resources consumed, and the ϕ_{ij} terms define the contribution of resources to the growth of the consumer populations at steady state (Tilman, 1980). The characteristic equation of this Jacobi matrix can be obtained with Mathematica, and is defined as

$$\lambda^4 + a_3\lambda^3 + a_2\lambda^2 + a_1\lambda + a_0 = 0 , \tag{9.25}$$

where

$$a_3 = \rho_1 + \rho_2 , \quad a_2 = \phi_{11}\gamma_{11} + \phi_{21}\gamma_{12} + \phi_{12}\gamma_{21} + \phi_{22}\gamma_{22} + \rho_1\rho_2 ,$$

$a_1 = \phi_{12}\rho_1\gamma_{21} + \phi_{22}\rho_1\gamma_{22} + \phi_{11}\gamma_{11}\rho_2 + \phi_{21}\gamma_{12}\rho_2$ and $a_0 = (\gamma_{11}\gamma_{22} - \gamma_{12}\gamma_{21})(\phi_{11}\phi_{22} - \phi_{12}\phi_{21})$.

The steady state will be stable when all four solutions of the eigenvalues in Eq. (9.25) are negative. Fortunately, there is a general method to test this without having to solve this fourth-order polynomial. This is so-called Routh-Horwitz stability criterion on the n coefficients, a_i, of an n^{th} order polynomial (May, 1974; Tilman, 1980). One of the Routh-Horwitz criteria is that all parameters, a_i, in Eq. (9.25) should be positive (or all negative as one can multiply the equation with -1). Thanks to the many zeros in the Jacobi matrix we here have a simple situation where $a_3 > 0, a_2 > 0, a_1 > 0$, and only a_0 can be negative. Hence testing $a_0 > 0$ may reveal a biological insight into the criteria for co-existence of two consumers of two resources.

For substitutable resources, we know that the steady state can only exist if the two consumers have a different diet (see Fig. 9.3a). Therefore consider a case where consumer one specializes on resource one, and consumer two on resource two, i.e., $c_{11} > c_{12}$ and $c_{22} > c_{21}$ (see Fig. 9.3b). Spelling out the first term of the a_0 equation, we see that in this case

$$(\gamma_{11}\gamma_{22} - \gamma_{12}\gamma_{21}) = (c_{11}\bar{R}_1 c_{22}\bar{R}_2 - c_{12}\bar{R}_2 c_{21}\bar{R}_1) > 0 \ ,$$

because $c_{11}c_{22} > c_{12}c_{21}$. For the second term of the a_0 equation we observe in Eq. (9.23) that $\phi_{11} > \phi_{12}$ when $c_{11} > c_{12}$ and that $\phi_{22} > \phi_{21}$ when $c_{22} > c_{21}$. As a consequence

$$\phi_{11}\phi_{22} - \phi_{12}\phi_{21} > 0 \quad \text{and, hence} \quad a_0 > 0 \ ,$$

which fulfills this Routh-Horwitz criterion, allowing the steady state to be stable. We conclude that two consumers using two substitutable resources can co-exist, i.e., when their quasi steady state nullclines intersect, this steady state is expected to be stable (see Fig. 9.3c).

Although we here considered the case where the resources are maintained by a source, little changes when we write

$$\frac{\mathrm{d}R_1}{\mathrm{d}t} = r_1 R_1(1 - R_1/K_1) - c_{11}N_1R_1 - c_{21}N_2R_1 \ , \tag{9.26}$$

$$\frac{\mathrm{d}R_2}{\mathrm{d}t} = r_2 R_2(1 - R_2/K_2) - c_{12}N_1R_2 - c_{22}N_2R_2 \ , \tag{9.27}$$

and Eqs. (9.18) and (9.19) for the consumers. The Tilman diagram remains the same because the ODEs for the consumer did not change. In the Jacobian of Eq. (9.23) only the upper two diagonal elements change into

$$\rho_1 = r_1 - \frac{2r_1}{K_1}\bar{R}_1 - c_{11}\bar{N}_1 - c_{21}\bar{N}_2 \quad \text{and} \quad \rho_2 = r_2 - \frac{2r_2}{K_2}\bar{R}_2 - c_{11}\bar{N}_1 - c_{21}\bar{N}_2 \ ,$$

both of which should remain negative. Hence, the Routh-Horwitz criteria remain the same and we again find that the steady state should be stable.

Essential resources

.

Can the Routh-Horwitz criteria also tell the difference between the stable and unstable situation in Fig. 9.4? Using Eqs. (9.16) and (9.17) for resources maintained by a source (or Eqs. (9.26) and (9.27) for self-renewing resources), and Eqs. (9.21) and (9.22) for the two consumers using two "essential" resources that cannot be substituted for one another, we obtain an Jacobian that

is quite similar to that of models with substitutable resources, as only the four $\partial_R N'$ elements change:

$$\begin{pmatrix} \partial_{R_1} N_1' & \partial_{R_2} N_1' \\ \partial_{R_1} N_2' & \partial_{R_2} N_2' \end{pmatrix} = \begin{pmatrix} \Phi_1 \frac{\bar{R}_2}{1+\bar{R}_1/H_{11}} & \Phi_1 \frac{\bar{R}_1}{1+\bar{R}_2/H_{12}} \\ \Phi_2 \frac{\bar{R}_2}{1+\bar{R}_1/H_{21}} & \Phi_2 \frac{\bar{R}_1}{1+\bar{R}_2/H_{22}} \end{pmatrix} = \begin{pmatrix} \phi_{11} & \phi_{12} \\ \phi_{21} & \phi_{22} \end{pmatrix} \tag{9.28}$$

where $H_{ij} = h_{ij}/c_{ij}$ and

$$\Phi_1 = \frac{\beta_1 \bar{N}_1}{(H_{11} + \bar{R}_1)(H_{12} + \bar{R}_2)} \quad \text{and} \quad \Phi_2 = \frac{\beta_2 \bar{N}_2}{(H_{21} + \bar{R}_1)(H_{22} + \bar{R}_2)} \, .$$

The full Jacobian therefore has the same signs and zeros as the matrix in Eq. (9.23), which means that the same $a_0 > 0$ criterion remains a condition for stability.

Again consider a case where consumer one specializes on resource one, and consumer two on resource two, i.e., $c_{11} > c_{12}$ and $c_{22} > c_{21}$. Like above the first term of the $a_0 > 0$ criterion, $\gamma_{11}\gamma_{22} > \gamma_{12}\gamma_{21}$, remains satisfied. However, the second term, $\phi_{11}\phi_{22} > \phi_{12}\phi_{21}$, need not be satisfied because the relative values of ϕ_{ij} elements are no longer determined by the corresponding consumption rates, c_{ij}. For instance, if species one, which consumes most of resource one, would require more of resource two, i.e., if $h_{11} < h_{12}$ (see Fig. 9.4b), the positive contribution of the first resource may become smaller than that of the second, and one can obtain that $\phi_{11} < \phi_{12}$. Setting the same "non-optimal" requirements for the second consumer one would also obtain that $\phi_{22} < \phi_{21}$ (see Fig. 9.4b). Whenever $(\phi_{11}\phi_{22} - \phi_{12}\phi_{21}) < 0$ and $(\gamma_{11}\gamma_{22} - \gamma_{12}\gamma_{21}) > 0$, the Routh-Horwitz criterion $a_0 > 0$ fails, and the steady state is expected to be unstable (see Fig. 9.4d).

Interestingly, we see that both consumers need to be restricted most by the resource they eat most, and that the condition $a_0 > 0$ has the biological interpretation that the species can coexist when they evolve consumption rates reflecting their resource requirements, i.e., when the ϕ_{ij} terms concur with the γ_{ij} terms (Tilman, 1980; McLean & May, 2007). Intuitively, one can understand that it is destabilizing when a consumer hardly consumes the resource it is mostly limited by (as an increase in the resource density would hardly increase is birth rate).

Finally, similar to deriving a graphical Jacobian from a local vector field, one can also estimate the relative sizes of the ϕ_{ij} terms from a Tilman diagram. In Fig. 9.4a we can see that $\partial_{R_1} N_1' = \phi_{11} > \partial_{R_2} N_1' = \phi_{12}$ because a small step to the right lands at a larger distance from the $\mathrm{d}N_1/\mathrm{d}t = 0$ nullcline that a small step to the top. Similarly, one can see that $\partial_{R_1} N_2 = \phi_{21} < \partial_{R_2} N_2' = \phi_{22}$, which tells us the Routh-Horwitz criterion, and the steady state should be stable (see Panel (c)). In Panel (b) the nullclines are reversed and these partial derivatives are just the other way around, which makes this un unstable steady state (see Panel (d)). This will become more clear in the exercises, where we simplify this model using a minimum function (Tilman, 1980, 1982). If we were to study this model with self-renewing resources, we would again obtain a very similar Jacobian and similar results (not shown).

Summarizing when consumers strongly require a resource that is more strongly depleted by another consumer than by themselves, they suffer more competition from the other consumer than from themselves. This destabilizes the steady state and leads to the "founder controlled" phase space of Fig. 9.4(d), where the initial condition determines which of the consumers survives.

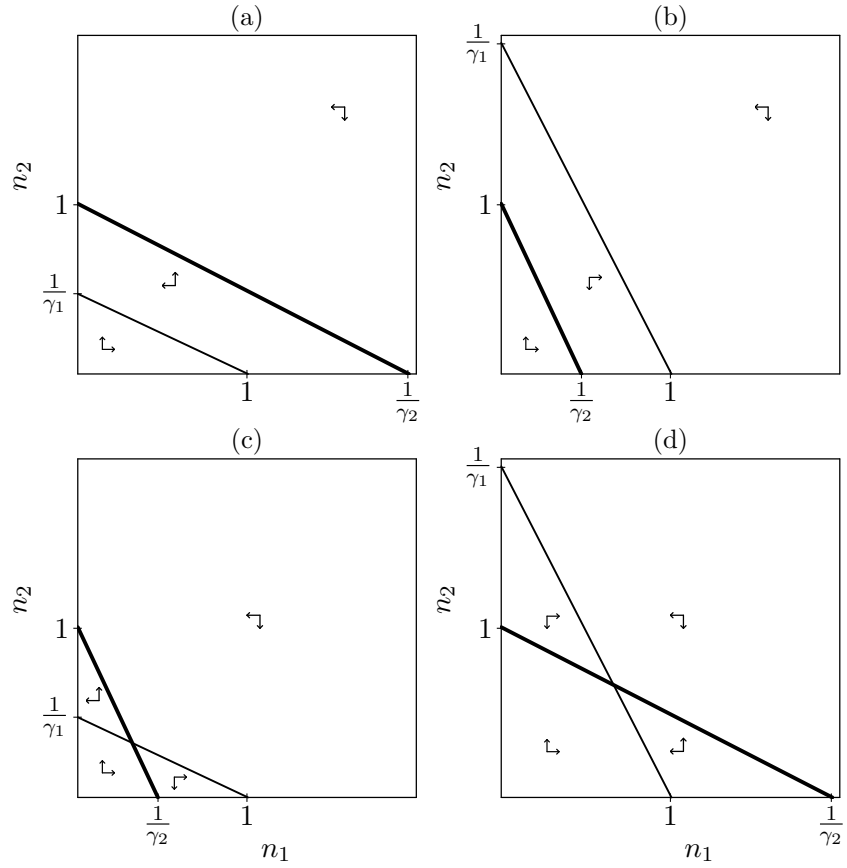

Figure 9.5: The four qualitatively different nullcline configurations of the scaled Lotka Volterra competition model given in Eq. (9.29). The heavy line is the $\mathrm{d}n_2/\mathrm{d}t = 0$ nullcline.

9.6 Scaled Lotka-Volterra competition model

In the model with two consumers using two essential resources we have seen that the QSSA nullclines can fail to intersect, or intersect in a stable or unstable steady state. This is summarized in most textbooks by the four phase space shown in Fig. 9.5, that one typically draws from a scaled version of the Lotka Volterra competition model,

$$\frac{\mathrm{d}n_1}{\mathrm{d}t} = r_1 n_1[1 - n_1 - \gamma_1 n_2] \quad \text{and} \quad \frac{\mathrm{d}n_2}{\mathrm{d}t} = r_2 n_2[1 - n_2 - \gamma_2 n_1] \; . \tag{9.29}$$

When both γ_i parameters are larger than one, the interspecific competition exceeds the intraspecific competition for both species (see Fig. 9.4b and d for a mechanistic example), and the nullclines intersect in an unstable equilibrium (Fig. 9.5c). This is called the "founder controlled" situation because the species that initially has the highest abundance has the highest chance to win (i.e., approach carrying capacity). When both γ_i parameters are smaller than one the steady state is stable; see Fig. 9.5d. Otherwise the nullclines fail to intersect (see Fig. 9.5a and b). Several textbooks start with an equation like Eq. (9.29) to discuss the possible outcomes of competition. Note how confusing this can be: it seems that the maximum rates of increase r_1 and r_2 have nothing to do with the competitive strength of a population because both parameters cancel from the nullcline equations, $\mathrm{d}n_1/\mathrm{d}t = \mathrm{d}n_2/\mathrm{d}t = 0$. Instead, we have seen above that all terms of this model, including the scaled carrying capacities, depend on the underlying parameters of the resource(s), the consumption rates, the resource requirements of the consumers, and their fitnesses.

9.7 Summary

The classical Lotka Volterra competition equations turn out to be bold simplifications of the equations that one obtains by QSS assumptions in a consumer-resource model, but part from the non-linearity of the nullclines, we do recover the same qualitatively phase diagrams with a stable or unstable steady state and non-intersecting nullclines. Replicating and non-replicating resources yield similar results for the outcome of the competition. Species will only co-exist if their niches are sufficiently different.

9.8 Exercises

Question 9.1. Migration
Extend the scaled Lotka Volterra competition model of Eq. (9.29) with a small constant immigration of individuals.
a. Write the new differential equations.
b. Analyse the model using nullclines: first sketch the phase space without this migration term, and reason how the nullclines change if you add a *small* immigration parameter.
c. What are the steady states and what is their stability?
d. Discuss competitive exclusion in this model.

Question 9.2. Nullclines
A series of experiments suggested that the nullclines of two populations are:

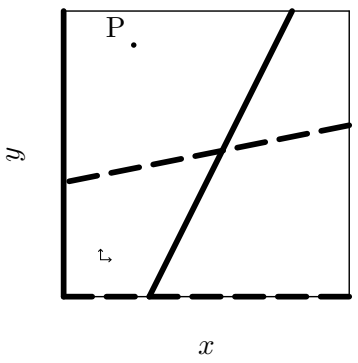

where the solid lines represent $\mathrm{d}x/\mathrm{d}t = 0$ and the dashed lines represent $\mathrm{d}y/\mathrm{d}t = 0$. Note that the vertical axis is part of the $\mathrm{d}x/\mathrm{d}t = 0$ nullcline.
a. Make a model matching these nullclines.
b. What type of ecological interaction could this be? Why is this not a model for obligate symbionts?
c. Give a correct definition of the "phase space" concept.
d. What is the state of point P in the figure?
e. Give a correct definition of a "nullcline" in a phase space.
f. Give a correct definition of a "nullcline" in a Tilman diagram.
g. Give a correct definition of a "trajectory".
h. Is it possible for trajectories to intersect?

	Gradient 1		Gradient 2	
Sample	Species A	Species B	Species C	Species D
1	80	0	80	0
2	75	0	90	10
3	80	0	70	20
4	85	0	50	40
5	70	0	40	55
6	80	0	30	60
7	10	80	20	70
8	0	80	10	90
9	0	70	0	70

Table 9.1: The data for the Gradients question.

Question 9.3. r/K selected
In this chapter we derived that two competitors that are using the same resource have to exclude each other, and that the species requiring the lowest level of resources, R^*, is expected to win. Traditionally, one distinguishes r-selected species that grow fast from K-selected species that are more competitive and have a higher carrying capacity. We have seen in Eq. (9.7) that the species requiring the lowest level of resources tends to have the highest carrying capacity, which would fit the r- and K-selected paradigm, but according to the same equations this need not always be true. Let us investigate this by considering the case where N_1 is a typical r-selected species, with fast birth and death rates, and a slower N_2 species is the winning K-selected species, and require that the carrying capacity of N_1 is lower than that of N_2.

a. Sketch the corresponding non-intersecting nullclines, with a trajectory starting close to the origin.

b. Why is the slowest species N_2 nevertheless the winner?

c. Given the presence of a long-lived K-selected species in some environment, would you expect that r-selected species can maintain themselves there?

d. Search for parameter values (or conditions) for which the species with the smallest carrying capacity wins, and sketch an example of a phase space corresponding to this situation (you may need `grind.R`).

Question 9.4. Patches
Two plant species compete for a certain type of patch. A single patch can only contain a single plant. The species have different generation times, i.e., the rate at which patches become empty is dependent on the plant species occupying the patch. In a temperate forest seeds of both plant species are abundant, making the contribution of seeds produced by the current plant populations negligible.

a. Make a differential equation model describing the population dynamics of these two plant species.

b. Analyse the model using nullclines.

c. What are the steady states and what is their stability?

d. Will all patches be occupied? What is the carrying capacity of the two species?

e. These two species are competing for the same resource: why is there no competitive exclusion?

Question 9.5. Gradients
Consider two vegetations in an environmental gradient. In the first gradient only one of the two dominant plant species (A or B) is present in each sample, whereas in the second gradient a gradual change in the abundance of the two species (C and D) is observed. A series of 9 samples

taken from one end of the gradient to the other end was recorded as in Table 9.1. Assume that these samples reflect equilibrium situations.
a. Provide an intuitive explanation for the above data.
b. Interpret these data in terms of nullclines of the Lotka-Volterra competition model.
c. What do you think of your intuitive explanation now?
d. What variation in the data is not reflected in the models?

Question 9.6. Density dependent birth rate
In this Chapter we used mass-action consumption terms, but made the birth rate of the consumer a saturation function of the amount of resources consumed. Since this seems realistic we will investigate what kind of density dependence this delivers for the consumers. To keep things simple start with a scaled resource equation for a replicating resource,

$$\frac{\mathrm{d}R}{\mathrm{d}t} = R(1-R) - aRN \quad \text{and} \quad \frac{\mathrm{d}N}{\mathrm{d}t} = \left[b\frac{aR}{h+aR} - d \right] N \ ,$$

where N is the consumer with a maximum birth rate b. We proceed as normal: make a QSS assumption for the resource and substitute this into the consumer equations.
a. What is the R_0 of the consumer?
b. Write the complete ODE for a single consumer and combine parameters to have it in its simplest form.
c. What is now the R_0 of the consumer?
d. Sketch the *per capita* birth rate of the consumer as a function of the consumer density.
e. Which of the growth models of Chapter 4 describes this best?
f. We considered a replicating resource in this question. If you have time you can also sketch the *per capita* birth rate of the consumer for a non-replicating resource, e.g., $\mathrm{d}R/\mathrm{d}t = 1-R-aRN$, where source and death have been scaled.

Question 9.7. Tilman's competition model
To simplify the model for two consumers using two essential resources Tilman (Tilman, 1980, 1982; McLean & May, 2007) used minimum functions rather than saturation functions, by assuming that for any combination of resource densities, there should be a single limiting resource, e.g.,

$$\frac{\mathrm{d}N_1}{\mathrm{d}t} = \left[b_1 \min\Big(\frac{c_{11}R_1}{h_{11}}, \frac{c_{12}R_2}{h_{12}} \Big) - d_1 \right] N_1 \quad \text{and} \quad \frac{\mathrm{d}N_2}{\mathrm{d}t} = \left[b_2 \min\Big(\frac{c_{21}R_1}{h_{21}}, \frac{c_{22}R_2}{h_{22}} \Big) - d_2 \right] N_2 \ , \quad (9.30)$$

where c_{ij} is the consumption rate of consumer i on resource j, and h_{ij} determines how much the consumer needs to eat from each resource. The minimum function makes the resources both "essential", i.e., both have to be consumed in sufficient amount, and the birth rate is limited by the resource that is most needed (i.e., high h_{ij}) and/or consumed less (i.e., low $c_{ij}R_j$).
a. Sketch Tilman diagrams of this model. Explain that this indeed corresponds to two essential resources.
b. One can simplify the model with two non-replicating resources by scaling the resource densities and time by setting $s = d = 1$, and write the quasi steady state resource densities as

$$R_1 = \frac{1}{1 + c_{11}N_1 + c_{21}N_2} \quad \text{and} \quad R_2 = \frac{1}{1 + c_{12}N_1 + c_{22}N_2} \ .$$

Use the model `tilman.R` to study the phase space of the two consumers. It is helpful to first consider two consumer with very different diets, i.e., give each species a unique preference in c_{ij} and h_{ij}, and see if you can get co-existence.
c. Change parameters to obtain both a stable and an unstable equilibrium in this model. Can you use the Routh-Horwitz criterion to read the stability directly from the Tilman diagram? Note, you can also use the `newton()` function in `grind.R` to check the Jacobian.

Question 9.8. Fitness (Extra exercise for cool students)
In this chapter we have used the fitness $R_0 = \beta/\delta$ to clean up the equations, and we have seen that the critical resource requirement, $R_i^* = h_i/[c_i(R_{0_i} - 1)]$ defines which species is the best competitor. In the model of Eqs. (9.1) to (9.3) one can also define a more complicated expression for the fitness as

$$\hat{R}_{0_i} = \frac{\beta_i}{\delta_i} \frac{c_i \bar{R}}{h_i + c_i \bar{R}} ,$$

where $\bar{R} = s/d$ is the "carrying capacity" of the resource (see Chapter 16). Since this contains all parameters defining R_i^*, and one could think that the species having the highest fitness, $\hat{R}_{0_i}$, should be the best competitor, i.e., have the lowest R_i^*. Due to the fact that the birth rates are saturation functions of the amount of resources consumed, one can already see that this need not always be true, as a consumer that is best at high resource densities, need not be the best one at low resource densities, i.e., around R^*. Can you think of a parameter setting where the species with the lowest fitness, $\hat{R}_{0_i}$, is the best competitor?

Chapter 10

Competition in large communities

The scaled Lotka Volterra competition model of Eq. (9.29) has been used in many different theoretical studies of competition in ecosystems. Thanks to its simplicity it has few parameters, and this has allowed theoretical ecologists to define "understandable" models composed of many competing species. We here discuss two examples. The first considers competition along a resource axis, and has the restriction discussed in Chapter 9 that all γ_{ij} parameters are smaller than one. In the second example the author did allow for the "founder controlled" situations shown in Fig. 9.4d and Fig. 9.5c.

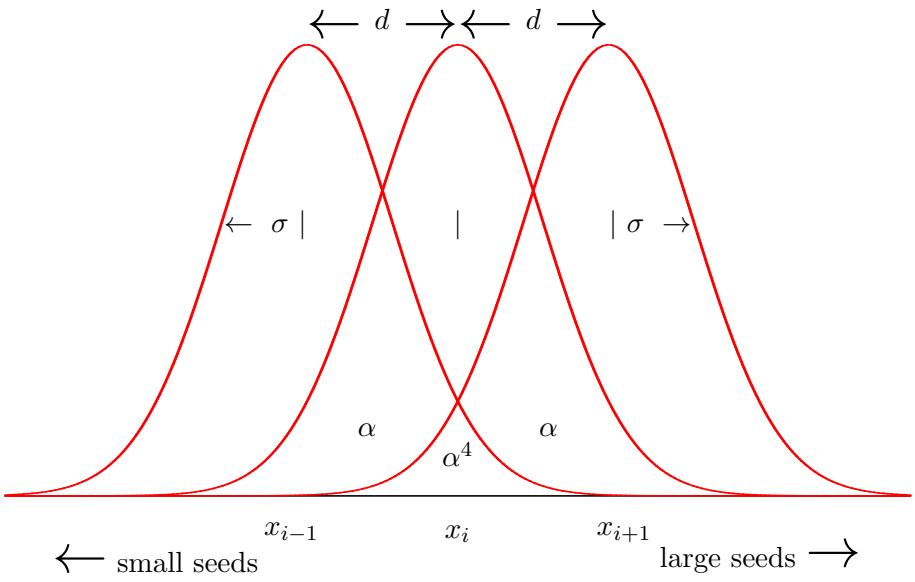

Figure 10.1: Resource usage of three "finch species" consuming seeds of different sizes. The distance between the preferred seed size of neighboring species is d, and σ is the standard deviation of the Gaussian seed size preferences. The niche overlap between neighboring species at distance d is α, and hence the overlap between species at distance $2d$ is α^4 (see Eq. (10.1)).

10.1 Niche space models

There is an interesting modeling formalism for resource competition that is based on a resource axis along which species are distributed (see Fig. 10.1) (MacArthur, 1972; May, 1974). Think of several species of Darwin finches that each have a preferred seed size because they evolved different beak sizes. The preference of each species can be modeled with a simple Gaussian function of the seed size x, i.e., $f_i(x) = \exp[-(x - x_i)^2/(2\sigma^2)]$ that is centered around the preferred seed size x_i of species i (see Fig. 10.1). One can interpret this function as the probability of using a seed of size x, i.e., seeds of the preferred size are consumed with probability one. For simplicity one assumes that the species are evenly distributed over the niche space. This boils the whole problem of niche overlap down to two parameters, i.e., σ for the standard deviation of the Gaussian functions, and d for the difference between the preferred seed sizes of neighboring species. The niche overlap between species is completely determined by the region where their respective Gaussian functions overlap. One can define the niche overlap as the probability of both species eating seeds of the same size, i.e., as the product of the Gaussian preference functions, which implies that the niche overlap is highest at the point where two neighboring species both use a resource most. To properly scale this one can normalize with the overlap that a species has with itself:

$$\alpha = \frac{\int_{-\infty}^{\infty} \mathrm{e}^{-\frac{x^2}{2\sigma^2}} \times \mathrm{e}^{-\frac{[x-d]^2}{2\sigma^2}} \,\mathrm{d}x}{\int_{-\infty}^{\infty} \mathrm{e}^{-\frac{x^2}{2\sigma^2}} \times \mathrm{e}^{-\frac{x^2}{2\sigma^2}} \,\mathrm{d}x} = \mathrm{e}^{-\left(\frac{d}{2\sigma}\right)^2} \;, \tag{10.1}$$

see Yodzis (1989) page 123. This confirms that the niche overlap α only depends on the distance d weighted by the standard deviation σ. With $\alpha = \mathrm{e}^{-\left(\frac{d}{2\sigma}\right)^2}$, the overlap of a species with itself is indeed defined by a distance $d = 0$ because $\alpha = \mathrm{e}^0 = 1$. The overlap between the first and the last species in Fig. 10.1 is determined substituting by their distance $2d$ into Eq. (10.1), i.e.,

$$\mathrm{e}^{-\left(\frac{2d}{2\sigma}\right)^2} = \mathrm{e}^{-4\left(\frac{d}{2\sigma}\right)^2} = \alpha^4 \;. \tag{10.2}$$

Likewise, one can see that the niche overlap between species at distance $3d$ will be α^9.

An ecosystem of n competing species that are equally distributed at distances d on a resource axis can therefore be described with the system of ODEs

$$\frac{\mathrm{d}N_i}{\mathrm{d}t} = rN_i \left(1 - \sum_{j=1}^{n} A_{ij} N_j\right) \;, \tag{10.3}$$

with the "interaction matrix"

$$A = \begin{pmatrix} 1 & \alpha & \alpha^4 & \alpha^9 & \alpha^{16} & \dots \\ \alpha & 1 & \alpha & \alpha^4 & \alpha^9 & \dots \\ \alpha^4 & \alpha & 1 & \alpha & \alpha^4 & \dots \\ \alpha^9 & \alpha^4 & \alpha & 1 & \alpha & \alpha^4 \quad \dots \\ \dots & & & & & \end{pmatrix} \tag{10.4}$$

where it is assumed that all species have the same natural rate of increase r.

One can analyse this model by increasing its diversity n one by one. A system of two species obeys

$$\frac{\mathrm{d}N_1}{\mathrm{d}t} = rN_1(1 - N_1 - \alpha N_2) \quad \text{and} \quad \frac{\mathrm{d}N_2}{\mathrm{d}t} = rN_2(1 - N_2 - \alpha N_1) \;. \tag{10.5}$$

We have learned in Section 9.3 that this 2-dimensional ecosystem will have a stable non-trivial steady state whenever $\alpha < 1$. By our definition of the maximal niche overlap of $\alpha = 1$ one concludes that two species can be located infinitely close on the resource axis and co-exist, i.e., we obtain for the critical niche overlap of a 2-dimensional system that $\alpha = 1$ and $d/\sigma \to 0$. Note that this is an "artifact" of using the scaled version of the competition model. If two species have different birth rates, death rates, and hence carrying capacities, they will not co-exist if they are located infinitely close on the resource axis (see Eq. (11.3)).

Next consider three species. What would be the maximal niche overlap, or the minimal distance d, required for co-existence of all three species? This can be analyzed by considering Fig. 10.1 and numbering the species from left to right as N_1, N_2, and N_3. This is a symmetric system, i.e., the ODEs of N_1 and N_3 should have the same structure, and $\mathrm{d}N_2/\mathrm{d}t$ should have the strongest competition because it has two direct neighbors, i.e.,

$$\begin{aligned} \frac{\mathrm{d}N_1}{\mathrm{d}t} &= rN_1(1 - N_1 - \alpha N_2 - \alpha^4 N_3) \ , \\ \frac{\mathrm{d}N_2}{\mathrm{d}t} &= rN_2(1 - N_2 - \alpha[N_1 + N_3]) \ , \\ \frac{\mathrm{d}N_3}{\mathrm{d}t} &= rN_3(1 - N_3 - \alpha N_2 - \alpha^4 N_1) \ . \end{aligned} \tag{10.6}$$

The existence and stability of the 3-dimensional steady state can be investigated by testing the invasion of the species in the middle, N_2, in the steady state of those at the ends. For this invasion criterion one first sets $N_2 = 0$ to compute the steady state of the 2-dimensional system. Employing the symmetry of the system one sets $N_1 = N_3$, and obtains their steady state by solving $\bar{N} = 1/(1 + \alpha^4)$ from $1 - N - \alpha^4 N = 0$. When $N_2 \to 0$ the invasion of N_2 is described by $\mathrm{d}N_2/\mathrm{d}t \simeq rN_2(1 - \alpha 2\bar{N})$. This means that co-existence is guaranteed whenever

$$1 - \frac{2\alpha}{1 + \alpha^4} > 0 \quad \text{or} \quad 1 + \alpha^4 - 2\alpha > 0 \ . \tag{10.7}$$

This fourth order equation can be solved numerically as $\alpha < 0.54$ (or $d/\sigma > 1.54$), which means that the maximal niche overlap of a 3-dimensional system is $\alpha \simeq 0.54$.

For four species one can test when one of the two species in the middle can invade in an (asymmetric) system of three species, and for five species one can again test the middle species in a steady state of four established species, and so on. The results of such a sequence are summarized in Fig. 10.2a which depicts the maximal niche overlap as a function of the diversity n of the ecosystem. The figure reveals a fast convergence to $\alpha \simeq 0.63$ (or $d/\sigma \simeq 1.3$). This convergence is due to the fact that the impact of the species at the very ends of the resource axis decreases when the diversity increases. The limit that is ultimately approached, i.e., $d/\sigma \simeq 1.3$, is called the "limiting similarity". This simply means that species cannot be too similar; otherwise they exclude each other. Because the maximum niche overlap converges to $\alpha \simeq 0.63$ when the diversity increases, one speaks of "diffuse competition": several species together determine the intensity of the competition on each species.

Infinite resource axis

The original analysis of this model by May (1974) addressed the relationship between the niche overlap and the diversity of the system by considering an infinite resource axis along which infinitely many species were distributed at distance d. An infinite system has the mathematical

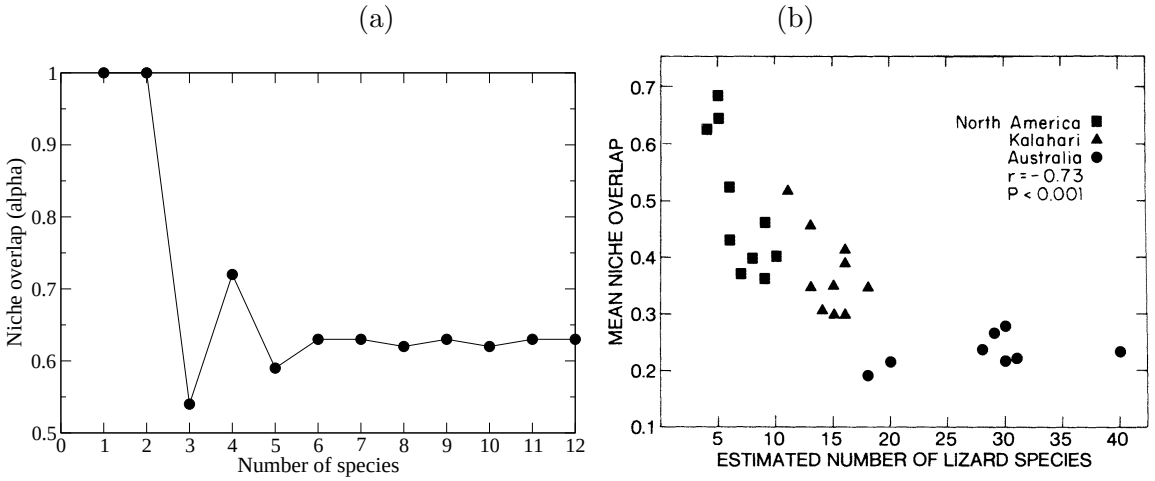

Figure 10.2: The limiting overlap computed numerically for the model of Eq. (10.3) (a), and the results of Pianka (1974) (b).

advantage that the effects of the edges disappear, which means that all equations become identical. Thanks to this simplification May (1974) was able to compute the Jacobian of the infinite system, and could compute the dominant eigenvalue of the Jacobian as a function of the niche overlap α. Because all equations were identical by the assumption of an infinite system, no single species could ever go extinct, and the dominant eigenvalues were simply approaching zero when the niche overlap α was approaching our limiting similarity of $\alpha \simeq 0.63$. In our analysis we were breaking the symmetry of the system by distinguishing the species in the middle from those at the borders, and were obtaining (transcritical) bifurcation points by increasing α, where the species in the middle disappeared. Because the symmetry could not break in the original infinite system, and the eigenvalues were approaching zero when the niche overlap was increased, May (1974) had to define variation in the abiotic circumstances that required the value of the dominant eigenvalue to remain below some critical negative level. Doing so he obtained a limiting similarity that is very similar to the one derived numerically in Fig. 10.2. The mathematical analysis of May (1974) is addressed further in the last (challenging) exercise.

Lizard man

Pianka (1974) measured the niche overlaps between several species of lizards in various desert habitats from all over the world. He distinguished three niche dimensions: (1) food, as determined from the contents of their stomachs, (2) habitat, and (3) the time of the day at which they were active. These observations were translated into a single measure of the niche overlap considering both additive and multiplicative measures for defining the total niche overlap. Pianka observed that the niche overlap decreased when the diversity of the ecosystem increased (see Fig. 10.2b). Thus, at low species numbers there was no evidence for a limiting niche overlap in the data (compare Fig. 10.2a with b). Because the diversity ranged from four to forty species, and the theoretical niche overlap of Fig. 10.2a converged already to 0.63 before a diversity of ten species, Pianka (1974) concluded that the data contradicted the theory.

A simple solution for this contradiction was proposed by Rappoldt & Hogeweg (1980) who argued that the niche space considered by Pianka (1974) was in fact not 1-dimensional. In a 2-dimensional niche space the Gaussian curves become circular and can be tiled in a hexagonal

lattice. In such a 2-dimensional lattice there are many more species at the borders of the niche space, and it takes a much higher diversity for the effects of the borders to peter out. The lizard data of Fig. 10.2b therefore confirm the theory, rather than contradict it, because Pianka indeed had more than one niche dimension in his data (Rappoldt & Hogeweg, 1980). Finally, Pianka (1974) observed that deserts with the highest amount of rain per year had the highest diversity, which is not suprising because the total production (and hence the length of the resource axis) is probably limited by the precipitation in deserts. Because the niche overlap decreased when the diversity increased (Fig. 10.2b), we can understand from this model that the amount of precipitation was correlated negatively with the average niche overlap (see Pianka (1974)).

10.2 Monopolization

For our second example we turn to Yodzis (1978) who was interested in the relation between the diversity of a community and the strength of its competitive interactions. It is indeed quite difficult to have a good intuition about this relation. One could argue that if there is more competition that there will be more competitive exclusion, and hence less diversity. Studies by Gardner & Ashby (1970) and May (1972) have also suggested that the more interactions there are in ecosystems, and the stronger the interaction strengths, the lower the probability that a diverse ecosystem will be stable (see Chapter 11).

Yodzis (1978) created diverse *in silico* ecosystems in computer simulations changing the intensity of the competitive interactions and the initial diversity of the simulation. Running the model on a computer, several of the species in the initial pool went extinct until the simulation approached a diversity that remained at a reasonably stable level over long periods of time. The model ecosystem had a large number of habitats in which all species could be present, and there was a diffusive flux of individuals from habitat to habitat. The abiotic circumstances were considered to be identical in each of the habitats, i.e., the same competition coefficients were used everywhere.

Yodzis (1978) considered an initial pool of n different species that were randomly distributed over m habitats, and defined N_{a_i} as the population size of species i in habitat a. The flux of individuals of species i between habitats a and b was described by a symmetric "dispersal" matrix D, where D_{ab} depends inversely on the distance from habitat a to b, and defines the rate at which individuals move from a to b. Since D_{ab} is a *per capita* flux, the total flux of individuals from species i at habitat a to b has to be multiplied with the local population density N_{a_i}. The net flux of individuals between two habitats is then given by

$$\frac{\mathrm{d}N_{a_i}}{\mathrm{d}t} = D_{ab}N_{b_i} - D_{ba}N_{a_i} = D_{ab}(N_{b_i} - N_{a_i}) \ , \tag{10.8}$$

given that $D_{ab} = D_{ba}$ because the distance from a to b is the same as that from b to a. Like in a diffusion equation, we observe that the net flux is proportional to the difference in the concentrations, i.e., the difference between population sizes in the two habitats.

Combining an n-dimensional form of Eq. (9.29) with Eq. (10.8) one ends up with a model ecosystem of $n \times m$ ODEs

$$\frac{\mathrm{d}N_{a_i}}{\mathrm{d}t} = N_{a_i}\Big(1 - \sum_{j=1}^{n} A_{ij}N_{a_j}\Big) + \sum_{b=1}^{m} D_{ab}(N_{b_i} - N_{a_i}) \ , \tag{10.9}$$

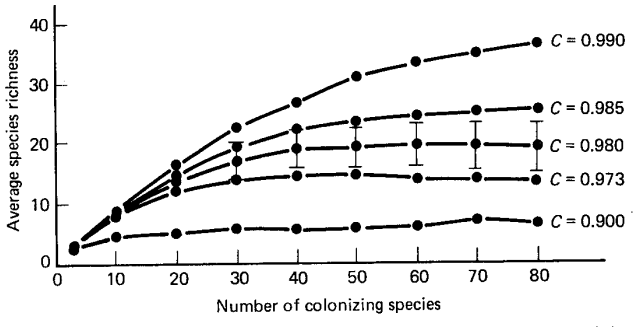

Figure 10.3: Figure 5.5 in Yodzis (1989) page 144: the steady state diversity as a function of the initial number of species, for various intensities of the competition C.

for $a = 1, \ldots, m$ and $i = 1, \ldots, n$. Here A_{ij} is the interaction matrix containing all competition coefficients. The growth rates were removed mathematically by giving all species the same growth rate, and scaling time by this fixed growth rate. All species were given the same intraspecific competition by setting $A_{ii} = 1, \forall i$. The other competition coefficients and the dispersal rates were drawn randomly.

From Eq. (9.29) and Fig. 9.5 we have learned that the outcome of competition between any two species depends crucially on the ratio of the interspecific competition parameters γ and the intraspecific competition strength (that was scaled to one). If both γ-s happen to be smaller than one, the nullclines intersect in a stable steady state, and if both are larger than one the non-trivial steady state is a saddle point leading to founder controlled competition (see Fig. 9.5). Yodzis (1978) varied the randomly chosen interaction strengths and defined a "global" competition strength parameter, C, for the probability that a randomly chosen matrix element was larger than one, i.e., $C = P(A_{ij} > 1)$. The values of the interaction matrix, A_{ij}, were drawn from a normal (or uniform) distribution. Knowing C, stable coexistence between any pair of species is expected with probability $(1 - C)^2$, and the unstable founder controlled phase space is expected with probability C^2. Competitive exclusion is expected when $A_{ij} < 1$ and $A_{ji} > 1$, or $A_{ij} > 1$ and $A_{ji} < 1$, which will occur with probability $2C(1 - C)$. We can do a sanity check and see that the sum $(1-C)^2+C^2+2C(1-C) = 1$. Yodzis (1978) considered systems in which stable coexistence should be rare, i.e., he was working with distributions yielding high values of C. Choosing $C \geq 0.9$ the probability of any species pair having a stable coexistence was small, i.e., maximally $(1 - C)^2 \leq 0.01$. The probability of finding the founder controlled situation is much higher, i.e., $C^2 \geq 0.81$. Having set all parameters, i.e., all matrix elements, the species were distributed randomly but scarcely over the patches, i.e., initially most species were only present in a few patches, and would only then start to disperse to all other patches.

Running the simulations until a steady state was approached, a fraction of the species in the initial species pool would typically go extinct, and the ecosystem approached the diversity depicted in Fig. 10.3. The figure shows that increasing the diversity of the initial species pool, and/or increasing the competition strengths, increased the final diversity of the ecosystem. This suggests that the more complex the ecosystem the higher its diversity, which is a controversial result (Gardner & Ashby, 1970; May, 1972, 1974; Grime, 1997; Hanksi, 1997; McCann *et al.*, 1998). The reason why the diversity increases with competition strength in these simulations is its spatial embedding, i.e., in each habitat one initially finds only a small selection of the species. Having many founder controlled situations the species that settle initially in a habitat can approach their carrying capacity before other species invade and approach sufficiently large numbers to have a chance to win the competition. Basically the model is a "resident always wins" system, and the final diversity is largely determined by the number of species that are

distributed initially over the habitats. Diversity does not come about by stable coexistence but by the spatial distribution of the species over the habitats. This is a fine example of the unexpected effects that spatial models may have over the well mixed ODE models.

10.3 Summary

The simplicity of the scaled Lotka-Volterra competition model has allowed us to formulate interesting and understandable models for large communities. When a sufficient number of species is packed along a (long) resource axis their degree of competition approaches a fixed niche overlap called "diffuse competition". The species diversity at which this happens depends on the number of resource axes taken into consideration. Ecosystem diversity may also come about by a spatial distribution of species that is largely determined historically by the initial seeding of the system.

Read the Scheffer & Van Nes (2006) paper to see a niche-space model where species co-exist by being similar.

10.4 Exercises

Question 10.1. Invasion criterion
Consider a species immigrating into an area in which two other species are present that do not compete with each other. Each of these two species therefore has a density equal to the carrying capacity, and let the new species compete equally with the other two species. Assume that the carrying capacities are the same for all three species.

a. Assume that competition takes place in a one dimensional resource space like the one depicted in Fig. 10.1. Redraw the figure for this system where the established species do not compete, and where the new species competes with both.
b. Make an ODE model of three equations.
c. Determine the parameter conditions for succesful invasion of the third species in the steady state of the other two.
d. Give a biological interpretation in terms of competition strengths.
e. Sketch the 3-dimensional phase space of this system for the invasion criterion. What do you expect to happen if the new species invades successfully?

Question 10.2. Symbiosis
This book has a strong emphasis on the resource competition between species that comes about whenever they are feeding on shared resources, and on direct interference competition. This seems a rather negative view on ecology because many species are also involved in symbiotic interactions. These come in two basic forms: obligatory symbionts cannot grow in the absence of each other, and facultative symbionts help each other but do not strictly require each other.

a. Write a model for two symbionts that strictly require each other, and study your model by phase plane analysis.
b. Change the previous model in an asymmetric symbiotic interaction. Let the first species be dependent on the second, and let the second be ignorant of the first. An example would be saprophytes.
c. Write a model for a facultative symbiosis.

d. Can you change the latter model into a model of obligatory symbionts by just changing the parameters?

Question 10.3. Larvae and adults

a. Write a simple model for an insect population with an early larval stage, and a late adult stage. Assume that larvae only compete among themselves, and make sure that the insect population as a whole has a carrying capacity.

b. Let there be two predators, one feeds on the larvae and the other on the adults. Since these predators are foraging on the same species they seem to occupy the same niche. Can these two predators co-exist?

Question 10.4. Control by parasites

Consider a population of songbirds with a birth rate that declines linearly with the population size, and have a death rate that is independent of the population density. Let the individuals be susceptible to an infection with a parasite that increases the death rate somewhat, but hardly affects the birth rate. Assume that transmission of parasites occurs upon contacts between infected and susceptible individuals, and obeys mass action kinetics. Let there be no vertical transmission, i.e., the parasite is not transmitted to eggs.

a. Write a natural model.

b. What is the R_0 and the carrying capacity of the population in the absence of the parasite?

c. What is the R_0 of the infection?

d. What is the population density of the susceptibles when the parasite is endemic?

e. Suppose this songbird competes with related bird species that occupies the same niche, but has a somewhat shorter life span, and is not susceptible to the parasite. Write a natural model for the 3-dimensional system.

f. Do you expect the resistant bird species to be present?

g. What would you expect for a large community of bird species, all sharing the same resource, but each being susceptible to a host specific parasite species?

Question 10.5. Monopolization

In the scaled Lotka Volterra model of Eq. (9.29) we have seen that the natural rate of increase of a species, r_i, has no effect on the competitive ability of a species. We know this is a consequence of the scaling because we also know that it is the species with the lowest resource requirements, R_i^*, that is the best competitor, and that R_i^* depends on several parameters, including the birth and death rates, and hence the natural rate of increase $r_i = b_i - d_i$. In the model of Yodzis (1989) the natural rates of increase were also removed, see Eq. (10.9).

a. Do you expect that if species were to have different growth rates, that those with fast growth rates would be expected to survive better in the simulations?

b. Would this make a difference for the general conclusion that the diversity increases with the intensity of the competition?

Question 10.6. Sex

All population models considered thus far fail to distinguish between the two sexes. Basically these models only consider the females in a population, and ignore the males. Extend the Lotka Volterra competition model with sexual reproduction, using a simple Hill function for the probability that a female finds a male, and see how this effects its possible phase spaces, and their biological interpretation. You will probably require a computer to draw these nullclines.

Question 10.7. Infinite niche space (Extra exercise for cool students)

In an infinite implementation of Eq. (10.3) all species obey the same ODE

$$\frac{\mathrm{d}N_i}{\mathrm{d}t} = N_i(1 - \sum_j A_{ij}N_j) \ ,$$

which implies that they all have the same steady state

$$\bar{N} = 1/\sum A_{ij} = 1/(1 + 2\alpha + 2\alpha^4 + 2\alpha^9 + \dots) \simeq 1/(1 + 2\alpha) \ .$$

a. What is the Jacobian of this steady state? Hint: do not substitute the expression for the equilibrium density, but write $\bar{N}$, and observe that the elements on the diagonal can be written as $1 - \bar{N} - \sum A_{ij}\bar{N}$.

b. Can one obtain the stability of the system directly from the interaction matrix A, or should one first compute the Jacobian?

Chapter 11

Stability and Persistence

The relationship between the complexity of an ecosystem and its stability has been debated over decades. Based on fairly romantic considerations ecologists have liked to think that the more diverse and complex an ecosystem, the higher its degree of stability. However, one could also turn this around by argueing that stable ecosystems have had more time to become diverse. Importantly, it remains unclear what one means with the stability of an ecosystem. This could vary from the local neighborhood stability that we have considered in this course, i.e., robustness against perturbations of the population sizes around the steady state (which was measured by the return time), to a mere persistence over time. It is rather obvious that most ecosystems are not persisting in stable steady states, because they are all driven by seasonal fluctuations and other disturbances. Robustness to invasion by new species can also be considered to be a form of stability. Unfortunately, we have no obvious modeling approach to study what properties of an ecosystem would make it resilient to disturbances like the removal or introduction of a species.

11.1 Stability

Classical studies of the properties of random Jacobian matrices representing the local neighborhood stability of steady states of complex systems have changed the thinking about the relationship between stability and complexity (Gardner & Ashby, 1970; May, 1972, 1974). Consider an arbitrary steady state of an arbitrary (eco)system, and address the question whether this steady state is expected to be stable. To do so, one can write a random Jacobian J, of a system with n species. To keep the analysis manageable one poses the following requirements:

1. Let every population have a carrying capacity and the same return time to this carrying capacity. For the Jacobian matrix this means that all elements on its diagonal have the value -1 (i.e., $\forall J_{ii} = -1$).
2. The off-diagonal elements of the matrix are set with a probability P. Thus, P determines the likelihood that two species are involved in an interaction. P determines the connectivity of the system, i.e., each species is expected to have $P(n-1)$ interactions with other species.
3. The interaction elements that are set are drawn from a normal distribution with mean $\mu = 0$ and standard deviation σ.

Summarizing, one draws a random matrix with dimension $n \times n$ of the following form

$$J = \begin{pmatrix} -1 & 0 & 0 & a & 0 & 0 & -b & 0 & \dots \\ 0 & -1 & 0 & 0 & 0 & c & \dots & & \\ 0 & 0 & -1 & 0 & \dots & & & & \\ -d & \dots & & -1 & \dots & & & & \end{pmatrix} , \tag{11.1}$$

and this matrix is interpreted as the Jacobian of a steady state of an (eco)system, where $a, b, \dots, d$ are randomly chosen values from a standard normal distribution.

Having drawn such a random Jacobian matrix, the question is how its stability depends on the parameters n, P, and σ. One can use the theory on the dominant eigenvalue of large random matrices to prove that the probability that the largest eigenvalue is negative, i.e., $\lambda_{\max} < 0$, strongly depends on the condition

$$\sigma\sqrt{nP} < 1 . \tag{11.2}$$

The biological interpretation of this rather abstract analysis is that increasing the number of interactions per species, nP, and/or increasing the absolute interactions strengths, σ, decreases the chance that the steady state is stable. This suggests that complex systems cannot *a priori* expected to be stable (Gardner & Ashby, 1970; May, 1972, 1974).

This result seemingly contradicts the co-existence of many species in the niche space model of Chapter 9. However, in the niche space model the average interaction strength decreases when the diversity increases (see Eq. (10.4)). Increasing the diversity n therefore implicitly decreases the interaction strength σ. This may also be true for natural ecosystems: when the number of species n increases, the number of connections per species, nP, need not increase, and their average connection strength, σ, may decrease.

A simple criticism on the analysis is that it only considers one steady state of the system, and that complex systems could have very many steady states, of which only one a few need to be stable to guarantee its persistence as a high-dimensional system. Thus, the ecosystem could be stable and still complex, after a few of its species have gone extinct. Despite these easy criticisms this work has changed the consensus view of "diversity entails stability" into the question "how come that complex systems persist over long periods of time?".

11.2 Permanence and persistence

Ecosystems are probably not persisting as steady states, and can also persist as stable attractors like stable limit cycles, chaotic attractors, or long transients. The persistence of ecosystems on attractors other than steady states can be studied with the invasion criterion that we also used in the niche space models of Chapter 9, and to determine stability of steady states in 3-dimensional phases spaces. A simple example is to ask the question when a new species can invade in an established ecosystem. For the 2-dimensional case one could define K as the average density of the established species and write

$$\frac{\mathrm{d}N}{\mathrm{d}t} = N[b(1 - \epsilon N - cK) - d] \quad \text{or} \quad \frac{\mathrm{d}N}{\mathrm{d}t} = N[b - d(1 + \epsilon N + cK)] , \tag{11.3}$$

for the invading species, with a linear density dependent birth or death term, respectively. The average density K of the established species could either be an equilibrium density, e.g., its carrying capacity, or an average density on some other attractor. The parameter c is the degree of competition that the invading species suffers from the established species.

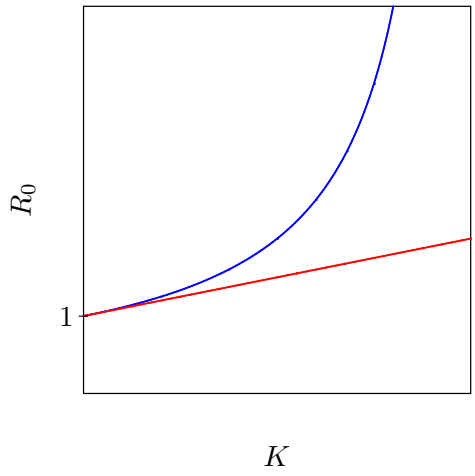

Figure 11.1: The invasion criterion of Eq. (11.4). The straight line corresponds to the species with density dependent death. The curved line is from the species with a density dependent birth rate. K is the average density of the established species.

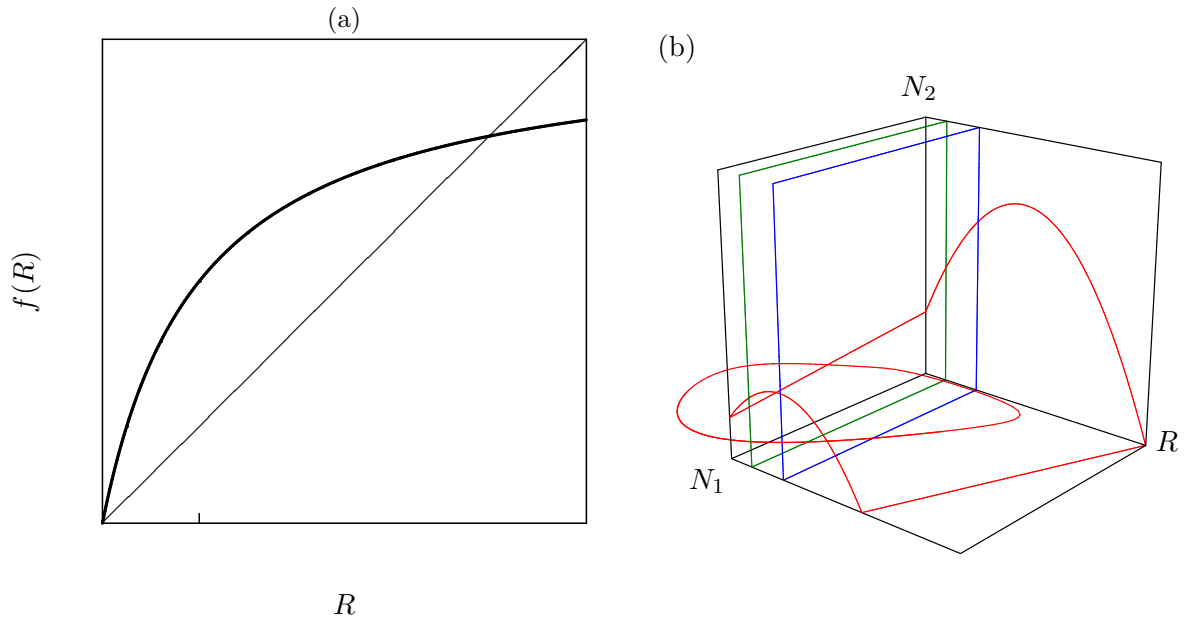

Figure 11.2: Panel (a) the functional response of Eq. (11.5). Panel (b) the 3-dimensional nullclines of Eq. (11.5) for a clever choice of the parameters allowing the two competing predators to co-exist on a stable limit cycle. The elipsoid curve in Panel (b) is a trajectory.

The fitness is in both models obviously defined as $R_0 = b/d$, and to test for invasion one asks whether $\mathrm{d}N/\mathrm{d}t > 0$ when $N \to 0$. The latter means that one can let $\epsilon \to 0$ in Eq. (11.3) and obtain from the condition $\mathrm{d}N/\mathrm{d}t > 0$ that

$$R_0 > \frac{1}{1 - cK} \quad \text{and} \quad R_0 > 1 + cK \ , \tag{11.4}$$

respectively. To be able to invade the fitness of a species not only has to be larger than one, but it has to exceed a value determined by the average population size and the competitive strength of the established species. The condition of Eq. (11.4) is depicted in Fig. 11.1.

A fine example of non-equilibrium co-existence of two predators on one prey was presented by Yodzis (1989). By making a smart choice of the functional response functions, one can make a system where one predator consumes faster at low prey densities, whilst another does better at high prey densities (see Fig. 11.2a). If the prey population oscillates between densities where the two predators differ in who performs best, the predators need not exclude each other (see Fig. 11.2b). Note that the two predator planes do run parallel in the phase space, i.e., there is no 3-dimensional steady state, which remains in agreement with the equilibrium analysis in Chapter 9. To find parameters corresponding to this behavior one should design an oscillatory predator prey system like we did in Chapter 6, and use invasion criteria allowing each of the predators to invade at the average prey density in the attractor set by the other predators (see the Exercises).

The relationship between ecosystem complexity and diversity has also been studied in non-equilibrium conditions (Law & Blackford, 1992; Yodzis, 1989; Pimm, 1980; Post & Pimm, 1983). The basic approach is to make ecosystems with a predefined food chain structure and create many species by giving them randomly selected parameter values. An example of such a study has been described in Chapter 10. Sometimes one finds that such randomly created ecosystems remain diverse in the absence of a stable steady state, i.e., they persist on a periodic or chaotic attractor (Law & Blackford, 1992). In other studies only a fraction of the randomly created ecosystems persists with all species present in an n-dimensional steady state (Roberts, 1974), and one could argue that these correspond to the type of systems one finds in nature. The last analysis confirms the classical random Jacobian analysis because the fraction of systems with an n-dimensional steady state decreases when the complexity increases (Roberts, 1974; Tilman *et al.*, 1997).

11.3 Summary

The relationship between the diversity or complexity of an ecosystem and its degree of stability is not well established. Most ecosystems are not persisting in the neighborhood of stable steady states anyway. Non-equilibrium persistence, and robustness to invasion by novel species, are better measures of the long-term stability of ecosystems.

11.4 Exercises

Question 11.1. Non-equilibrium co-existence
We have seen in Chapter 9 that two species competing for the same resource cannot co-exist in a steady state. In the absence of such a steady state, species might still be able to co-exist on a non-equilibrium attractor such as a stable limit cycle or a chaotic attractor. An example of a model allowing for the non-equilibrium co-existence depicted in Fig. 11.2b is

$$\begin{aligned}
\frac{\mathrm{d}R}{\mathrm{d}t} &= rR(1-R/K) - a_1RN_1 - \frac{a_2RN_2}{h+R} \ , \\
\frac{\mathrm{d}N_1}{\mathrm{d}t} &= a_1RN_1 - d_1N_1 \ , \\
\frac{\mathrm{d}N_2}{\mathrm{d}t} &= \frac{a_2RN_2}{h+R} - d_2N_2 \ ,
\end{aligned} \tag{11.5}$$

where one predator has a linear functional response and the other a saturated Holling type II response.

a. Find parameter values for which the predators co-exist. Use pencil and paper to find parameters delivering functional responses that agree with Fig. 11.2a, and to check the invasion of each of the predators in the attractor of the other.

b. Can one obtain the same result when both predators have a saturated functional response?

Chapter 12

Metapopulations

Metapopulation models describe the distribution of a population over a large number of different habitats or patches. With metapopulation models one is interested in how the migration and extinction rates of a species determine the fraction of suitable habitats that is actually occupied by the species. Because rich ecosystem habitats become more and more fragmented by our destruction of nature, metapopulation models have become very popular among nature conservation biologists (Hanksi, 1998; Hanski & Gaggiotti, 2004). Typically, in metapopulation models one only considers the presence or absence of a species in a habitat, and is no longer interested in the population size, or the birth and death rates.

12.1 The Levins model

The basic metapopulation model was proposed by Levins (1969) and Levins & Culver (1971), and has the utterly simple form of the logistic growth model considered in Chapter 3. Instead of modeling the population size, one now describes the fraction, $0 \leq p \leq 1$, of patches occupied by a species. There is a fixed probability, or rate, that an occupied patch looses the species of interest, which is described by a extinction parameter m (for mortality). One assumes that individuals emigrate from occupied patches and have a certain probability to settle in another patch. The number of migrants that are traveling between the patches was therefore assumed to be proportional to the number of occupied patches, p. Only if the migrants colonize an empty patch, which occurs with probability $(1 - p)$, the migration event should be counted as an increase in the fraction of occupied patches, i.e.,

$$\frac{\mathrm{d}p}{\mathrm{d}t} = cp(1 - p) - mp \ , \tag{12.1}$$

where the colonization parameter c collects the number of migrants leaving an occupied patch and the rate at which they land in another patch. Solving $\mathrm{d}p/\mathrm{d}t = 0$ gives the non-trivial steady state $\bar{p} = 1 - m/c$, which simply says that the degree at which patches are occupied depends on the ratio of the extinction and colonization parameters. The fraction of empty patches at steady state, i.e., m/c, reflects the ratio of the extinction and the colonization rate. The colonization parameter will be large if the habitats are located close to each other, and the extinction parameter will be small when the habitats are large. This equation therefore formalizes the "Single Large Or Several Small" (SLOSS) discussion on the optimal design of fragmented ecosystems.

The metapopulation model and its application to the SLOSS discussion resembles the famous island theory of MacArthur & Wilson (1967). Island theory describes the number of species in appropriate habitats, i.e., islands, rather than the distribution of a single species. In the classical island theory one ignores the migration between the islands, and considers the migration of species from a large "continent" (or ecosystem) to several small islands located in an area of unsuitable habitat. Considering a continent with N different species one describes the number of species n on an island with

$$\frac{\mathrm{d}n}{\mathrm{d}t} = i(N-n) - dn \ , \tag{12.2}$$

where i is the rate at which each species settles on the island, and where d is the rate at which a species goes extinct from the island. The term $(N-n)$ resembles the $(1-p)$ term of the metapopulation model, and counts only those species that are not present on the island as novel immigrations. The steady state is $\bar{n} = iN/(i+d) < N$, which is a saturation function of the immigration rate i, approaching the maximum number of species $\bar{n} \to N$ when $i \to \infty$ or $d \to 0$. Like in the metapopulation model, the ultimate number of species on the island depends on the ratio of the rates of immigration and extinction. The former will be large if the island is located close to the continent, and the latter will be large when the island is small. Again one can see the application of this model to the SLOSS discussion. Finally, note that the metapopulation model can easily be rewritten for the situations where many small suitable habitats are invaded from a much larger area as

$$\frac{\mathrm{d}p}{\mathrm{d}t} = C(1-p) - mp \ , \tag{12.3}$$

where C reflects the number of migrants invading from the continent, and where all migration between the island has been ignored.

Hanksi (1998) estimated colonization and extinction probabilities for a large population of butterflies in Finland. The colonization rate was estimated from the average distance between suitable habitats, and was written as $c = c_0 \mathrm{e}^{-aD}$, where D is the average distance between the habitats. The extinction rate was estimated from the average size of the habitat, and was written as $m = m_0 \mathrm{e}^{-bA}$ where A is the average area of the preferred habitats. The parameters a and b describe how strongly colonization and extinction depend on the distance and the area size. Substitution of the new functions c and m into Eq. (12.1) delivers that the fraction of habitats occupied by the butterfly approaches $\bar{p} = 1 - (m_0/c_0)\mathrm{e}^{aD-bA}$, which decreases with the distance and increases with the area size. Habitat destruction by removing suitable patches, which increases the average distance D, or by decreasing the size of the habitats, A, are therefore expected to have a similar detrimental effect on the distribution of the butterfly over Finland.

Destruction of suitable habitats

To study the effect of removing a fraction of the suitable habitats on a metapopulation, Nee & May (1992) have generalized Eq. (12.1) into

$$\frac{\mathrm{d}p}{\mathrm{d}t} = cp(P-p) - mp \ , \tag{12.4}$$

where $P = 1 - D$ is the fraction of undamaged habitats, and D is the fraction of destructed habitats. The steady steady of this model is $\bar{p} = P - m/c$. The fraction of empty patches, m/c, therefore remains the same as in the original Levins model, and is independent of P or D. One can now study at what fraction D of habitat destruction the metapopulation is driven to extinction. Mathematically this boils down to solving

$$\bar{p} = 0 = 1 - D - \frac{m}{c} \quad \text{yielding} \quad D = 1 - \frac{m}{c} \ , \tag{12.5}$$

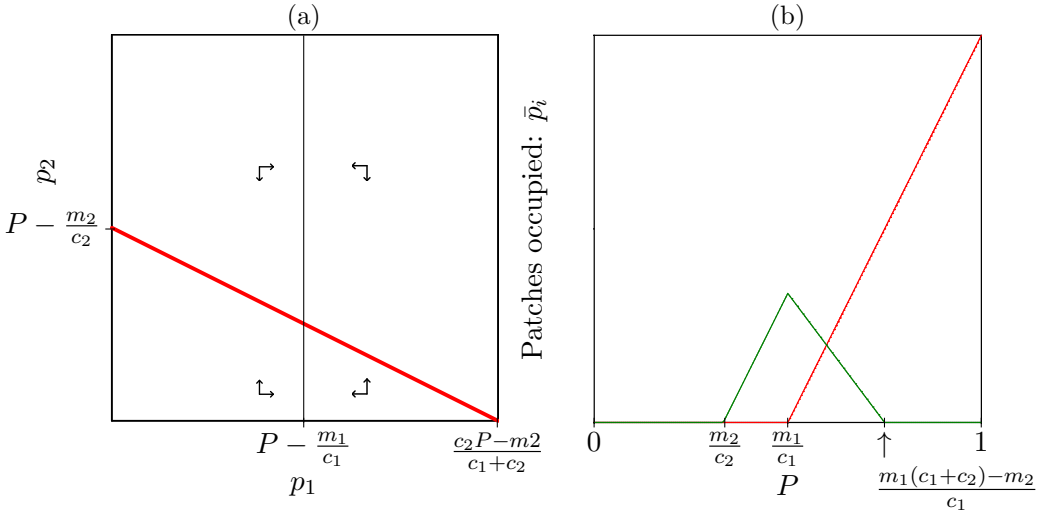

Figure 12.1: The nullclines (a) and the steady states (b) of the two superior species of the Tilman *et al.* (1994) model.

where the critical damage $D = 1 - m/c$ is the same as the fraction of habitats occupied by this species in an undisturbed situation (where $P = 1$). To prevent the extinction of a "rare" species occupying a small fraction $\alpha = 1 - m/c$ of the suitable habitats, one should keep the level of habitat destruction below the same $D = \alpha$ (Nee & May, 1992; Tilman *et al.*, 1994). This seems a strange and unexpected result, but in retrospect one can see that this comes about by the condition that rare species are poor colonizers, and therefore need many patches to survive.

12.2 The Tilman model

Nee & May (1992) and Tilman *et al.* (1994) extended the metapopulation model of Levins (1969) with competition. Tilman *et al.* (1994) considered a large number of species competing with each other in a particular kind of habitat, and recorded the presence or absence of each species over a large number of habitats (or patches). The competition between the species was incorporated in the model by ordering the species by their competitive ability. This is a clever trick that keeps the model simple, and delivers surprising results when one studies the effects of habitat destruction in the model.

Eq. (12.1) was simply extended by writing that p_i is the fraction of patches occupied by species i, and because species are ordered by competitive ability one obtains

$$\frac{\mathrm{d}p_i}{\mathrm{d}t} = c_i p_i \Big(P - \sum_{j=1}^{i} p_j \Big) - m_i p_i - \sum_{j=1}^{i-1} c_j p_i p_j \ , \tag{12.6}$$

where the differences with the original model are (1) the term between the brackets, which is the "perceived" fraction of empty patches, and (2) the final colonization term, which is the chance that a patch occupied by species i is colonized by species j. The sum terms in this model run from $j = 1$ to $j = i$ (and to $i - 1$ in the second term) because of the ordering by competitive ability. For instance, the strongest competitor (for which $i = 1$), will perceive patches occupied by other species as "empty", and will itself never be colonized by other species. Hence, the sum term between the brackets only contains the first species, and the colonization term at the end is ignored. The second species, with $i = 2$, sums the first two between the brackets, and can be

taken over by the first one, and so on. The parameter P in this model is one when there is no habitat destruction, and one can again substitute $P = 1 - D$ to study the effect of destructing a fraction D of the habitats.

Tilman *et al.* (1994) derive the steady state of model by canceling the $p_i = 0$ solution and rewriting the first sum term,

$$\begin{aligned} 0 &= c_i\Big(P - p_i - \sum_{j=1}^{i-1} p_j\Big) - m_i - \sum_{j=1}^{i-1} c_j p_j \ , \\ \bar{p}_i &= P - \frac{m_i}{c_i} - \sum_{j}^{i-1} p_j\Big(1 + \frac{c_j}{c_i}\Big) \ , \end{aligned} \tag{12.7}$$

which for $i = 1$ is indeed identical to the steady state of the Levins (1969) model. The density of the other species is lower than that predicted by the Levins model, because one has to subtract the ratio of the colonization rates times the density of all species that are superior competitors.

To learn about the co-existence of several metapopulation on a shared set of habitats it is instructive to study the first two equations of this model, i.e.,

$$\frac{\mathrm{d}p_1}{\mathrm{d}t} = c_1 p_1(P - p_1) - m_1 p_1 \quad \text{and} \quad \frac{\mathrm{d}p_2}{\mathrm{d}t} = c_2 p_2(P - p_1 - p_2) - m_2 p_2 - c_1 p_1 p_2 \ . \tag{12.8}$$

The nullclines of the model are simple straight lines. Solving $\mathrm{d}p_1/\mathrm{d}t = 0$ gives $p_1 = P - m_1/c_1$, and the p_2 nullcline is given by $p_2 = P - m_2/c_2 - p_1(1 + c_1/c_2)$; see also Eq. (12.7). In a phase space with p_1 on the horizontal, and p_2 on the vertical axis, the former is a vertical line, and the latter is a straight line from $p_2 = P - m_2/c_2$ on the vertical axis to $p_1 = (c_2 P - m_2)/(c_2 + c_1)$ on the horizontal axis (see Fig. 12.1a). This phase plane analysis shows that the two species will co-exist whenever

$$\frac{c_2 P - m_2}{c_1 + c_2} > P - \frac{m_1}{c_1} \ . \tag{12.9}$$

One can directly solve P from this condition, or follow Nee & May (1992) who proposed a convenient analysis by plotting the steady states as a function of the number of patches P. For the first species this is $\bar{p}_1 = P - m_1/c_1$, which is a line with slope one, intersecting the horizontal axis at $P = m_1/c_1$ (see Fig. 12.1b). This repeats the result derived above: the first species is driven to extinction when the total patch density P drops below the steady state number of empty patches m_1/c_1.

In the absence of the first species, the second species has the same steady state expression $\bar{p}_2 = P - m_2/c_2$. Thus, whenever $\frac{m_2}{c_2} < \frac{m_1}{c_1}$ the second species will be present at low values of P where the first species cannot be maintained yet. In the presence of the first species, i.e., when $P > m_1/c_1$, Eq. (12.7) gives the steady state of the second species as

$$\bar{p}_2 = P - \frac{m_2}{c_2} - \bar{p}_1\left(1 + \frac{c_1}{c_2}\right) = \frac{m_1}{c_1}\left(1 + \frac{c_1}{c_2}\right) - \frac{m_2}{c_2} - \frac{c_1}{c_2}P \ , \tag{12.10}$$

which is a straight line with a negative slope $-c_1/c_2$; see Fig. 12.1b. Since the steady state of the inferior species declines with increasing P when the superior species is present, the inferior species can only coexist when its steady state was positive in the absence of the first species. Thus, the second species can therefore only persist in this system if it has better migration parameters, i.e., if $c_2/m_2 > c_1/m_1$. Fig. 12.1b shows that increasing the number of patches P

ultimately drives the second species to extinction. This critical value can be obtained by solving $\bar{p}_2 = 0$. Co-existence is therefore only possible when

$$\frac{m_2}{c_2} < \frac{m_1}{c_1} \quad \text{and} \quad \frac{m_1}{c_1} < P < \frac{m_1(c_1 + c_2) - m_2}{c_1} \ . \tag{12.11}$$

Above we have already seen that one will drive the superior species to extinction when its pristine steady state density $1 - m_1/c_1$ of the suitable habitats is destructed. Suppose now that the two species are co-existing in a pristine environment: what would happen with the second species when a fraction of the habitats were destructed (Nee & May, 1992; Tilman *et al.*, 1994)? One can see from Fig. 12.1b that in the co-existence region $\bar{p}_2$ would increase when P is decreased. At the critical amount of habitat destruction where the first species is driven to extinction, the second species will not go extinct. This requires more damage, i.e., requires that the patch availability is decreased to $P = m_2/c_2$. Although this seems strange, it is a natural result because co-existence required that the second species had better superior migration parameters, which implies that it can better handle the decreased habitat availability.

12.3 Summary

Metapopulation models are used for describing the fraction of habitats occupied by a species, and resemble the classical Island Theory model. Both have been applied in conservation biology. One should be careful with habitat destruction because removing a small fraction of the habitats may drive rare species to extinction.

12.4 Exercises

Question 12.1. Islands in a lake
Consider the metapopulation of shrews living in Finland (Hanksi, 1991). The mice live on many islands in a lake, and migrate between them. Additionally, mice from the large population on the "continent" swim from the borders of the lake to the islands.

a. Combine Eq. (12.1) with Eq. (12.3) into a simple model for the metapopulation of shrews on the islands.
b. Compute the steady state.
c. Will this steady state be stable?

Question 12.2. Population size
Hanksi (1991) extended the metapopulation model of Eq. (12.1) with a population size per patch. His model is difficult and not completely correct because the model was written in terms of the average size of a subpopulation per patch. In this exercise you will stay closer to the original concept of describing the total metapopulation, and will derive a much simpler model. Assuming that all patches have approximately the same size (or writing a "mean field model"), one would have to argue that the carrying capacity of the total population, N, should be proportional to the total number of patched occupied, i.e.,

$$\frac{\mathrm{d}N}{\mathrm{d}t} = rN(1 - \frac{N}{kp}) - dN \ .$$

a. Rewrite the ODE for the patches, i.e., Eq. (12.1), to connect it with the total population size N.
b. Sketch the nullclines in a 2-dimensional phase space.
c. Determine the stability of the steady state(s).
d. If you have not already done so, extend your model for the situation where the extinction rate decreases with the average population size in a patch.
e. Will such a density dependent extinction have a strong impact on the phase space?
f. What do you learn from this?

Question 12.3. Tilman
Consider the first two species of the Tilman *et al.* (1994) model under habitat destruction.
a. Can the second species invade at the critical destruction level $D = 1 - m_1/c_1$?
b. Can one increase the diversity of an ecosystem by habitat destruction?
c. How does the total fraction of occupied patches depend on the habitat destruction?

Chapter 13

Maps

All models considered hitherto have neglected seasonal variation and have all been formulated in differential equations. One area of ecological modeling implements seasonal variation by means of a periodic function, i.e., typically a sine or cosine function, influencing some of the parameters of the model. These periodically forced models will not be covered in this book, but such systems are capable of rich and complicated behavior (Scheffer *et al.*, 1997). Insect populations are strongly influenced by the season, and many of the insect species in the temperate climate zones have a relatively short season in which they are active, and a long period around winter during which they survive as larvae. Because the growth season is short, insect populations are often modeled with maps, or difference equations, that describe the population size in the next year as a function of the population size in the current year. Since the behavioral properties of maps differ significantly from those of ODEs we will first do some theory on maps, and then derive the Beverton-Holt model ourselves from a seasonally reproducing insect population.

13.1 Stability

We will first consider one-dimensional maps for the growth of a single population, i.e.,

$$N_{t+1} = f(N_t) \ , \tag{13.1}$$

where $f()$ is an arbitrary function mapping the population size at time t to a new population size at time $t+1$. Between times t and $t+1$ the population size is undefined, and can be interpreted as the hibernation stage during a winter season. Typical examples of maps used in ecology are

$$f(N) = rN(1 - N/k) \quad \text{and} \quad f(N) = \frac{rN}{1 + N/k} \ , \tag{13.2}$$

which are called the "logistic map" and the "Beverton-Holt" model, respectively. Because we have used similar functions to describe the birth rate in ODEs, we are already familiar with the shape of these two functions. The logistic map is a parabola, which by being non-monotonic assumes that the maximum population size in the next year is attained from an intermediate population size in the current year. Importantly, by intraspecific competition, large populations tend to be mapped into small populations in the next year. The second model is a monotonically increasing Hill function assuming the population size in the next year is a saturation function of the population size in the current year. Below we will derive the Beverton & Holt (1957) model

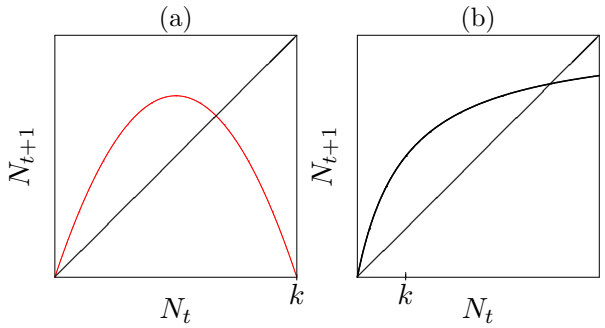

Figure 13.1: Stability of maps. Panel (a) depicts the logistic map, which is a parabola, and Panel (b) shows the saturation function underlying the map of Eq. (13.2)b. The diagonal line is the line at which $N_{t+1} = N_t$. Steady states therefore correspond to the intersections of the map with the diagonal line.

ourselves. The same equation has also been proposed by Maynard Smith & Slatkin (1973) and later by Hassell (1975).

The steady states and the stability properties of maps differ from those of ODEs. To compute the steady state of a map one should not set $f(N)$ to zero, but compute the population size, $\bar{N}$, for which $N_{t+1} = N_t$. To see how one computes the stability of a steady state of a map, one should redo the linearization, i.e.,

$$N_{t+1} = f(N_t) \simeq f(\bar{N}) + \partial_N f(\bar{N})\,(N_t - \bar{N}) = \bar{N} + \lambda h_t \ , \tag{13.3}$$

where we have defined $\lambda = \partial_N f(\bar{N})$ and $h_t = N_t - \bar{N}$. Subtracting $\bar{N}$ from the left hand side and the right hand side one obtains

$$h_{t+1} \simeq \lambda h_t \ , \tag{13.4}$$

because $h_{t+1} = N_{t+1} - \bar{N}$. Thus, like in ODEs, λ remains to be the derivative of the population growth function at the steady state value, $\bar{N}$. The difference with ODEs is that the steady state is not stable when $\lambda < 0$, but when the next size of the perturbance, h_{t+1}, is smaller than the current, h_t. In maps this is the case when $-1 < \lambda < 1$, where for $-1 < \lambda < 0$ the sign of h_t is alternating in time, which corresponds to a dampened oscillation approaching $h_t = 0$. Since λ is the slope of the map at the steady state, one immediately sees an important difference between the two maps in Eq. (13.2). Since the function of Eq. (13.2)b is monotonically increasing, λ is always larger than zero, and the behavior of the map will never be oscillatory. Conversely, the logistic map has a positive slope when $N < k/2$, and a negative slope when $N > k/2$, and should therefore be capable of oscillatory behavior when the steady state is located above $N > k/2$.

A graphic method for finding steady states of maps is to sketch the map, and the diagonal $N_{t+1} = N_t$ in one graph (see Fig. 13.1). The points at which the two lines intersect are steady states. We have learned above that the slope of the map at these intersection points determines the stability of the steady state. For illustration let us determine the stability of the steady state of the logistic map. One solves the steady state from

$$N = rN(1 - N/k) \quad \text{or} \quad \bar{N} = \frac{r-1}{r}\ k \ . \tag{13.5}$$

Because $\partial_N f(N) = r - 2rN/k$ one obtains by substitution of the steady state value that $\lambda = 2 - r$. Since the steady state is stable when $-1 < \lambda < 1$, i.e., when $-1 < 2 - r < 1$, the condition for stability is that $2 - r < 1$ and $-1 < 2 - r$, i.e., that $1 < r < 3$. The requirement that $r > 1$ is trivial because the population cannot maintain itself when the next population size is always smaller than the current one. The instability at $r = 3$ leads to oscillatory behavior: when $r \to 3$

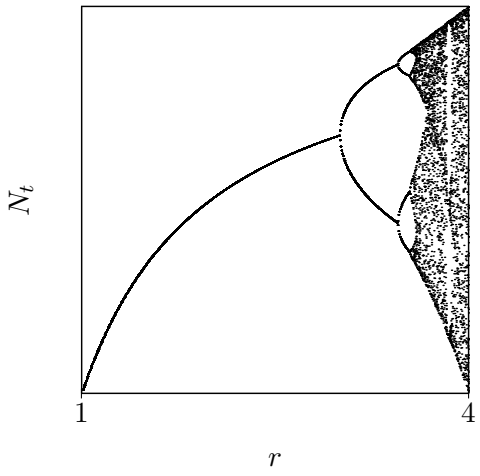

Figure 13.2: The behavior of the logistic map as a function of its natural rate of increase r. For each value of r the map is run for a long time until the attractor is approached. Subsequently the map is run for twenty time steps, and each value of N_t is depicted as a point. For $r < 3$ all points collaps onto the steady state value $\bar{N} = k(r-1)/r$, for $3 < r < 3.45$ N_t oscillates between two values, for $3.45 < r < 3.55$ N_t oscillates between four values, and so on. Note the window of r values where the logistic map has a three point cycle. This led to the famous paper by Li & Yorke (1975) with the title "Period three implies chaos".

the slope $\lambda = 2 - r \to -1$, and the steady state is approached by a dampened oscillation. For $r > 3$ the oscillation is no longer dampened but a stable limit cycle. For $3 < r < 4$ this limit cycle undergoes period doubling giving rise to the famous chaotic behavior of the logistic map (see Fig. 13.2).

The stability of the steady state of the second example in Eq. (13.2) is computed similarly. The steady state is derived from

$$\bar{N} = \frac{rN}{1 + N/k} \quad \text{, i.e.,} \quad \bar{N} = k(r-1) \ , \tag{13.6}$$

and because

$$\partial_N f = \frac{r}{1 + N/k} - \frac{rN/k}{(1 + N/k)^2} \ , \tag{13.7}$$

one obtains for the slope at the steady state $\bar{N}$ that

$$\lambda = \frac{r}{r} - \frac{r(r-1)}{r^2} = \frac{r - (r-1)}{r} = \frac{1}{r} \ . \tag{13.8}$$

Whenever the population can maintain itself, i.e., whenever $r > 1$, the steady state will always be stable.

Oscillatory behavior is therefore not necessarily expected for populations described by maps. This is important because the insect populations that one typically models with maps often have a very large natural rate of increase r, i.e., an insect can lay thousands of eggs. The logistic map has $r = 4$ as the maximum rate of increase; for larger r the population size becomes negative. Finally, note that the second example in Eq. (13.2) generalizes to the Maynard Smith & Slatkin (1973) model

$$N_{t+1} = \frac{rN}{1 + (N/k)^n} \ , \tag{13.9}$$

where the density dependence is a simple inverse Hill function. For $n = 1$ this delivers the Beverton-Holt model considered above. Whenever the exponent, n, of the Hill function becomes larger than one, the function will no longer be monotonic (see Chapter 4), and chaos and oscillations will be possible (Hassell *et al.*, 1976).

13.2 Deriving a map mechanistically

The two examples of maps of Eq. (13.2) have frequently been used for describing seasonal population growth. The logistic map is typically used for convenience, however, and not because one really has data supporting the so crucial humped shape of the map. The chaotic behavior that theoretical ecologists generally attribute to seasonally growing populations could therefore well be an artifact of too easily adopting humped or logistic equations. To develop an opinion of what type of maps would be appropriate we develop the model ourselves (by essentially following the derivation proposed by Beverton & Holt (1957)).

The biology that is typically neglected when populations are described with maps is that seasonal populations do have a season in which they are active, and which could be modeled with a conventional ODE. Think of insects that lay their eggs at the end of the season shortly before they die, and where the new generation hatches from the eggs at the start of the next season. During the season the insects do not reproduce, as all growth is determined by the number of eggs deposited at the end of the season. Density dependent regulation of the population most likely takes place during the season, as the eggs probably have a density independent chance to survive the winter season. It could therefore be that most of the population regulation takes place during a normal continuous part of the year. What we will do next is to derive a map for the seasonal insect population sketched in this paragraph.

Let the population size during the season be described by $n(t)$, where t is the time (e.g., in days) since the start of the season. Let N_j be the population size at the end of the season, where j measures times in years, i.e., $j = 0, 1, 2, \ldots$. For a season length of τ days, one should have in year j that $N_j = n(\tau)$. Assuming that at the end of the season each individual lays g eggs that are expected to survive the winter season, one obtains that at the start of the season $n(0) = gN_{j-1}$ (see Fig. 13.3a).

The main challenge is to write a natural model for the population during the active season. Since there is no reproduction one could assume a straightforward density dependent death model like

$$\frac{\mathrm{d}n}{\mathrm{d}t} = -dn(1 + n/k) \quad \text{with the solution} \quad n(t) = \frac{kn(0)}{k\mathrm{e}^{dt} + n(0)[\mathrm{e}^{dt} - 1]} \ , \tag{13.10}$$

where d is a normal density independent death rate, e.g., due to predation by birds, and the parameter k determines the density dependent death rate (i.e., at $n(t) = k$ the death rate has doubled). For a season of a fixed length of τ days, and a starting number of $n(0) = gN_{j-1}$ the solution becomes

$$N_j = n(\tau) = \frac{kgN_{j-1}}{k\mathrm{e}^{d\tau} + gN_{j-1}[\mathrm{e}^{d\tau} - 1]} \ , \tag{13.11}$$

and because $\mathrm{e}^{d\tau}$ is just a certain value (for which we happen to known that $\mathrm{e}^{d\tau} - 1 > 0$), this can be rewritten into

$$N_{j+1} = \frac{rN_j}{1 + N_j/c} \quad \text{where} \quad r = g\mathrm{e}^{-d\tau} \quad \text{and} \quad c = \frac{k}{g(1 - \mathrm{e}^{-d\tau})} \ . \tag{13.12}$$

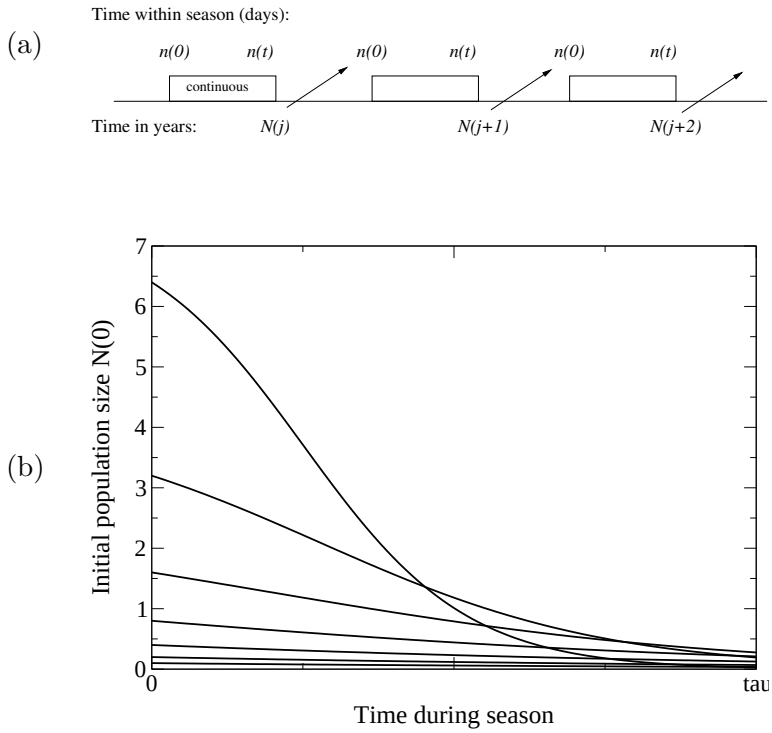

Figure 13.3: Discrete and continuous seasons in an population of insects (a). To obtain a humped relationship between the initial and the final population size trajectories have to cross (b).

This has the form of the Beverton-Holt model that we have studied above, which implies that we expect our seasonal insect population to approach a stable state value over the years, and never be oscillatory or chaotic (see Eq. (13.8)). This does not mean that we predict that insect populations should typically approach a steady state, but demonstrates that we need not expect that seasonal populations readily become chaotic.

An even simpler alternative of Eq. (13.10) is to ignore the density independent death and write

$$\frac{\mathrm{d}n}{\mathrm{d}t} = -dn^2 \quad \text{with the solution} \quad n(t) = \frac{n(0)}{1 + dtn(0)} \ , \tag{13.13}$$

which for a fixed length of the season also assumes the form of the Beverton-Holt model.

The fact that we fail to obtain periodic behavior with a single ODE describing density dependent death during the season seems quite general. We learned that oscillatory behavior can be obtained only when the map has a maximum, and hence has a region where its slope $\lambda < 0$. This can only come about when there is a range of large $n(0)$ values for which the number of individuals, $n(\tau)$, at the end of the season is smaller than what would have survived at intermediate $n(0)$ values. This cannot happen in the one-dimensional phase space of any ODE, because at some point in time the trajectory with a large starting number should cross the one with an intermediate starting number. At this point in time the two trajectories should obey the same derivative, and cannot end differently (see Fig. 13.3b).

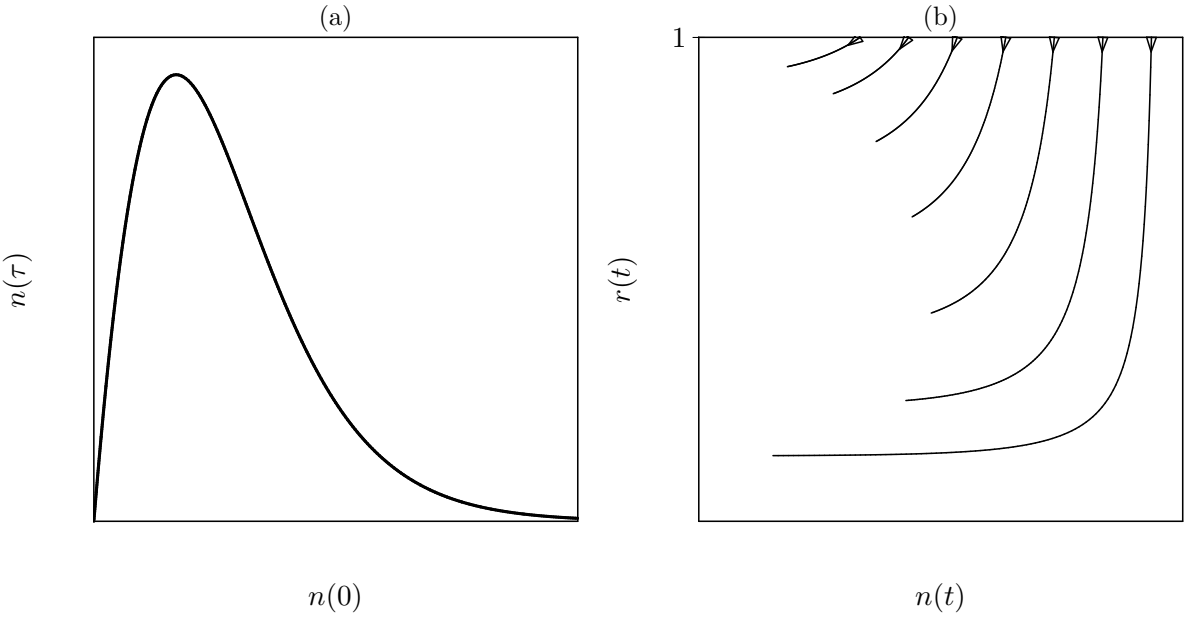

Figure 13.4: The solution of Eq. (13.15) (a) and various simulations of the model of Eq. (13.14) for one season of $\tau = 10$ days, and $c = d = 0.1$ per day, starting at a scaled food density of $r(0) = 1$.

How to obtain oscillations?

As simple one-dimensional death models fail to do the job, we apparently have to do some work to allow for oscillations in biologically realistic maps. One could argue that if a large initial population depletes most of the available food during the early days of the season, that many will die by starvation during the later half of the season. Intuitively, it seems that too large populations could be at a disadvantage, and end up with less survivors than populations of an intermediate size. Since we know this requires a 2-dimensional model one could propose

$$\frac{\mathrm{d}r}{\mathrm{d}t} = -crn \quad \text{and} \quad \frac{\mathrm{d}n}{\mathrm{d}t} = -dn/r \ , \tag{13.14}$$

where r is the amount of resource, c is the feeding rate of the insects on the resource, and d/r is the *per capita* death rate of the insects. It is somewhat disturbing to divide by the resource density r in $\mathrm{d}n/\mathrm{d}t$, but because r will always remain larger than zero, and because we need a model that can be solved analytically, this seems allowable here. One can scale the initial food availability to $r(0) = 1$, such that d is a normal *per capita* death rate when food is abundant, which increases rapidly when the amount of food declines. Because we have deliberately kept the model simple one can still obtain the solution

$$n(t) = f[n(0)] = \frac{cn(0) + d}{c + d\mathrm{e}^{t[cn(0)+d]}/n(0)} \ . \tag{13.15}$$

Plotting the population size at the end of the season, i.e., $n(\tau)$, as a function of the initial population size, $n(0)$, one obtains a humped shape for $f[n(0)]$ because Eq. (13.15) is an increasing function when $n(0)$ is small, while it approaches zero when $n(0)$ is large, i.e.,

$$\lim_{n(0)\to 0} f[n(0)] = \mathrm{e}^{-d\tau} n(0) \quad \text{and} \quad \lim_{n(0)\to\infty} f[n(0)] = 0 \ . \tag{13.16}$$

Substituting parameter values indeed reveals a humped relationship (see Fig. 13.4a), and simulations of the 2-dimensional model confirm that large population have fewer survivors because they deplete the resource faster (see Fig. 13.4b).

13.3 Eggs produced during the season

Geritz & Kisdi (2004) also derived maps from populations competing within a continuous season. Working with models where eggs are produced during the season there were able to provide a mechanistic underpinning of various different maps, such as the logistic map, the Beverton-Holt model, and the Ricker model. Their basic model was a single ODE for the number of eggs produced over the season. The number of eggs at the end of the season depended on the total number of adults and the availability of resource during the season, and they easily obtain a non-monotonic relation between the initial number of adults and the final number of eggs. Starting with few adults few eggs are produced. Starting with too many adults the resource availability is low, and again few eggs are produced. The maximum number of eggs is produced when the season starts with an intermediate number of adults. Eggs also "die" during the season.

One example of their models has a a resource growing logistically:

$$\frac{\mathrm{d}R}{\mathrm{d}t} = rR(1-R) - bRA \quad \text{and} \quad \frac{\mathrm{d}E}{\mathrm{d}t} = cbRA - dE \ , \tag{13.17}$$

where R is the resource, E is the egg density, and A is the fixed number of adults the season starts with, e.g., for a season of length τ one would write $A_j = \alpha E(\tau)_{j-1}$. Assuming that the dynamics of the resource is fast compared to that of the eggs, Geritz & Kisdi (2004) simplified by writing the quasi state state of the resource, $R = 1 - bA/r$, obtaining for the eggs

$$\frac{\mathrm{d}E}{\mathrm{d}t} = cb(1-bA/r)A - dE \ . \tag{13.18}$$

Since $cb(1-bA/r)A$ does not depend on time, t, this is a source/death model similar to those solved in Chapter 2, i.e.,

$$E(t) = \frac{cb(1-bA/r)A}{d}\left(1 - \mathrm{e}^{-dt}\right) \ . \tag{13.19}$$

For a fixed length of the season of τ days $E(\tau)$ is therefore completely defined by the parameters and the number of adults A. Defining a map for the number of adults A_{j+1} in year $j+1$ as a function of those in year j, one obtains

$$A_{j+1} = \alpha E(\tau)_j = \rho A_j[1 - A_j/K] \ , \tag{13.20}$$

where $\rho = \alpha cb[1 - \mathrm{e}^{-d\tau}]/d$ and $K = r/b$, which is the conventional logistic map. Taking non-logistic growth functions of the resource other maps were obtained (Geritz & Kisdi, 2004); see the exercises.

The within season models studied by Geritz & Kisdi (2004) provide a non-monotonic map with just one ODE, whereas we needed at least two ODEs to obtain this with the density dependent death model of Eq. (13.10). How can this be? The simple reason is that in the model of Eq. (13.10) the information transferred between the years is an *initial* condition, i.e., $n(0)$ is the number of adults hatching from the eggs produced the year before. In the models of Geritz & Kisdi (2004) the number of adults in the current year is a *parameter* set by the within season dynamics of the previous year. The problem that trajectories cannot cross if just the initial condition is different (see Fig. 13.3) therefore never arises: if the continuous dynamics in a season are parameterized by the previous year it is perfectly possible to have a humped relation between the initial population size and the final population size. An interesting question now is if we can identify populations where the information transfer between the years goes via an initial condition (e.g., the number of eggs) or via a parameter (e.g., a fixed number of adults). It is again somewhat disturbing that such a technical difference seems so important for the expected behavior of the population.

13.4 Summary

Oscillations and chaos are by no means the expected behavior of seasonally reproducing populations. Periodic behavior or chaos is not difficult to obtain, but we had to do work to obtain this when the information transfer between the years was just an initial condition. Finding chaos or oscillations by modeling populations with an arbitrary humped map could well be artificial, and one basically needs evidence, or a good argument, to use a humped survival function.

13.5 Exercises

Question 13.1. Geritz & Kisdi (2004)
Follow the procedure of Geritz & Kisdi (2004) explained in this Chapter to show that the Gomperz equation for population growth, i.e., $\mathrm{d}R/\mathrm{d}t = rR(1-\ln[R]) - bRA$, delivers the Ricker map, $N_{t+1} = aN_t\mathrm{e}^{-bN_t}$.

Question 13.2. Insect population
In the model of Eq. (13.14) the death rate of the insects will go the infinity when the amount of resource approaches zero. This was done to keep the model simple, such that it remained feasible to obtain a solution.

a. Write a more realistic version of Eq. (13.14).

b. Study the model numerically to see if the humped relationship between $n(\tau)$ at the end of the season and $n(0)$ at the start of the season remains a possibility. Begin with studying one season with various initial values of $n(0)$ (and keep $r(0) = 1$).

c. On the website you will find a file `discreteSeason.R` as an example of the seasonal population of Eq. (13.14). Try to obtain oscillations and/or chaos in your extension of this model.

Question 13.3. Periodic forcing
Instead of writing maps for seasonal populations, one can also change parameter values with a periodic function to represent seasonality. Extend the Monod saturated algae zooplankton model of Chapter 6 with a seasonal variation of the birth rates to model the bloom of algae in the spring (Scheffer *et al.*, 1997). In `grind.R` one would write something like:

```
b <- b0 + e*(sin(2*3.1416*(t-Delta)/365))
dA  <- b*A*(1-A/k) - d*A ....
```

where the paramater `Delta` can be used to shift the peak of the seasonal variation to the appropriate time of the year, and the parameter `e` defines the amplitude of the variation around the average value `b0` (see the file `season.R`).

Chapter 14

Bifurcation analysis

In several chapters of this course we have encountered examples where the properties of a steady state changes at some critical parameter value. A good example is the steady state of the Monod saturated predator prey model which changes stability precisely when the vertical predator nullcline intersects the top of the parabolic prey nullcline. We have seen that at this "Hopf bifurcation point" the stability of the steady state is carried over to a stable limit cycle. In the same model there was another bifurcation point when the predator nullcline crosses the carrying capacity of the prey. This is a so-called "transcritical bifurcation" at which the presence of the predator is determined. In ODE models there are only four different types of bifurcations that can happen if one changes a single parameter. This chapter will illustrate all four of them and explain each of them in simple phase plane pictures.

Bifurcation diagrams depict what occurs when one changes a parameter, and therefore provide a powerful graphical representation of the different behaviors a model may exhibit for different values of its parameters. Bifurcation diagrams are typically made with special purpose software tools (like MatCont or XPPAUT); `Grind.R` has a fairly primitive algorithm for continuing steady states. In the exercises you will be challenged to sketch a few bifurcation diagrams with pencil and paper.

Several other bifurcations may occur if one changes two parameters at the same time. These can be summarized in 2-dimensional bifurcation diagrams, which can provide an even better overview of the possible behaviors of a model. Such 2-dimensional bifurcations will not be discussed here, and we refer you to books or courses on bifurcation analysis.

14.1 Hopf bifurcation

At a Hopf bifurcation a limit cycle is born from a spiral point switching stability. This was already discussed at length in Chapter 6 for models with a saturated functional response. Fig. 14.1 depicts the nullclines of a predator prey model with a sigmoid functional response for several different values of the death rate, d, of the predator N. In Chapter 6 we already calculated for the model

$$\frac{\mathrm{d}R}{\mathrm{d}t} = rR(1-R/K) - \frac{bR^2N}{h^2+R^2} \quad \text{and} \quad \frac{\mathrm{d}N}{\mathrm{d}t} = \frac{cbNR^2}{h^2+R^2} - dN \ , \tag{14.1}$$

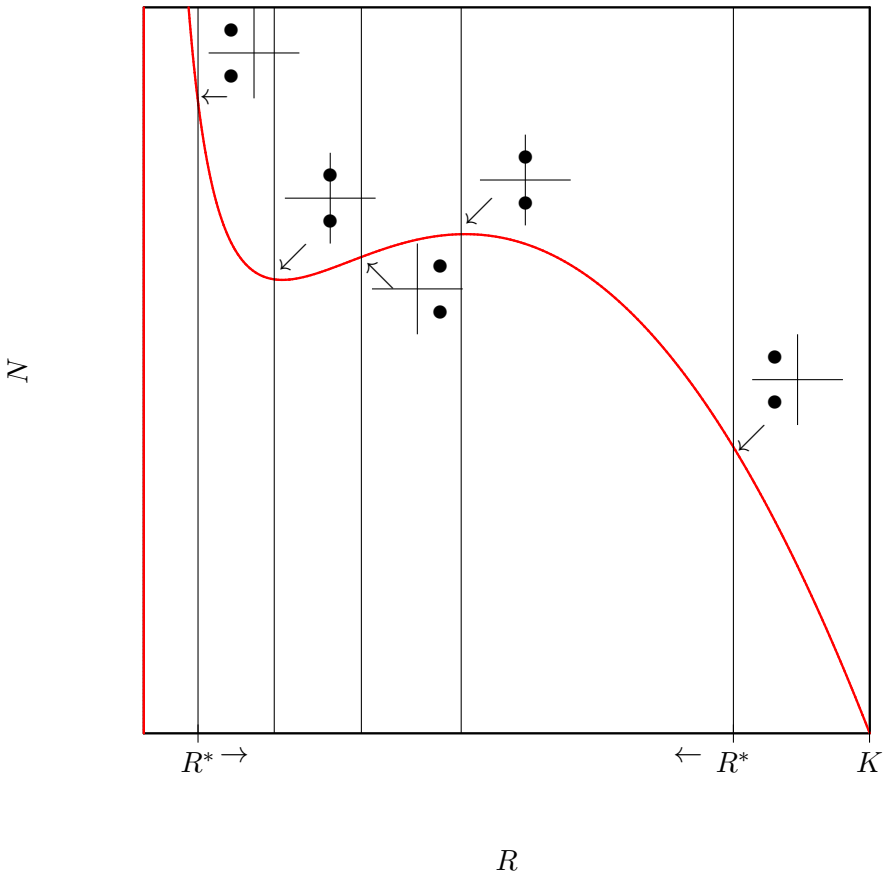

Figure 14.1: Two Hopf bifurcations in the sigmoid predator prey model. The vertical lines depict the $\mathrm{d}N/\mathrm{d}t = 0$ nullcline for various values of $R^* = \frac{h}{\sqrt{R_0-1}}$. The "Argand diagrams" depict the eigenvalues by plotting the real part on the horizontal, and the imaginary part on the vertical axis (see also Fig. 18.8). Hopf bifurcations corresponds to a complex pair moving through the imaginary axis.

that the non-trivial predator nullcline is a vertical line located at the prey density $R = \sqrt{\frac{h^2}{cb/d-1}} = h/\sqrt{R_0-1}$. Thus by changing the predator death rate d one moves the predator nullcline, and because the predator death rate is not part of the ODE of the prey, the prey nullcline remains identical.

First consider values of the death rate d in Fig. 14.1 for which the predator nullcline is located at the right side of the top of the humped prey nullcline. The graphical Jacobian is

$$A = \begin{pmatrix} -a & -b \\ c & 0 \end{pmatrix} \quad \text{such that} \quad \mathrm{tr} = -a < 0 \quad \text{and} \quad \det = bc > 0 \; . \tag{14.2}$$

Close to the top of the prey nullcline the discriminant of this matrix, $D = a^2 - 4bc$, will become negative, and the steady state is a stable spiral point with eigenvalues $\lambda_\pm = -a \pm \mathrm{i}b$. (Below we will see that the same steady state will be a stable node when the nullcline intersects in the neighborhood of the carrying capacity.) Decreasing the parameter d the predator nullcline is shifted to the left, and will cross through the top of the prey nullcline. When located left of this top the graphical Jacobian is

$$A = \begin{pmatrix} a & -b \\ c & 0 \end{pmatrix} \quad \text{such that} \quad \mathrm{tr} = a > 0 \quad \text{and} \quad \det = bc > 0 \; . \tag{14.3}$$

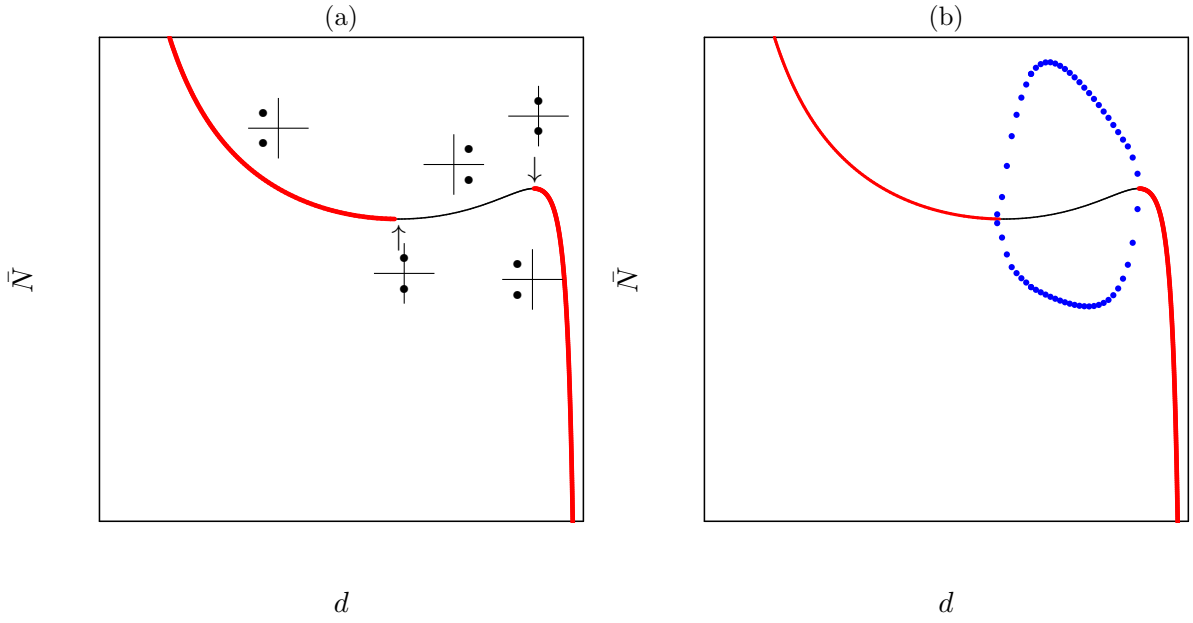

Figure 14.2: A bifurcation diagram with the two Hopf bifurcations of Fig. 14.1. The circles in panel (b) depict the stable limit cycle that exist between the two Hopf bifurcations for many different values of the parameter d.

Close to the top the discriminant, $D = a^2 - 4bc = \mathrm{tr}^2 - 4\det$, will remain to be negative, and the steady state is an unstable spiral point.

For the critical value of d where the nullcline is located at the top, i.e., at $(K-h)/2$ (see Chapter 6) the graphical Jacobian is

$$A = \begin{pmatrix} 0 & -b \\ c & 0 \end{pmatrix} \quad \text{such that} \quad \mathrm{tr} = 0 \quad \text{and} \quad \det = bc > 0\ . \tag{14.4}$$

The imaginary eigenvalues $\lambda_\pm = \pm \mathrm{i}\sqrt{bc}$ have no real part and correspond to the structurally unstable equilibrium point of the Lotka Volterra model lacking a carrying capacity of the prey (see Eq. (5.11)). Summarizing, at a Hopf bifurcation a complex pair of eigenvalues moves through the imaginary axis. At the bifurcation point the steady state has a neutral stability, and a limit cycle is born.

Fig. 14.1 has little diagrams displaying the nature of the eigenvalues in so-called "Argand diagrams". These diagrams simply depict the real part of an eigenvalue on the horizontal axis, and the imaginary part on the vertical axis (see Fig. 18.8). In these diagrams a complex pair of eigenvalues is located at one specific x-value with two opposite imaginary parts, and a real eigenvalue will be a point on the horizontal axis. The Hopf bifurcation can neatly be summarized as a complex pair moving horizontally through the vertical imaginary axis (see Fig. 14.1).

This is summarized in the bifurcation diagram of Fig. 14.2 which depicts the steady state value of the predator as a function of its death rate d. Stable steady states are drawn as heavy lines, and unstable steady states as light lines. We have chosen to have the predator on the vertical axis to facilitate the comparison with the phase portrait of Fig. 14.1, which also has the predator on the vertical axis (note that if we had chosen the prey on the vertical axis the steady state would be a line at $\bar{R} = h/\sqrt{R_0 - 1}$). Sometimes one depicts the "norm", i.e., $N^2 + R^2$, on the vertical axis, but this all remains rather arbitrary because it is not so important what is

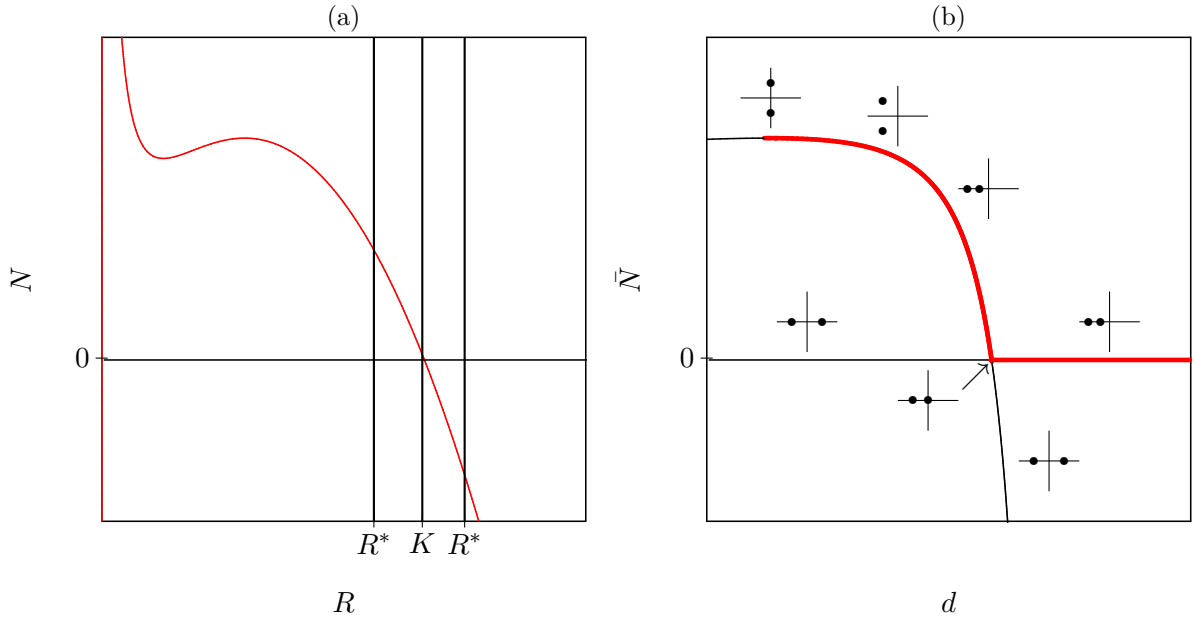

Figure 14.3: The phase space for three values of d around a transcritical bifurcation (a), and the bifurcation diagram (b) of a transcritical bifurcation with d as the bifurcation parameter on the horizontal axis.

exactly plotted on the vertical axis as long as it provides a measure of the location of the steady state. The bifurcation diagram displays another Hopf bifurcation that occurs when the predator nullcline goes through the minimum of the prey nullcline. Between these critical values of d there exits a stable limit cycle, of which we depict the amplitude by the bullets in Fig. 14.2b. Decreasing d the limit cycle is born at the top and dies at the bottom of the prey nullcline, increasing d this would just be the other way around. Fig. 14.2 does provide a good summary of the behavior of the model as a function of the death rate d.

In Fig. 14.2b the amplitude of limit cycle is depicted by the bullets reflecting predator densities at some predefined prey density. Conventionally closed circles are used to depict stable limit cycles, and open circles are used for unstable limit cycles (that we have not discussed explicitly in this book; but there is one in Fig. 6.7d). To depict and study limit cycles one typically plots the predator value when the limit cycles crosses through a particular prey value. Such a prey value is called a Poincaré section, and on this Poincaré plane one can define the limit cycle as a map, mapping one point on the section to the next crossing by the limit cycle. The stability of the limit cycle is then determined from the "Floquet multipliers" of this map. This will not be explained any further in this book.

14.2 Transcritical bifurcation

If one increases the death rate d in the same model, the predator nullcline moves to the right. As long as this nullcline remains left of the carrying capacity the non-trivial steady state will remain stable. However, at one specific value of d it will change from a stable spiral into a stable node. In the Argand diagram this means that the complex pair collapses into a single point on the horizontal axis, after which the eigenvalues drift apart on the horizontal (real) axis (see Fig. 14.3). When the predator nullcline is about to hit the carrying capacity, one can be sure the

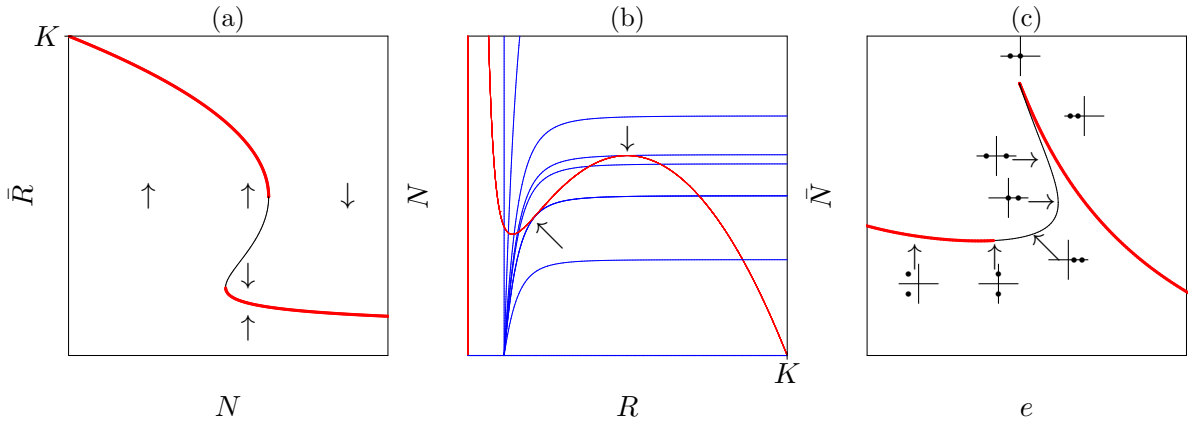

Figure 14.4: The bifurcation diagram of the saddle node bifurcations in Eq. (14.1)a with a fixed number of predators N as a bifurcation parameter, and the phase space (b) and bifurcation diagram (c) of the full model of Eq. (14.5) with the density dependent death rate e as a bifurcation parameter. The phase space in (b) is drawn for several values of e, and the arrows denote the two saddle-node bifurcations.

steady state has become a stable node, i.e., it will have two real eigenvalues smaller than zero.

Increasing d further leads to a transcritical bifurcation at $K = h/\sqrt{R_0 - 1}$. Here the stable node collapses with the saddle point $(\bar{N}, \bar{R}) = (K, 0)$. After increasing d further the saddle point becomes a stable node, and the non-trivial steady state becomes a saddle point located at a negative predator density. At the bifurcation point one of the eigenvalues goes through zero (see Fig. 14.3b), which again corresponds to the structurally unstable neutral stability. Transcritical bifurcations typically take place in a situation where the steady state value of one of the variables becomes zero, i.e., correspond to situations where one of the trivial steady states changes stability. Because in biological models a population size of zero often corresponds to an equilibrium, transcritical bifurcations are very common in biological models.

14.3 Saddle node bifurcation

The saddle-node bifurcations that occur in the sigmoid predator prey model of Eq. (14.1) are famous because of their interpretation of catastrophic switches between rich and poor steady states that may occur in arid habitats like the Sahel zone (Noy-Meir, 1975; May, 1977; Rietkerk & Van de Koppel, 1997; Scheffer *et al.*, 2001; Scheffer, 2009; Hirota *et al.*, 2011; Veraart *et al.*, 2012). To illustrate this bifurcation one can treat the predator density as a parameter, representing the number of cattle (herbivores) that people let graze in a certain habitat. This reduces the model of Eq. (14.1) to the $\mathrm{d}R/\mathrm{d}t$ equation. The steady states of this 1-dimensional model are depicted in Fig. 14.4a with the number of herbivores, N, as a bifurcation parameter plotted on the horizontal axis. Because this parameter is identical to the predator variable plotted on the vertical axis of the phase spaces considered before, these steady states simply correspond to the $\mathrm{d}R/\mathrm{d}t = 0$ nullcline. The bifurcation diagram shows two saddle-node bifurcations (see Fig. 14.4a). At some critical value of the herbivore density on the upper branch, corresponding to a rich vegetation, disappears. At intermediate herbivore densities the vegetation can be in one of two alternative steady states, that are separated by an unstable branch (see Fig. 14.4a). This bifurcation diagram has the famous hysteresis where, after a catastrophic collapse of the vegetation, one has to sell a lot of cattle before the vegetation recovers (Noy-Meir, 1975; May, 1977; Rietkerk & Van de Koppel, 1997; Scheffer *et al.*, 2001; Scheffer, 2009).

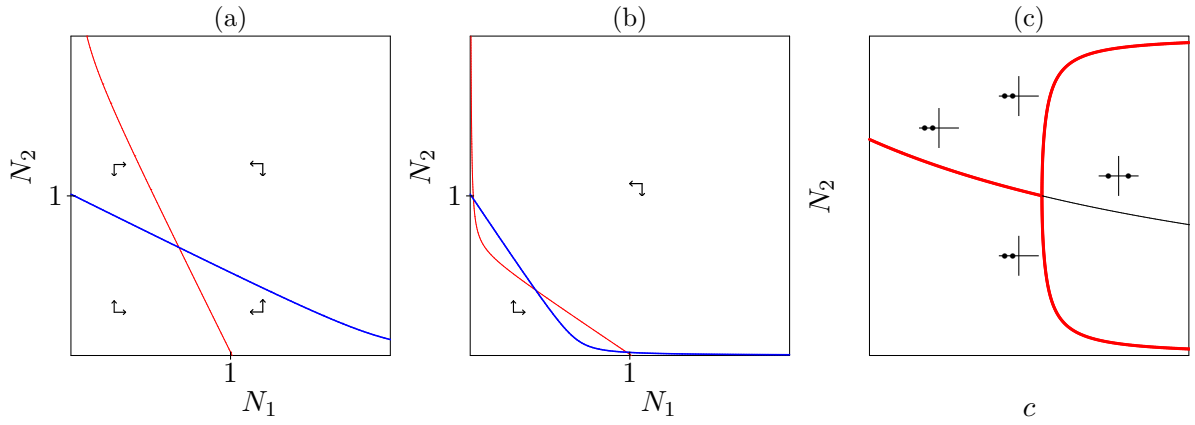

Figure 14.5: The Pitchfork bifurcation of the Lotka Volterra competition model. Panel (a) and (b) show the phase spaces for $c < 1$ and $c > 1$, and Panel (c) shows the bifurcation diagram.

To show a more complicated bifurcation diagram with a Hopf bifurcation, and two different saddle-node bifurcations in the same predator prey model, we extend Eq. (14.1) with direct interference competition between the predators, i.e.,

$$\frac{\mathrm{d}N}{\mathrm{d}t} = \frac{cbNR^2}{h^2 + R^2} - dN - eN^2 \ . \tag{14.5}$$

To illustrate the saddle node bifurcations we will study the model as a function of the competition parameter e, and will sketch a bifurcation diagram with e on the horizontal axis (see Fig. 14.4).

First, choose a value of the death rate, d, such that the predator nullcline intersects at the left of the valley in the prey nullcline (see Fig. 14.4a). For $e = 0$ there is a single stable steady state. Increasing e the predator nullcline will bend because the predator nullcline can be written as the sigmoid function

$$N = \frac{(cb/e)R^2}{h^2 + R^2} - d/e \ , \tag{14.6}$$

intersecting the horizontal axis at the now familiar $R^* = h/\sqrt{R_0 - 1}$. The prey nullcline remains the same because it does not depend on the e parameter. By increasing the curvature with e, this low steady state first undergoes a Hopf bifurcation in the valley of the prey nullcline (see Fig. 14.4b & c). Then the predator nullcline will hit the prey nullcline close its top (see the arrow), which creates two new steady states at a completely different location in phase space. Increasing e a little further leads to the formation of two steady states around this first intersection point (see the other arrow). One is a saddle point and the other a unstable node (see Fig. 14.4c). A "saddle node" bifurcation is a catastrophic bifurcation because it creates (or annihilates) a completely new configuration of steady states located just somewhere in phase space.

14.4 Pitchfork bifurcation

Thus far we have discussed three bifurcations, i.e., the Hopf, transcritical, and saddle node bifurcation, and we could all let them occur in a conventional predator prey model. The fourth, and final, bifurcation is called the pitchfork bifurcation, and can be demonstrated from the scaled competition model of Eq. (9.29) extended with a small immigration term:

$$\frac{\mathrm{d}N_1}{\mathrm{d}t} = i + rN_1(1 - N_1 - cN_2) \quad \text{and} \quad \frac{\mathrm{d}N_2}{\mathrm{d}t} = i + rN_2(1 - N_2 - cN_1) \ . \tag{14.7}$$

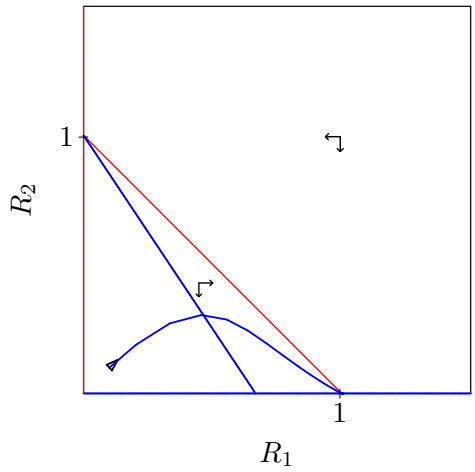

Figure 14.6: The nullclines of the two prey species of Eq. (14.8) in the absence of the predator. The curved line is a trajectory.

Whenever the competition parameter c is smaller than one, the species are hampered more by intraspecific competition than by interspecific competition, and they will co-exist in a stable node (see Fig. 14.5a), and there will be one stable steady state. Increasing c above one will change this node into the saddle point corresponding to the unstable founder controlled competition (see Fig. 14.5b). In between these two cases there is a bifurcation point of c, where one real eigenvalue goes through zero (see Fig. 14.5c). Because of the hyperbolic nature of the nullclines, one can see that when the non-trivial steady state becomes a saddle, the nullclines form new steady states around the two carrying capacities. These new states are stable nodes (see Fig. 14.5b & c). In the bifurcation diagram this is depicted as two branches, one for the stable node becoming a saddle point, and one for the stable nodes born at the bifurcation point. Because of the shape of the solutions in this bifurcation diagram this is called a pitchfork bifurcation.

Both the pitch fork bifurcation and the Hopf bifurcation have mirror images. At a so-called subcritical Hopf bifurcation point an unstable limit cycle is born from an unstable spiral point becoming stable. In a subcritical pitchfork bifurcation, an unstable branch of two outward steady states encloses a stable branch in the middle. Both will not further be discussed here.

14.5 Period doubling cascade leading to chaos

Having covered all possible bifurcations of steady states in ODE models we will illustrate one bifurcation that limit cycles may undergo when one parameter is changed, i.e., the period doubling bifurcation. This bifurcation will again be explained by means of a simple example, because it occurs in a large variety of models (including maps, see Fig. 13.2). The bifurcation is interesting because a cascade of period doubling bifurcations is a route to chaotic behavior. In ODE models we have discussed two types of attractors: stable steady states and stable limit cycles. A chaotic attractor, or strange attractor, is a third type of attractor that frequently occurs in ODE models (with at least three variables).

The example is taken from Yodzis (1989) and is a model with two prey species that are eaten

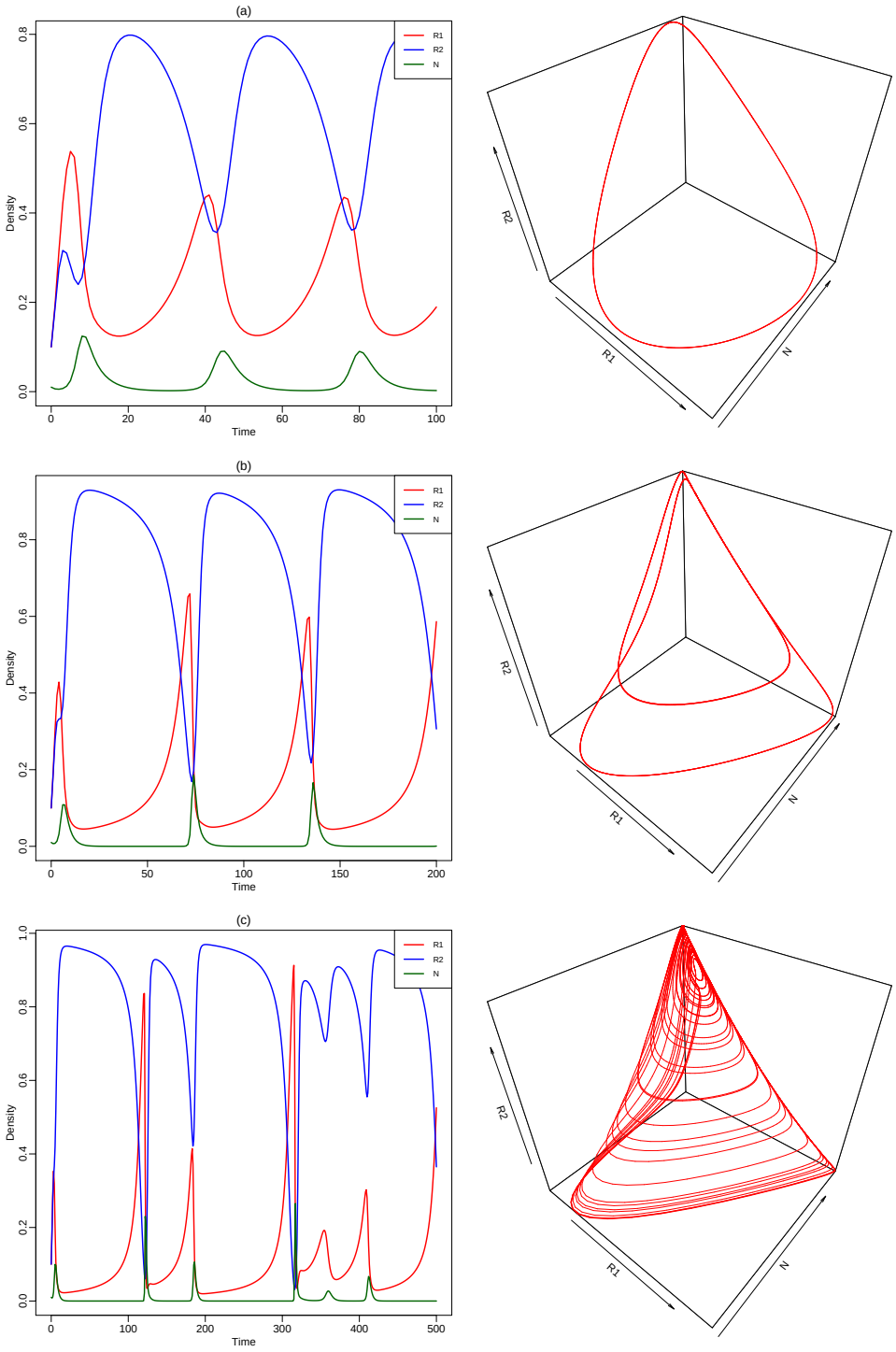

Figure 14.7: Period doubling cascade of the limit cycle of Eq. (14.8). In Panel (a) the model behavior is a simple limit cycle, in Panel (b) the limit cycle makes two loops before returning to the same point, in Panel (c) we see a chaotic attractor. This Figure was made with the file `rrn.R`.

by a single predator

$$\begin{aligned}
\frac{\mathrm{d}R_1}{\mathrm{d}t} &= R_1(1 - R_1 - \alpha_{12}R_2) - a_1R_1N \ , \\
\frac{\mathrm{d}R_2}{\mathrm{d}t} &= R_2(1 - R_2 - \alpha_{21}R_1) - a_2R_2N \ , \\
\frac{\mathrm{d}N}{\mathrm{d}t} &= N(ca_1R_1 + ca_2R_2 - 1) \ ,
\end{aligned} \tag{14.8}$$

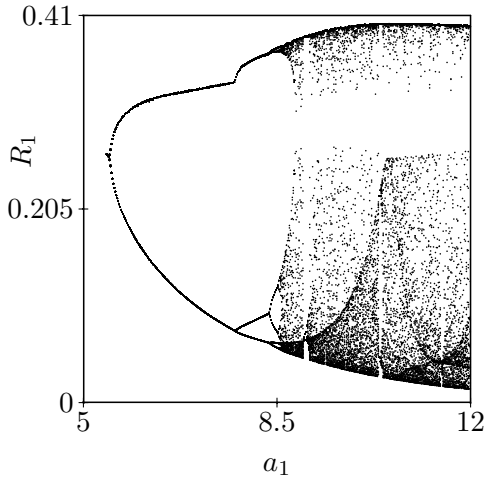

Figure 14.8: Period doubling cascade of the limit cycle of Eq. (14.8) illustrated by plotting 200 values of R_1 obtained for many different values of a_1. The values of R_1 are recorded when the trajectory crosses a Poincaré plane located around $R_2 = 0.8$. Note how similar this is to the bifurcation diagram of the Logistic map (Fig. 13.2).

with simple mass-action predation terms. Time is scaled with respect to the death rate of the predator, and both carrying capacities have been scaled to one. Setting the parameters $\alpha_{12} = 1$ and $\alpha_{21} = 1.5$ the prey species exclude each other in the absence of the predator (see Fig. 14.6). The behavior of the model is studied by varying the predation pressure, a_1, on the winning species. By setting $a_2 = 1$ and $c = 0.5$, i.e., $ca_2 = 0.5$, the model is designed such that the predator cannot survive on R_2 alone. For $3.4 \leq a_1 \leq 5.5$ one obtains a stable steady state where all three species co-exist. Around $a_1 = 5.5$ this steady state undergoes a Hopf bifurcation, and a stable limit cycle is born. (Note that at $a_1 = 3.4$ a transcritical bifurcation allows the second prey to invade (because the first one suffers sufficiently from the predation), and that at $a_1 = 2$ a second transcritical bifurcation occurs when the predator can invade.)

Fig. 14.7 shows what happens if a_1 is increased further. For $a_1 = 6$ there is a simple stable limit cycle that was born at the Hopf bifurcation (see Fig. 14.7a). At $a_1 = 8$ this limit cycle makes two rounds before returning to its starting point: the period has approximately doubled at a period doubling bifurcation somewhere between $6 < a_1 < 8$. This repeats itself several times, and at $a_1 = 10$ the system is already chaotic (see Fig. 14.8).

Chaotic behavior is defined by two important properties:

1. An extreme sensitivity for the initial conditions. An arbitrary small deviation from a chaotic trajectory will after sufficient time expand into a macroscopic distance. This is the famous "butterfly" effect where the disturbance in the air flow caused by a butterfly in Africa flying to the next flower causes a rainstorm in Europe after a week.
2. A fractal structure: a strange attractor has a layered structure that will appear layered again when one zooms in (e.g., see Fig. 13.2 and Fig. 14.8).

The first property is obviously important for the predictability of ecological models. It could very well be that one will never be able to predict the precise future behavior of several ecosystems (like we will never be able to predict the weather on June 17 in the next year). This sensitivity comes about from the "folding" and "stretching" regions in strange attractors where many trajectories collapse and are torn apart again.

14.6 Summary

Varying a single parameter of an ODE model its steady states may undergo four different bifurcations. Some are catastrophic because they involve a large jump in phase space. Bifurcation diagrams provide an excellent summary of the possible behaviors of a model. We have discussed chaotic behavior to demonstrate that it is one of the common and expected behaviors of simple ecological models. Despite being strange it is a normal behavior.

14.7 Exercises

Question 14.1. Biomanipulation
In Chapter 15 you studied a model with zooplankton, algae, and a fixed population of fish. Sketch the bifurcation diagram of the model with the carrying capacity K on the horizontal axis.

Chapter 15

Numerical phase plane analysis

Most phase portraits in this book were made with a computer program called GRIND, for GReat INtegrator Differential equations. In this course you will work with an R-script called `grind.R` that is somewhat easier to use, and can perform very similar phase plane analysis. Thanks to the R-packages `deSolve` and `rootSolve` developed by Karline Soetaert and colleagues (Soetaert & Herman, 2009; Soetaert *et al.*, 2010; Soetaert, 2009), it was relatively easy to copy most of GRIND's capabilities into R. People liking R may also like this simple interface to phase plane analysis. Thanks to their `FME` package (Soetaert & Petzoldt, 2010), it was also feasible to extend GRIND with non-linear parameter estimation. This resulted in an R-script `grind.R` defining five easy-to-use functions:

- `run()` integrates a model numerically and provides a time plot or a trajectory in the phase plane,
- `plane()` draws nullclines and can provide a vector field or phase portrait,
- `newton()` finds steady states (using the Newton-Raphson method) and can provide the Jacobian with its eigenvalues and eigenvectors.
- `continue()` performs parameter continuation of a steady state, providing a bifurcation diagram,
- `fit()` fits a model to data by estimating its parameters, and depicts the result in a timeplot.

The `run()` function calls `ode()` from the `deSolve` library, the `fit()` function calls `modFit` from the `FME` library, and `newton()` and `continue()` call `steady()` from the `rootSolve` library. One can get help on the `grind.R` functions by typing `args(run)`, etcetera. For the library functions one can get more help by typing `?ode`, etcetera. The following sections are tutorials illustrating the usage of the `grind.R` functions.

The best way to get started is to download our example analyzing the Lotka Volterra model. We will work in the RStudio environment, which has a window for the code, a console window, a window defining the environment, and a help or graphics window. Download the `grind.R` and the `lotka.R` files from the `http://tbb.bio.uu.nl/rdb/te/models/` webpage, store them in a local directory, and open both of them via the `File` menu. Both will be tabs in the code window. It may anyway be useful to set the working directory to the folder where your R-codes are stored (`Set working directory` in the `Session` menu of RStudio). Files with then be opened and saved in that directory.

First "source" the `grind.R` file (button in right hand top corner) to define the five functions. (In case you get an error message like "Error in library(deSolve): there is no package called deSolve", the Soetaert libraries have to be installed by using `Install Packages` in the `Tools`

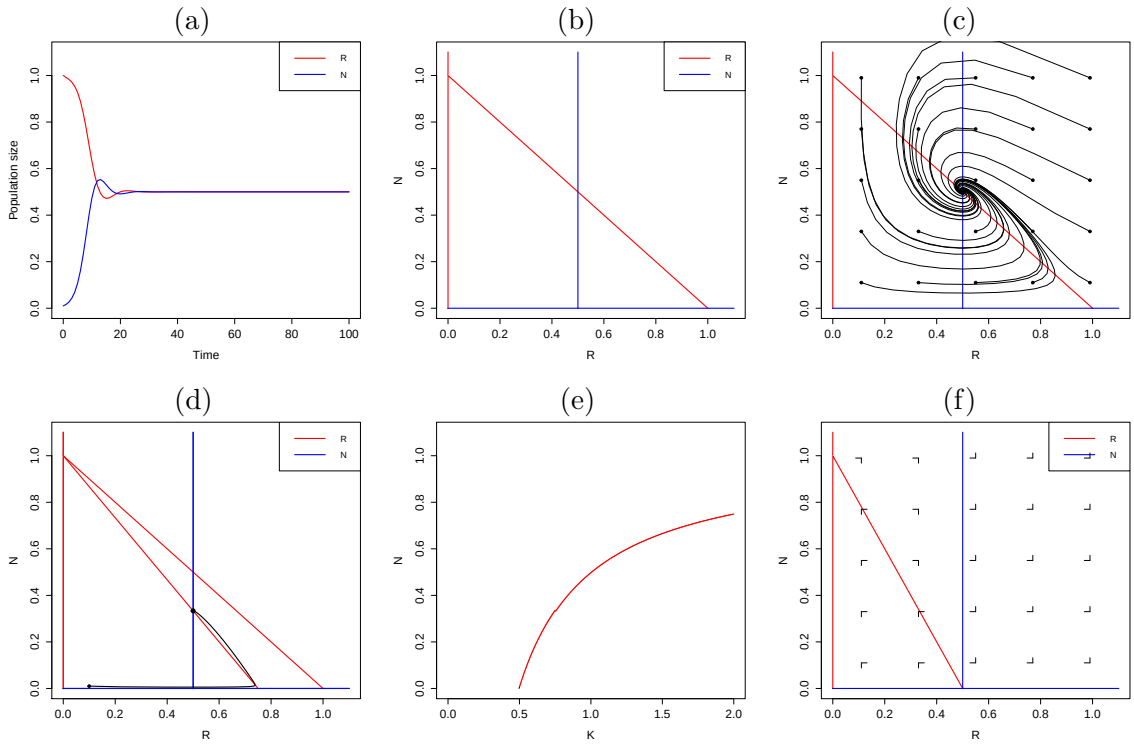

Figure 15.1: Numerical integration, phase plane analysis, and a bifurcation diagram of the Lotka Volterra model. The six panels collect the graphical output of the example session listed above.

menu of RStudio). When `grind.R` is successfully "sourced", it is time to "run" the model with its parameter and state definitions from the `lotka.R` script. In the R-console below the `lotka.R` panel, one can then type the function calls given in the example session below. Once you have a picture that you like, you may copy the lines creating that figure into the `lotka.R` window for later usage. (Use "Run" or "Control Enter" to execute lines from the `lotka.R` panel into the console).

15.1 Tutorial 1: Lotka Volterra model

The ODEs of the model are defined in the simple notation defined for the `deSolve` package. The following is an example of the Lotka Volterra model, here defined by the function `model()`:

```
model <- function(t, state, parms) {
  with(as.list(c(state,parms)), {
    dR <- r*R*(1 - R/K) - a*R*N
    dN <- c*a*R*N - delta*N
    return(list(c(dR, dN)))
  })
}

p <- c(r=1,K=1,a=1,c=1,delta=0.5) # p is a named vector of parameters
s <- c(R=1,N=0.01)                # s is the state
```

where the two lines below the function define the parameter values in the vector `p`, and the

initial state of the variables in the vector `s`. Note that the function returns a list of derivatives `(dR,dN)`. The names `model`, `s`, and `p` are the default designations for the model, state, and parameter values in all `grind.R` functions. This example should be self explanatory as it just defines the Lotka Volterra model $\mathrm{d}R/\mathrm{d}t = rR(1-R/K) - aRN$, and $\mathrm{d}N/\mathrm{d}t = caRN - \delta N$, with its parameter values and initial state as R-vectors, `p <- c(r=1,K=1,a=1,c=1,d=1,delta=0.5)`, and `s <- c(R=1,N=0.01)`, respectively. Note that the order of the variables in the state vector should be the same as the order of their ODEs in the model. The following tutorial is an example session illustrating the usage of the four `grind.R` functions analyzing this Lotka Volterra model (see Fig. 15.1 for its graphical output):

```
run()                                  # run the model and make a timeplot          (Fig 15.1a)
plane()                                # make a phase plane with nullclines
plane(xmin=-0.001,ymin=-0.001)         # include the full axis in the phase plane   (Fig 15.1b)
plane(tstep=0.5,portrait=T)            # make a phase portrait                      (Fig 15.1c)
plane()                                # make a clean phase plain again             (Fig 15.1d)
p["K"] <- 0.75                         # change the parameter K from 1 to 0.75
plane(add=T)                           # add the new nullclines
s["R"] <- 0.1                          # change the initial state to (R=0.1,N=0.01)
run(traject=T)                         # run the model and plot a trajecory
newton(c(R=0.5,N=0.5),plot=T)          # find a steady state around (R=0.5,N=0.5)a  (Fig 15.1d)
f <- newton(c(R=0.5,N=0.5))            # store this steady state in f
continue(f,x="K",xmax=2,y="N")         # continue this steady state while varying K (Fig 15.1e)
continue(f,x="K",xmax=2,y="N",step=0.001)  # get a better value with a smaller step size
p["K"] <- 0.5                          # set K to the value at which N goes extinct
plane(vector=T)                        # make a phase plane for this value of K     (Fig 15.1f)
```

15.2 Tutorial 2: Combining numerical integration with events

The `deSolve` package allows one to execute discrete events while integrating the model numerically by using the `events` argument (see the `ode()` manual). This remains possible in `grind.R` because `run()` passes additional options to `ode()` via the ellipsis (`...`) argument in R. We have added a somewhat simpler option (`after`) to handle events that are executed after each time step within `run()`. For instance `run(after="state<-ifelse(state<1e-9,0,state)")` will set small variables to zero after each time step. This new option is illustrated by the following three examples each providing an R-command as a text, `after="text"` in a call of `run()` of the Lotka Volterra model introduced above.

For example, `after="parms[\"r\"]<-rnorm(1,1,0.1)"` sets the parameter r to a random value, drawn from a normal distribution with a mean of one and a standard deviation of 0.1 (see the result in Fig. 15.2a). Note that `p` is called `parms` within `run()` (see the Manual), and the backslashes in `\"r\"` before the quotes around the parameter name, because these quotes would otherwise mark the beginning or ending of a text. (Since r is the first parameter, one can also just write `"parms[1]<-rnorm(1,1,0.1)"` to achieve the same effect). This random resetting of r is done every timestep (as defined by the parameter `tstep=1` in `run()`).

The second example, `run(after="if(t==20)state[\"N\"]<-0")`, sets the predators $N = 0$ when time $t = 20$ (see Fig. 15.2b). Note again that `s` is called `state` in `run()` (see the Manual), and the backslashes in `\"N\"`. Again, the more simple `state[2]<-0` would achieve the same effect, because N is the second variable. Finally, the third example adds Gaussian noise to both variables, e.g., `after="state<-state+rnorm(2,0,0.01)"` (see Fig. 15.2c). Note that `rnorm(2,0,0.01)` provides two random values, that are added to the two variables, respectively.

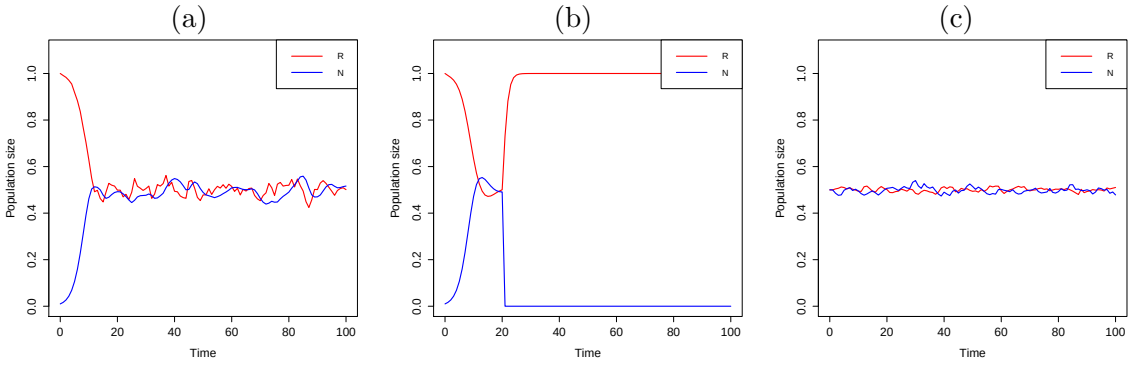

Figure 15.2: The three runs with `after="text"` executed after every timestep

The integration starts close to the steady state to prevent problems arising from random values setting a population to a negative value. These three examples are combined in the R-script `events.R`:

```
model <- function(t, state, parms) {
  with(as.list(c(state,parms)), {

    dR <- r*R*(1 - R/K) - a*R*N
    dN <- c*a*R*N - delta*N

    return(list(c(dR, dN)))
  })
}
p <- c(r=1,K=1,a=1,c=1,delta=0.5)
s <- c(R=1,N=0.01)

run(after="parms[\"r\"]<-rnorm(1,mean=1,sd=0.1)")

run(after="if(t==20)state[\"N\"]<-0")
# Use arrest to handle events at time points within time steps:
run(50,arrest=33.14,after="if(t==33.14)state[\"N\"]<-0",table=T)

f <- newton(c(R=0.5,N=0.5))
run(state=f,after="state<-state+rnorm(2,mean=0,sd=0.01)",ymax=1)
```

Most models that you will need for this course are provided on the course webpage `tbb.bio.uu.nl/rdb/te/models/`. The sections above are more or less copy pasted from the `grind.R` tutorial, which has additional sections on vectors of equations and parameter fitting. The official webpage for `grind.R` is `tbb.bio.uu.nl/rdb/practicals/grindR`, where you can find the complete tutorial and several more examples. The remainder is a reference manual explaining all options of the five functions. Consult this when needed.

15.3 Manual

A model can be solved numerically from the initial state by calling `run()`, and the output will be a timeplot, trajectory or table. Next to the graphics output, `run()` returns the final state attained by the simulation (or all data when `table=TRUE`). The former can be helpful if

one wants to continue from the previous state (e.g., `f<-run(); f<-run(state=f)`). The full definition of `run()` is:

```
run <- function(tmax=100, tstep=1, state=s, parms=p, odes=model, ymin=0,
ymax=NULL, log="", x=1, y=2, xlab="Time", ylab="Density", tmin=0, draw=lines,
times=NULL, show=NULL, arrest=NULL, after=NULL, tweak=NULL, timeplot=TRUE,
traject=FALSE, table=FALSE, add=FALSE, legend=TRUE, solution=FALSE, lwd=2,
...)
```

`run()` calls the `ode()` function from the `deSolve` package. Additional arguments (...) are passed on to `ode()` and `plot()`.

The phase plane function `plane()` sets up a space with the first variable on the horizontal axis, and the second on the vertical axis. The full definition of `plane()` is:

```
plane <- function(xmin=0, xmax=1.1, ymin=0, ymax=1.1, log="", npixels=500,
state=s, parms=p, odes=model, x=1, y=2, time=0, grid=5, eps=0, show=NULL,
portrait=FALSE, vector=FALSE, add=FALSE, legend=TRUE, zero=TRUE, lwd=2, ...)
```

Additional arguments (...) are passed on to `run()` (for the phase portrait) and to `plot()`. Note that `plane()` calls the "vectorized" R-function `outer()`, which implies that if one calls functions in the ODEs they should also be vectorized, e.g., one should use `pmax()` instead of `max()`.

The function `newton()` finds a steady state from a nearby initial state, and can report the Jacobi matrix with its eigenvalues and eigenvectors. The full definition of `newton()` is:

```
newton <- function(state=s, parms=p, odes=model, time=0, x=1, y=2,
positive=FALSE, jacobian=FALSE, vector=FALSE, plot=FALSE, ...)
```

`newton()` calls the function `steady()` from the `rootSolve` package (which calls `stode()`). Additional arguments (...) are passed on to both of them. `newton()` needs an initial state close to an equilibrium point.

The function `continue()` continues a steady state by changing a "bifurcation" parameter defined by the horizontal axis of the bifurcation diagram. The full definition of `continue()` is:

```
continue <- function(state=s, parms=p, odes=model, x=1, step=0.01, xmin=0,
xmax=1, y=2, ymin=0, ymax=1.1, log="", time=0, positive=FALSE, add=FALSE,
...)
```

`continue()` calls the function `steady()`from the `rootSolve` package (additional arguments (...) are passed on), and needs an initial state close to an equilibrium point. Note that there is much more proper software for bifurcation analysis like XPPAUT or MatCont, which reports the type of bifurcations encountered, and automatically continues all branches of branch points.

The function `fit()` fits a model to data by non-linear parameter estimation. The output is an object (class of `modFit`) containing the estimated parameters, the summed squared residuals, confidence ranges, and correlations (see the `modFit()` manual). The data and the model behavior for its best fit parameters are depicted in a timeplot. Its full definition is:

```
fit <- function(datas=data, state=s, parms=p, odes=model, free=NULL,
differ=NULL, fixed=NULL, tmin=0, tmax=NULL, ymin=0, ymax=NULL, log="",
xlab="Time", ylab="Density", bootstrap=0, show=NULL, fun=NULL, costfun=cost,
initial=FALSE, add=FALSE, timeplot=TRUE, legend=TRUE, main=NULL, sub=NULL,
pchMap=NULL, ...)
```

`fit()` calls the function `modFit()` from the `FME` package (which calls `modCost()`). Additional arguments (...) are passed on to both of them, and to `run()` and `ode()`.

Finally the internal function `timePlot()` can be used to plot data and is defined as:

```
timePlot <- function(data, tmin=0, tmax=NULL, ymin=0, ymax=NULL, log="",
xlab="Time", ylab="Density", show=NULL, legend=TRUE, draw=lines, lwd=2,
add=FALSE, main=NULL, sub=NULL, colMap=NULL, pchMap=NULL, ...)
```

These functions have many arguments, and fortunately most of them have good default values, and can hence typically be omitted. The arguments can be used to define various options and adjustments:

- `state=s, parms=p, odes=model` define the names of the state vector, parameter vector, and the model.
- `tmax=100, tstep=1` set the integration time and the reporting interval. `tmin` allows one to start a specific time point (which can be convenient when a run is continued). One can also provide a vector of time points where the `run()` should provide output with the `times` option (see the `ode()` manual).
- `x=1, y=2` define the variables on the axes of phase planes and bifurcation diagrams. One can also use the names of the variables to define the axes, e.g., `x="R",y="N"`.
- `xmin=0, xmax=1.1, ymin=0, ymax=1.1, log=""` define the scaling of the horizontal and vertical axes of phase planes and bifurcation diagrams (`log="y"` makes the vertical axis logarithmic).
- `step=0.01` defines the maximum change of the bifurcation parameter in a bifurcation diagram. When the axis is linear the parameter is increased, or decreased, in steps not exceeding `step` × `xmax`. When the axis is logarithmic the parameters is maximally multiplied by 1+`step`. `continue()` will decrease the step size to maximally `step`/100 when it looses the steady state.
- `xlab="Time", ylab="Density"` allow one to redefine the labels of the axes of a time plot.
- `show=NULL` defines the variables appearing in a time plot, fit, or phase plane. By default all are shown. By explicitly providing a list of variables, one can omit some of the variables. `show` is typically a list of names (`show=c("P","Q")`).
- `after=NULL` defines a command to be executed after each time step, e.g., `after="state <- ifelse( state<1e-9, 0, state)"` sets small variables to zero.
- `arrest=NULL` defines a vector of values, or parameter names, defining time points where the integrator should stop, and report the current state (i.e., these time points are added to the `times` vector of `ode()`). This can be helpful when fitting a piece-wise model for which the discontinuous time points have to be estimated (e.g., `arrest=c("T1","T2")`).
- `tweak=NULL` allows one to modify the data delivered by `run()`. For instance one can add columns that can be fitted to data: (`tweak<-"nsol<-cbind(nsol,nsol[,2]+nsol[,3]);names(nsol)[4]<- \"T\""`), or transform the simulation data before they are fitted to data that is already transformed.
- `timeplot=TRUE, traject=FALSE, table=FALSE` determine the output of `run()` in the form of a time plot (default), trajectory in a phase plane, and/or a table with all data.
- `draw=lines` draws the timeplot as continuous lines. The alternative is `draw=points`.
- `lwd=2` sets the line width of the graphs, `colMap=NULL` and `pchMap=NULL` can be used to re-map the colors or symbols, e.g., `pchMap=c(3,2,1)` reverts the order of the first three R-symbols (see `pch` in `points()`). Note that `grind.R` defines its own color table (of dark colors that print well). If you don't like this, uncomment the second `colors <-` line in the `grind.R` script.
- `main=NULL, sub=NULL` allow one to put a title at the top and/or a subtitle at the bottom of the graph (these are passed on to the R-function `plot()`). Note that these titles are set in a plain font (to set that back to bold face, change the two `font` lines in the `grind.R` file).
- `add=FALSE, legend=TRUE` define whether or not the new plot should be added to the current one, and a legend should be placed.
- `solution=FALSE` tells `grind.R` whether or not the model provides time derivatives (default),

or a full solution, This is particularly useful when fitting data to functions, and should obviously not be used in combination with phase plane analysis, nor with searching steady states (`newton(), continue()`). Models returning a solution obey the same format as the ODE models required by `deSolve`, except for the fact that they should return a value, or a vector of values (and not a list).

- `npixels=500` defines the resolution of the phase space in `plane()`
- `time=0` defines the time point for which nullclines are computed and steady states are computed (for non-autonomous ODEs).
- `grid=5` defines the number of grid points for which the vector field or phase portrait is drawn.
- `eps=0` is a shortcut in `plane()` to include or exclude the axis in the nullclines: `eps` is added to both `xmin` and `ymin`.
- `portrait=FALSE, vector=FALSE` define whether or not `plane()` should include a phase portrait or vector field.
- `zero=TRUE` draws the phase plane for all variables other than `x` and `y` set to zero (also important when drawing nullclines of variables not appearing on the axes).
- `positive=FALSE`, setting `positive=TRUE` will restricts the search of `newton()` and `continue()` to positive steady states only.
- `jacobian=FALSE,vectors=FALSE,plot=FALSE` define whether or not `newton()` should print the Jacobian and eigenvectors, and indicate the steady state by a symbol in the phase plane.
- `datas=data` in `fit()` defines the name of the data frame containing the data, or defines a list of data frames.
- `free=NULL` defines the names of the parameters to be fitted. By default `free` equals `c(names(state), names(parms))`.
- `differ=NULL` defines the names of the parameters that differ between the data sets and need to be fitted separately. `differ` can also be a named list containing the individual guesses for each data set. (One can use `makelist(differ,state,parms,nsets)` to set up such a list).
- `fixed=NULL` defines a named list of the parameters that differ between the data sets and have known fixed values. (One can use `makelist(fixed,state,parms,nsets)` to set up such a list).
- `initial=FALSE` allows one to read the initial condition from the data (and not estimate it).
- `fun=NULL` defines a function to transform the data and (numerical) solution before fitting.
- `costfun=cost` allows one to redefine the cost-function measuring the distance between the model and the data. This can be useful when different data sets need different models. The default `cost`-function loops over the various data sets, and calls `run()` for each of them. That call can easily be adapted for each data set (the index of the loop is called `iset`).
- `bootstrap=0` defines the number of samples to be taken randomly from the data (with replacement). This prints a summary and adds an element `bootstrap` to the `modFit` list, containing a matrix with all parameter estimates. Use `pairs(f$bootstrap)` to see the correlations between the estimates.
- `...` can be used to define parameters that are passed on to other functions

15.4 Exercises

Question 15.1. Fishing herring
In Chapter 3 you made an exercise on fishing a population of herring. We had the following model

$$\frac{\mathrm{d}H}{\mathrm{d}t} = rH(1 - H/k) - Q$$

where Q is the quotum that was allowed to be caught per unit of time. Although the maximum yield was $rk/4$ we showed that one cannot set the quotum to $Q = rk/4$.

a. Confirm your earlier analysis by setting $Q = rk/4$ and study a population of herring with a carrying capacity that fluctuates somewhat due to weather conditions (you may use the file `herring.R` for this).

b. Now replace the fixed quotum by a fraction f that one can maximally catch, i.e., study $\mathrm{d}H/\mathrm{d}t = rH(1 - H/k) - fH$, again allowing for a noisy carrying capacity.

c. What is economically speaking the optimal value of f? Hint: compute the steady state, $\bar{H}$, and the expected harvest, $f\bar{H}$, and compute its maximum by taking the derivative ∂_f.

d. Study the model for this optimal f for a noisy carrying capacity. What happens if you allow for "human error", i.e., if you allow for noise on f?

e. What is the expected harvest at this optimal f? Is that lower than $Q = rk/4$?

Question 15.2. Allee effect

We have seen in Chapter 5 that the prey nullcline reflects the *per capita* prey growth function whenever there is a mass action predation term. Consider a prey species with an unusual growth function, e.g., consider a prey with an Allee effect,

$$\frac{\mathrm{d}R}{\mathrm{d}t} = \frac{bR}{1 + R/k}\frac{R}{h + R} - d_1 R - eRN \quad \text{and} \quad \frac{\mathrm{d}N}{\mathrm{d}t} = ceRN - d_2 N \ ,$$

and study the phase space of this model (you may use the model `allee.R` for this).

a. Check with pencil and paper that the prey nullcline indeed reflects the *per capita* growth function of the prey.

b. Draw the nullclines for all qualitatively different cases.

c. What is the model behavior in each case?

d. Remove the predators from the model and add a term representing the hunting of whales by humans. Assuming a fixed quotum, Q, redo the "Herring question", and study whether or not the conditions for "saving the whales" are stronger than those for saving a herring population without an Allee effect.

Question 15.3. Paradox of Enrichment

Repeat the Rosenzweig (1971) analysis with the Holling type II consumer resource model:

$$\frac{\mathrm{d}R}{\mathrm{d}t} = bR(1 - R/k) - d_1 R - \frac{eNR}{h + R} \ ,$$

$$\frac{\mathrm{d}N}{\mathrm{d}t} = -d_2 N + \frac{ceNR}{h + R} \ ,$$

which is provided on the website as `rosenzweig.R`.

a. Think about simple and reasonable parameter values. Use pencil and paper during your computer exercises: make sure that populations can grow, i.e., have an $R_0 > 1$.

b. Draw nullclines, check the various possibilities, and run trajectories for each case.

c. Study the effect of eutrophication by increasing the carrying capacity.

d. Continue the non-trivial steady state as a function of k (with the `continue()` command).

e. Do the same for a model having a functional response with "predator interference".

f. Replace the $f = R/(h + R)$ functional reponse by one with a refugium with a size of r prey individuals, i.e., $\hat{R} = \max[0, R - r]$ and $f = \hat{R}/(h + \hat{R})$; see Page 37 and the R-file `refugium.R` where the `pmax()` function is called.

g. Replace the functional response with the one defined by Eq. (6.14), with $H = h/(1 - \gamma/2)$ (see the `hyper.R` file).

Question 15.4. Luckinbill
Study the analysis by Luckinbill (1973) with the same Holling type II consumer resource model. You will need the examples on how to add events for drawing noise and setting small populations to zero (see the `luckinbill.R` file on the website).

a. Use pencil and paper to find reasonable parameters that confirm with your earlier analysis of this model in Chapter 6.

b. Repeat the Luckinbill experiments.

c. Try to repeat them with a linear functional response.

Question 15.5. Biomanipulation
Lakes often look green because of eutrophication. Such lakes have a high density of algae and fish, and little zoo-plankton. Experiments show that catching sufficient fish can make the water clear again. Scheffer (1991) proposed the following model:

$$\frac{\mathrm{d}A}{\mathrm{d}t} = A(1 - A/k) - pZ\frac{A}{1+A} \ ,$$

$$\frac{\mathrm{d}Z}{\mathrm{d}t} = -mZ + pZ\frac{A}{1+A} - F\frac{Z^2}{h^2+Z^2} \ ,$$

where A represents algae and Z zoo-plankton. Basically, this is the same Holling type II model as considered above, extended with predation with a fixed density of the fish, F. Study the model for the parameters: $h = 1, m = 0.4, p = 0.5$, $5 \leq k \leq 15$, and $0 \leq F \leq 1$; see the model `fish.R`.

a. Choose different values for the parameters indicated by the ranges, and draw nullclines.

b. Is it possible to have a permanent effect by temporarily (e.g., once) removing a large fraction of the fish?

c. What steady states do you find when a system is enriched? Draw several phase spaces and enumerate all steady states. Is that realistic? How would you change the model to repair this if you find it unrealistic?

Question 15.6. Density dependent growth
In Eq. (4.2) we defined models with a density dependent birth rate, and in Fig. 4.1 these were analyzed graphically by plotting the *per capita* growth and death rates. Substitute the various forms for $f(N)$ defined in Eq. (4.3) into this model and:

a. Rescale the models such that they have the same carrying capacity and the same natural rate of increase.

b. Simulate the rescaled models on a computer to study the differences in behavior. Start far below the carrying capacity to get a sigmoidal time plot (see the file `density.R`).

Question 15.7. Linear models
Study the linear system

$$\frac{\mathrm{d}x}{\mathrm{d}t} = ax + by \quad \text{and} \quad \frac{\mathrm{d}y}{\mathrm{d}t} = cx + dy \ .$$

What is the steady state of this system? Derive the Jacobi matrix for this system and use your knowledge of the eigenvalues of this matrix to choose values of a, b, c, and d such that you obtain a stable node, a spiral, and a saddle point. The model is provided as the file `linear.R`.

Question 15.8. Noise and r and K-selected species
Study the logistically growing population

$$\frac{\mathrm{d}N}{\mathrm{d}t} = rN(1 - N/K) \ ,$$

by adding noise to one of its parameters, and by adding noise to the population density (use the file `rknoise.R` for this). Use the concept of r and K-selected species and study species with different growth rates r (the population size can always be scaled to $K = 1$).

Chapter 16

The basic reproductive ratio R_0

In this book we frequently use the fitness, R_0, of a population to simplify steady state values, and the expressions for nullclines, which has facilitated their biological interpretation. Analyzing resource competition we have seen that the population with the largest R_0, and not necessarily the one with the largest carrying capacity, is expected to win the competitive exclusion. In our predator prey models we observed that the depletion of prey species is (at least partly) determined by the R_0 of the predator. We have defined R_0 as a fitness, namely as the maximum number of offspring that is produced over the expected lifespan of an individual, in a situation without competition or predation, i.e., as the mean lifetime reproductive success of a typical individual (Heffernan *et al.*, 2005). The R_0 plays a central role in epidemiology, where it is defined as the expected number of individuals that is successfully infected by a single infected individual during its entire infectious period, in a population that is entirely composed of susceptible individuals (Anderson & May, 1991; Diekmann *et al.*, 1990). Epidemics will grow whenever $R_0 > 1$. In order to provide a more general understanding of the basic reproductive ratio, R_0, this Chapter reviews some of the classical epidemiological approaches to define and calculate R_0.

16.1 The SIR model

The most classical model in epidemiology is the "SIR" model, for Susceptible, Infected, and Recovered individuals, e.g.,

$$\frac{\mathrm{d}S}{\mathrm{d}t} = s - dS - \beta SI \ , \quad \frac{\mathrm{d}I}{\mathrm{d}t} = \beta SI - (\delta + r)I \ , \quad \text{and} \quad \frac{\mathrm{d}R}{\mathrm{d}t} = rI - dR \ , \tag{16.1}$$

where s defines the source of susceptibles, d is their death rate, β is an infection rate, δ the death rate of infected individuals (with $\delta \geq d$), r is a recovery rate, and where recovered individuals have the same death rate as susceptibles. Let us consider a time scale of days, i.e., all death rates are per day. Note that in this version of the SIR model the subpopulation of recovered individuals does not feed back onto the dynamics of the other two subpopulations, which means that they need not be considered when analyzing the establishment of an epidemic. Also note that setting $r = 0$ defines the "SI" model of anndemic infection that no one recovers from.

The disease-free steady state is defined as $\bar{S} = s/d$ and $\bar{I} = \bar{R} = 0$, and the endemic equilibrium

is defined as

$$\bar{S} = \frac{\delta + r}{\beta} \ , \quad \bar{I} = \frac{s}{\delta + r} - \frac{d}{\beta} \ , \quad \text{and} \quad \bar{R} = \frac{r}{d}\,\bar{I} = \frac{rs}{d(\delta + r)} - \frac{r}{\beta} \ , \tag{16.2}$$

which can only be present when $\bar{I} > 0$, i.e.,

$$\frac{s}{\delta + r} > \frac{d}{\beta} \quad \text{or} \quad \frac{s}{d}\,\frac{\beta}{\delta + r} > 1 \ . \tag{16.3}$$

The R_0 of this model is defined by the rate, βS, at which new cases are produced per infected individual over its entire infectious period of $1/(\delta + r)$ days, in a fully susceptible population $\bar{S} = s/d$. R_0 is therefore defined as

$$R_0 = \beta \bar{S}\,\frac{1}{\delta + r} = \frac{s}{d}\,\frac{\beta}{\delta + r} \ . \tag{16.4}$$

Since the epidemic will only spread if an infected individual is replaced by more than one secondary case, we require $R_0 > 1$, which indeed corresponds to the threshold derived in Eq. (16.3). This also means that we could have derived the same condition from the Jacobian of the disease-free steady state, i.e., for the 2-dimension "SI" model,

$$J = \begin{pmatrix} -d & -\beta\bar{S} \\ 0 & \beta\bar{S} - \delta - r \end{pmatrix} \ , \tag{16.5}$$

with eigenvalues $\lambda_1 = \beta\bar{S} - \delta - r$ and $\lambda_2 = -d$. The parameter condition $R_0 > 1$ indeed corresponds to the transcritical bifurcation point, $\lambda_1 = 0$, at which the endemic steady state becomes positive.

Note that R_0 is dimensionless, i.e., it is the expected number of secondary cases per infectious period. Since R_0 is not a rate, it cannot define how fast the epidemic is expanding. Indeed the initial rate at which an epidemic is expected to grow is here defined by

$$\frac{\mathrm{d}I}{\mathrm{d}t} = \beta\bar{S}I - (\delta + r)I = \left(\frac{\beta s}{d} - \delta - r\right) I = r_0 I \ , \tag{16.6}$$

where the rate r_0 is the initial *per capita* net growth rate of the infected individuals. Observe that this growth rate, r_0, corresponds to the dominant eigenvalue of the Jacobi matrix in Eq. (16.5), and that applying the "invasion criterion" $r_0 > 0$, i.e., $\frac{\beta s}{d} > \delta + r$ or $\frac{s}{d}\,\frac{\beta}{\delta + r} > 1$, is again the same as requiring $R_0 > 1$. The net growth rate, r_0, over the entire infectious period, $L = 1/(\delta + r)$, should obviously be related to the R_0, i.e.,

$$R_0 = 1 + r_0 L = 1 + \frac{r_0}{\delta + r} = \frac{s}{d}\,\frac{\beta}{\delta + r} \tag{16.7}$$

where the 1 is required to compensate for the fact that R_0 is defined by the new cases only, whereas the rate r_0 includes the death rate.

Finally, defining the disease free steady state as a carrying capacity, $K = s/d$, one can see that the ultimate degree of depletion of the susceptibles is fully determined by the R_0, i.e., in Eq. (16.2) we see that $\bar{S} = K/R_0$. Summarizing, R_0 is a valuable and meaningful concept in epidemiology, there are several methods to compute an R_0, where the one that calculates the number of secondary cases produced during the infectious period of an infected individual seems the most intuitive.

16.2 The SEIR model

The definition of the R_0 becomes more complicated in systems where the infection involves several stages. Adding a stage of exposed individuals, E, that are not yet infectious, one obtains the SEIR model

$$\frac{\mathrm{d}S}{\mathrm{d}t} = s - dS - \beta SI \ , \ \frac{\mathrm{d}E}{\mathrm{d}t} = \beta SI - (\gamma + d)E \ , \ \frac{\mathrm{d}I}{\mathrm{d}t} = \gamma E - (\delta + r)I \ , \ \frac{\mathrm{d}R}{\mathrm{d}t} = rI - dR \ , \quad (16.8)$$

where the exposed individuals become infectious at a rate γ (and have the same death rate as the susceptibles). A general method for deriving the R_0 for multi-stage models is the "next generation method" devised by Diekmann *et al.*(Diekmann *et al.*, 1990), and involves the definition of a matrix collecting the rates at which new infections appear in each compartment, and a matrix defining the loss and gains in each compartment. This method is general but its explanation would be too involved for a short summary like this Chapter (if you are interested read any of the following citations (Heffernan *et al.*, 2005; Diekmann *et al.*, 2012, 1990)). Eq. (16.8) is simple enough to define the R_0 by the more intuitive "survival" method. The initial rate at which an infected individual produces novel infections remains $\beta\bar{S}$, and this will occur over an infectious period of $1/(\delta + r)$ time steps, but since not all exposed individuals become infectious (i.e., only a fraction $\gamma/(\gamma + d)$ are expected to survive and become infectious), we need to multiply with this fraction and obtain

$$R_0 = \frac{s}{d} \ \frac{\beta}{\delta + r} \ \frac{\gamma}{\gamma + d} \ . \quad (16.9)$$

Solving $\bar{E} = \frac{\delta+r}{\gamma} I$ from $\mathrm{d}E/\mathrm{d}t = 0$, and substituting that into $\mathrm{d}I/\mathrm{d}t = 0$ delivers $\bar{S} = \frac{\gamma+d}{\gamma} \ \frac{\delta+r}{\beta}$, which when substituted in $\mathrm{d}S/\mathrm{d}t = 0$ gives

$$\bar{I} = \frac{s}{\beta\bar{S}} - \frac{d}{\beta} = \frac{\gamma}{\gamma + d} \ \frac{s}{\delta + r} - \frac{d}{\beta} \ , \quad (16.10)$$

which can only be positive when

$$\frac{\gamma}{\gamma + d} \ \frac{s}{\delta + r} > \frac{d}{\beta} \quad \text{or} \quad \frac{s}{d} \ \frac{\beta}{\delta + r} \ \frac{\gamma}{\gamma + d} > 1 \quad \text{or} \quad R_0 > 1 \ , \quad (16.11)$$

confirming that the R_0 derived by the survival method again corresponds to the parameter threshold at which the epidemic steady state becomes positive. The initial growth rate, r_0, of an epidemic in the SEIR model now depends on two ODEs, $\mathrm{d}E/\mathrm{d}t$ and $\mathrm{d}I/\mathrm{d}t$, and can still be computed because these ODEs are linear around the disease-free steady state $\bar{S} = s/d$. Solving these ODEs and applying the invasion criterion $\mathrm{d}I/\mathrm{d}t > 0$, or deriving the dominant eigenvalue of the Jacobian of the disease-free equilibrium, would therefore be alternative means to calculate the R_0 of this SEIR model. Summarizing, there are various ways to one can compute an R_0 for infections involving multiple stages, where the next generation method (Diekmann *et al.*, 1990, 2012) is the most general (but is not explained here).

16.3 Fitnesses in predator prey models

In this book we have similarly defined the R_0 of prey and predator populations to facilitate the biological interpretations of otherwise more complicated expressions. For instance re-consider the Lotka-Volterra model with explicit birth and death rates for the prey,

$$\frac{\mathrm{d}R}{\mathrm{d}t} = bR(1 - R/k) - dR - aRN \quad \text{and} \quad \frac{\mathrm{d}N}{\mathrm{d}t} = caRN - \delta N \ , \quad (16.12)$$

with a carrying capacity $\bar{R} = K = k(1 - d/b)$. Using the survival method, the R_0 of the prey is defined by the maximum number of offspring, b per day (note that the $(1 - R/k)$ term can only decrease the birth rate), over its expected life span of $1/d$ days, i.e., $R_{0_R} = b/d$. One can also easily see that the prey population can only invade when the maximum birth rate, b, exceeds the death rate, d, i.e., when $b/d > 1$, and define the R_0 this way (like above for the SIR model). Given this R_0 of the prey the carrying capacity can be written as $K = k(1-1/R_{0_R})$ (see Chapter 3).

Similarly, the R_0 of the predator is its maximum birth rate, $ca\bar{R}$, times its expected life span, $1/\delta$, i.e., $R_{0_N} = caK/\delta$. Likewise, see that the maximum predator birth rate, caK, should exceed its death rate, δ, implying that $R_{0_N} = caK/\delta > 1$. Hence, one can again derive the R_0 parameters of this model in several ways. The R_0 of the predator can be used to simplify the expression for the non-trivial steady state of the prey, which is solved from $\mathrm{d}N/\mathrm{d}t = 0$, i.e., $\bar{R} = \frac{\delta}{ca}$, and can now be expressed as $\bar{R} = K/R_{0_N}$. This reveals the biological insight that the depletion of the prey population is proportional to the R_0 of the predator (like in the SIR model), which even means that one can estimate the R_0 from an observed level of depletion.

We have also considered models where the birth rate of the predator is a saturation function of its consumption, e.g.,

$$\frac{\mathrm{d}R}{\mathrm{d}t} = bR(1 - R/k) - dR - aRN \quad \text{and} \quad \frac{\mathrm{d}N}{\mathrm{d}t} = \frac{\beta RN}{h + R} - \delta N \ , \tag{16.13}$$

with the same equation, R_0, and carrying capacity of the prey. Now the R_0 of the predator can either be defined as $R_0 = \beta/\delta$, because β is a maximum birth rate of the predator at infinite prey densities, or —more classically— as $R_0 = \frac{\beta K}{\delta(h+K)}$, which uses the predator birth rate at carrying capacity of the prey for the maximum predator birth rate. Since we aim for simplifying mathematical expressions, the simpler $R_0 = \beta/\delta$ is typically the most useful definition. When $h \ll K$ the two definitions of R_0 approach one another. If not, an invasion criterion would correspond to the more complicated R_0, because predators can only invade into a prey population at carrying capacity when $\frac{\beta K}{h+K} > \delta$. The simpler form of the predator fitness, $R_0 = \beta/\delta$, instead allows us to simplify the expression for the steady state of the prey, which is again solved from $\mathrm{d}N/\mathrm{d}t = 0$, i.e., $\bar{R} = \frac{\delta h}{\beta - \delta} = \frac{h}{R_0 - 1}$, revealing that the depletion of the prey still increases with the R_0 of the predator, but that this is no longer proportional the R_0.

Chapter 17

Extra questions

17.1 Exercises

Question 17.1. Space
Consider two plant species that compete for space and have the same lifespan. One species is twice as large as the other. Because of this, the birth rate of the large species is twice as slow as that of the small species. Assume that the rate at which empty space is occupied depends on the density of the two species. In addition assume that seeds are distributed homogeneously in space.
a. Make a model of this system and analyse it using nullclines.
b. What are the steady states and what is their stability?
c. Will all patches always be occupied? What is the carrying capacity of the two species?
d. In case of competitive exclusion, which species will win and why?

Question 17.2. Nitrogen
Consider two algae species in a lake that are competing for nitrogen. The total amount of nitrogen, T, is not changing over time. Nitrogen is either freely available (N) for algal growth, or is taken up by the algae, A_1 and A_2. Thus we can write a conservation equation for the total amount of nitrogen (i.e., $T = N + A_1 + A_2$). For the algae we write a standard birth death model with a maximum birth rate b_i:

$$\frac{\mathrm{d}A_1}{\mathrm{d}t} = A_1\left(\frac{b_1 N}{h_1 + N} - d_1\right) \quad \text{and} \quad \frac{\mathrm{d}A_2}{\mathrm{d}t} = A_2\left(\frac{b_2 N}{h_2 + N} - d_2\right) \ ,$$

where $N = T - A_1 - A_2$ is the amount of free nitrogen.
a. What is the R_0 of the algae species?
b. What is the carrying capacity of each species?
c. Sketch the nullclines.
d. At high total nitrogen levels both algae become independent of the nitrogen concentration because they both approach their maximum growth rate. Explain why the algae nevertheless cannot co-exist.
e. Which species is expected to win the competition: the species with the lowest resource requirement, N^*, or the one with the highest carrying capacity (or is that the same here)?

Question 17.3. Food chain
Consider the following food chain of a resource, R, a consumer, N, and a (top)predator, M.

This is a non-replicating resource!

$$\frac{\mathrm{d}R}{\mathrm{d}t} = s - d_R R - aRN \ , \quad \frac{\mathrm{d}N}{\mathrm{d}t} = caRN - d_N N - bNM \quad \text{and} \quad \frac{\mathrm{d}M}{\mathrm{d}t} = cbNM - d_M M \ .$$

a. What is the steady state of the resource when there are no consumers?
b. What is the steady state of the resource when there are consumers, but no predators?
c. What is the steady state of the resource if all species are present?
d. What is the fitness, R_0, of the consumers?
e. Sketch a bifurcation diagram plotting the steady state of the resource as a function of its source, s, and name all bifurcations that occur.
f. Sketch for the same bifurcation analysis the steady state of the consumers.

Question 17.4. Write a natural model
Consider a lake that is visited by a large population of kingfishers (a colorful fish-eating bird species). The kingsfishers have no suitable nesting places at this particular lake and fly in depending on the amount of fish in the lake, and out after a little while. The fish in the lake grow logistically and are eaten by kingsfishers. Write a natural model for the total fish density and the density of kingsfishers present at this lake.

Chapter 18

Appendix: mathematical prerequisites

18.1 Phase plane analysis

Most mathematical models in biology have non-linearities and can therefore not be solved explicitly. One can nevertheless obtain insight into the behavior of the model by numerical (computer) analysis, and/or by sketching nullclines and solving for steady states. One determines the stability of the steady states from the vector field, and by linearization around the steady states.

The long-term behavior of a model typically approaches a stable steady state, a stable limit cycle, or a chaotic attractor. Phase plane analysis is a graphical method to analyze a model to investigate these behavioral properties of a model. Consider a model of two variables x and y,

$$\frac{\mathrm{d}x}{\mathrm{d}t} = f(x,y) \quad \text{and} \quad \frac{\mathrm{d}y}{\mathrm{d}t} = g(x,y)\ . \tag{18.1}$$

One can define a "phase space" with x on the horizontal axis and y on the vertical axis, where each point in this space is one particular "state" of the model. To obtain further insight in the model one sketches the "nullclines" $f(x,y) = 0$ and $g(x,y) = 0$. This is useful because at the former nullcline $\mathrm{d}x/\mathrm{d}t$ switches sign, and at the latter $\mathrm{d}y/\mathrm{d}t$ switches sign. Two simple nullclines therefore typically define regions with qualitatively different signs of the two differential equations. Nullclines enable one to localize all steady states of the model because these correspond to the intersections of the nullclines (i.e., $f(x,y) = g(x,y) = 0$). This is very useful because models may have multiple steady states.

For each steady state one has to determine whether it is an attractor, i.e., a stable steady state, or a repellor, i.e., an unstable equilibrium. The local vector field around a steady state in a phase space with nullclines often provides sufficient information to see whether the steady state is stable or unstable. In 2-dimensional phase spaces there are three classes of steady states: nodes, saddles, and spirals. Nodes and spirals are either stable or unstable, and a saddle point is always unstable because it has a stable and an unstable direction. The two nullclines intersecting at the equilibrium point define four local regions of phase space, each with its unique local vector field. The four local vector fields define the nature of the steady state.

A simple example is a "stable node", for which all four vector fields point towards the steady state

(see Fig. 18.1a). A stable node is therefore approached by trajectories from all four directions (Fig. 18.1b). When the vector fields point outward in all four regions the equilibrium is an "unstable node" (Fig. 18.1c), and trajectories are repelled in all four directions (Fig. 18.1d). The local vector fields in Fig. 18.1e define a "saddle point", which has a stable and an unstable direction (Fig. 18.1f). The stable direction of a saddle point defines a "separatrix" because all trajectories starting at either side of this line end up in another attractor (i.e., a separatrix defines different basins of attractions).

The local vector field can also suggest rotation (see Fig. 18.2). Rotating vector fields are typical for spiral points. The local vector field fails to provide sufficient information to determine with absolute certainty whether a spiral point is stable or unstable. However, one can get some good suggestion for the stability from the vector field. In Fig. 18.2c, for instance, and one can see that increasing y from its steady state value makes $\mathrm{d}y/\mathrm{d}t > 0$. Locally, there must be some positive feedback allowing y to increase further when y increases. This is definitely destabilizing, and the trajectory in Fig. 18.2d confirms that this is an "unstable spiral" point. Conversely, the spiral point in Fig. 18.2a is stable, and locally has negative feedback for both x and y (i.e., increasing x makes $\mathrm{d}x/\mathrm{d}t < 0$ and increasing y makes $\mathrm{d}y/\mathrm{d}t < 0$), which has a stabilizing influence. Because the stability of spiral points also depends on the local difference in time scales of the horizontal (x) and vertical (y) variables, the local vector field is not always sufficient to determine the stability of the steady state. Even the suggestion of rotation in a local vector field is not sufficient to determine with certainty that the steady state is a spiral. Fig. 18.2e & f show that the same vector field defining a stable spiral point in Fig. 18.2a can actually also correspond to a stable node.

Example: Lotka Volterra model

Using the famous Lotka Volterra model as an example we review a few methods for analyzing systems of non-linear differential equations. The Lotka-Volterra predator prey model can be written as:

$$\frac{\mathrm{d}R}{\mathrm{d}t} = aR - bR^2 - cRN \qquad \frac{\mathrm{d}N}{\mathrm{d}t} = dRN - eN \;, \tag{18.2}$$

where a, b, c, d, and e are positive constant parameters, and R and N are the prey and predator densities. The derivatives $\mathrm{d}R/\mathrm{d}t$ and $\mathrm{d}N/\mathrm{d}t$ define the rate at which the prey and predator densities change in time.

A first step is to sketch nullclines (0-isoclines) in phase space. A nullcline is the set of points (R, N) for which the corresponding population remains constant. Thus, the R-nullcline is the set of points at which $\mathrm{d}R/\mathrm{d}t = 0$. Setting $\mathrm{d}R/\mathrm{d}t = 0$ and $\mathrm{d}N/\mathrm{d}t = 0$ in Eq. (18.2) one finds

$$R = 0 \;, \quad N = \frac{a - bR}{c} \quad \text{and} \quad N = 0 \;, \quad R = \frac{e}{d} \;, \tag{18.3}$$

for the prey nullclines and the predator nullclines, respectively. These four lines are depicted in Fig. 18.3. For biological reasons we only consider the positive quadrant.

A second step is to determine the vector field. Not knowing the parameter values, one considers extreme points in phase space. In the neighborhood of the point $(R, N) = (0, 0)$, for example, one can neglect the quadratic bR^2, cRN, and dRN terms, such that

$$\frac{\mathrm{d}R}{\mathrm{d}t} \approx aR \;, \quad \frac{\mathrm{d}N}{\mathrm{d}t} \approx -eN \;. \tag{18.4}$$

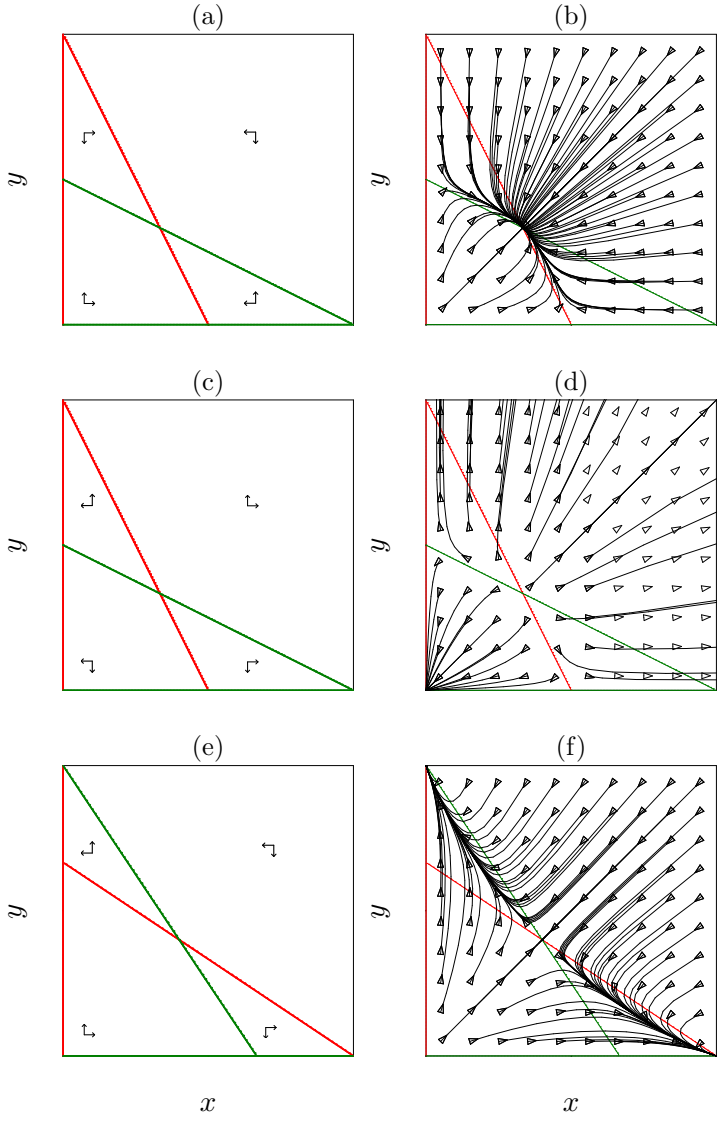

Figure 18.1: Qualitatively different steady states determined by the local vector field in the four regions defined by the nullclines. Stable node (a,b): the vector field points inwards in all four sections. Unstable node (c,d): the vector field points outwards in all four sections. Saddle point (e,f): the vector field points inwards in two sections, and outwards in the other two regions. A saddle point is an unstable steady state with a stable and an unstable direction.

Since the former is strictly positive, and the latter strictly negative, we assign $(+-)$ to the local direction of the vector field (see Fig. 18.3). This means that $\mathrm{d}R/\mathrm{d}t > 0$ below the R-nullcline, i.e., we sketch arrows to the right, and that at the left hand side of the N-nullclines $\mathrm{d}N/\mathrm{d}t < 0$, i.e., we sketch arrows pointing to the bottom. At the R and N-nullclines the arrows are vertical and horizontal, respectively. The derivatives switch sign, and the arrows switch their direction, when one passes a nullcline. Nullclines therefore separate the phase space into regions where the derivatives have the same sign.

An important step is to determine the steady states of the system. A steady state, or equilibrium, is defined as $\mathrm{d}R/\mathrm{d}t = \mathrm{d}N/\mathrm{d}t = 0$. Graphically steady states are the intersects of the nullclines.

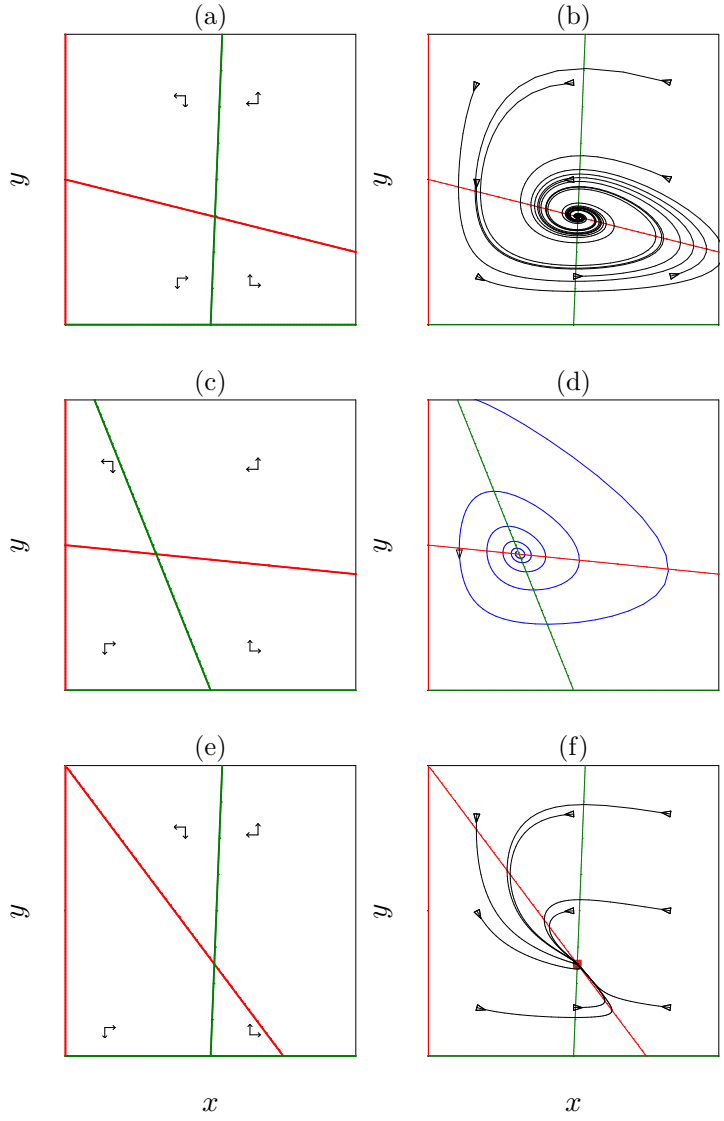

Figure 18.2: Qualitatively different steady states determined by the local vector field in the four regions defined by the nullclines. Spiral points (a-d): the vector field suggests rotation. The spiral point in (a,b) is stable, which can be guessed because increasing x at the steady states makes $\mathrm{d}x/\mathrm{d}t < 0$, and increasing y at the steady states makes $\mathrm{d}y/\mathrm{d}t < 0$ (which is stabilizing). The spiral in (c,d) is unstable, which can be guessed because increasing y at the steady states makes $\mathrm{d}y/\mathrm{d}t > 0$ (which is destabilizing). Panels (e & f) illustrate that nodes can also have a rotating vector field, i.e., that one cannot tell with certainty from the local field whether or not a steady state is a spiral point.

Analytically, one finds

$$(R, N) = (0, 0)\ , \quad (R, N) = (a/b, 0) \quad \text{and} \quad (R, N) = \left(\frac{e}{d}, \frac{da - eb}{dc}\right) \tag{18.5}$$

as the three steady states of this system. Note that the non-trivial steady state only exists when $\frac{da-eb}{dc} > 0$. We will further analyze the model for the parameter condition that all three steady states exist, i.e., we consider $da > eb$.

Finally, one has to determine the nature of the steady states. For the steady states $(0, 0)$ and $(a/b, 0)$ one can read from the vector field that they are saddle points. Around $(a/b, 0)$ the

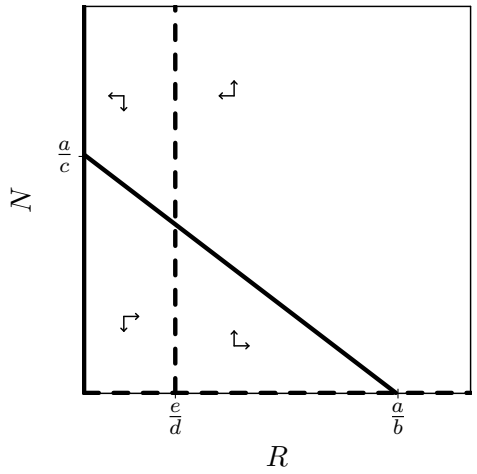

Figure 18.3: The phase space of the Lotka Volterra model with the vector field indicated by the arrows.

vertical component is the unstable direction, and around $(0, 0)$ the horizontal component is the unstable direction. This is not so simple for the non-trivial point. Because there is no stable and unstable direction in the vector field the non-trivial steady state cannot be a saddle point, and it has to be a node or a spiral point. To determine its stability one can check for local feedback. Increasing R in the steady state makes $\mathrm{d}R/\mathrm{d}t < 0$, and increasing N in the steady state keeps $\mathrm{d}N/\mathrm{d}t = 0$ because one lands exactly on the $\mathrm{d}N/\mathrm{d}t = 0$ nullcline (see Fig. 18.3). Because locally there is no positive feedback we suggest that the non-trivial steady state is stable. One can derive the full Jacobian of this model and confirm that this non-trivial steady state is stable.

18.2 Graphical Jacobian

Very often it is sufficient to determine the signs of the Jacobi matrix from the local vector field around the steady state (see the accompanying Ebook (Panfilov *et al.*, 2016)). Consider the vector field around the steady state of some system $\mathrm{d}x/\mathrm{d}t = f(x, y)$ and $\mathrm{d}y/\mathrm{d}t = g(x, y)$. Around the steady state $(\bar{x}, \bar{y})$ in the phase space (x, y) the sign of $\mathrm{d}x/\mathrm{d}t$ is given by the horizontal arrows, i.e., the horizontal component of the vector field. The sign of $\partial_x f$ can therefore be determined by making a small step to the right, i.e., in the x direction, and reading the sign of $\mathrm{d}x/\mathrm{d}t$ from the vector field. Similarly, a small step upwards gives the effect of y on $\mathrm{d}x/\mathrm{d}t$, i.e., gives $\partial_y f$, and the sign can be read from the vertical arrow of the vector field. Repeating this for $\partial_x g$ and $\partial_y g$, while replacing x, y with R, N, one finds around the steady state $(0, 0)$ in Fig. 18.3:

$$J = \begin{pmatrix} \partial_x f & \partial_y f \\ \partial_x g & \partial_y g \end{pmatrix} = \begin{pmatrix} \alpha & 0 \\ 0 & -\beta \end{pmatrix} , \tag{18.6}$$

where α and β are positive constants. Because $\det(J) = -\alpha\beta < 0$ the steady state is a saddle point (see Fig. 18.8). For the steady state without predators one finds

$$J = \begin{pmatrix} -\alpha & -\beta \\ 0 & \gamma \end{pmatrix} , \tag{18.7}$$

Because $\det(J) = -\alpha\gamma < 0$ the equilibrium is a saddle point. For the non-trivial steady state one finds

$$J = \begin{pmatrix} -\alpha & -\beta \\ \gamma & 0 \end{pmatrix} , \tag{18.8}$$

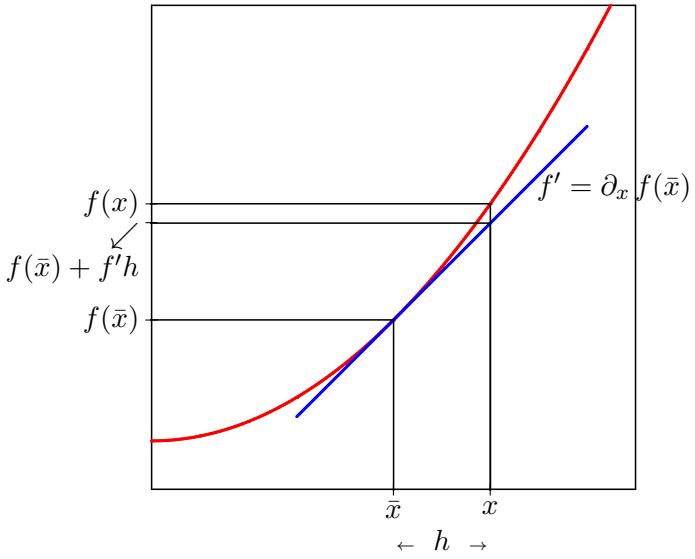

Figure 18.4: Linearization of a non-linear function: $f(x) \simeq f(\bar{x}) + \partial_x f(\bar{x})\,(x - \bar{x}) = f(\bar{x}) + f'h$. The heavy line is the local tangent $f' = \partial_x f(\bar{x})$ at $x = \bar{x}$.

and because $\mathrm{tr}(J) = -\alpha < 0$ and $\det(J) = \beta\gamma > 0$ the equilibrium is stable. This method is also explained in the book of Hastings (1997).

18.3 Linearization

Complicated non-linear functions, $f(x)$, can be approximated by a local linearization around any particular value of x (see the accompanying Ebook (Panfilov *et al.*, 2016)). Fig. 18.4 shows that the local tangent at some point linearizes the function so that nearby function values can be estimated. This derivative can be used to approximate the curved $f(x)$ around a particular value $\bar{x}$, and from Fig. 18.4 we can read that

$$f(x) \simeq f(\bar{x}) + \partial_x f(\bar{x})\,(x - \bar{x})\ ,$$

where $h = x - \bar{x}$ is a small step in the x-direction that we multiply with the local slope, $\partial_x f(\bar{x})$, to approximate the required change in the vertical direction. Basically, one estimates the vertical displacement by multiplying the local slope with the horizontal displacement. A simple example would be the function $f(x) = 3\sqrt{x}$ (with derivative $f' = 3/[2\sqrt{x}]$). The true function values for $x = 4$ and $x = 5$ are $f(4) = 6$ and $f(5) = 6.71$, respectively. We can approximate the latter by writing

$$f(5) \simeq f(4) + \frac{3}{2\sqrt{4}} \times 1 = 6 + 3/4 = 6.75\ , \tag{18.9}$$

which is indeed close to $f(5) = 6.71$. The same can be done for 2-dimensional functions, i.e.,

$$f(x, y) \simeq f(\bar{x}, \bar{y}) + \partial_x f(\bar{x}, \bar{y})\,(x - \bar{x}) + \partial_y f(\bar{x}, \bar{y})\,(y - \bar{y})\ . \tag{18.10}$$

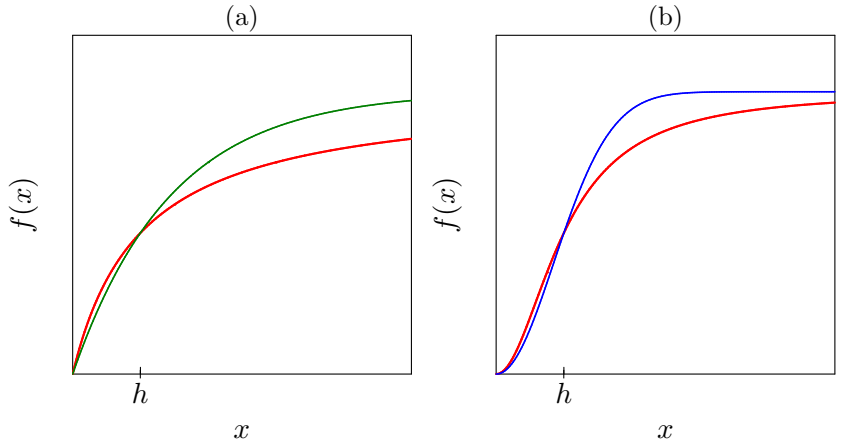

Figure 18.5: The increasing saturation functions defined by Eq. (18.11). The left panel depicts $f(x) = x/(h+x)$ and $f(x) = 1 - \mathrm{e}^{-\ln[2]x/h}$ which both have the convenient property that $0 \leq f(x) < 1$ and $f(x) = 0.5$ when $x = h$. In the panel on the right we draw their corresponding sigmoid variants $f(x) = x^2/(h^2+x^2)$ and $f(x) = 1 - \mathrm{e}^{-ln[2](x/h)^2}$.

18.4 Convenient functions

Once we have a sketch of how some process should depend on a variable of the model, we need to translate this graph into a mathematical function. We here let you become familiar with a few families of convenient functions, i.e., Hill-functions and exponential functions. These will be used to formulate positive and negative effects of populations onto each other. Because these functions are dimensionless and remain bounded between zero and one, i.e., $0 \leq f(x) \leq 1$, one can easily multiply any term in a model (corresponding to some biological process) with such a function. We here define two families of functions $f(x)$ that increase with x, are zero when $x = 0$, and approach a maximum $f(x) = 1$ when $x \to \infty$. Whenever one would need a different maximum in the model, one could simply multiply $f(x)$ with some parameter. Having increasing functions $0 \leq f(x) \leq 1$, one can easily define decreasing functions by taking $g(x) = 1 - f(x)$.

Hill-functions are a very conventional and convenient family of saturation functions:

$$f(x) = \frac{x^n}{h^n + x^n} \quad \text{and} \quad g(x) = 1 - f(x) = \frac{1}{1 + (x/h)^n} \ , \tag{18.11}$$

in which you may recognize the classical Michaelis-Menten saturation function for $n = 1$ (see Fig. 18.5a). The "saturation constant" h is the value of x where $f(x)$ or $g(x)$ attains half of its maximal value. The exponent n determines the steepness of the function. Whenever $n > 1$ the function is sigmoid (see Fig. 18.5b), and for $n \to \infty$ both $f(x)$ and $g(x)$ become step functions switching between zero and one at $x = h$. The slope of $f(x)$ in the origin is determined from its derivative, which for $n = 1$ equals

$$\partial_x f(x) = \frac{1}{h+x} - \frac{x}{(h+x)^2} \ , \tag{18.12}$$

which delivers a slope of $1/h$ for $x = 0$. For $n > 1$ the derivative is

$$\partial_x f(x) = \frac{nx^{n-1}}{h^n + x^n} - \frac{nx^{2n-1}}{(h^n + x^n)^2} \ , \tag{18.13}$$

which means that for $x = 0$ the slope is zero. An advantage of using Hill functions in mathematical models is that solving steady states corresponds to solving polynomial functions.

The **exponential functions**

$$f(x) = 1 - \mathrm{e}^{-\ln[2]x/h} \quad \text{and} \quad g(x) = \mathrm{e}^{-\ln[2]x/h} \ . \tag{18.14}$$

are as conventional as Hill functions. They may be more convenient for finding solutions of equations, but they are more cumbersome when it comes to finding steady states. Like Hill functions we have $f(0) = 0$. For finding the half maximal value of $f(x)$ one solves $0.5 = \mathrm{e}^{-\ln[2]x/h}$ to find that $x = h$. The slope in the origin is determined from the derivative $\partial_x[1 - \mathrm{e}^{-\ln[2]x/h}] = (\ln[2]/h)\mathrm{e}^{-\ln[2]x/h}$ which for $x = 0$ gives a slope of $\ln[2]/h$. The sigmoid form of the exponential function is known as the Gaussian distribution

$$f(x) = 1 - \mathrm{e}^{-\ln[2](x/h)^2} \ , \text{and} \quad g(x) = \mathrm{e}^{-\ln[2](x/h)^2} \ . \tag{18.15}$$

Thanks to our scaling with ln[2] these sigmoid functions are also half maximal when $x = h$ (and $x = -h$); see Fig. 18.5b.

Finally, in Section 6.3 we have presented the Holling I/II function that can be tuned between a discontinuous minimum function and a classical saturated Hill function with a single curvature parameter γ. We have seen that discontinuous saturation functions can easily be written with minimum and maximum functions. For instance, $f(x) = \min[1, x/(2h)]$ has its half-maximal value $f(x) = 0.5$ when $x = h$, but has a sharp corner at $x = 2h$. Another convenient function is

$$f(x) = \sqrt[\alpha]{1 - (x/k)^\alpha} \ , \tag{18.16}$$

which declines from one to zero over the interval $x = 0$ to $x = k$. When $\alpha = 1$ the decline is linear, when $\alpha > 1$ the function is concave, and when $\alpha < 1$ it is convex.

18.5 Scaling

Models can be simplified by scaling variables and time such that one loses a number of parameters. Such scaled variables are said to be dimensionless. Reducing the number of parameters of a model can be very helpful to completely understand its behavior. The technique is explained by writing a dimensionless logistic growth model.

Write the logistic equation as

$$\frac{\mathrm{d}N}{\mathrm{d}T} = rN[1 - N/k] \ , \tag{18.17}$$

where r is the *per capita* maximum rate of increase, and k is the carrying capacity. The parameter r is a rate, with dimension $1/T$, and the parameter k has the dimension "biomass" or "number of individuals". First scale the biomass such that the carrying capacity becomes one. We introduce a new variable n with the property $n = N/k$ such that $n = 1$ when $N = k$. Now substitute $N = kn$ in Eq. (18.17), i.e.,

$$\frac{\mathrm{d}kn}{\mathrm{d}T} = k\frac{\mathrm{d}n}{\mathrm{d}T} = rkn[1 - kn/k] \ , \tag{18.18}$$

which simplifies into

$$\frac{\mathrm{d}n}{\mathrm{d}T} = rn[1 - n] \ , \tag{18.19}$$

which indeed has a carrying capacity $\bar{n} = 1$.

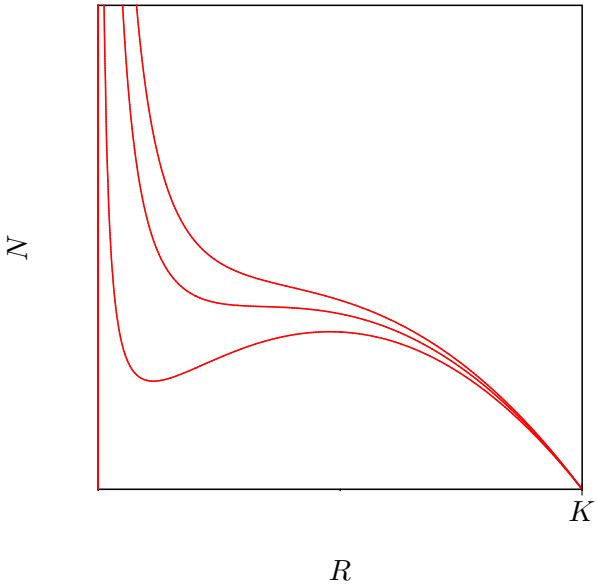

Figure 18.6: The function defined by Eq. (18.22) for three values of h. The inflection point is located at $R = \sqrt[3]{Kh^2}$.

Having lost one parameter one can scale time, T, such that the parameter r disappears, i.e.,

$$r\frac{\mathrm{d}n}{\mathrm{d}t} = rn[1-n] \ , \tag{18.20}$$

implying that $t = rT$. This defines a new time scale for which

$$\frac{\mathrm{d}n}{\mathrm{d}t} = n[1-n] \ . \tag{18.21}$$

This non-dimensional form of the logistic growth equation proves that its solution is always the same sigmoid function. Thus, plotting $N(T)$ as a function of time, the only effect of choosing different parameter values of r and k is a scaling of the horizontal and vertical axis.

18.6 The prey nullcline with a sigmoid functional response

In Section 6.2 we wrote the prey nullcline of the Holling type III functional response as the following function

$$N = \frac{r(h^2+R^2)}{aR}\left(1-\frac{R}{K}\right) \ , \tag{18.22}$$

which has a vertical asymptote at $R = 0$ and is zero when $R = K$ (see Fig. 18.6). The derivative f' of this function is negative when $R \to 0$ and around $R = K$. The function will be non-monotonic, and have a minimum and a maximum, when the derivative is positive in the inflection point. The first and second derivative with respect to R are

$$f' = \frac{r(KR^2-2R^3-h^2K)}{aKR} \quad \text{and} \quad f'' = \frac{2r(h^2K-R^3)}{aKR^3} \ , \tag{18.23}$$

respectively. Solving $f'' = 0$ shows that the inflection point is located at $R = \sqrt[3]{Kh^2}$ (see Fig. 18.6). Substituting this value of R into f' and solving $f' > 0$ yields $h < \frac{K}{3\sqrt{3}} \simeq \frac{K}{5}$, which says that the function is non-monotonic whenever the saturation constant h is sufficiently small.

18.7 Mathematical background

Sketching functions

Most models in this course are analyzed graphically by sketching nullclines in phase space. Some experience with sketching functions is therefore required. To fresh up these techniques we here discuss the general approach, and give a few examples. Since most of the models have free parameters, we also have to sketch functions with free parameters. This implies that one cannot simply resort to a computer program or a graphical calculator.

The general procedure is:
1. Determine the intersects with the horizontal and vertical axes.
2. Check for vertical asymptotes, i.e., x values leading to division by zero.
3. Check for horizontal asymptotes by taking the limit $x \to \infty$ and $x \to -\infty$.
4. Check where the function has positive values and where it has negative values.
5. We typically **do not need** to determine minimum values, maximum values, or inflexion points.

Example 1
Sketch the function

$$y = \frac{ax}{b-x} \tag{18.24}$$

in a graph plotting y as a function of x:
a. For $x = 0$ one finds $y = 0$ as the intersect with the y-axis. This is the only intersect with the horizontal axis.
b. There exists a vertical asymptote at $x = b$. When $x \uparrow b$ one finds that $y \to \infty$, when $x \downarrow b$ one sees that $y \to -\infty$.
c. To find horizontal asymptotes one rewrites the function into

$$y = \frac{a}{b/x - 1} \ . \tag{18.25}$$

Both for $x \to \infty$ and for $x \to -\infty$ one sees $y \to -a$. Thus, we find one horizontal asymptote at $y = -a$.
d. When $x < 0$ one sees that $y < 0$, when $0 \leq x < b$ one sees that $y \geq 0$, and when $x > b$ one finds $y < 0$. The function is sketched in Fig. 18.7a.

Example 2
Sketch the system

$$0 = \sigma + \frac{aX}{b+X} - cY \ , \tag{18.26}$$

$$0 = -\alpha + \beta X - \gamma Y \tag{18.27}$$

in one graph. Because both equations can easily be solved for the Y variable, it is most easy to draw Y as a function of X. For the second equation one finds

$$Y = -\alpha/\gamma + (\beta/\gamma)X \ , \tag{18.28}$$

which is a straight line with slope β/γ.
a. The intersect with the Y-axis $-\alpha/\gamma$, and that with horizontal axis $X = \alpha/\beta$.
b. No vertical asymptotes.
c. No horizontal asymptotes.
d. When $X < \alpha/\beta$ one finds $Y < 0$, otherwise $Y \geq 0$.

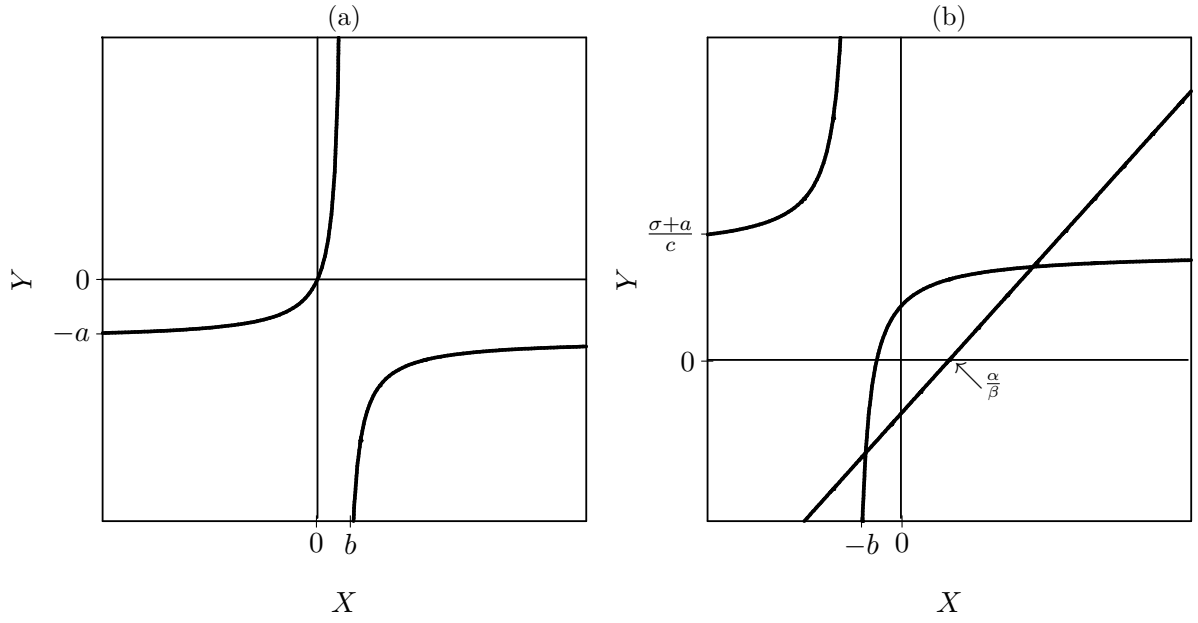

Figure 18.7: Two examples for **qualitatively** sketching functions.

For the first equation we also write Y as a function of X

$$Y = \sigma/c + \frac{(a/c)X}{b+X} \ . \tag{18.29}$$

a. The intersect with the vertical axis is $Y = \sigma/c$. That with the X axis is $X = -b\sigma/(\sigma + a)$.
b. There exists a vertical asymptote at $X = -b$. When $X \downarrow -b$ one finds that $Y \to -\infty$ and when $X \uparrow -b$ we see $Y \to \infty$.
c. For the horizontal asymptotes one first writes

$$Y = \sigma/c + \frac{(a/c)}{b/X + 1} \ , \tag{18.30}$$

to see that for $X \to \infty$ and for $X \to -\infty$, $Y \to (\sigma + a)/c$.
d. One finds that $Y > 0$ if $X > -b\sigma/(\sigma + a)$ or if $X < -b$.
Although one does not know the parameters for this system, one can be sure that in the positive quadrant the two curves have to intersect. Thus, qualitatively, there is only one unique situation, which is depicted in Fig. 18.7b.

Useful mathematical formulas

To fresh up your memory of earlier education in mathematics we provide a few standard formulas

$$\ln 1 = 0 \ , \quad \ln xy = \ln x + \ln y \ , \quad \ln x/y = \ln x - \ln y \ , \quad \mathrm{e}^{\mathrm{i}x} = \cos x + \mathrm{i}\sin x \ , \tag{18.31}$$

and the two roots of the quadratic equation

$$ax^2 + bx + c = 0 \quad \text{are} \quad x_\pm = \frac{-b \pm \sqrt{b^2 - 4ac}}{2a} \ . \tag{18.32}$$

The standard rules of differentiation are

$$[cx]' = c \ , \quad [cx^n]' = ncx^{n-1} \ , \quad [f(x) + g(x)]' = f'(x) + g'(x) \ , \tag{18.33}$$

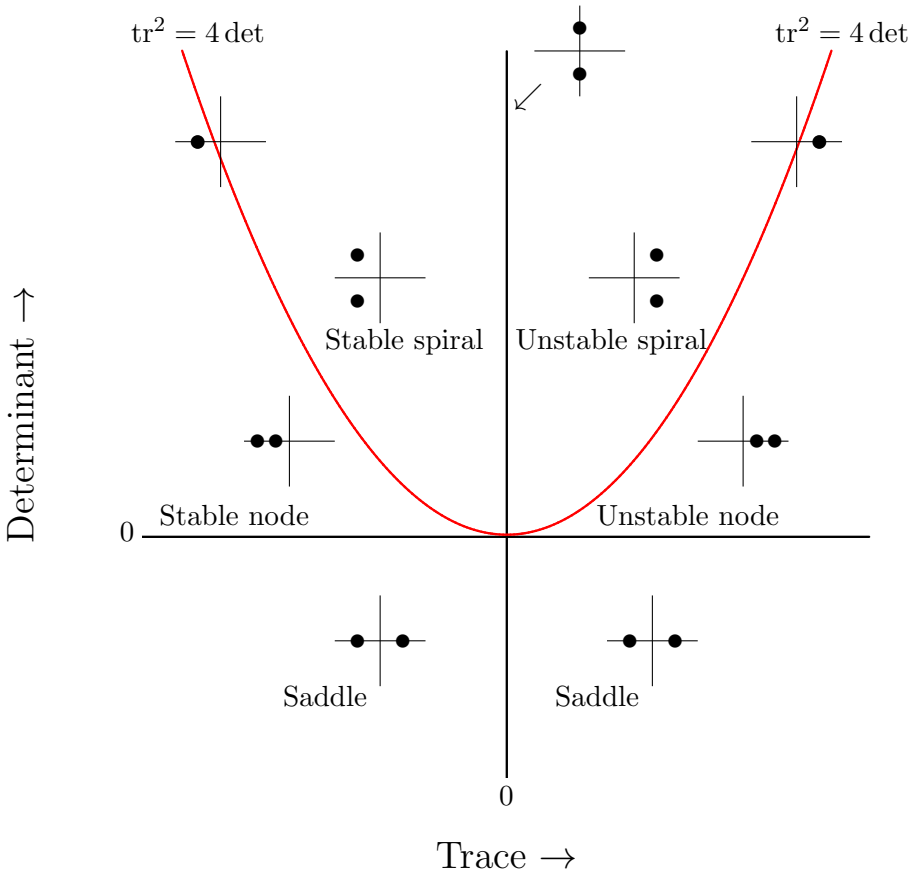

Figure 18.8: The stability of a steady state as a function of the trace and determinant of a 2-dimensional Jacobi-matrix. The bullets depict the real and imaginary parts of the eigenvalues in so-called Argand diagrams (where the horizontal axis reflects the real part, and the vertical axis the imaginary part of the eigenvalue).

where the $'$ means ∂_x, and

$$[f(x)g(x)]' = f'(x)g(x) + f(x)g'(x) \ , \quad \left[\frac{f(x)}{g(x)}\right]' = \frac{f'(x)}{g(x)} - \frac{f(x)g'(x)}{g(x)^2} \ , \tag{18.34}$$

and the famous chain rule

$$f[g(x)]' = f'(g)\ g'(x) \quad \text{, e.g.,} \quad \sqrt{1+ax}\,' = \left[\frac{1}{2}(1+ax)^{-\frac{1}{2}}\right] a = \frac{a}{2\sqrt{1+ax}} \ . \tag{18.35}$$

Trace and determinant

In the accompanying Ebook (Panfilov *et al.*, 2016) we explain that the eigenvalues of an arbitrary matrix

$$A = \begin{pmatrix} p & q \\ r & s \end{pmatrix} \tag{18.36}$$

are the solutions of the characteristic equation

$$(p-\lambda)(s-\lambda) - rq = \lambda^2 - \lambda(p+s) + (ps - rq) = 0 \ . \tag{18.37}$$

Defining the "trace" of the matrix as $\mathrm{tr} = p + s$ and the "determinant" as $\det = ps - rq$, the characteristic equation simplifies into

$$\lambda^2 - \mathrm{tr}\lambda + \det = 0 \tag{18.38}$$

with solutions

$$\lambda_\pm = \frac{\mathrm{tr} \pm \sqrt{\mathrm{tr}^2 - 4\det}}{2} = \frac{\mathrm{tr} \pm \sqrt{D}}{2} \ , \tag{18.39}$$

where $D \equiv \mathrm{tr}^2 - 4\det$ is the "discriminant" of the matrix. If $D < 0$ the $\sqrt{D}$ delivers imaginary solutions that correspond with oscillations ($\mathrm{e}^{\mathrm{i}x} = \cos[x] + \mathrm{i}\sin[x]$).

Summing the two eigenvalues $\lambda_\pm$ yields

$$\frac{\mathrm{tr} + \sqrt{\mathrm{tr}^2 - 4\det}}{2} \ + \ \frac{\mathrm{tr} - \sqrt{\mathrm{tr}^2 - 4\det}}{2} = \mathrm{tr} \ , \tag{18.40}$$

and the product gives

$$\frac{\mathrm{tr} + \sqrt{\mathrm{tr}^2 - 4\det}}{2} \ \times \ \frac{\mathrm{tr} - \sqrt{\mathrm{tr}^2 - 4\det}}{2} = \det \ . \tag{18.41}$$

If this matrix was the Jacobian of a steady state, we now observe that to check for stability, i.e., $\lambda_+ < 0$ and $\lambda_- < 0$, it is therefore in many cases sufficient to know the values of the trace and the determinant. When $\det > 0$ one knows that either both eigenvalues are negative or that they are both positive. Having $\det > 0$ and $\mathrm{tr} < 0$ one knows that they cannot be positive, and therefore that they are both negative and the steady state has to be stable. Summarizing an easy test for stability is $\mathrm{tr}[J] < 0$ and $\det[J] > 0$ (see Fig. 18.8).

18.8 Exercises

Question 18.1. Sketch a few functions
In this course we sketch nullclines from models with free parameters. It is very important therefore to know how to sketch arbitrary functions with free parameters.
a. Sketch $y = \frac{h}{h+x}$.
b. Sketch $y = \frac{x}{h+x}$.
c. Sketch $aA - bLA - cL = 0$ plotting L as a function of A, and plotting A as a function of L.
d. Sketch $0 = aY(1-Y) - \frac{bYX}{c+Y}$. Hint: think beforehand which variable can best be expressed as a function of the other variable.
e. Sketch $y = a\ \frac{k-x}{q+k-x} - d$ assuming that $a > d$.
f. Sketch $y = a\sqrt{x}(1-x)$. What is the derivative when $x = 0$? At what value of x will y have a maximal value?

Question 18.2. Linearization
Consider the function $f(x) = x^2$.
a. What is the derivative $\partial_x f(x)$?
b. Use linearization around $x = 3$ to estimate the function value at $x = 3.1$. What is the true value at $x = 3.1$?

Question 18.3. Scaling
Scale the Lotka-Volterra predator prey model by introducing non-dimensional population densities, and scale time by the natural rate of increase of the prey.
a. Write the new model.
b. How many parameters did you lose?

Chapter 19

Answers to the exercises

Question 2.1. Red blood cells
A possible good answer has the following sketches:

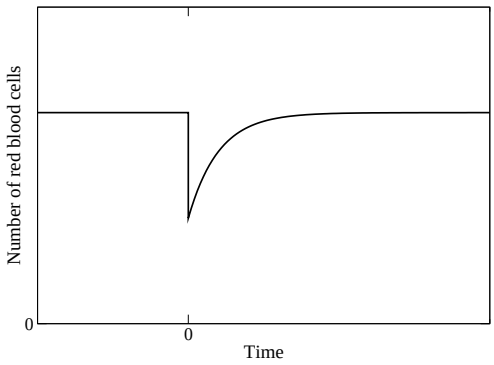

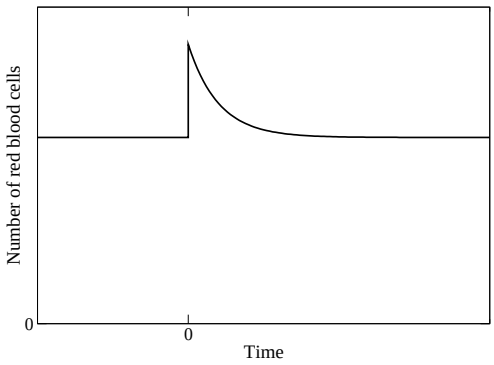

a. $\mathrm{d}N/\mathrm{d}t = m - dN$.
b. See the sketch in Panel (a)
c. See the sketch in Panel (b)

Question 2.2. Pesticides on apples
A possible good answer has the following sketch:

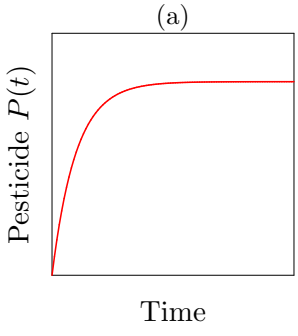

a. See the sketch in Panel (a)

b. $\bar{P} = \sigma/\delta$.
c. The model becomes $\mathrm{d}P/\mathrm{d}t = -\delta P$ with the initial condition $P(0) = \sigma/\delta$. Solving $P(0)/2 = P(0)\mathrm{e}^{-\delta t}$ yields $t_{1/2} = \ln[2]/\delta$.
d. From $\mathrm{d}P/\mathrm{d}t = 2\sigma - \delta P$ with $\bar{P} = 2\sigma/\delta$, one obtains the same $\ln 2/\delta$ days for the half life.
e. From $50 = \ln 2/\delta$ one obtains $\delta = 0.014$ per day.

Question 2.3. Bacterial growth

a. $t = \ln[2]/r$.
b. From $rB - kNB = 0$ we neglect the trivial $B = 0$ solution to obtain $N = r/k$.
c. The dimension of r is per hour. Since the total term kNB has dimension "number of bacteria per ml per hour", the dimension of k should be "per neutrophil per ml per hour". This can also be checked from the expression $N = r/k$ that should be "neutrophils per ml" on the both the left- and right-hand side.
d. "bacteria per neutrophil per hour". This is the maximum number of bacteria that one neutrophil can encounter and kill per hour.
e. $N = (r/k)(h + B)$, which is a straight line with slope r/k, intersecting the vertical axis at $N = rh/k$. This line is a nullcline: below this line $\mathrm{d}B/\mathrm{d}t > 0$, and above it $\mathrm{d}B/\mathrm{d}t < 0$.
f. h has the dimension number of bacteria per ml. When $B = h$ the model is $\mathrm{d}B/\mathrm{d}t = rB - kN/2$ saying the neutrophils are killing at a rate $k/2$, i.e., half their half-maximal killing rate.

Question 2.4. Injecting anesthesia

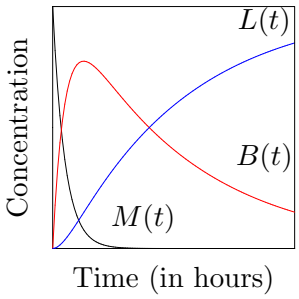

a. See the sketch.
b. $\ln 2/e$ hours.
c. No, it all depends on the clearance rate from the blood, and how long the operation takes. If c is small one should wait longer than $\ln 2/e$ hours.
d. For $\delta = 0$ everything ends op in the liver: $L(\infty) = M(0)$.

Question 2.5. SARS

a. First count the total number of infected patients $I(t)$. $R_0 = 3$ in two weeks means that $\beta = 1.5$ per week. For a time scale of weeks the model therefore is $\mathrm{d}I/\mathrm{d}t = 1.5I - 0.5I = I$. The equation to solve is $3 \times 10^9 = I(0)\mathrm{e}^{rt}$, where $r = (\beta - \delta) = 1$, and where one starts with one infected individual, i.e., $I(0) = 1$. Solving $3 \times 10^9 = \mathrm{e}^t$ yields $t = 22$ weeks for the time required to have $I(t) = 3 \times 10^9$.
One could argue that it is more interesting to calculate the time required to have killed half of the population, but this is more difficult. For that one also should keep track of the total number of dead individuals $\mathrm{d}D/\mathrm{d}t = \delta I$. With $I(t) = \mathrm{e}^{(\beta-\delta)t}$ and $D(0) = 0$ the solution of $\mathrm{d}D/\mathrm{d}t = \delta\mathrm{e}^{(\beta-\delta)t}$ is $D(t) = \frac{\delta[\mathrm{e}^{(\beta-\delta)t}-1]}{\beta-\delta}$. Solving $I(t) + D(t) = 3 \times 10^9$ for $\beta = 1.5$ and $\delta = 0.5$ per week gives a total time of $t = 21$ weeks. The difference is small because the number of dead patients approaches a fixed fraction $\frac{\delta}{\beta-\delta} = 0.5$ of the total number of patients that are alive.
b. No, it will go slower because the epidemic will limit itself by depleting the number of susceptibles. A better model is to add an ODE for the susceptibles, S, where $S(0) = 6 \times 10^9$ is the initial population size. Redefining β as the chance to meet and infect a susceptible person the model becomes

$$\frac{\mathrm{d}I}{\mathrm{d}t} = \beta IS - \delta I \quad \text{and} \quad \frac{\mathrm{d}S}{\mathrm{d}t} = -\beta IS \ .$$

Another improvement of the model that would slow down the epidemic is to allow for an incubation period, i.e., to introduce a time lag in the two week period during which patients are not yet infective.

Question 2.6. Physics

a. The dimension of v is m/s and that of a is m/s^2.

b. The derivative of the $v(t)$ solution is $\mathrm{d}v/\mathrm{d}t = a$ and that of the $x(t)$ solution is $\mathrm{d}x/\mathrm{d}t = at + v(0)$.

Question 3.1. Seed bank

Since plants are born from a fixed seed bank, one can use a simple source term for modeling the growth. Assuming a simple density independent death rate one would write

$$\frac{\mathrm{d}N}{\mathrm{d}t} = s - dN \ .$$

Since this has $\bar{N} = s/d$ as a well-defined carrying capacity, the model seems well-behaved, and one apparently does not need to invoke any density dependent factors.

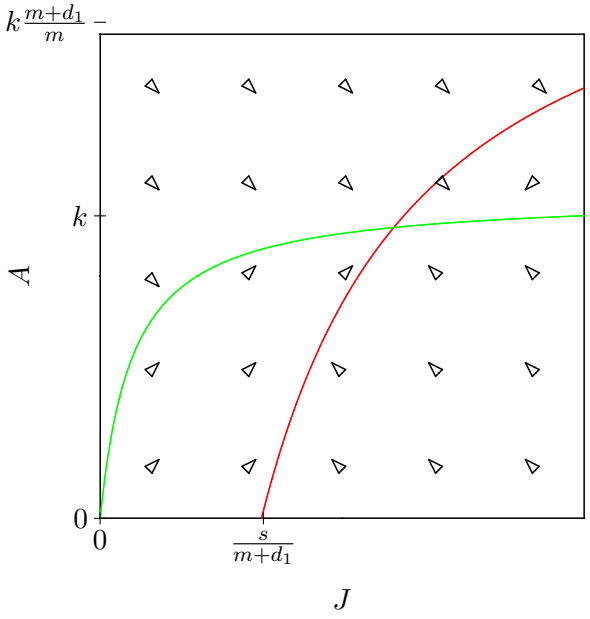

For a more elaborate extension of this model, where seedlings that are growing in the shade of adult plants take longer to mature, one could write:

$$\frac{\mathrm{d}J}{\mathrm{d}t} = s - d_1 J - mJ(1 - A/k) \quad \text{and} \quad \frac{\mathrm{d}A}{\mathrm{d}t} = mJ(1 - A/k) - d_2 A \ ,$$

where J are the (juvenile) seedlings, A are the (adult) plants, and k is the plant density at which the maturation rate becomes zero. For the juvenile nullcline we solve

$$s - d_1 J - mJ + mJA/k = 0 \quad \text{or} \quad A = k\frac{m + d_1}{m} - \frac{ks}{mJ} \ ,$$

which is a function of the form $y = a - b/x$, i.e., an increasing function with a horizontal asymptote $k\frac{m+d_1}{m}$. For low values of J one obtains negative values, and the nullcline intersects the line $A = 0$ at $J = s/(m + d_1)$. For the adult nullcline we solve

$$mJ - mJA/k - d_2 A = 0 \quad \text{or} \quad A = \frac{mJ}{d_2 + mJ/k} = \frac{kJ}{kd_2/m + J} \ ,$$

which is a conventional increasing saturation function with maximum k, saturation constant kd_2/m, and going through the origin. Since the horizontal asymptote of the $\mathrm{d}A/\mathrm{d}t = 0$ isocline, k, is smaller than that of the $\mathrm{d}J/\mathrm{d}t = 0$ isocline, i.e., $k < k\frac{m+d_1}{m}$, and the $\mathrm{d}J/\mathrm{d}t = 0$ isocline intersects the horizontal axis at $J = s/(m + d_1)$, the nullclines will always intersect. The vector field shows that the —one and only— steady state is stable.

Question 3.2. Carrying capacity

When a population approaches its carrying capacity:

a. the *per capita* birth rate is minimal

b. the *per capita* death rate is maximal.

c. The individual well-being is expected to be best in an expanding population: the *per capita* birth rate is maximal and the *per capita* death rate is minimal.

d. With $\mathrm{d}N/\mathrm{d}t = rN[1 - N/(k\sqrt{N})] = 0$ one obtains the carrying capacity from $N/(k\sqrt{N}) = 1$ or $\sqrt{N} = k$ giving $\bar{N} = k^2$ which is still a finite carrying capacity, at which circumstances are poor. For the best circumstances the population has to remain below its carrying capacity.

Question 3.3. Assumptions

Every mathematical model comes with assumptions.

a. Unrealistic assumptions of ODEs are

1. All individuals are equal or average.
2. The population size remains so large that discrete effects of having only a few individuals can be ignored.
3. The parameters are fixed constant.
4. The individuals are well-mixed and there are no spatial effects.

b. Models simplify reality and can therefore help to give insight into population dynamics.

Question 3.4. Fishing herring

A possible good answer has the following sketches:

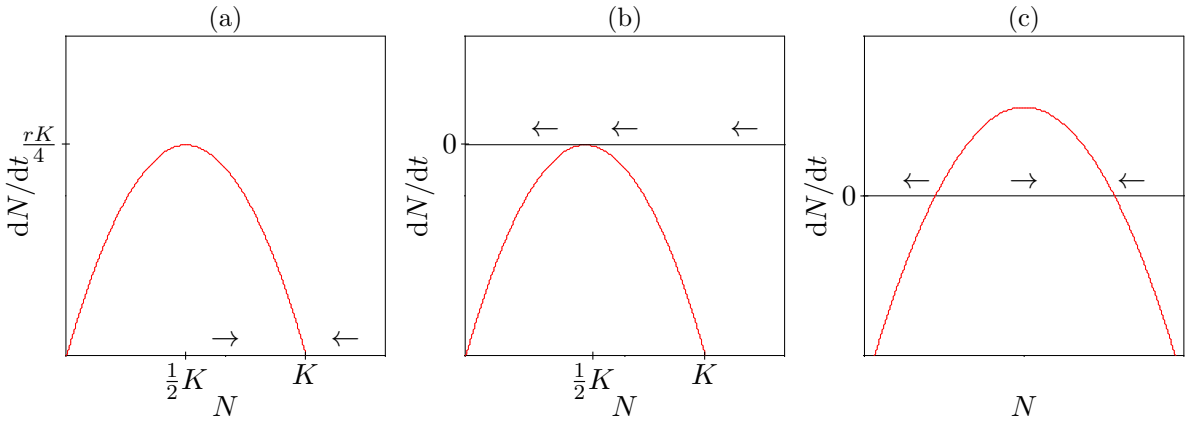

a. $\mathrm{d}N/\mathrm{d}t = f(N) = rN(1 - N/K)$, which is a parabola crossing the horizontal axis at $N = 0$ and $N = K$. See the sketch in Panel (a).

b. The maximum of the function, $f(N) = rN - rN^2/K$, is found by setting its derivative, $\partial_N f = r - 2rN/K$, to zero. This delivers $\hat{N} = K/2$ (see Panel (a)). Substituting this maximum into the population growth function, one obtains the maximum population growth of $f(\hat{N}) = rK/4$.

c. The optimal population size is that yielding maximum growth, i.e., $N = K/2$, and the total population growth, $rK/4$, could in principle be harvested.

d. $\mathrm{d}N/\mathrm{d}t = rN(1 - N/K) - rK/4$.

e. See the sketch in Panel (b): at the maximum harvest there is a steady state where $\mathrm{d}N/\mathrm{d}t = 0$. Starting at $N = K$ and allowing for this maximum harvest, one mathematically approaches this steady at $N = K/2$. This steady state is not structurally stable, however, as any disturbance of the population size, bringing it below the steady state at $N = K/2$, will let the fish go extinct.

f. One should never catch the maximum yield. This allows for a stable population size while the population is harvested. See the sketch in Panel (c). The population remains vulnerable to extinction by large perturbations due to the saddle point at low population densities. In the computer practical you will revisit this problem and discover that by catching an optimal *fraction* of the population one can on average catch this maximum yield, without threatening the population with extinction.

Question 3.5. Owls

An essential element of this question is that you have to implement the statement that the owls find the tree hollows easily. This calls for a minimum function that switches discontinuously between all trees occupied and still having some empty trees. A minimum function like $y = \min(N, h)$ allows for that since $y = N$ when $N < h$ and $y = h$ otherwise. A possible good answer has the following sketches:

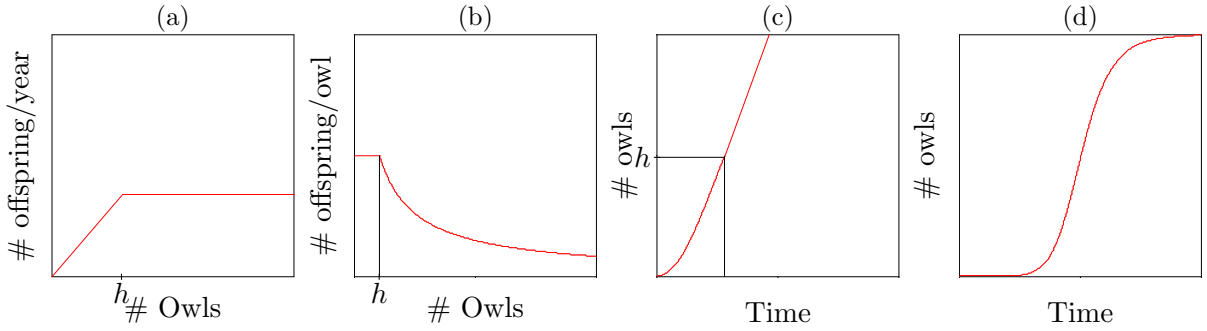

a. See the sketch in Panel (a).

b. A simple model is $\mathrm{d}N/\mathrm{d}t = b\min(N, h) - dN$, where b and d are birth and death rates, and h is the number of tree hollows.

c. The *per capita* birth rate is b when $N < h$ and bh/N when $N \geq h$. See the sketch in Panel (b).

d. When $N \geq h$ the population growth becomes maximal, and the curve becomes a straight line with the slope of the growth at $N = h$. See the sketch in Panel (c).

e. When $N \geq h$ the *per capita* growth slows down due to the death, and $\mathrm{d}N/\mathrm{d}t = b\min(N, h) - dN$ approaches the steady state $\bar{B} = bh/d$. See the sketch in Panel (d).

Question 3.6. Patches

A possible good answer has the following sketches:

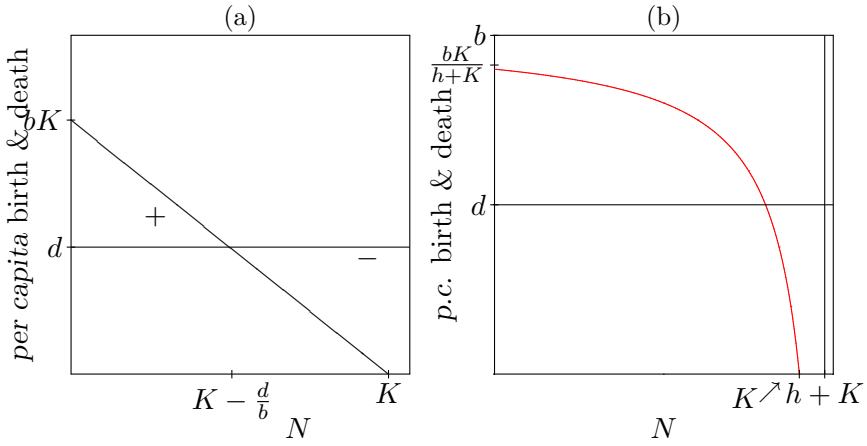

a. $\mathrm{d}N/\mathrm{d}t = bNL - dN$ with $L = \max(0, K - N)$. Note that bK is the maximum birth rate. The parameter b would have the usual interpretation of a maximal birth rate when one writes L as a probability to find an empty patch, i.e., $L = \max[0, (K - N)/K]$.

b. The fitness is $R_0 = bK/d$, and the steady states are solved from $\mathrm{d}N/\mathrm{d}t = bN(K-N) - dN = 0$ giving $N = 0$ and $K - N = d/b$ or $\bar{N} = K - d/b = K[1 - d/(bK)] = K[1 - 1/R_0]$. Note that $\bar{N} < K$ so that at this steady state we can ignore the maximum function, i.e., $L = \max(0, K - N) = K - N$. There is no steady state when $N > K$ and $L = \max(0, K - N) = 0$

c. No, K is not the carrying capacity, the steady state is at $\bar{N} = K(1 - 1/R_0)$ which is smaller than K.

d. The *per capita* birth rate $b(K - N)$ is a straight line intersecting the vertical axis at $y = bK$ and the horizontal axis at $N = K$. The *per capita* death rate is a horizontal line at $y = d$. See the sketch in Panel (a). The lines intersect in the carrying capacity, which is stable because increasing N decreases $\mathrm{d}N/\mathrm{d}t$, decreasing N increases $\mathrm{d}N/\mathrm{d}t$.

e. Adopting a saturation function of the form $f(L) = \frac{L}{h+L}$ where $L = K - N$, one obtains $\mathrm{d}N/\mathrm{d}t = bN\frac{L}{h+L} - dN$. The shape of $f(L)$ when plotted as a function of L is shown in Fig. 18.5a: after increasing almost linearly, it approaches a horizontal asymptote $f(L) \to 1$ when $L \to \infty$. The half-maximal value $f(L) = 1/2$ is reached when $L = h$.

f. The *per capita* birth rate is

$$y = b\frac{L}{h+L} = \frac{b(K-N)}{h+K-N} \ .$$

When $N = 0$ the birth rate is $y = bK/(h + K)$, and $y = 0$ when $N = K$. To find the horizontal asymptote we first divide both the numerator and the denominator by the highest order of N (here N^1) to obtain

$$y = \frac{bK/N - b}{(h+K)/N - 1} \quad \text{which for} \quad N \to \infty \quad \text{and} \quad N \to -\infty \quad \text{gives} \quad y = b \ ,$$

and the function has a vertical asymptote at $N = h + K$. This enables us to sketch the biologically relevant part of the *per capita* birth rate in Panel (b). The death rate is density independent, and corresponds to the horizontal line in Panel (b).

g. No, see the intersection point in Panel (b). Because the *per capita* birth rate is zero at $N = K$, whereas the *per capita* death rate is d, $N = K$ cannot be a steady state. The carrying capacity is again smaller than the total number of patches, and can be solved from $b\frac{K-N}{h+K-N} = d$, i.e., $\bar{N} = K - \frac{dh}{b-d}$. Note that the first question in Chapter 18 asks for a sketch of $\mathrm{d}N/\mathrm{d}t$ versus N.

Question 3.7. Return Time

a. For $\mathrm{d}N/\mathrm{d}t = bN - dN(1+N/K)$ with $R_0 = b/d$ there are two steady states, the origin $\bar{N} = 0$, and the carrying capacity $\bar{N} = K(R_0 - 1)$. For the return time of the carrying capacity one computes the derivative $\partial_N = b - d - 2dN/K$ and substitutes the steady state value to obtain

$$\lambda = b - d - \frac{2d}{K}\, K(R_0 - 1) = b - d - 2d(b/d - 1) = d - b$$

The return time

$$T_R = \frac{-1}{\lambda} = \frac{1}{b-d} = \frac{1}{d(R_0 - 1)} \ .$$

Thus, if R_0, or the death rate, is increased the return time will decrease.

b. For $\mathrm{d}N/\mathrm{d}t = s - dN$ with steady state $\bar{N} = s/d$, the derivative $\partial_N[s - dN] = -d$. This immediately gives $\lambda = -d$ and $T_R = 1/d$. Note that one can always scale the population size by its steady state, i.e., define a scaled population as $n = \frac{d}{s}N$ (hence $N = \frac{s}{d}n$) obeying the new ODE $\frac{s}{d}\mathrm{d}n/\mathrm{d}t = s - \frac{s}{d}dn$, or $\mathrm{d}n/\mathrm{d}t = d - dn$.

Question 3.8. Regulation of birth rates

The model uses a simple Hill function for the decline of the birth rate with the population size.

a. The *per capita* growth is $b/(1 + N)$ which is maximal if there is no competition, i.e., when $N = 0$.

b. R_0 is the maximum *per capita* growth multiplied by the expected life span, $R_0 = b(1/d) = b/d$.

c. Solving $\mathrm{d}N/\mathrm{d}t = \frac{bN}{1+N} - dN = 0$ gives $N = 0$ and

$$\frac{b}{1+N} - d = 0 \quad \text{giving} \quad \frac{b}{d} = 1 + N \quad \text{or} \quad \bar{N} = R_0 - 1 \ .$$

The stability can be obtained from the graphic method shown in Fig. 3.1 or by linearizing. Defining $\mathrm{d}N/\mathrm{d}t = g(N)$ the derivative of the growth function $g(N)$ is

$$\partial_N g = \frac{b}{1+N} - \frac{bN}{(1+N)^2} - d = \frac{b}{(1+N)^2} - d \ ,$$

which for $\bar{N} = 0$ gives a slope $\lambda = b - d$, which is positive whenever $R_0 > 1$. Substituting $\bar{N} = R_0 - 1$ gives

$$\lambda = \frac{b}{R_0^2} - d = \frac{d}{R_0} - d = d(1/R_0 - 1) \ ,$$

which is less than zero whenever $R_0 > 1$. Thus, for $R_0 > 1$, the origin is unstable and the carrying capacity is stable.

d. We have already computed for the carrying capacity that $\lambda = d(1/R_0 - 1)$. The return time $T_R = -1/\lambda$ therefore becomes $T_R = 1/[d(1 - 1/R_0)]$, which is positive whenever $R_0 > 1$, and which approaches a minimum of $T_R = 1/d$ when R_0 is large.

e. The density at which the growth is maximal is found from setting the derivative $\partial_N g$ to zero, and solving for N: $\frac{b}{d} = (1 + N)^2$ giving $N = \sqrt{R_0} - 1$.

f. Insert the solution of **e** into the original growth equation, delivering

$$\frac{\mathrm{d}N}{\mathrm{d}t} = \frac{b(\sqrt{R_0} - 1)}{\sqrt{R_0}} - d(\sqrt{R_0} - 1) \ .$$

Question 4.1. Lichens

A possible good answer has the following sketches:

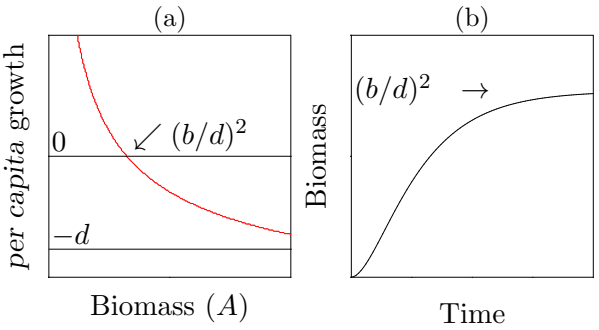

a. Since the total biomass is given by $A = c\pi r^2$, one obtains that $r = \sqrt{\frac{A}{c\pi}} = c'\sqrt{A}$, where c' is a new scaling constant. The total growth rate is proportional to the circumference $2\pi r$, which after substituting the radius becomes $2\pi c'\sqrt{A} = b\sqrt{A}$, where b is a "birth rate" that is proportional to the square root of the biomass. On the other hand, the total death rate is proportional to the total biomass. A simple model would therefore be $\mathrm{d}A/\mathrm{d}t = b\sqrt{A} - dA$.

b. The carrying capacity is solved from $b\sqrt{A} - dA = 0$ or $b - d\sqrt{A} = 0$ giving $\bar{A} = (b/d)^2$.

c. The *per capita* growth $\frac{\mathrm{d}A/\mathrm{d}t}{A} = \frac{b}{\sqrt{A}} - d$. Which for $A \to \infty$ approaches the horizontal asymptote $-d$, which seems perfectly reasonable. For small population size, i.e., $A \to 0$, the *per capita* growth blows up, however, which is not a good property of the model. See the sketch in Panel (a).

d. The initial population growth will not be exponential, and will slow down until the lichen approaches its equilibrium size. See the sketch in Panel (b).

e. One could make the birth rate linear at low densities: $\mathrm{d}A/\mathrm{d}t = b\min(A, \sqrt{hA}) - dA$, where h is the density at which the growth becomes proportional to the circumference.

f. Defining the width of the ring as w, the total biomass would be proportional to $A = \pi r^2 - \pi(r-w)^2 = 2\pi rw - \pi w^2$. For large lichens, $w \ll r$, this approaches $A = 2\pi rw$, which is proportional to the radius, i.e., $r = A/(2\pi w) = cA$, where c is yet another scaling constant. The model would therefore approach $\mathrm{d}A/\mathrm{d}t = (\beta - d)A$, i.e., exponential growth.

Question 4.2. Life stages

A possible good answer has the following sketches:

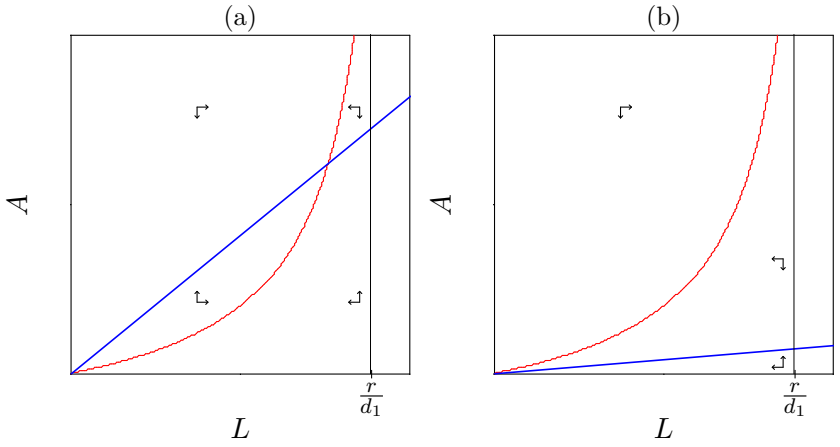

a. For the larvae, L, and the adults, A, one could write

$$\frac{\mathrm{d}L}{\mathrm{d}t} = rA - mL - d_1LA \quad \text{and} \quad \frac{\mathrm{d}A}{\mathrm{d}t} = mL - d_2A\ ,$$

where m is the maturation of the larvae, and r the reproduction of the adults.

b. The larvae nullcline is solved from $\mathrm{d}L/\mathrm{d}t = rA - mL - d_1LA = 0$ giving $A = \frac{mL}{r-d_1L}$, which is zero when $L = 0$ and has a vertical asymptote at $L = r/d_1$. The slope in the origin is computed from the derivative

$$\frac{m}{r - d_1L} + \frac{md_1L}{(r - d_1L)^2} \quad \text{which for } L = 0 \text{ gives} \quad \frac{m}{r} \ .$$

See the sketch in Panel (a). For the adults $\mathrm{d}A/\mathrm{d}t = mL - d_2A = 0$ gives $A = \frac{mL}{d_2}$, which is a line with slope m/d_2. If $m/d_2 > m/r$ the two nullclines intersect in a non trivial stable steady state. Otherwise the origin is the only steady state (see Panel (b)).

c. Assuming a quasi steady state for the larvae, one has to solve L from $\mathrm{d}L/\mathrm{d}t = 0$, giving $\hat{L} = \frac{rA}{m+d_1A}$.

d. Substituting $\hat{L}$ into the adult equation gives $\mathrm{d}A/\mathrm{d}t = \frac{mrA}{m+d_1A} - d_2A$ for the quasi steady state model. This is one of the models with a density dependent birth rate (see Table 4.1).

e. From $A = (m/d_2)L$ we get $\mathrm{d}L/\mathrm{d}t = (r' - m)L - dL^2$ where $r' = rm/d_2$ and $d = d_1m/d_2$, which has the form of a logistic equation.

f. In many insect species the adults live much shorter than the larvae. Then $\mathrm{d}A/\mathrm{d}t = 0$ would be most realistic.

Question 4.3. Allee effect

To develop a model for the whales we have to consider three biological processes: birth, death, and the likelihood of finding a male. We write a model for the number of females, N, in the population, and assume that there is a similar number of males. The true population size would therefore be similar to $2N$. The probability that an individual female finds a male should increases with the number of males, and approach one at large densities of males. A simple saturation function $p = N/(m + N)$, where p is the probability, and m is the population size at which there is a 50% probability of finding a male. Assuming density dependent birth one would write

$$\frac{\mathrm{d}N}{\mathrm{d}t} = \frac{bN}{1 + N/h} \ \frac{N}{m + N} - dN \ ,$$

and assuming density dependent death one would write

$$\frac{\mathrm{d}N}{\mathrm{d}t} = bN\frac{N}{m + N} - dN(1 + eN) \ ,$$

and in reality one could have a combination of the two.

Question 4.4. Nullcline

A possible good answer has the following sketch:

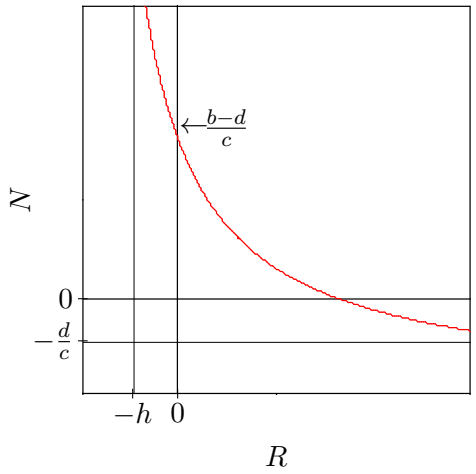

Setting $\mathrm{d}R/\mathrm{d}t = \frac{bR}{1+R/h} - dR - cRN = 0$ gives $\bar{R} = 0$ or $\frac{b}{1+R/h} - d - cN = 0$ which is most easily written as

$$N = \frac{1}{c}\left[\frac{b}{1+R/h} - d\right] .$$

The intersect with the vertical axis is found by setting $R = 0$, which gives $N = (b-d)/c$. The horizontal asymptote is found by letting $R \to \infty$, which gives a horizontal asymptote at $N = -\frac{d}{c}$. There is a vertical asymptote at $R = -h$ giving $N \to \infty$. All in all this results in the sketch depicted above, in which one only needs to consider the positive quadrant.

Question 5.1. Desert
A possible good answer has the following sketches:

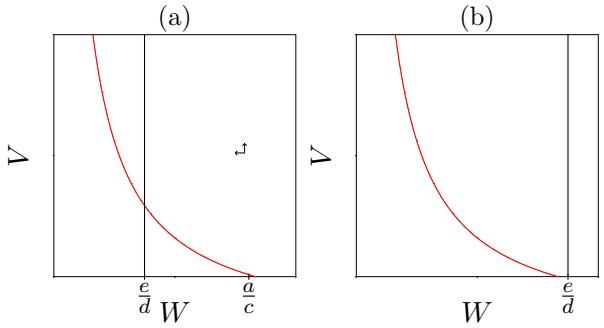

a. If there is no vegetation one sets $V = 0$ to obtain $\mathrm{d}W/\mathrm{d}t = a - cW$ with the steady state $\bar{W} = a/c$

b. If there is twice the amount of rain the parameter a becomes $2a$, which means $\bar{W} = 2a/c$.

c. The steady state is now solved from the system $\mathrm{d}W/\mathrm{d}t = \mathrm{d}V/\mathrm{d}t = 0$. Since $V = 0$ cancels from $\mathrm{d}V/\mathrm{d}t = 0$ one obtains the steady state $\bar{W} = e/d$ from the vegetation equation. This is independent of rain and evaporation!

d. The steady state remains $\bar{W} = e/d$ and all the extra water ends up in the vegetation.

e. The vegetation nullcline is solved from $\mathrm{d}V/\mathrm{d}t = dWV - eV = 0$ which means that $V = 0$ and $W = e/d$. The water nullcline is solved from $\mathrm{d}W/\mathrm{d}t = a - bWV - cW = 0$ or $a - cW = bWV$, i.e., $V = \frac{a}{bW} - \frac{c}{b}$, which is a decreasing hyperbolic function with horizontal asymptote $V = -(c/b)$ and vertical asymptote $W = 0$. There are two possibilities: See the sketch in Panel (a) and (b). The vector field shows steady state $\bar{W} = a/c$ without a vegetation is a

unstable saddle in Panel (a) and is stable in Panel (b). For the non-trivial steady state in Panel (a) we derive the Jacobian

$$J = \begin{pmatrix} - & - \\ + & 0 \end{pmatrix} \quad \text{giving} \quad \mathrm{tr}J < 0 \quad \text{and} \quad \det J > 0 \ ,$$

i.e., it is stable.

f. Increased rainfall increases a, which will move the water nullcline up and to the right. Since the vertical vegetation nullcline is unaffected, the amount of water in the soil remains the same, and the vegetation increases.

Question 5.2. Monkeys

A possible good answer has the following sketches:

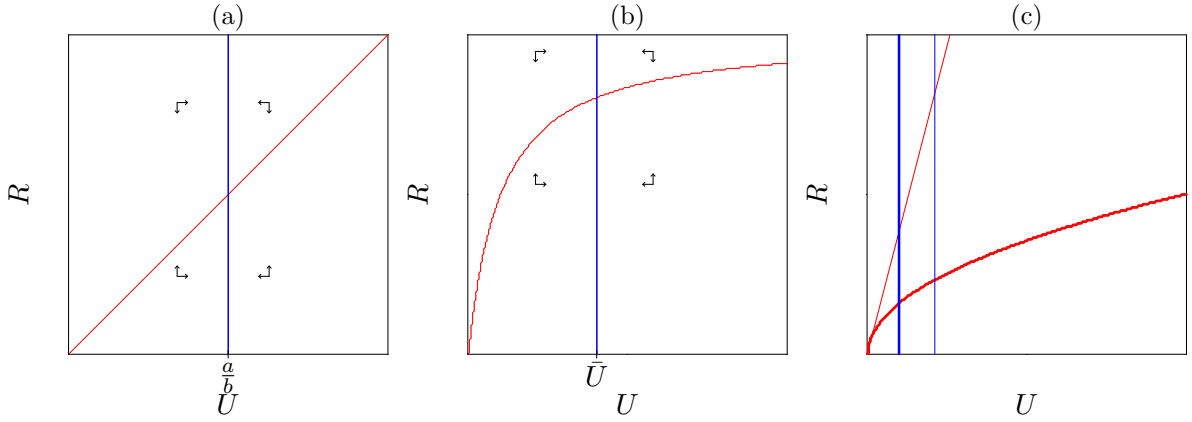

a. For the monkeys eating unripe fruits, M_U, and those eating ripe fruits, M_R, one would write

$$\frac{\mathrm{d}M_U}{\mathrm{d}t} = i - \frac{eM_U}{1+U/h} \quad \text{and} \quad \frac{\mathrm{d}M_R}{\mathrm{d}t} = i - \frac{eM_R}{1+R/h} \ ,$$

where e is the maximal emigration rate, and h the fruit density at which the emigration is half maximal. For the fruits we write

$$\frac{\mathrm{d}U}{\mathrm{d}t} = a - bU - c_1 M_U U \quad \text{and} \quad \frac{\mathrm{d}R}{\mathrm{d}t} = bU - c_2 M_R R - dR \ .$$

b. The immigration is independent of the amount of fruit available and there is no direct competition (interference) between the two species of monkeys.

c. In absence of monkeys the fruits obey $\mathrm{d}U/\mathrm{d}t = 0 = a - bU$ $\mathrm{d}R/\mathrm{d}t = bU - dR$ with nullclines $U = a/b$ and $R = bU/d$, respectively. See the sketch in Panel (a).

d. A quasi steady state assumption for both monkey species gives

$$\frac{\mathrm{d}M_U}{\mathrm{d}t} = 0 \quad \text{gives} \quad i = \frac{eM_U}{1+U/h} \quad \text{or} \quad M_U = \frac{i}{e}(1+U/h) \ ,$$

$$\frac{\mathrm{d}M_R}{\mathrm{d}t} = 0 \quad \text{gives} \quad i = \frac{eM_R}{1+R/h} \quad \text{or} \quad M_R = \frac{i}{e}(1+R/h) \ .$$

This is substituted into the equations for the fruits

$$\frac{\mathrm{d}U}{\mathrm{d}t} = a - bU - \frac{c_1 i}{e}U(1+U/h) \quad \text{and} \quad \frac{\mathrm{d}R}{\mathrm{d}t} = bU - dR - \frac{c_2 i}{e}R(1+R/h)$$

e. For the nullcline of the unripe fruits one sets $\mathrm{d}U/\mathrm{d}t = a - bU - \frac{c_1 iU}{e} - \frac{c_1 iU^2}{eh} = 0$ which is independent of R and will have one or two solutions. From the quadratic equation,

$$U_\pm = \frac{b + c_1 i/e \pm \sqrt{(b + c_1 i/e)^2 + 4ac_1 i/(eh)}}{-2c_1 i/(eh)} \ ,$$

one can easily see that this has only one positive solution, i.e., U_-. Call this root $\bar{U}$, and draw a vertical line in Panel (b). For the nullcline of the ripe fruits one sets $\mathrm{d}R/\mathrm{d}t = bU - \frac{c_2 iR}{e} - \frac{c_2 iR^2}{eh} - dR = 0$, which can easily be expressed in terms of the unripe fruits:

$$U = \frac{c_2 iR^2}{ehb} + \left(\frac{c_2 i}{eb} + \frac{d}{b}\right) R \quad \text{or} \quad U = \alpha R^2 + \beta R \ ,$$

which is the parabola depicted in Panel (b). From the vector field we see that the steady state is a stable node.

f. Because we have monkeys at steady state, their number reacts immediately to changes in R and U. So if we know R and U we also know how many monkeys there are.

g. In the presence of monkeys there should be an equilibrium with less fruit. See the sketch in Panel (c): the heavy nullclines represent the situation with monkeys.

Question 5.3. Return time

We calculate the return time of the non-trivial steady state of the Lotka Volterra model considering both density dependent birth and density dependent death. For simplicity we do this for the case where this equilibrium is a stable spiral point. To save time we first write the model in a general form and compute the return time for this general model. The two cases of density dependent birth and death can then be "substituted" into the general form. A general form of the Lotka Volterra model is

$$\frac{\mathrm{d}R}{\mathrm{d}t} = rR - \gamma R^2 - aRN \quad \text{and} \quad \frac{\mathrm{d}N}{\mathrm{d}t} = caRN - \delta N \ .$$

a. For the return time of the general form we first solve the non-trivial steady state by setting $\mathrm{d}N/\mathrm{d}t = 0$ and $\mathrm{d}R/\mathrm{d}t = 0$, which gives

$$\bar{R} = \frac{\delta}{ca} \quad \text{and} \quad \bar{N} = \frac{r}{a} - \frac{\gamma}{a}\bar{R} = \frac{r}{a} - \frac{\gamma\delta}{ca^2} \ ,$$

respectively. The Jacobian of the general model is

$$J = \begin{pmatrix} r - 2\gamma\bar{R} - a\bar{N} & -a\bar{R} \\ ca\bar{N} & ca\bar{R} - \delta \end{pmatrix} = \begin{pmatrix} -\frac{\gamma\delta}{ca} & -\frac{\delta}{c} \\ cr - \frac{\gamma\delta}{a} & 0 \end{pmatrix} \ ,$$

where $cr - \gamma\delta/a > 0$ because $ca\bar{N} > 0$. The trace of this matrix is negative, i.e., $\mathrm{tr} = -\frac{\gamma\delta}{ca}$, and the eigenvalues of this Jacobian are given by

$$\lambda_\pm = \frac{\mathrm{tr} \pm \sqrt{\mathrm{tr}^2 - 4\det}}{2} = -\frac{\gamma\delta}{2ca} \pm \frac{\sqrt{D}}{2} \ ,$$

where $D = \mathrm{tr}^2 - 4\det$ is the discriminant of the matrix (and "det" the determinant). Since we are considering a spiral point, the eigenvalues have to be complex, implying that the discriminant $D < 0$. The imaginary part of the eigenvalues defines the period of the dampened oscillation, and the real part how fast its amplitude grows or contracts, i.e., the return time depends on the real part only. Thus, for the return time we consider the real part, $\mathrm{Re}(\lambda) = -\frac{\gamma\delta}{2ca}$, to obtain a return time

$$T_R = \frac{-1}{\mathrm{Re}(\lambda)} = \frac{2ca}{\gamma\delta} = \frac{2}{\gamma}\ \frac{1}{\bar{R}} \ .$$

Thus, the return time is independent of the net rate of increase, r, depends on the density dependence parameter, γ, and is inversely related to the steady state of the prey.

b. We write the model with density dependent birth as

$$\frac{\mathrm{d}R}{\mathrm{d}t} = bR(1 - R/k) - dR - aRN = bR - bR^2/k - dR - aRN \ ,$$

which in the general form means that $r = (b - d)$ and $\gamma = b/k$. To obtain the return time of the non-trivial steady state of this model, we only need to substitute $\gamma = b/k$ into the general expression for the return time, because the return time is independent of r, and because $\bar{R}$ came from $\mathrm{d}N/\mathrm{d}t = 0$, which has not changed. We obtain that

$$T_R = \frac{2}{b}\frac{k}{\bar{R}} = \frac{2cak}{b\delta} \ ,$$

where $k/\bar{R}$ is a ratio of prey densities (i.e., k is the density at which the birth rate become zero). Note that the dimension is correct: $k/\bar{R}$ is dimensionless and $2/b$ has the dimension time. Thus, the return time of this density dependent birth depends on the birth rate parameters, b and k, and not on the density independent death rate, d.

c. We write the model with density dependent death as

$$\frac{\mathrm{d}R}{\mathrm{d}t} = bR - dR(1 + R/k) - aRN = bR - dR - dR^2/k - aRN \ ,$$

which in the general form means that $r = (b - d)$ and $\gamma = d/k$. Now we substitute $\gamma = d/k$ into T_R and obtain that

$$T_R = \frac{2}{d}\frac{k}{\bar{R}} = \frac{2cak}{d\delta} \ ,$$

where $k/\bar{R}$ is another ratio of prey densities (i.e., k is the density at which the death rate doubles). Now the return time depends on the density dependent death rate parameters, d and k.

d. In both cases the return time is determined by a self-dampening effect of the prey onto itself, i.e., $\mathrm{Re}(\lambda) = -(\gamma/2)\bar{R}$. Increasing the birth rate, or the death rate, decreases the return time because it speeds up the dynamics around the steady state. Increasing k increases the return time because it weakens the density dependent regulation. Weakening the predator, i.e., increasing $\bar{R}$, decreases the return time because that also increases the self-dampening effect of the prey.

Question 6.1. Parameters

The biological interpretation and dimension of the parameters are:

a. 1. a_1: Maximal *per capita* growth rate $(1/t)$
2. K: Carrying capacity (numbers or biomass).
3. b_1: Maximal *per capita* catch rate $(1/t)$.
4. c_1: Population density R where N catches/feeds at its half maximal rate (numbers or biomass).
5. a_2: *per capita* death rate $(1/t)$.
6. b_2: Maximum *per capita* birth rate $(1/t)$.
7. c_2: Population R where N grows at half its maximum rate (numbers or biomass).

b. $b_2 = \alpha b_1$ where α is the conversion factor. If population sizes are measured in biomass the normal trophic conversion factor is $\alpha = 0.1$, i.e., typically there is a 90% loss between tropic levels. If the population sizes are measured in numbers this could be anything because small predators could feed on large prey.

c. $c_1 = c_2$ means that the growth of the predator is proportional to what it eats. $c_1 > c_2$ means that the growth rate saturates earlier than the catching rate, which is to be expected when the birth rate of the predator saturates as a function of its consumption; see Eq. (6.4). $c_1 < c_2$ seems strange and means that the catching rate is saturated earlier than the growth rate.

Question 6.2. Eutrophication: 2D
A possible good answer has the following sketches:

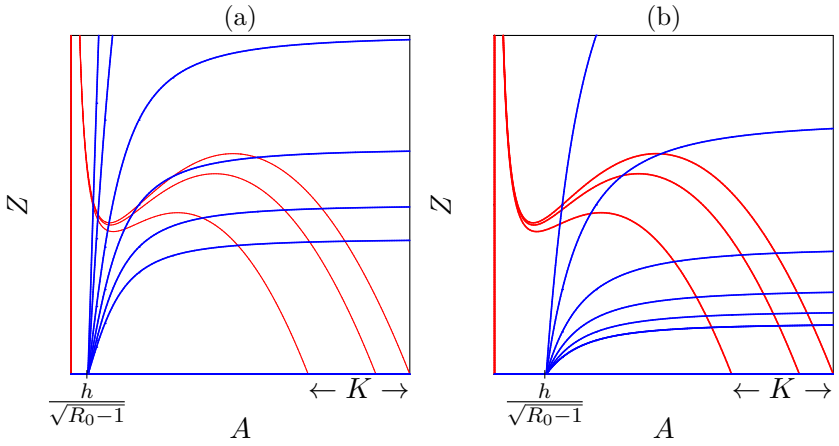

a. For the algae, A, and zooplankton, Z, one writes

$$\frac{\mathrm{d}A}{\mathrm{d}t} = rA(1 - A/K) - bZ\frac{A^2}{h^2 + A^2} \quad \text{and} \quad \frac{\mathrm{d}Z}{\mathrm{d}t} = cbZ\frac{A^2}{h^2 + A^2} - dZ(1 + eZ) \ ,$$

where e is the extra death due to intra-specific competition. The nullcline for the algae has been constructed in the text. For the zooplankton one obtains from $\mathrm{d}Z/\mathrm{d}t = 0$ that $Z = 0$ or

$$cb\frac{A^2}{h^2 + A^2} - d - deZ = 0 \quad \text{or} \quad Z = \frac{cb}{de}\frac{A^2}{h^2 + A^2} - \frac{1}{e} \ ,$$

which is a sigmoid function intersecting the vertical axis at $Z = -1/e$ and the horizontal axis at $A = h/\sqrt{R_0 - 1}$, where $R_0 = cb/d$. When $e = 0$ the Z-nullcline is a vertical line.

b. the carrying capacity K

c. There are many possibilities. See the sketch in Panel (a) and (b). Eutrophication corresponds to moving along a sigmoid zooplankton nullcline from the lowest to the highest algae nullcline. Steady states may stabilize or destabilize and appear or disappear.

d. Models suggest that changing a single parameter can have various different effects, depending on the precise initial circumstances. It is difficult to generalize, and reliable predictions are nearly impossible to make. A model plays the important role of suggesting various possible outcomes; possibly including undesired outcomes.

Question 6.3. Luckinbill
A possible good answer has the following sketches:

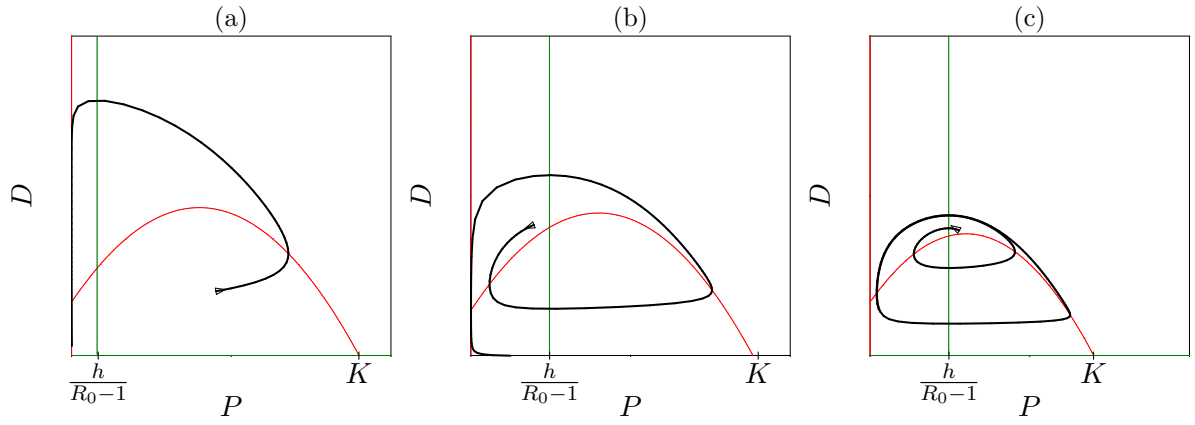

a. The oscillatory behavior suggests a Monod saturation

$$\frac{\mathrm{d}P}{\mathrm{d}t} = aP(1-P/K) - \frac{bDP}{h+P} \quad \text{and} \quad \frac{\mathrm{d}D}{\mathrm{d}t} = \frac{cDP}{h+P} - dD \ .$$

b. Increasing the viscosity of the medium decreases the likelihood of meeting prey, which corresponds to increasing the h parameter; see Panel (b). Halving the concentration of food decreases the K parameter; see Panel (c).

c. See Panels (a)–(c).

d. The agreement between model and data seems perfect; a simple Monod saturated functional response provides a good explanation.

e. Formally the populations cannot go extinct in the model; the noise in the data would require stochasticity in the model.

Question 6.4. Filter feeders

A possible good answer has the following sketches:

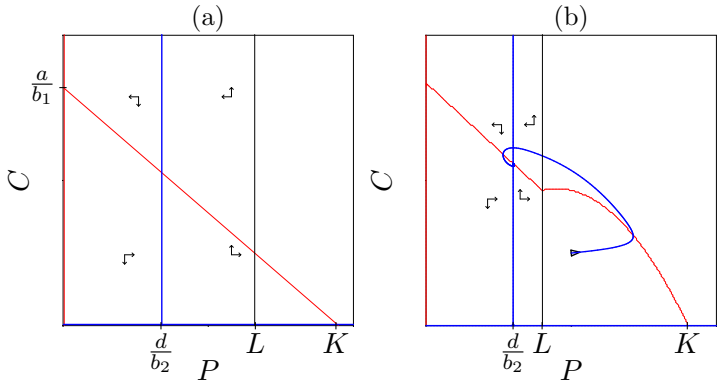

a. For the phytoplankton, P, and the copepods, C, one could write

$$\frac{\mathrm{d}P}{\mathrm{d}t} = aP(1-P/K) - b_1PC \quad \text{and} \quad \frac{\mathrm{d}C}{\mathrm{d}t} = b_2\min(P,L)C - dC \ ,$$

where L is the phytoplankton level at which the copepods are saturated.

b. Solving $\mathrm{d}P/\mathrm{d}t = 0$ one obtains $P = 0$ or

$$a - \frac{aP}{K} = b_1C \quad \text{or} \quad C = \frac{a}{b_1}\left(1 - \frac{P}{K}\right) \ ,$$

which is a Lotka Volterra type prey nullcline. Solving $\mathrm{d}C/\mathrm{d}t = 0$ gives $C = 0$ and $b_2\min(P,L) - d = 0$. For $P < L$ this yields $P = \frac{d}{b_2}$ and for $P > L$ there is no solution.

The case $P = L$ we do not consider because it is not generic. Thus, the P-nullcline exists when $\frac{d}{b_2} < L$. See the sketch in Panel (a). The non trivial steady state is stable because the graphical Jacobian

$$J = \begin{pmatrix} - & - \\ + & 0 \end{pmatrix} \quad \text{has a} \quad \mathrm{tr}J < 0 \quad \text{and} \quad \det J > 0 \ .$$

The carrying capacity $P = K$ is stable when $\frac{d}{b_2} > L$ because then $\mathrm{d}C/\mathrm{d}t < 0$ everywhere.

c. The return time is calculated from a neighborhood stability close to a steady state. The threshold L has not changed the properties of the steady state, so there is no difference in the return time.

d. When $P > L$ the vertical arrows in the vector field remain constant. Trajectories in this region therefore move less slowly upward than when $L \to \infty$. This slows the trajectory down and changes its angle.

e. The mussels would correspond to a normal Holling type I functional response

$$\frac{\mathrm{d}P}{\mathrm{d}t} = aP(1 - P/K) - b_1 C \min(P, L) \quad \text{and} \quad \frac{\mathrm{d}C}{\mathrm{d}t} = b_2 C \min(P, L) - dC$$

corresponding to the following nullclines

$$\begin{cases} C = \frac{a}{b_1}\left(1 - \frac{P}{K}\right) & \text{and} \quad P = 0 \quad \text{when } P < L \text{ and} \\ C = \frac{aP}{b_1 L}(1 - \frac{P}{K}) & \text{otherwise.} \end{cases}$$

See the sketch in Panel (b).

Question 6.5. Exponential functional response

A possible good answer has the following sketch:

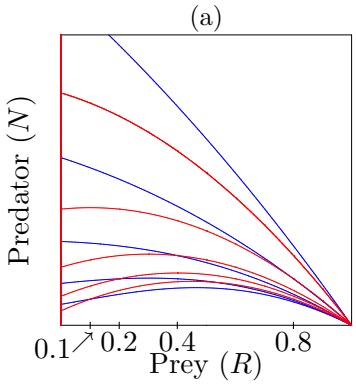

a. For $R \to \infty$ the functional response $(1 - \mathrm{e}^{-\ln[2]R/h}) \to 1$, which means that at high prey densities the *per capita* predator consumption is a prey per unit of time.

b. Since one can scale time by the natural rate of increase r, the prey density by its carrying capacity, and the predator by the a parameter, the generic form of both models is:

$$\frac{\mathrm{d}R}{\mathrm{d}t} = R(1 - R) - \frac{NR}{h + R} \quad \text{and} \quad \frac{\mathrm{d}R}{\mathrm{d}t} = R(1 - R) - N(1 - \mathrm{e}^{-\ln[2]R/h}) \ ,$$

which has only one parameter h. Panel (a) shows the nullclines for $h = 0.1, 0.2, 0.4, 0.8$ and $h = 1.6$. The nullclines intersect when $R = h$ because the functional response then equals 0.5. There is no qualitative difference between the two sets of nullclines, i.e., we expect similar behavior for these two models.

Question 7.1. Wolves
A possible good answer has the following sketch:

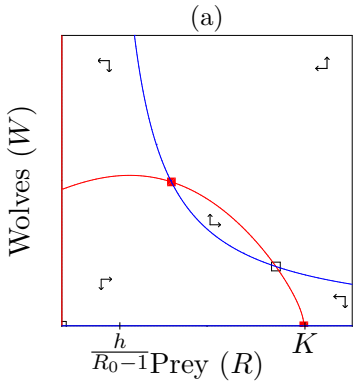

There are many different possibilities. For instance, let R be the prey, and W be the wolves:

a. One could define $\hat{R} = RW/(c+W)$ as the number of prey that can be caught, i.e., if there are enough wolves ($W \gg c$) all prey can be caught ($\hat{R} \to R$). Taking $\hat{R}$ through a normal Monod saturation gives

$$f(R,W) = \frac{\hat{R}}{h+\hat{R}} = \frac{RW}{hc+hW+RW}$$

$$\frac{\mathrm{d}R}{\mathrm{d}t} = rR(1-R/K) - \frac{aRW^2}{hc+hW+RW} \quad \text{and} \quad \frac{\mathrm{d}W}{\mathrm{d}t} = \frac{aRW^2}{hc+hW+RW} - dW \ ,$$

with $R_0 = a/d$.

b. To sketch the predator nullcline one solves

$$\frac{aRW}{hc+hW+RW} = d \quad \text{or} \quad W = \frac{hc}{R(R_0-1)-h} \ ,$$

which has a vertical asymptote at $R = h/(R_0-1)$ and a horizontal asymptote at $W = 0$. The only intersection with the vertical axis ($R = 0$) is at the negative value $W = -c$. The prey nullcline is not so easy to sketch. We have drawn it with `grind.R` in the picture above, where it looks like a parabola. From the vector field one can see that the carrying capacity is stable. This is an Allee effect because the wolves cannot invade in small numbers. The upper non-trivial steady state is stable when the intersection points is located at the right hand side of the top of the parabola. The lower intersection point is a saddle point, with a separatrix defining the Allee effect.

Alternatively, one could use a mass action predation term and write

$$\frac{\mathrm{d}R}{\mathrm{d}t} = rR(1-R/K) - \frac{aRW^2}{c+W} \quad \text{and} \quad \frac{\mathrm{d}W}{\mathrm{d}t} = \frac{aRW^2}{c+W} - dW \ .$$

One could even define $f(R,W) = \frac{R}{h(1-cW)+R}$ as a phenomenological functional response that decreases the saturation constant when the number of wolves increases (and use a maximum function to prevent that $1-cW$ becomes negative).

Question 7.2. Saturation in predators
A possible good answer has the following sketches:

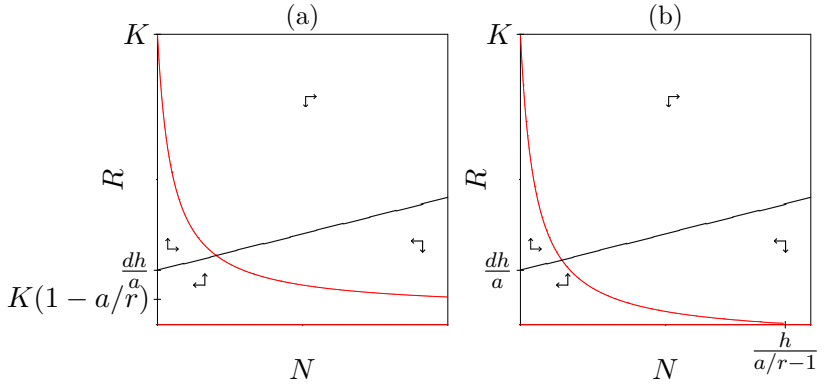

The prey nullcline is solved from

$$r(1-R/K) = \frac{aN}{h+N} \quad \text{or} \quad R = K\left(1 - \frac{a/rN}{h+N}\right) ,$$

which is an inverse Hill function intersecting the vertical R-axis at $R = K$. If $a/r < 1$ one obtains a "limited predation" nullcline with an asymptote at $R = K(1 - a/r)$; see Panel (a). Otherwise the nullcline intersects the horizontal N-axis $N = h/(a/r - 1)$; see Panel (b). The predator nullcline is solved from

$$\frac{aR}{h+N} = d \quad \text{or} \quad R = (d/a)(h+N) ,$$

which is a straight line with slope d/a that intersects the vertical axis at $R = dh/a$.

For the non-trivial steady states in both panels we derive the Jacobian

$$J = \begin{pmatrix} - & + \\ - & - \end{pmatrix} \quad \text{giving} \quad \mathrm{tr}J < 0 \quad \text{and} \quad \det J > 0 ,$$

i.e., they are stable.

Question 8.1. Nullclines
A possible good answer has the following sketches:

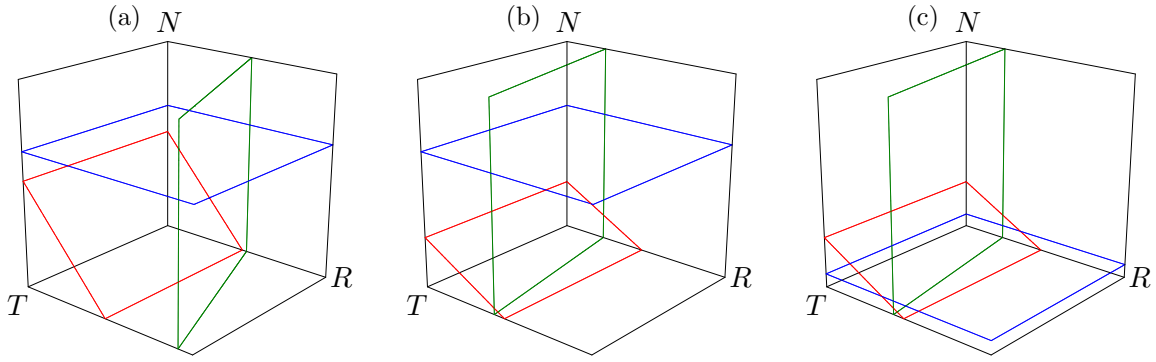

In Panel (a) we have a situation where $d/b > K$, or $R_0 < 1$. In Panel (b) we have $R_0 > 1$ and a top-predator nullcline that is located above the 2-dimensional $(\bar{R}, \bar{N})$ steady state. In Panel (c) we have sketched a situation where $R_0 > 1$ and $R_0' > 1$.

Question 8.2. Kaunzinger
A possible good answer has the following sketch:

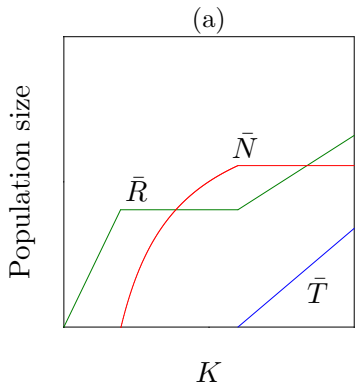

a. $\bar{T} = \frac{1}{c}[b\bar{R} - d] = \frac{bK}{c}\left[1 - \frac{be}{rc}\right] - \frac{d}{c}$, which increases proportional to the carrying capacity K.
b. See the sketch in Panel (a)
c. The figures are close but not identical. The main difference is the saturated increase of $\bar{N}$ in Panel (a). This is not so important because exact shape of this lines also depends on the form of the interaction functions.
d. One could add interference competition between the predators.

Question 8.3. Chaos
A possible good answer has the following sketches:

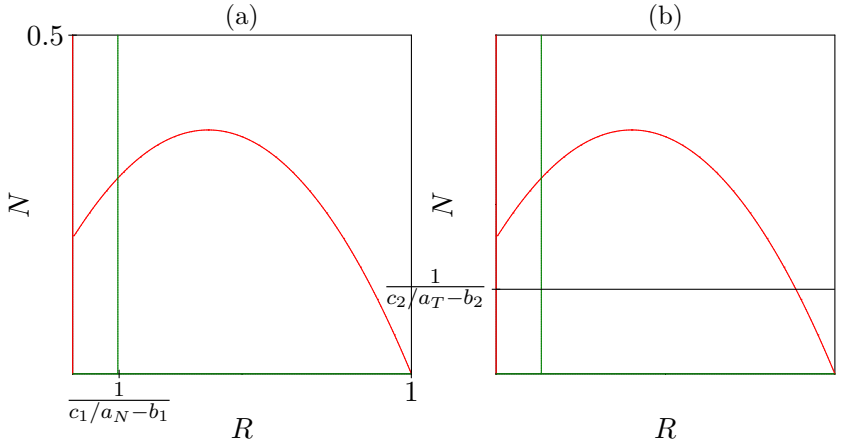

a. See the sketch in Panel (a). Yes, for their values of b_1 the steady state is unstable.
b. See the sketch in Panel (b). Yes, the unstable steady state around which the trajectory cycles is located above the top-predator nullcline, and we expect the average predator density to be higher than the top-predator nullcline.
c. use `grind.R`.
d. use `grind.R`.
e. use `grind.R`.

Question 8.4. Detritus
A possible good answer has the following sketches:

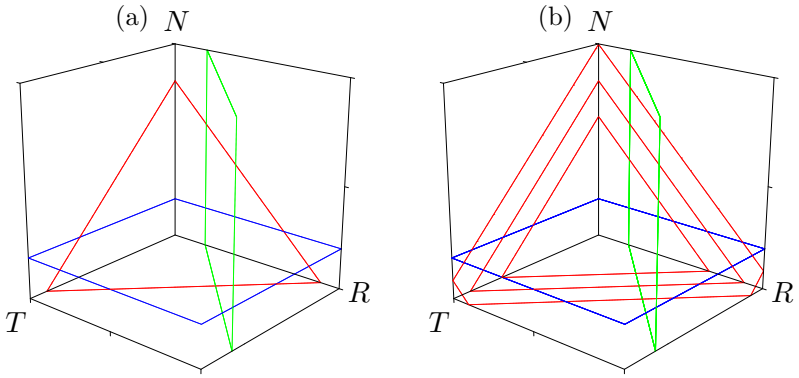

A simple model would be

$$\frac{\mathrm{d}R}{\mathrm{d}t} = [bF - d_R - c_1 N]R \ , \quad \frac{\mathrm{d}N}{\mathrm{d}t} = [c_1 R - d_N - c_2 T]N \quad \text{and} \quad \frac{\mathrm{d}T}{\mathrm{d}t} = [c_2 N - d_T]T \ ,$$

where $F = K - R - N - T$. This shows that the $\mathrm{d}N/\mathrm{d}t$ and $\mathrm{d}T/\mathrm{d}t$ equations do not change. The 3-dimensional nullclines of the predator, N, and the top-predator T therefore stay the same. That of the resource is solved from $[b(K - R - N - T) - d_R - c_1 N] = 0$, which gives a negative linear relation in each of the sides of the 3-dimensional phase space. The plane will look like a triangle (Panel a) that moves vertically when K is changed (Panel b).

For $N = T = 0$ one now obtains $\bar{R} = K - d_R/b$, which increases linearly with the total amount of nutrients, K, in the system. When $N > 0$ and $T = 0$, one solves $\bar{R} = d_N/c_1$ from $\mathrm{d}N/\mathrm{d}t = 0$, and from $[b(K - \bar{R} - N) - d_R - c_1 N] = 0$ one solves that

$$\bar{N} = \frac{c_1 bK - bd_N - c_1 d_R}{c_1(b + c_1)}$$

which increases linearly with K, and becomes positive when $K > (bd_N - c_1 d_R)/(c_1 b)$. When $N > 0$ and $T > 0$ one again solves $\bar{N} = d_T/c_2$ from $\mathrm{d}T/\mathrm{d}t = 0$, $\bar{T}$ from $\mathrm{d}N/\mathrm{d}t = 0$, and $\bar{R}$ from $\mathrm{d}R/\mathrm{d}t = 0$. The steady state resource density again only depends on K when the food chain has an odd length.

Question 9.1. Migration

A possible good answer has the following sketches:

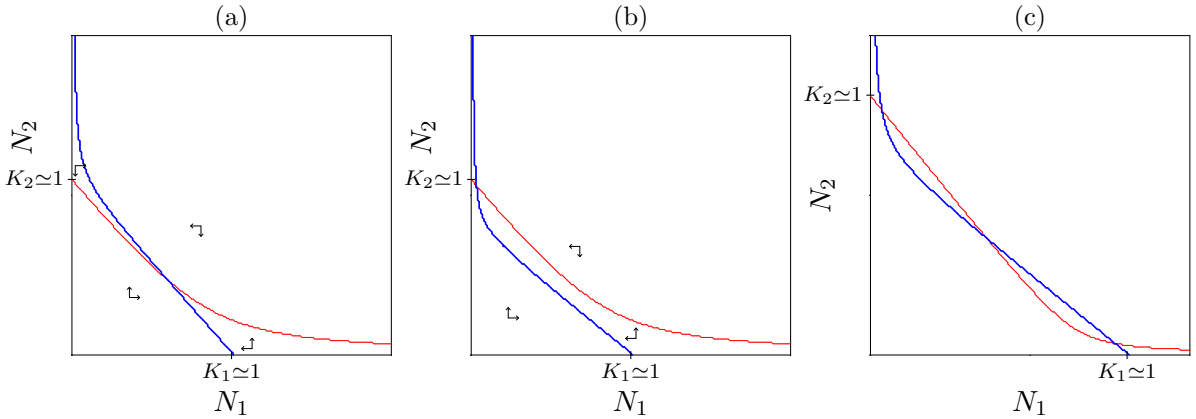

a. The model would become

$$\frac{\mathrm{d}N_1}{\mathrm{d}t} = i + r_1 N_1(1 - N_1 - \gamma_1 N_2) \quad \text{and} \quad \frac{\mathrm{d}N_2}{\mathrm{d}t} = i + r_2 N_2(1 - N_2 - \gamma_2 N_1)$$

b. Given that $i \ll 1$ one obtains the sketches in Panels (a)–(c).

c. From the vector field one can see that the steady states close to the carrying capacity are stable. The steady state in the middle of Panel (a) is stable, whereas that in the middle of Panel (c) is unstable.

d. In Panel (a) there is normal coexistence. In the other Panels there is no true competitive exclusion. However, at the steady state near the carrying capacity the density of the rarest species is very low.

Question 9.2. Nullclines

a. The $\mathrm{d}x/\mathrm{d}t = 0$ nullcline obeys $y = -e + dx$ which means that $e + y - dx = 0$. To explain the $x = 0$ part of the nullcline, we could assume that x is a replicating population. Thus a model would be $\mathrm{d}x/\mathrm{d}t = ex + yx - dx^2$. This model in agreement with the vector field in the figure. The $\mathrm{d}y/\mathrm{d}t = 0$ nullcline obeys $y = a + bx$ which means that $a + bx - y = 0$, and a possible model would be $\mathrm{d}y/\mathrm{d}t = ay + bxy - y^2$.

b. They stimulate each other, so this would be a symbiosis or mutualism. These are not obligatory symbionts because they will grow (invade) in the absence of the other.

c. The set of all possible states of x and y.

d. The state at $P(x, y)$ is the value of x and y at point P.

e. The set of (x, y) values where the variable does not change.

f. The set of resource values where the consumer does not change.

g. The consecutive points in phase space defined by the solution of the differential equations.

h. No, at one point in phase space there is only one derivative, and trajectories cannot go through at different angles.

Question 9.3. r/K selected

A possible good answer has the following sketches:

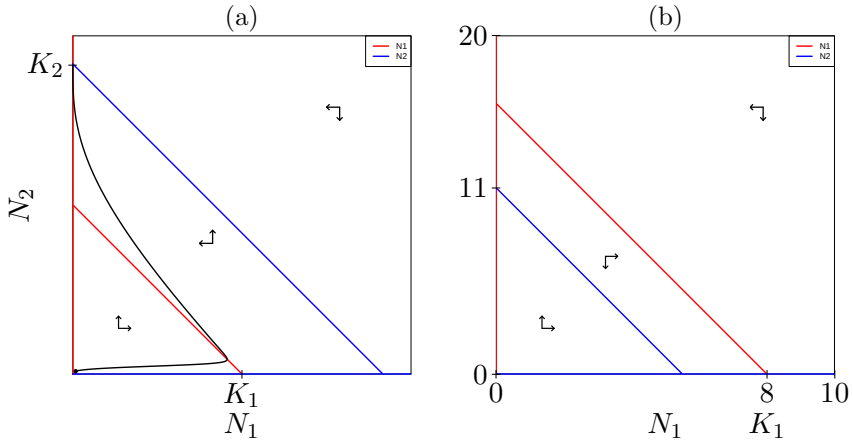

a. Using the QSSA model of Eq. (9.2), (9.3), and (9.5), and setting $\beta_1 \gg \beta_2$, $\delta_1 \gg \delta_2$, $c_1 = c_2$, and $h_1 < h_2$, N_1 is r-selected and N_2 is a K-selected species. The trajectory therefore remains close to the horizontal axis because N_1 grows much faster (see Panel a). After crossing the N_1-nullcline, the trajectory moves in the direction of the carrying capacity of N_2.

b. Although N_1 grows faster, N_2 has lower resource requirements, R_2^* and wins.

c. r-selected species can be maintained by short transients if there is enough noise or disturbance in the system.

d. By Eq. (9.4), i.e., $R_i^* = h_i/[c_i(R_{0_i} - 1)]$, the species with the lowest resource requirements, h_i, the highest R_{0_i} and the fastest consumption c_i is the best competitor. The carrying capacity, $K_i = s(R_{0_i} - 1)/h_i - d/c_i$ in Eq. (9.7), is an increasing saturation function of the consumption rate, c_i. Hence by increasing c_1 of the r-selected species until it wins, i.e., $R_1^* < R_2^*$, the carrying capacity, K_1, may still be smaller than than of the K-selected species. See the sketch in Panel (b).

Question 9.4. Patches

A possible good answer has the following sketch:

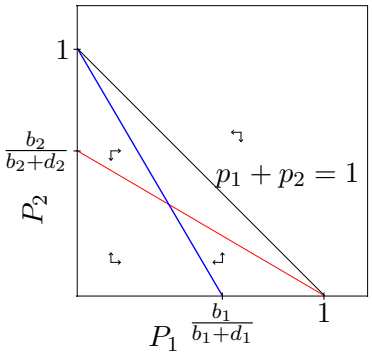

a. If $L = 1 - P_1 - P_2$ is the fraction of empty patches one would write

$$\frac{\mathrm{d}P_1}{\mathrm{d}t} = b_1 L - d_1 P_1 \quad \text{and} \quad \frac{\mathrm{d}P_2}{\mathrm{d}t} = b_2 L - d_2 P_2 \ ,$$

because the reproduction is not related to the current population size.

b. Solving

$$\frac{\mathrm{d}P_1}{\mathrm{d}t} = b_1 - b_1 P_1 - b_1 P_2 - d_1 P_1 = 0 \quad \text{gives} \quad P_2 = 1 - P_1(1 + \frac{d_1}{b_1}) \ ,$$

and solving

$$\frac{\mathrm{d}P_2}{\mathrm{d}t} = b_2 - b_2 P_2 - b_2 P_1 - d_2 P_2 = 0 \quad \text{gives} \quad P_2 = \frac{b_2}{b_2 + d_2}\ (1 - P_1) \ ,$$

which intersect the horizontal, $P_2 = 0$, axis at $P_1 = \frac{b_1}{b_1+d_1}$ and $P_1 = 1$, respectively (see the sketch).

c. There is only one steady state, and the vector field shows that it is stable.

d. The carrying capacities $\bar{P}_1 = \frac{b_1}{b_1+d_1} < 1$ and $\bar{P}_2 = \frac{b_2}{b_2+d_2} < 1$, and the steady state lies below the $P_1 + P_2 = 1$ line. Thus the patches are never fully occupied.

e. Because the size of the seed bank is not proportional to population size, these populations are expanding by a source, and not by replication. Extinction is impossible in the presence of a source.

Question 9.5. Gradients

A possible good answer has the following sketches:

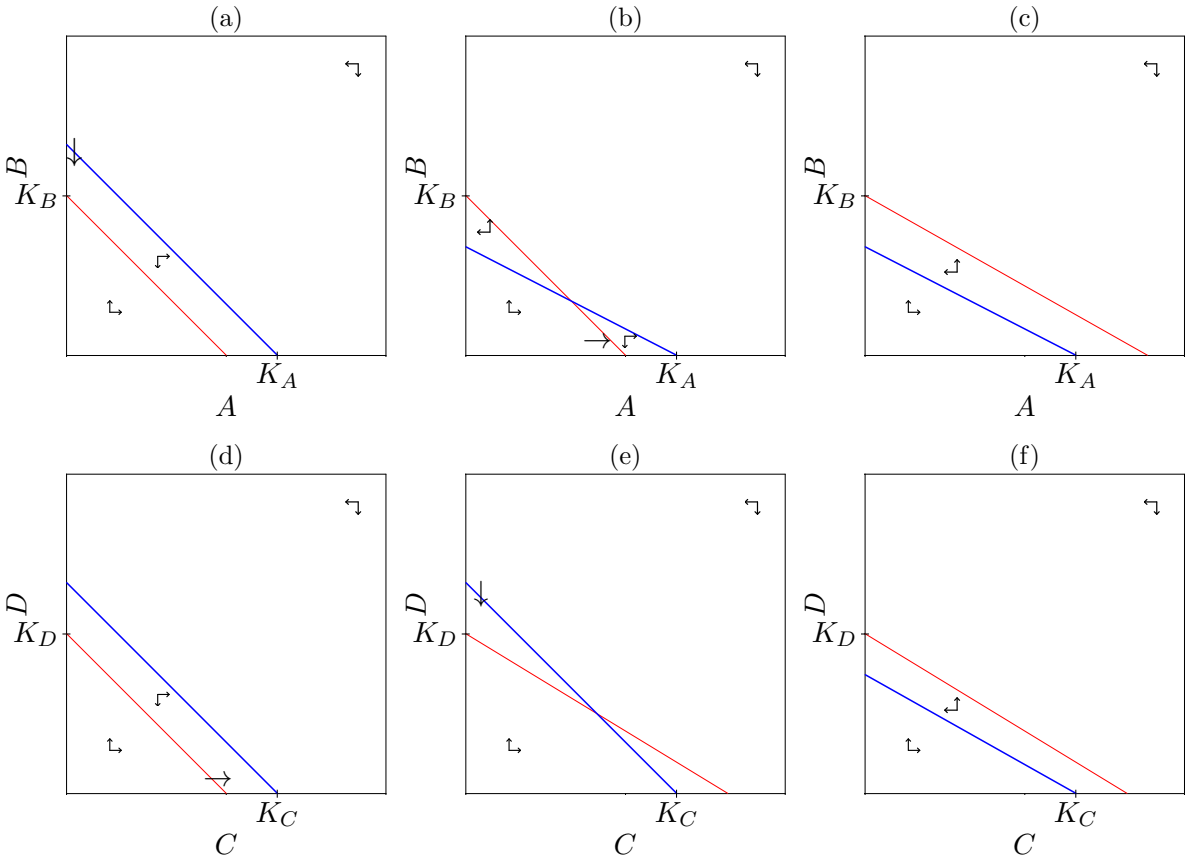

a. In gradient 1 there is a sharp transition, as if there is a abrupt change in the environmental conditions in sample seven. In gradient 2 it seems that environmental conditions change more gradually.

b. Turn the nullclines in the direction of the arrows, while keeping the carrying capacities the same. See the sketch in Panel (a)-(f).

c. Both environmental gradients can be gradual. If this gradient affects the inter-specific competition the gradual change in the environment can give rise to the sharp cline in gradient 1 or to the continuous transition in gradient 2.

d. The samples have some variation that could be due to noise.

Question 9.6. Density dependent birth rate

A possible good answer has the following sketches:

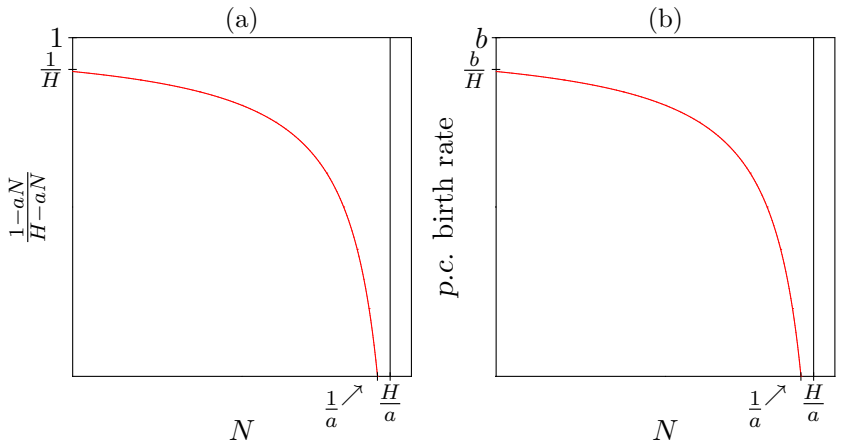

a. $R_0 = b/d$ or $R_0 = \frac{b}{d}\frac{a}{h+a}$, depending on its definition.
b. The QSS of the resource is $R = 1 - aN$ which when substituted into

$$\frac{aR}{h + aR} \quad \text{gives} \quad \frac{1 - aN}{H - aN}$$

where $H = 1 + h/a$, which is larger than one. The new consumer equation becomes

$$\frac{\mathrm{d}N}{\mathrm{d}t} = \left[b\frac{1 - aN}{H - aN} - d\right] N \ .$$

c. The maximum birth rate is $b/H = \frac{ab}{a+h}$. Hence $R_0 = \frac{b}{d}\frac{a}{h+a}$, which is the same as the second answer in **a**.
d. To sketch the *per capita* birth rate as a function of N we first consider the function $y = \frac{1-aN}{H-aN}$ knowing that $H > 1$. For $N = 0$ this delivers $y = 1/H$, and for $y = 0$ we find $N = 1/a$. A horizontal asymptote is found by dividing numerator and denominator by N, i.e., $y = \frac{1/N-a}{H/N-a}$, and letting $N \to \infty$ to find that $y \to 1$. A vertical asymptote is located at $N = H/a$. Because $H > 1$ we know that the intersections with the horizontal and vertical axis fall below the asymptotes. See the sketch in Panel (a). Finally we multiply (scale) the whole function with the birth rate b to obtain the sketch in Panel (b).
e. This resembles a sigmoid function.
f. The QSS now equals $R = 1/(1 + aN)$ which gives a *per capita* birth rate of $\frac{b}{1+h/a+hN}$ which is convex.

Question 9.7. Tilman's competition model
A possible good answer has the following sketches:

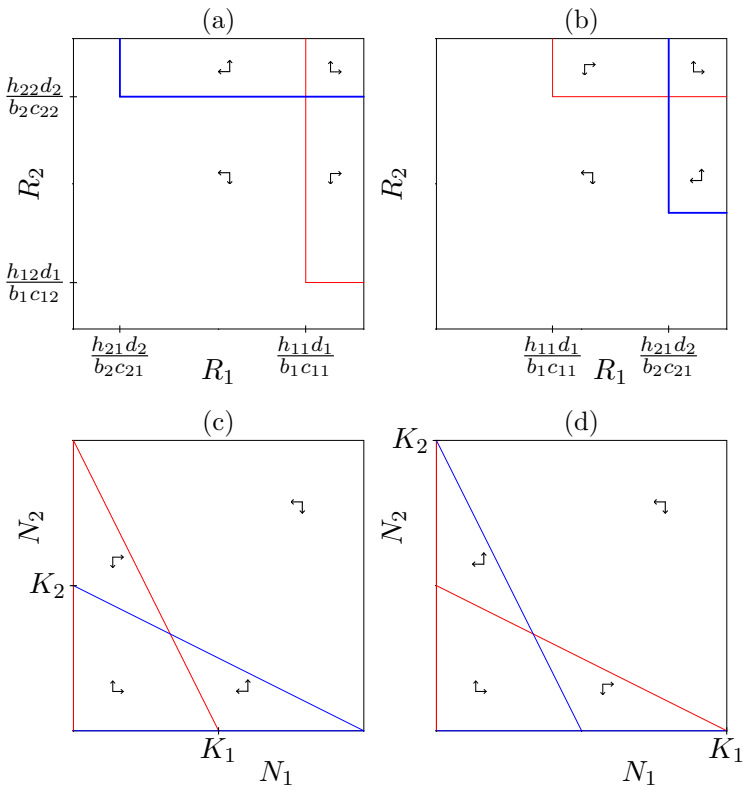

a. The red $\mathrm{d}N_1/\mathrm{d}t = 0$ nullcline has a vertical part at $R_1 = \frac{h_{11}d_1}{b_1c_{11}}$ where the first resource is limiting, and a horizontal part at $R_2 = \frac{h_{12}d_1}{b_1c_{12}}$ where the second resource is limiting. Above

and on the right hand side of this nullcline $\mathrm{d}N_1/\mathrm{d}t > 0$ (which is "arbitrarily" indicated by horizontal arrows). The blue $\mathrm{d}N_2/\mathrm{d}t = 0$ nullcline as a horizontal part located at $R_2 = \frac{h_{22}d_2}{b_2c_{22}}$, and a vertical part located at $R_1 = \frac{h_{21}d_2}{b_2c_{21}}$. The upwards arrows indicate the region where $\mathrm{d}N_2/\mathrm{d}t > 0$. The derivatives of the resources are not (yet) defined because this diagram is based upon Eq. (9.30) only. Both resources are essential because the horizontal and vertical parts of these nullclines define the minimum amounts the species require for growth. Two qualitatively different examples with intersecting nullclines are given in Panels (a) and (b). When these nullclines fail to intersect there is no resource density (R_1, R_2) where $\mathrm{d}N_1/\mathrm{d}t = \mathrm{d}N_2/\mathrm{d}t = 0$.

b. The nullclines in Panels (c) and (d) correspond to Tilman diagrams of (a) and (b), respectively All Panels were made by assuming that N_1 consumes more of resource one, whereas N_2 specializes on R_2, i.e., $c_{11} = c_{22} = 0.5$, and $c_{12} = c_{21} = 0.25$. All Panels have the same birth and death rates ($b_1 = b_2 = 0.5$, $d_1 = d_2 = 0.1$), and we have located the intersection point at the same resource densities by setting

$$\frac{h_{11}d_1}{b_1c_{11}} = \frac{h_{21}d_2}{b_2c_{21}} = \frac{h_{22}d_2}{b_2c_{22}} = \frac{h_{12}d_1}{b_1c_{12}} = 0.4\ ,$$

i.e., $h_{11} = h_{22} = 1$, and $h_{21} = h_{12} = 0.1$ in Panel (a) and $h_{11} = h_{22} = h_{21} = h_{12} = 0.5$ in Panel (b). The steady state is then located at $\bar{R}_1 = \bar{R}_2 = 0.4$ and $\bar{N}_1 = \bar{N}_2 = 2$ (this can be studied with the file `tilman.R`). In Panels (a & c) each species therefore consumes most of the resource it requires most. In Panels (b & d) they require the same amount of each resource, but they consume them at different rates. The former leads to stable co-existence (Panel c), the latter to a "founder controlled" phase plane with an unstable steady state (Panel d).

c. We can study the difference between the two parameter settings by studying the Jacobian of the 4-dimensional system. Since N_1 consumes more of R_1 and N_2 more of R_2 we obtain that $\partial R_1'/\partial N_1 = -c_{11}\bar{R}_1 = -0.5\times 0.4 = -0.2$ and that $\partial R_1'/\partial N_2 = -c_{21}\bar{R}_1 = -0.25\times 0.4 = -0.1$. For resource two this is just the other way around. The local effect of a specialized consumer on its resource is thus 2-fold larger than that of the other consumer. This is the same in both parameter settings. The effect of the resources on the consumers can be read by combing the graphical Jacobian with the full Jacobian. In Panel (a) where the steady state is located at the vertical part of the $\mathrm{d}N_1/\mathrm{d}t = 0$ nullcline and hence R_1 is limiting, a small increase of R_1 will increase $\mathrm{d}N_1/\mathrm{d}t$, i.e., $\partial N_1'/\partial R_1 = (b_1c_{11}/h_{11})\bar{N}_1 = (0.5 \times 0.5/1)\bar{N}_1 = 0.25 \times 2 = 0.5$, whereas $\partial N_1'/\partial R_2 = 0$ because R_2 is not limiting (and we stay on the $\mathrm{d}N_1/\mathrm{d}t = 0$ nullcline if R_2 is increased). For the second consumer this is just the other way around. Conversely, in Panel (b) the steady state is located at the horizontal part of the $\mathrm{d}N_1/\mathrm{d}t = 0$ nullcline and hence R_2 is limiting, a small increase of R_1 will not affect $\mathrm{d}N_1/\mathrm{d}t$ i.e., $\partial N_1'/\partial R_1 = 0$ whereas whereas $\partial N_1'/\partial R_2 = (b_1c_{12}/h_{12})\bar{N}_1 = (0.5 \times 0.25/0.5)\bar{N}_1 = 0.25 \times 2 = 0.5$. For the second consumer this is just the other way around. Thus, in Panels (a & c) the species that consumes most of R_1 is also limited by R_1, whereas in Panels (b & d) the species that consumes most of R_1 is limited by R_2. The former is a stable situation and the latter is not (see Section 9.5 and (Tilman, 1980, 1982)).

Question 10.1. Invasion criterion

A possible good answer has the following sketches:

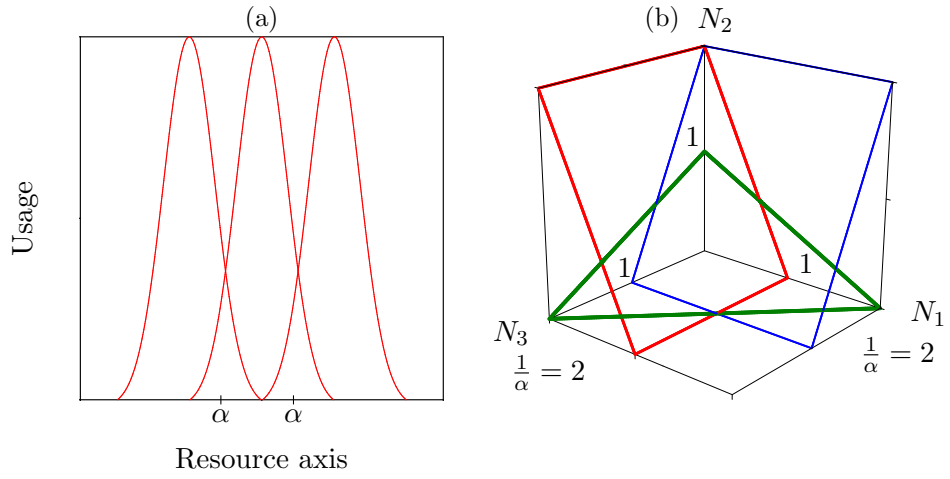

a. See the sketch in Panel (a)

b. Since N_1 and N_3 do not compete the model simplifies to

$$\frac{\mathrm{d}N_1}{\mathrm{d}t} = rN_1(1-N_1-\alpha N_2)\,, \frac{\mathrm{d}N_2}{\mathrm{d}t} = rN_2(1-N_2-\alpha N_1-\alpha N_3) \quad \text{and} \quad \frac{\mathrm{d}N_3}{\mathrm{d}t} = rN_3(1-N_3-\alpha N_2)$$

c. Because $N_2 \approx 0$ the steady states before invasion is $\bar{N}_1 = \bar{N}_3 = 1$ and $\mathrm{d}N_2/\mathrm{d}t \simeq rN_2(1-2\alpha)$. For invasion one requires $\mathrm{d}N_2/\mathrm{d}t > 0$ or $1-2\alpha > 0$ giving that $\alpha < 1/2$.

d. Since N_2 has an overlap of one with itself the total overlap with the other species should be less than the overlap with itself.

e. For $N_2 = 0$ the nullclines of N_1 and N_3 are perpendicular lines at $N_1 = 1$ and $N_3 = 1$, respectively. The N_2 nullcline intersects the N_1 and the N_3 axis at $1/\alpha$. At the critical invasion point the $\mathrm{d}N_2/\mathrm{d}t = 0$ nullcline should go exactly through the point $N_2 = 0$ and $N_1 = N_3 = 1$. See the sketch in Panel (b) When N_2 can invade the $\mathrm{d}N_2/\mathrm{d}t = 0$ nullcline will intersect at larger $N_1 = N_3$ values, and there will be a stable 3-dimensional steady state.

Question 10.2. Symbiosis

A possible good answer has the following sketches:

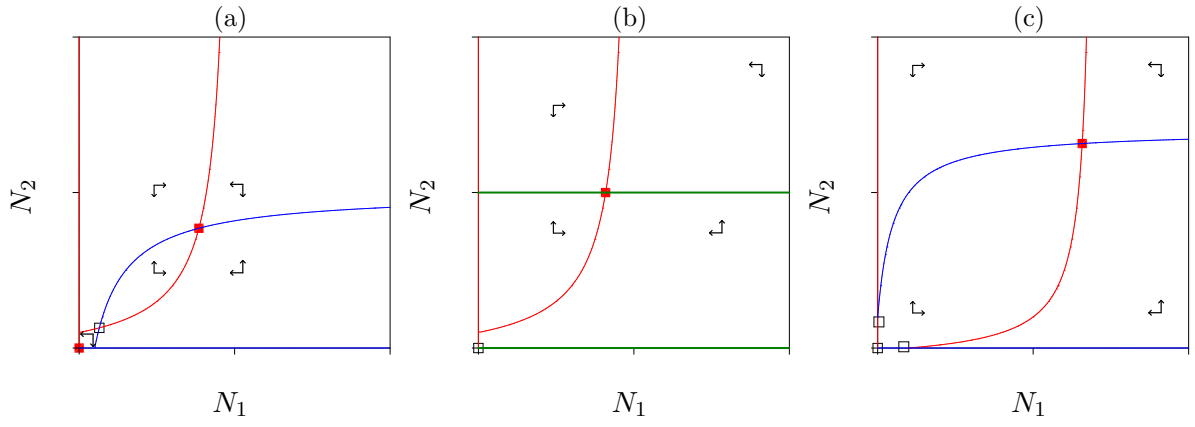

a. A simple model makes the birth rate a saturation function of the other species and assumes density dependent death:

$$\frac{\mathrm{d}N_1}{\mathrm{d}t} = N_1\left[\frac{b_1N_2}{h+N_2} - d_1(1+e_1N_1)\right] \quad \text{and} \quad \frac{\mathrm{d}N_2}{\mathrm{d}t} = N_2\left[\frac{b_2N_1}{h+N_1} - d_2(1+e_2N_2)\right]\,.$$

The $\mathrm{d}N_2/\mathrm{d}t = 0$ nullcline is given by

$$N_2 = \frac{1}{e_2}\left[R_{0_2}\frac{N_1}{h+N_1} - 1\right] ,$$

where $R_{0_2} = b_2/d_2$. This is a saturation function starting at $N_2 = -1/e_2$ when $N_1 = 0$. See the sketch in Panel (a).

b. Let N_1 be the saprophyte:

$$\frac{\mathrm{d}N_1}{\mathrm{d}t} = N_1\left[\frac{b_1 N_2}{h+N_2} - d_1(1+e_1 N_1)\right] \quad \text{and} \quad \frac{\mathrm{d}N_2}{\mathrm{d}t} = N_2\left[b_2 - d_2(1+e_2 N_2)\right] .$$

c. The other species could merely increase the birth rate:

$$\frac{\mathrm{d}N_1}{\mathrm{d}t} = N_1\left[b_1 + \frac{\beta_1 N_2}{h+N_2} - d_1(1+e_1 N_1)\right] \quad \text{and} \quad \frac{\mathrm{d}N_2}{\mathrm{d}t} = N_2\left[b_2 + \frac{\beta_2 N_1}{h+N_1} - d_2(1+e_2 N_2)\right] ,$$

where β_i is the maximum birth rate due to the presence of the symbiont, and b_i is the maximum birth rate in the absence of the symbiont.

d. Yes, just make sure that $R_{0_i} = b_i/d_i < 1$ in the absence of the other species, and $(b_i+\beta_i)/d_i > 1$ to enable growth in the presence of the symbiont. Panel (c) depicts the typical phase space when $R_{0_i} > 1$.

Question 10.3. Larvae and adults

a. A simple model would be:

$$\frac{\mathrm{d}L}{\mathrm{d}t} = rA - dL(1+eL) - mL \quad \text{and} \quad \frac{\mathrm{d}A}{\mathrm{d}t} = mL - \delta A ,$$

where we assume density dependent death by competition between the larvae. The steady state can be solved by first setting $\mathrm{d}A/\mathrm{d}t = 0$ delivering $A = mL/\delta$. Substituting this into $\mathrm{d}L/\mathrm{d}t = 0$ gives

$$\bar{L} = \frac{1}{e}\left[\frac{m}{d}\left(\frac{r}{\delta} - 1\right) - 1\right] , \bar{A} = \frac{m}{\delta}\,\bar{L} ,$$

which requires $\alpha = r/\delta > 1$ and $m(\alpha-1)/d > 1$.

b. Adding two predators changes to model into

$$\frac{\mathrm{d}L}{\mathrm{d}t} = rA - dL(1+eL) - mL - c_1 L N_1 , \quad \frac{\mathrm{d}A}{\mathrm{d}t} = mL - \delta A - c_2 A N_2 ,$$

$$\frac{\mathrm{d}N_1}{\mathrm{d}t} = (c_1 L - d_1)N_1 \quad \text{and} \quad \frac{\mathrm{d}N_2}{\mathrm{d}t} = (c_2 A - d_2)N_2 .$$

Solving the steady state of the latter two gives $\bar{L} = d_1/c_1$ and $\bar{A} = d_2/c_2$. Substituting this into $\mathrm{d}L/\mathrm{d}t = 0$ and $\mathrm{d}A/\mathrm{d}t = 0$ gives

$$\bar{N}_1 = \frac{r d_2}{c_2 d_1} - \frac{m}{c_1} - \frac{d}{c_1}\left(1 + \frac{e d_1}{c_1}\right) \quad \text{and} \quad \bar{N}_2 = \frac{m d_1}{c_1 d_2} - \frac{\delta}{c_2} .$$

Since one can always choose parameters such that $\bar{N}_1 > 0$ and $\bar{N}_2 > 0$ co-existence seems possible.

Question 10.4. Control by parasites

a. Define $T = S + I$ as the total population size of susceptible and infected birds, and write

$$\frac{\mathrm{d}S}{\mathrm{d}t} = bT(1-T) - dS - \beta SI \quad \text{and} \quad \frac{\mathrm{d}I}{\mathrm{d}t} = \beta SI - \delta I$$

b. The R_0 of the birds is b/d and the carrying capacity is $K = 1 - 1/R_0$.
c. The R_0 of the parasites is $R_0' = \beta K/\delta$.
d. $S = \delta/\beta = K/R_0'$.
e. Defining O as the other species one could write $\mathrm{d}S/\mathrm{d}t = bT(1-T-O) - dS - \beta SI, \mathrm{d}I/\mathrm{d}t = \beta SI - \delta I$ and $\mathrm{d}O/\mathrm{d}t = bO(1-T-O) - d_0 O$, with $d_0 > d$. Whenever $b(1-T)/d_0 > 1$ the other species can invade.
f. Thus, if the infection is sufficiently harmful, i.e., $\bar{T} \ll K$, the other species can invade despite its lower fitness.
g. If each species is sufficiently down-regulated by its parasite the resource density can stay high and many species can be maintained (Scheffer & Van Nes, 2006).

Question 10.5. Monopolization

a. Yes, since most competition situations are "founder controlled", species that grow faster are more likely to outcompete the species that grow slower.
b. No, one would still have that species will survive in a few patches just because they arrived there earlier, or in greater numbers, than other species.

Question 10.6. Sex

A possible good answer has the following sketches:

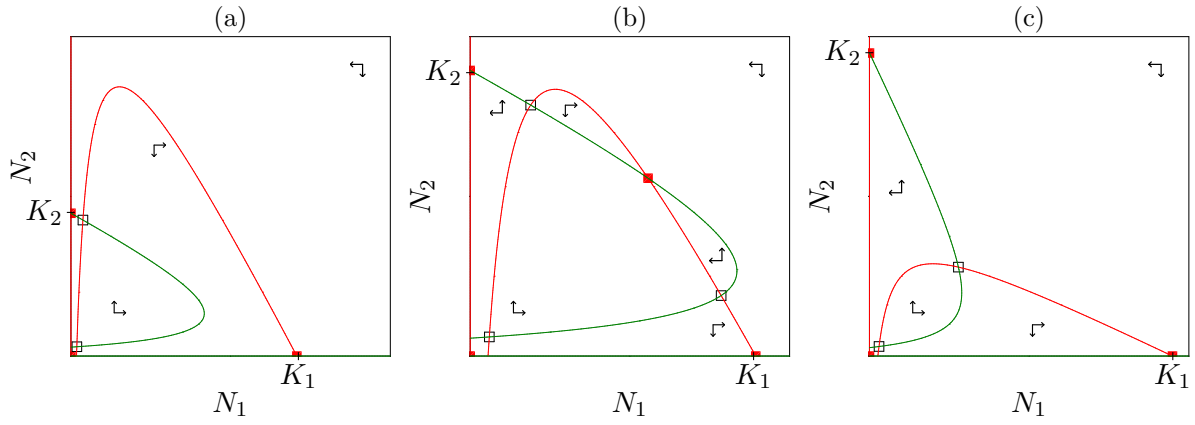

A model with density dependent death rates would be something like

$$\frac{\mathrm{d}N_1}{\mathrm{d}t} = N_1\left[\frac{b_1 N_1}{h+N_1} - d_1(1+e_1N_1+c_1N_2)\right] \quad \text{and} \quad \frac{\mathrm{d}N_2}{\mathrm{d}t} = N_2\left[\frac{b_2 N_2}{h+N_2} - d_2(1+e_2N_2+c_2N_1)\right]$$

Note that one has to separate birth from death because the sexual reproduction should only affect reproduction, and not the death. Assuming that the chance to find a mate approaches one when the population is close to its carrying capacity, i.e., assuming $h \ll K$, the carrying capacity is approximately $K_i \simeq (R_{0_i} - 1)/e_1$. In the absence of sex, i.e., when $h \to 0$, the nullclines are solved from $b_i - d_i(1 + e_iN_i + c_iN_j) = 0$ delivering the normal straight lines

$$N_2 = \frac{R_{0_1} - 1}{c_1} - \frac{e_1}{c_1}N_1 \quad \text{and} \quad N_2 = \frac{R_{0_2} - 1}{e_2} - \frac{c_2}{e_2}N_1 \ ,$$

which may or may not intersect, intersect in a stable state when there is resource competition, and intersect in an unstable steady state when there is interference competition. From these three situations one can sketch the three Panels depicted above. For instance, the $\mathrm{d}N_1/\mathrm{d}t = 0$ nullcline is given by

$$N_2 = \frac{1}{c_1}\left[R_{0_1}\,\frac{N_1}{h+N_1} - 1\right] - \frac{e_1}{c_1}N_1\ ,$$

which resembles the straight line with slope $-e_1/c_1$ for $N_1 \gg h$, and which gives $N_2 = -1/c_1$ when $N_1 = 0$. Panel (a) would correspond to non-intersecting nullclines, Panel (b) to resource competition (i.e., $c_i < e_i$), and Panel (c) to resource competition (i.e., $c_i > e_i$). Note that sex implies an Allee effect, and that (0,0), and the two carrying capacities are always stable (stable states are marked by closed boxes, unstable states by open boxes).

Question 10.7. Infinite Niche-matrix

a. The partial derivatives of the off-diagonal elements

$$\partial_{N_j} \quad N_i - \sum_j A_{ij}N_iN_j \quad \text{are} \quad 0, 0, \ldots, -A_{ij}N_i, 0, \ldots\ .$$

Because all populations have the same steady state, $\bar{N}$, they become $-\alpha\bar{N}$, $-\alpha^4\bar{N}$, $-\alpha^9\bar{N}$. The partial derivatives on the diagonal

$$\partial_{N_i} \quad N_i - \sum_j A_{ij}N_iN_j \quad \text{are} \quad 1 - 2\bar{N} - \sum_{j\neq i} A_{ij}\bar{N}\ ,$$

and hence the Jacobian is:

$$J = \begin{pmatrix} \ldots & -\alpha\bar{N} & 1-2\bar{N}-\sum_{j\neq i}A_{ij}\bar{N} & -\alpha\bar{N} & -\alpha^4\bar{N} & -\alpha^9\bar{N} & \ldots \\ \ldots & -\alpha^4\bar{N} & -\alpha\bar{N} & 1-2\bar{N}-\sum_{j\neq i}A_{ij}\bar{N} & -\alpha\bar{N} & -\alpha^4\bar{N} & \ldots \\ \ldots & & & & & & \end{pmatrix}$$

Moving one of the $2\bar{N}$ on the diagonal into the sum we obtain

$$J = \begin{pmatrix} \ldots & -\alpha\bar{N} & 1-\bar{N}-\sum A_{ij}\bar{N} & -\alpha\bar{N} & -\alpha^4\bar{N} & -\alpha^9\bar{N} & \ldots \\ \ldots & -\alpha^4\bar{N} & -\alpha\bar{N} & 1-\bar{N}-\sum A_{ij}\bar{N} & -\alpha\bar{N} & -\alpha^4\bar{N} & \ldots \end{pmatrix}$$

Finally because $\bar{N} = 1/\sum A_{ij}$ all diagonal elements can be simplified as $-\bar{N}$, i.e.,

$$J = \begin{pmatrix} \ldots & -\alpha\bar{N} & -\bar{N} & -\alpha\bar{N} & -\alpha^4\bar{N} & -\alpha^9\bar{N} & \ldots \\ \ldots & -\alpha^4\bar{N} & -\alpha\bar{N} & -\bar{N} & -\alpha\bar{N} & -\alpha^4\bar{N} & \ldots \end{pmatrix}$$

b. The Jacobian is equal to $-\bar{N}\mathbf{A}$, where $\mathbf{A}$ is the interaction matrix. The signs of the eigenvalues of the Jacobian are equal to those of the interaction matrix.

Question 11.1. Non-equilibrium co-existence

The best approach is to first make a system where the Monod saturated predator co-exists with the prey on a stable limit cycle. Then add the second predator, and make sure that it can invade on this limit cycle. The nullcline of the Monod saturated predator has to be located at a lower prey value than that of the linear predator to enable the Monod saturated predator to invade in the steady state of the linear predator with the prey, i.e., $\frac{h}{a_2/d_2-1} < \frac{d_1}{a_1}$.

Question 12.1. Islands in a lake

a. Since there will be a constant source of immigrants from the continent the model would be something like:

$$\frac{\mathrm{d}p}{\mathrm{d}t} = (C + cp)(1 - p) - mp \ .$$

b. The steady state is

$$\bar{p}_{\pm} = \frac{[c - C - m] \pm \sqrt{[c - C - m]^2 + 4cC}}{2c},$$

and since the term in the square root is larger than $[c - C - m]^2$, there is only one positive solution.

c. The "*per capita*" growth $f = \mathrm{d}p/\mathrm{d}t/p$ as a function of p is $f = c - C - m + C/p - cp$, which is a line having the vertical axis as an asymptote and a negative slope approaching $-c$. Since the slope $\lambda = -c$ is negative the steady state is stable.

Question 12.2. Population size

A possible good answer has the following sketches:

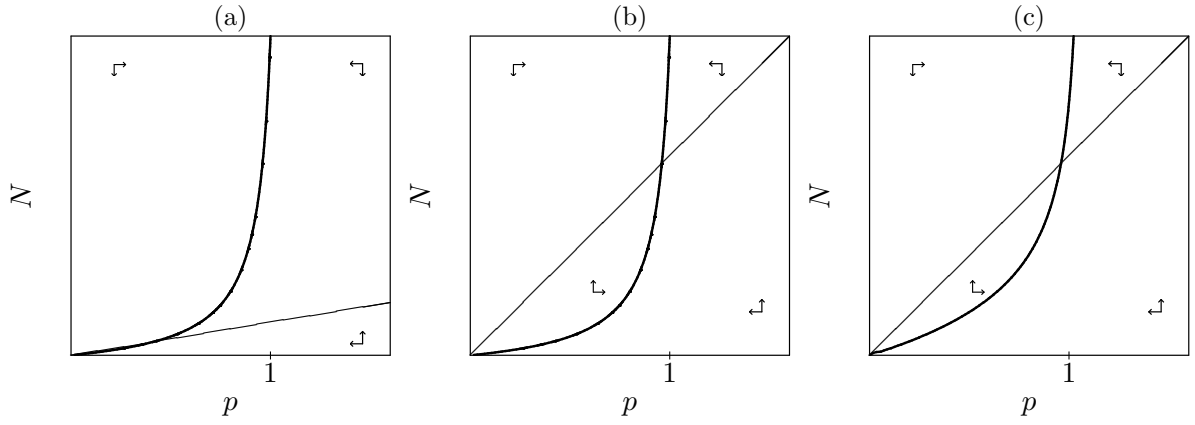

a. The number of migrants should be proportional to the total population size: $\mathrm{d}p/\mathrm{d}t = cN(1 - p) - mp$.

b. $\mathrm{d}N/\mathrm{d}t = 0$ delivers the diagonal line $N = kp(1 - d/r)$, and the $\mathrm{d}p/\mathrm{d}t = 0$ nullcline is $N = mp/[c(1 - p)]$. Plotting N as a function of p, the latter line leaves the origin with a slope m/c, and has a vertical asymptote at $p = 1$. Whenever $m/c < k(1 - d/r)$ there will be an intersection point (see panel (b)). Otherwise there is no intersection point (see panel (a)).

c. The vector field demonstrates that the non-trivial steady state is stable.

d. When the extinction rate decreases with the average population size per patch, i.e., $n = N/p$, we will have a very strong effect with a simple model

$$\frac{\mathrm{d}p}{\mathrm{d}t} = cN(1 - p) - m\frac{p}{n} = cN(1 - p) - m\frac{p^2}{N} \ ,$$

which approaches infinite extinction rates when $n \to 0$.

e. The p-nullcline now becomes $N = p\sqrt{m/[c(1 - p)]}$, which when plotted as a function of p leaves the origin with a slope $\sqrt{m/c}$, and also has a vertical asymptote at $p = 1$. Whenever $\sqrt{m/c} < k(1 - d/r)$ one obtains the non-trivial steady state shown in panel (c).

f. One should conclude that adding an average population size to the model of Levins & Culver (1971) hardly changes the behavior of the model. The saddle point obtained by Hanksi (1991), delivering an Allee effect, was an artifact of this particular model.

Question 12.3. Tilman

a. Yes, this can occur when the second species is a better colonizer (i.e., when $\frac{c_2}{m_2} > \frac{c_1}{m_1}$).

b. Yes, if the second species is absent in the pristine environment, it can invade after the right amount of habitat destruction if it is a better colonizer.

c. This declines monotonically, just add the two curves in Fig. 12.1b.

Question 13.1. Geritz & Kisdi (2004)

The quasi steady assumption for the resource gives $R = \mathrm{e}^{1-bA/r}$ and $\mathrm{d}E/\mathrm{d}t = cbA\mathrm{e}^{1-bA/r} - dE$ with solution

$$E(t) = \frac{cbA\mathrm{e}^{1-bA/r}}{d}\left(1 - \mathrm{e}^{-dt}\right) \quad \text{and} \quad A_{j+1} = \rho A_j \mathrm{e}^{-\beta A_j} \ ,$$

where $\rho = cb\mathrm{e}(1 - \mathrm{e}^{-d\tau})/d$ and $\beta = b/r$.

Question 13.2. Insect population

Since the death rate should increase when the amount of resource declines one could write for the *per capita* death rate

$$d = d_0 + \frac{d_1}{1 + r/h} \quad \text{such that} \quad \frac{\mathrm{d}n}{\mathrm{d}t} = -d_0 n - \frac{d_1 n}{1 + r/h} \ .$$

Question 13.3. Periodic forcing

Question 14.1. Biomanipulation

A possible good answer has the following sketches:

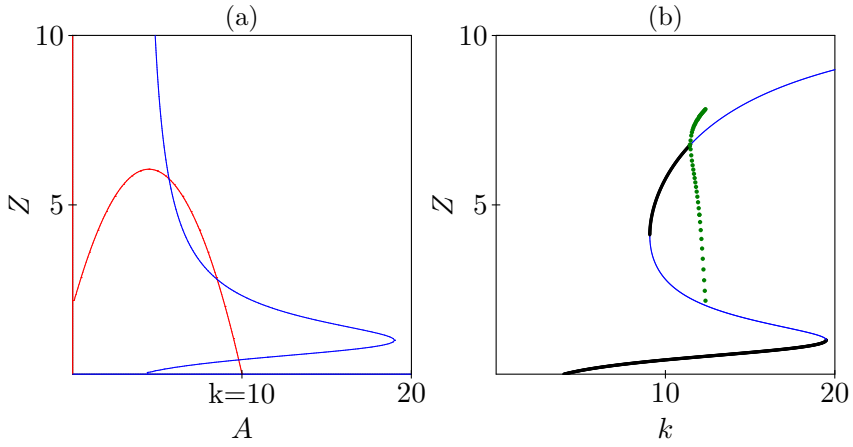

Scheffer (1991) proposed the following model:

$$\frac{\mathrm{d}A}{\mathrm{d}t} = A(1 - A/k) - pZ\frac{A}{1 + A} \ ,$$

$$\frac{\mathrm{d}Z}{\mathrm{d}t} = -mZ + pZ\frac{A}{1 + A} - F\frac{Z^2}{h^2 + Z^2} \ .$$

For $F = 0.15, h = 1, k = 10, m = 0.4$ and $p = 0.5$ the phase space is given by Panel (a), which has three steady states. Following any of these by changing the carrying capacity k yields the bifurcation diagram of Panel (b). There is a transcritical bifurcation at $k = 4$, a saddle-node bifurcation at $k \simeq 9$, a Hopf bifurcation at $k \simeq 11.5$, and another saddle-node bifurcation at $k \simeq 19.5$. The stable limit cycle that is born at the Hopf bifurcation dies by a so-called "global bifurfaction" around $k = 12$ when it glues with the stable manifold of the saddle point in the middle. The heavy solid line depicts stable steady states, the light solid line unstable steady states, and the dots are Z values where the limit cycle crosses a Poincaré plane located at an average A value.

Question 15.1. Fishing herring

The first thing to think about is the parameters of the model. For instance, one could consider the Herring population in the North sea, and realize that the population will have a carrying capacity amounting to an enormous number of individuals, or an enormous amount of biomass. Fortunately, one can always scale the population density in a model by the carrying capacity of the population. Thus, we can set the carrying capacity, $k = 1$, realizing that $H = 1$ actually corresponds to this enormous Herring population at carrying capacity in the North sea. The next parameter is the natural rate of increase, r. We first need to define a time-scale, and for a Herring population with a yearly reproduction cycle, a time-scale of years seems a proper choice. If t is measured in years we can think of a growth rate per year, and using our biological intuition about fish of the size of Herring, it seems obvious that a growth rate of 1% per year seems slow and that they will not easily grow faster than 100% per year. Thus, setting $r = 0.1$ per year or $r = 0.2$ per year seem reasonable choices. One can actually check this by studying the recovery rate of a crashed Herring population in the absence of fishing: setting $H = 0.01$ and $Q = 0$, and run the model for a few decades to test how long it takes for the population to recover and approach its carrying capacity. Once you think you have found realistic parameters, you can start on the rest of the exercise.

a. Starting at the carrying capacity, and setting $Q = rk/4$ to study the impact of this maximum yearly harvest, one finds that the population approaches $H = k/2$ in the absence of noise. However, the population will always go extinct if there is enough noise.

b. Now the population will not go extinct.

c. At the steady state $\mathrm{d}H/\mathrm{d}t = rH(1 - H/k) - fH = 0$, or $\bar{H} = k(1 - f/r)$, the total harvest is $f\bar{H}$. Taking the derivative, ∂_f, of $f\bar{H}$, and setting that to zero gives $k - (2k/r)f = 0$ or $f = r/2$. Substituting that into $\bar{H}$ gives $\bar{H} = k/2$, i.e., half of the carrying capacity.

d. The population will no longer go extinct. Even noise on the "optimal" f will not drive the population to extinction.

e. The optimal harvest $f\bar{H}$ at $f = r/2$ is $rk/4$, which is equal to Q. Thus, catching a fraction of the Herring population on average allows for the same maximum harvest, but is much more robust. Note that a shortcut to the same result is to see that this optimum is reached when the harvest function, fH, crosses the growth function, $rH(1 - H/k)$, in its maximum $rk/4$ at $H = k/2$.

Question 15.2. Allee effect

a. The prey nullcline can be described by $N = \frac{b/e}{1+R/k}\frac{R}{h+R} - d_1/e$, which indeed reflects the shape of the *per capita* growth function.

b. Before you can do this you have to think of a particular population, and about what is causing the Allee effect. We could continue with the Herring of the previous exercise, and let $k = 1$ be the Herring density at which the birth rate has reduced to half its maximum value. The maximum birth rate we could then set to $b = 0.3$ per year, and argue that the Herring

have an expected life span of about ten years, by setting $d_1 = 0.1$ per year. Hence, we would have a natural rate of increase of $b - d_1 = 0.2$ per year (if you thought this was slow, just increase b). In the absence of an Allee effect (i.e., for $h \to 0$) the carrying capacity of the population is $K = k(R_0 - 1)$ (see Table 4.1), which for $k = 1, b = 0.3$ and $d_1 = 0.1$ boils down to $K = 2$. If the Allee effect is due to low rates of sexual reproduction at low population densities, one would have to set $h \ll 2$ because a low density corresponds to a small fraction of the carrying capacity. The predator, N, could be some predatory fish. It seems natural to allow for a $c = 0.1$ trophic conversion factor (or scale this to one), and to give the species at a higher trophic level a longer expected life-span, e.g., set $d_2 = d_1/2 = 0.05$ per year to have a life span of twenty years. Finally we have to make sure that the predator can actually persist by giving it an $R_0 > 1$. For the current parameters, the R_0 of the predator in a prey population at carrying capacity is $0.1 \times e \times 2/0.05$, implying that we need to set $e > 0.25$ per predator per year. Qualitatively different cases can be set by varying e: the predator nullcline can be placed above the carrying capacity ($e < 0.25$) or below it ($e > 0.25$), and then it can be put in the rising or the declining part of the prey nullcline.

c. Just run `grind.R` in every regime.

d. To re-interpret the $\mathrm{d}R/\mathrm{d}t$ equation in terms of whales, we better give them a long life-span, e.g., setting $d_1 = 0.02$ gives 50 years, and a slow birth rate, e.g., $b = 0.04$ allowing for a maximum yearly growth rate of $b - d_1 = 0.02$ per year, which is slightly slower than that of humans. Scaling the population size such that $k = 1$ is the density at which the birth rate is half-maximal, the carrying capacity of such a population of whales, in the absence of the Allee effect, remains $K = k(R_0 - 1)$ (see Table 4.1), which for $k = 1, b = 0.04$ and $d_1 = 0.02$ boils down to $K = 1$. The Allee effect can then be incorporated by setting $h \ll 1$. If the whales were to grow logistically, the maximum quotum would be $Q = rK/4$, i.e., $Q = 0.02/4 = 0.005$. We can study the maximum quotum for whales obeying this non-logistic equation by plotting the whale nullcline as a function of Q for different values of the Allee effect parameter h. For instance, set $h = 0$ and have whales (R) and quotum (Q) on the axes of a 2-dimensional phase space, and read of what the maximum value of Q is.

Question 15.3. Paradox of enrichment

a. Scale the density of the algae at which the birth rate vanishes to $k = 2$ and scale time by their expected life span such that $d_1 = 1$ (which implies a time scale of about one week). We could give the algae a maximum rate of increase of $b - d_1 = 1$ by setting $b = 2$. Because the carrying capacity $K = k(1 - 1/R_0)$ (see Table 4.1) we obtain that $K = 1$. Because the saturation of the functional response probably occurs at prey densities below the carrying capacity, it seems wise to set $h \ll K$, e.g., $h = 0.1$. We could scale the predator biomass such that the trophic conversion factor becomes $c = 1$, and let us give the predators a 2-fold longer life span , i.e., $d_2 = 0.5$. To give the predator an $R_0 = ce/d_2 = e/0.5 > 1$ we could set $e = 0.6$ such that the initial growth rate of the predator at high prey densities is about 0.1, i.e., 10-fold slower than the algae. For these values the predator nullcline is located at $h/(R_0 - 1) = 0.1/(0.6/0.5 - 1) = 0.5$, which is just at the right hand side of the maximum of the prey nullcline at $(K - h)/2 = 0.45$.

b. Different possibilities for the location of the predator nullcline, without changing that of the prey, can be made by changing the death rate of the predator.

c. The carrying capacity can be changed by altering the density k at which the birth rate of the algae vanishes.

d. First settle into a non-trivial steady state by giving proper initial values and then issuing the `f<-newton()` command. Then call `continue(f,x="k",xmin=0.1,xmax=5,y="N")` to define a horizontal axis (where we avoid $k = 0$ because the model is dividing by k), and we keep the predator on the vertical axis.

e. Replace the death rate of the predators by $d_2(1 + \epsilon N)$.

f.

g.

Question 15.4. Luckinbill

a. Using the model

$$\frac{\mathrm{d}P}{\mathrm{d}t} = aP(1 - P/K) - \frac{bDP}{h + P} \quad \text{and} \quad \frac{\mathrm{d}D}{\mathrm{d}t} = \frac{cDP}{h + P} - dD \ ,$$

we could set $a = 1$ and $K = 1$ to scale time and carrying capacity by the growth rate and carrying capacity of the prey *Paramecium*. A typical value of h would then be $h = 0.1$. Scaling the predator *Didinium* density such that the conversion factor disappears we could basically set $b = c$. This implies that we should keep $d < c$ to allow the predator to possibly persist.

b. First find values of h and $b = c$ such that the predator nullcline is located at very low prey densities. Increase h such that it moves to the right, and decrease K such that the top of the prey nullcline moves to the left.

c. Replacing the saturated functional response with the mass-action bDP term allows for similar results because the noise will not allow trajectories to approach the stable spiral point. In the experiments this will look like an oscillation.

Question 15.5. Biomanipulation

A possible good answer has the following sketches:

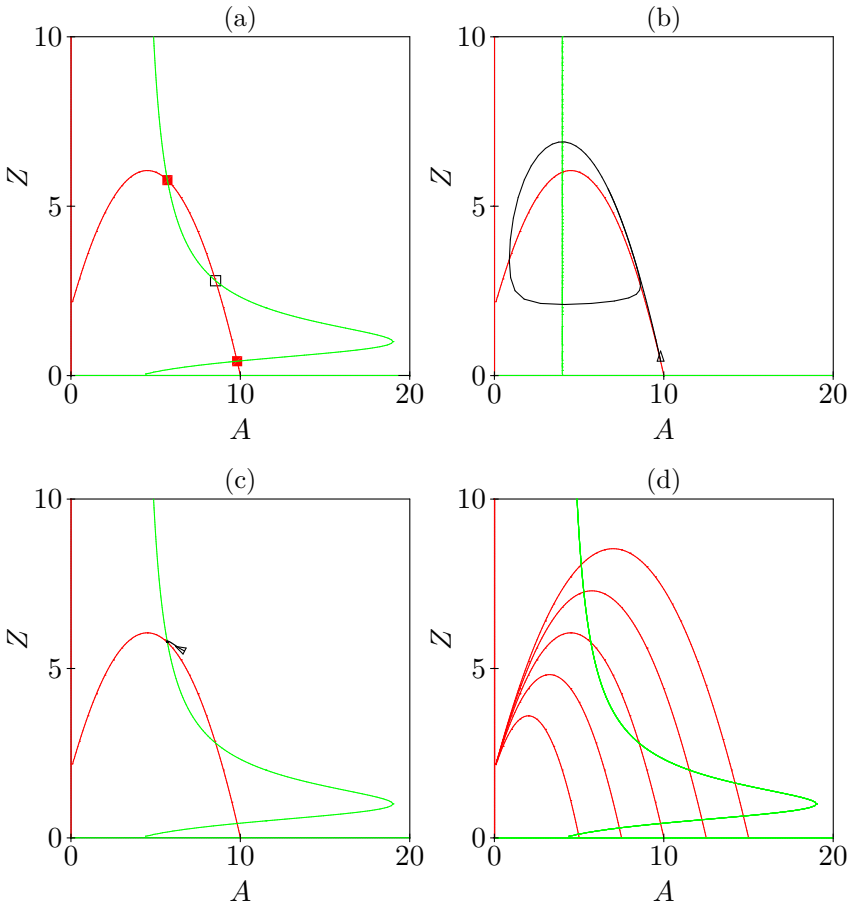

a. For $F = 0.15$ and $k = 10$ one obtains Panel (a). The "green starting point" where the lake is turbid due to eutrophication would correspond to the stable steady state close to the carrying capacity.

b. Removing the fish by setting $F = 0$ would lead to a trajectory approach the limit cycle shown in Panel (b). Setting $F = 0.15$ after this limit cycle has been approached, leads to the picture in Panel (c) where the system approaches the steady state with less algae and much more zooplankton. Thus the lake has switched states and has become much more clear permanently by a single perturbation.

c. Keeping $F = 0.15$ one could increase the carrying capacity from $k = 5$ to $k = 15$ (see Panel (d)). At $k = 5$ the only steady state is the one close to the carrying capacity, which should now correspond to a relatively clear lake (because $A < 5$). Increasing the carrying capacity the system is expected to stay in the same steady state, but when $k = 10$ or $k = 15$ we call the same state the turbid steady state, while a new "clear" steady state appears at high values of Z when $k \simeq 9$. Note that this analysis is not completely realistic because the fish density should actually change when we change the carrying capacity. One could try this by adding a $\mathrm{d}F/\mathrm{d}t$ equation.

Question 15.6. Non-linear density dependence

a. The four models already have the same natural rate of increase, $b - d$, and the same fitness $R_0 = b/d$ (see Chapter 16). To rescale the carrying capacities, one can define $K = 1$, and compute the corresponding k parameters:
1. $1 = 2k[1 - 1/R_0]$ gives $k = 1/(2[1 - 1/R_0])$.
2. $1 = k[R_0 - 1]$ gives $k = 1/(R_0 - 1)$.
3. $1 = k\sqrt{R_0 - 1}$ gives $k = 1/\sqrt{R_0 - 1}$.
4. $1 = \frac{k}{\ln[2]} \ln[R_0]$ gives $k = \frac{\ln 2}{\ln R_0}$

b. Computer simulations with models where the carrying capacities and the initial growth rates, $b - d$, are identical, will show that the four sigmoid curves are very similar.

Question 15.7. Linear models

The steady state is $x = y = 0$ and the Jacobian, $J = \begin{pmatrix} a & b \\ c & d \end{pmatrix}$, is the same as the interaction matrix. Use Fig. 18.8 to create an interaction matrix with the eigenvalues corresponding to the different types of steady states.

Question 15.8. Noise and r and K-selected species

r-selected species recover more quickly from disturbances of the population density, but can also fluctuate more than K-selected species by tracing the variation in parameter values.

Question 17.1. Space

A possible good answer has the following sketch:

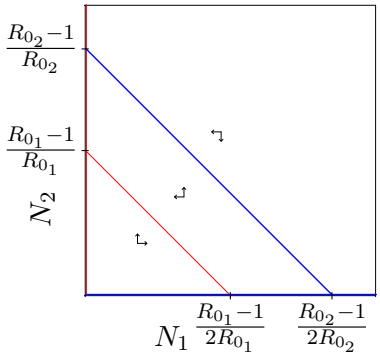

a. Let N_1 be the population size of the large species that grows slowly, N_2 be that of the small species, and define the amount of empty space as $L = 1 - 2N_1 - N_2$, where the total amount of space as scaled to one. One writes

$$\frac{\mathrm{d}N_1}{\mathrm{d}t} = bN_1L - dN_1 \quad \text{and} \quad \frac{\mathrm{d}N_2}{\mathrm{d}t} = 2bN_2L - dN_2 \quad \text{with} \quad R_{0_1} = \frac{b}{d} \quad \text{and} \quad R_{0_2} = 2R_{0_1}\ .$$

From the fitnesses one can conclude that the small species N_2 should win.

b. Solving $\mathrm{d}N_1/\mathrm{d}t = 0$ gives $N_1 = 0$ and $1 - 2N_1 - N_2 - d/b = 0$ or $N_2 = 1 - 1/R_{0_1} - 2N_1$. Solving $\mathrm{d}N_2/\mathrm{d}t = 0$ gives $N_2 = 0$ and $1 - 2N_1 - N_2 - d/(2b) = 0$ or $N_2 = 1 - 1/R_{0_2} - 2N_1$. The nullclines are parallel and intersect the N_2 axis at $N_2 = 1 - 1/R_{0_1}$ and $N_2 = 1 - 1/R_{0_2}$, respectively. Since $R_{0_2} = 2R_{0_1}$ the N_2 nullcline is the upper line, and N_2 wins. See the phase space, note that the axes have different scales.

c. The carrying capacities are $\bar{N}_1 = 0.5[1 - 1/R_{0_1}]$ and $\bar{N}_2 = 1 - 1/R_{0_2}$, respectively. Both are smaller than one, which was the total amount of space.

d. N_2 wins because of its higher fitness, it also has a larger carrying capacity.

Question 17.2. Nitrogen

a. $R_0 = b_i/d_i$

b. From $b_i \frac{T-A_i}{h_i+T-A_i} - d_i = 0$, or $R_{0_i} \frac{T-A_i}{h_i+T-A_i} = 1$, one obtains $\bar{A}_i = K_i = T - \frac{h_i}{R_{0_i}-1}$ for each species.

c. For the intersect of the A_1 nullcline with the A_2 axis we solve the very similar $R_{0_1} \frac{T-A_2}{h_1+T-A_2} = 1$ to obtain $A_2 = K_1$. From the general $R_{0_1} \frac{T-A_1-A_2}{h_1+T-A_1-A_2} = 1$ we solve $A_2 = K_1 - A_1$. The A_1 nullcline has slope -1 and runs from $A_2 = K_1$ on the vertical axis to $A_1 = K_1$ on the horizontal axis. The A_2 nullcline runs parallel to this, from $A_2 = K_2$ on the vertical axis to $A_1 = K_2$ on the horizontal axis.

d. The nullclines cannot intersect, so there is no equilibrium co-existence. Around the equilibrium nitrogen will always be depleted, so it makes no difference that the birth rate saturates at high nitrogen levels.

e. Because the nullclines run from $A_2 = K_i$ to $A_1 = K_i$, the species with the largest carrying capacity always wins. Computing the critical nitrogen density, N_i^*, for the each species from $R_{0_i} \frac{N}{h_i+N} = 1$, we find that $N_i^* = \frac{h_i}{R_{0_i}-1}$, and hence that $K_i = T - N_i^*$. Thus, the species with the lowest resource requirement, N_i^*, necessarily has the largest carrying capacity.

Question 17.3. Food chain

A possible good answer has the following sketches:

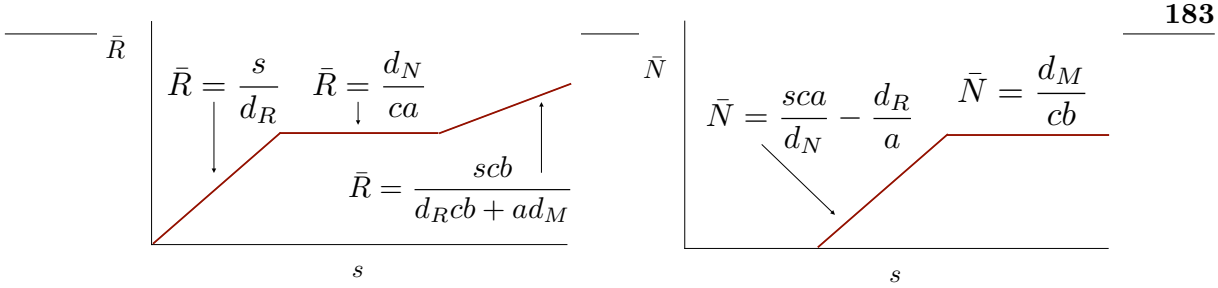

a. From $\mathrm{d}R/\mathrm{d}t = 0$ with $N = 0$ one solves $\bar{R} = \frac{s}{d_R}$.
b. From $\mathrm{d}N/\mathrm{d}t = 0$ with $M = 0$ one solves $\bar{N} = 0$ and $\bar{R} = \frac{d_N}{ca}$.
c. Starting with the simplest equation, i.e., $\mathrm{d}M/\mathrm{d}t = 0$, one solves $M = 0$ $\bar{N} = \frac{d_M}{cb}$. Substituting the latter into $\mathrm{d}R/\mathrm{d}t = 0$ gives $s = R(d_R + \frac{ad_M}{cb}$ or $\bar{R} = \frac{scb}{d_R cb + a d_M}$.
d. Since their maximum per capita birth rate is $ca\bar{R}$, one obtains $R_0 = \frac{ca\bar{R}}{d_N} = \frac{cas}{d_N d_R}$.
e. See the sketch in Panel (a). Two transcritical bifurcations, one where the consumer becomes non-zero, and one where the predator invades.
f. See the sketch in Panel (b)

Question 17.4. Write a natural model

$$\frac{\mathrm{d}F}{\mathrm{d}t} = rF(1 - F/K) - aFB \quad \text{and} \quad \frac{\mathrm{d}B}{\mathrm{d}t} = \frac{iF}{h + F} - eB \ ,$$

where F are the fish, B the birds, h the fish density where immigration (i) is half maximal, and e is the emigration.

Question 18.1. Sketch a few functions
A possible good answer has the following sketches:

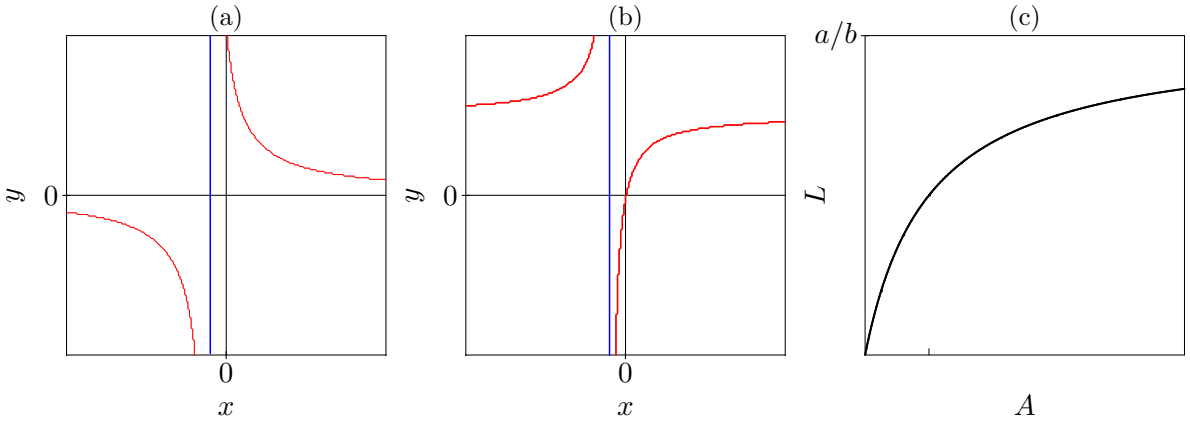

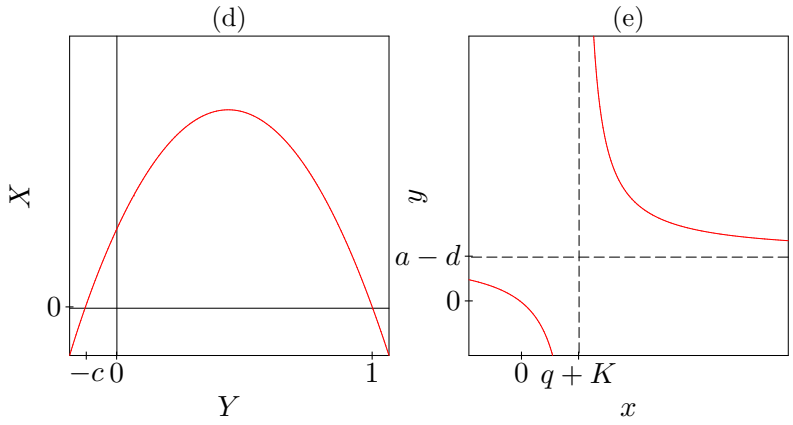

a. $y = \frac{h}{h+x} = 1$ when $x = 0$. For $x \to \infty, y \to 0$. For $x \to -\infty, y \to 0$. There is an vertical asymptote at $x = -h$. See the sketch in Panel (a).
b. $y = \frac{x}{h+x} = 0$ when $x = 0$. For $x \to \infty, y \to 1$. For $x \to -\infty, y \to 1$. There is an vertical asymptote at $x = -h$. See the sketch in Panel (b).
c. $L = \frac{aA}{c+bA}$ with horizontal asymptote $L = a/b$ or $A = \frac{cL}{a-bL}$ with vertical asymptote $L = a/b$. See the sketch in Panel (c).
d. Write $Y = 0$ and $X = (a/b)(1 - Y)(c + Y)$. See the sketch in Panel (d).
e. Intersection with x-axis: $x = \frac{ak-dq-dk}{a-d}$,
intersection with y-axis: $y = \frac{ak}{q+k} - d$
Horizontal asymptote: $y = a - d$, and vertical asymptote: $x = q + k$. See the sketch in Panel (e), where the dashed lines denote the two asymptotes.

Question 18.2. Linearization

a. $\partial_x x^2 = 2x$
b. For $x = 3$ one obtains $x^2 = 9$
c. $y = 9 + 0.1 \times 2 \times 3 = 9.6$. The true value is $3.1^2 = 9.61$.

Question 18.3. Scaling

The Lotka Volterra equations are

$$\frac{\mathrm{d}R}{\mathrm{d}t} = [r(1 - R/K) - aN]R \quad \text{and} \quad \frac{\mathrm{d}N}{\mathrm{d}t} = [caR - d]N$$

a. Defining $x = R/K$ and dividing all rates by r one obtains

$$\frac{\mathrm{d}Kx}{\mathrm{d}t} = [(1 - Kx/K) - aN/r]Kx \quad \text{and} \quad \frac{\mathrm{d}N}{\mathrm{d}t} = [\frac{ca}{r}Kx - d/r]N$$

and by defining $\alpha = a/r$ this simplifies into

$$\frac{\mathrm{d}x}{\mathrm{d}t} = [(1 - x) - \alpha N]x \quad \text{and} \quad \frac{\mathrm{d}N}{\mathrm{d}t} = [c\alpha Kx - d/r]N$$

with only one parameter in the prey equation. Defining $y = \alpha N$, i.e., $N = y/\alpha$, we remove that parameter from $\mathrm{d}x/\mathrm{d}t$

$$\frac{\mathrm{d}x}{\mathrm{d}t} = [(1 - x) - y]x \quad \text{and} \quad \frac{1}{\alpha}\frac{\mathrm{d}y}{\mathrm{d}t} = [c\alpha Kx - \frac{d}{r}]\frac{y}{\alpha}$$

where $\mathrm{d}y/\mathrm{d}t$ can be simplified by lumping the parameters

$$\frac{\mathrm{d}y}{\mathrm{d}t} = [\gamma x - \delta]y \ ,$$

where $\gamma = c\alpha K = cKa/r$ and $\delta = d/r$.

b. We went from five to two parameters for which we even know that is a scaled fitness $R_0 = \gamma/\delta$, and that $\gamma/\delta > 1$ is required for co-existence.

Bibliography

Abrams, P. A. (1994). The fallacies of "ratio-dependent" predation. *Ecology* **75**, 1842–1850.

Adler, F. R. (1997). *Modeling the Dynamics of Life. Calculus and Probabilty for Life Scientists*. Pacific Grove: Brooks/Cole.

Anderson, R. M. & May, R. M. (1991). *Infectious diseases of humans. Dynamics and Control*. Oxford: Oxford U.P.

Arditi, R. & Ginzburg, L. R. (1989). Coupling in predator-prey dynamics: Ratio-dependence. *J. theor. Biol.* **139**, 311–326.

Arditi, R. & Ginzburg, L. R. (2012). *How Species Interact: Altering the Standard View on Trophic Ecology*. Oxford: Oxford U.P.

Beddington, J. R. (1975). Mutual interference between parasites or predators and its effect on searching efficiency. *J. Anim. Ecol.* **51**, 597–624.

Beverton, R. J. H. & Holt, S. J. (1957). In: *On the dynamics of exploited fish populations*, vol. 19 of *Fish. Invest. Ser. 2*. London: Her majesty's stationery office.

Campbell, N. A. & Reece (2002). *Biology, sixth edition*. Redwood city CA: Benjamin/Cummings.

Campbell, N. A. & Reece (2005). *Biology, Seventh edition*. San Francisco, CA: Pearson/BenjaminCummings.

Campbell, N. A. & Reece, J. B. (2008). *Biology, Eighth edition*. San Francisco, CA: Pearson/BenjaminCummings.

Cohen, J. E. (1995). Population growth and earth's human carrying capacity. *Science* **269**, 341–346.

Diekmann, O., Heesterbeek, H. & Britton, T. (2012). *Mathematical tools for understanding infectious disease dynamics*. Princeton University Press.

Diekmann, O., Heesterbeek, J. A. & Metz, J. A. (1990). On the definition and the computation of the basic reproduction ratio R0 in models for infectious diseases in heterogeneous populations. *J. Math. Biol.* **28**, 365–382.

Fussmann, G. F., Ellner, S. P., Shertzer, K. W. & Hairston, Jr, N. G. (2000). Crossing the hopf bifurcation in a live predator-prey system. *Science* **290**, 1358–1360.

Gardner, M. R. & Ashby, W. R. (1970). Connectivity of large, dynamical (cybernetic) systems: critical values for stability. *Nature* **228**, 784.

Geritz, S. A. & Kisdi, E. (2004). On the mechanistic underpinning of discrete-time population models with complex dynamics. *J. theor. Biol.* **228**, 261–269.

Ginzburg, L. R. & Akçakaya, H. R. (1992). Consequences of ratio-dependent predation for steady-state properties of ecosystems. *Ecology* **93**, 1536–1543.

Grime, J. P. (1997). Biodiversity and ecosystem function: the debate deepens. *Science* **277**, 1260–1261.

Hanksi, I. (1991). Single-species metapopulation dynamics: concepts, models and observations. *Biol. J. Linnean Soc.* **42**, 17–38.

Hanksi, I. (1997). Be diverse, be predicatable. *Nature* **390**, 440–441.

Hanksi, I. (1998). Metapopulation dynamics. *Nature* **396**, 41–49.

Hanski, I. & Gaggiotti, O. (2004). *Ecology, genetics, and evolution of metapopulations*. Amsterdam: Elsevier Academic Press.

Hassell, M. P. (1975). Density-dependence in single-species populations. *J. Anim. Ecol.* **44**, 283–295.

Hassell, M. P., Lawton, J. H. & May, R. M. (1976). Patterns of dynamical behaviour in single-species populations. *J. Anim. Ecol.* **45**, 471–486.

Hastings, A. (1997). *Population biology: concepts and models*. New York: Springer.

Hastings, A. & Powell, T. (1991). Chaos in a three-species food chain. *Ecology* **72**, 896–903.

Heffernan, J. M., Smith, R. J. & Wahl, L. M. (2005). Perspectives on the basic reproductive ratio. *J. R. Soc. Interface* **2**, 281–293.

Hirota, M., Holmgren, M., Van Nes, E. H. & Scheffer, M. (2011). Global resilience of tropical forest and savanna to critical transitions. *Science* **334**, 232–235.

Hogeweg, P. & Hesper, B. (1978). Interactive instruction on population interactions. *Comput. Biol. Med.* **8**, 319–327.

Holling, C. S. (1959). The components of predation as revealed bij a study of small mammal predation of the european pine sawfly. *Can. Entomol.* **91**, 293–320.

Huisman, G. & De Boer, R. J. (1997). A formal derivation of the "Beddington" functional response. *J. theor. Biol.* **185**, 389–400.

Kaunzinger, C. M. K. & Morin, P. J. (1998). Productivity controls food-chain properties in microbial communities. *Nature* **395**, 495–497.

Law, R. & Blackford, J. C. (1992). Self-assembling food webs - a global viewpoint of coexistence of species in Lotka-Volterra communities. *Ecology* **73**, 567–578.

Levins, R. (1969). Some demographic and genetic consequences of environmental heterogeneity for biological control. *Bull. Ent. Soc. Am.* **15**, 237–240.

Levins, R. & Culver, D. (1971). Regional Coexistence of Species and Competition between Rare Species. *Proc. Nat. Acad. Sci USA.* **68**, 1246–1248.

Li, T. A. & Yorke, J. A. (1975). Period three implies chaos. *Amer. Math. Monthly* **82**, 985–992.

Lipsitch, M., Cohen, T., Cooper, B., Robins, J. M., Ma, S., James, L., Gopalakrishna, G., Chew, S. K., Tan, C. C., Samore, M. H., Fisman, D. & Murray, M. (2003). Transmission dynamics and control of severe acute respiratory syndrome. *Science* **300**, 1966–1970.

Lotka, A. J. (1913). A natural population norm. *J. Wash. Acad. Sci.* **3**, 289–293.

Luckinbill, L. S. (1973). Coexistence in laboratory populations of *Paramecium aurelia* and its predator *Didinium nasutum*. *Ecology* **54**, 1320–1327.

MacArthur, R. H. (1972). *Geographical Ecology*. New York: Harper & Row.

MacArthur, R. H. & Wilson, E. O. (1967). *The Theory of Island Biogeography*. Princeton, NJ: Princeton University Press.

May, R. M. (1972). Will a large complex system be stable? *Nature* **238**, 413–414.

May, R. M. (1974). *Stability and complexity in model ecosystems*, vol. 6 of *Monographs in population biology*. Princeton, New Jersey: Princeton University Press, second edn.

May, R. M. (1977). Thresholds and breakpoints in ecosystems with a multiplicity of stable states. *Nature* **269**, 471–477.

May, R. M. (2004). Uses and abuses of mathematics in biology. *Science* **303**, 790–793.

Maynard Smith, J. & Slatkin, M. (1973). The stability of predator-prey systems. *Ecol.* **54**, 384–391.

McCann, K., Hastings, A. & Huxel, G. R. (1998). Weak trophic interactions and the balance of nature. *Nature* **395**, 794–798.

McCauley, E., Nisbet, R. M., Murdoch, W. W., De Roos, A. M. & Gurney, W. S. C. (1999). Large-amplitude cycles of Daphnia and its algal prey in enriched environments. *Nature* **402**, 653–656.

McLean, A. & May, R. M. (2007). *Theoretical Ecology: Principles and Applications*. Oxford: Oxford University Press.

Murdoch, W. W., Kendall, B. E., Nisbet, R. M., Briggs, C. J., McCauley, E. & Bolser, R. (2002). Single-species models for many-species food webs. *Nature* **417**, 541–543.

Mylius, S. D. & Diekmann, O. (1995). On evolutionarily stable life histories, optimization and the need to be specific about density dependence. *Oikos* **74**, 218–224.

Nee, S. & May, R. M. (1992). Dynamics of metapopulations: habitat destruction and competitive coexistence. *J. Anim. Ecol.* **61**, 37–40.

Noy-Meir, I. (1975). Stability of grazing systems: an application of predator-prey graphs. *J. Ecology* **63**, 459–483.

Panfilov, A. V., Ten Tusscher, K. H. W. J., Van Zon, L. & De Boer, R. J. (2016). *Matrices, Linearization, and the Jacobi matrix*. EBook: http://tbb.bio.uu.nl/rdb/books/math.pdf.

Pianka, E. R. (1974). Niche overlap and diffuse competition. *Proc. Natl. Acad. Sci. U.S.A.* **71**, 2141–2145.

Pimm, S. L. (1980). Properties of food webs. *Ecology* **61**, 219–225.

Post, W. M. & Pimm, S. L. (1983). Community assembly and food web stability. *Math. Biosci.* **64**, 169–192.

Rappoldt, C. & Hogeweg, P. (1980). Niche packing and number of species. *Am. Nat.* **116**, 480–492.

Rietkerk, M. & Van de Koppel, J. (1997). Alternate stable states and threshold effects in semi-arid grazing systems. *Oikos* **79**, 69–76.

Roberts, A. (1974). The stability of a feasible random ecosystem. *Nature* **251**, 608.

Rosenzweig, M. L. (1971). Paradox of enrichment: destabilization of exploitation ecosystems in ecological time. *Science* **171**, 385–387.

Scheffer, M. (1991). Fish and nutrients interplay determines algal biomass - a minimal model. *Oikos* **62**, 271–282.

Scheffer, M. (2009). *Critical Transitions in Nature and Society*. Princeton: Princeton U.P.

Scheffer, M., Carpenter, A., Foley, J. A., Folke, C. & Walker, B. (2001). Catastrophic shifts in ecosystems. *Nature* **413**, 591–596.

Scheffer, M. & De Boer, R. J. (1995). Implications of spatial heterogeneity for the paradox of enrichment. *Ecology* **76**, 2270–2277.

Scheffer, M., Rinaldi, S., Kuznetsov, Y. A. & VanNes, E. H. (1997). Seasonal dynamics of Daphnia and algae explained as a periodically forced predator-prey system. *Oikos* **80**, 519–532.

Scheffer, M. & Van Nes, E. H. (2006). Self-organized similarity, the evolutionary emergence of groups of similar species. *Proc. Natl. Acad. Sci. U.S.A.* **103**, 6230–6235.

Soetaert, K. (2009). *rootSolve: Nonlinear root finding, equilibrium and steady-state analysis of ordinary differential equations*. R package 1.6.

Soetaert, K. & Herman, P. M. (2009). *A Practical Guide to Ecological Modelling. Using R as a Simulation Platform*. Springer. ISBN 978-1-4020-8623-6.

Soetaert, K. & Petzoldt, T. (2010). Inverse modelling, sensitivity and Monte Carlo analysis in R using package FME. *Journal of Statistical Software* **33**, 1–28.

Soetaert, K., Petzoldt, T. & Setzer, R. W. (2010). Solving differential equations in R: Package deSolve. *Journal of Statistical Software* **33**, 1–25.

Stenseth, N. C., Chan, K., Tong, H., Boonstra, R., Boutin, S., Krebs, C. J., Post, E., O'Donoghue, M., Yoccoz, N. G., Forchhammer, M. C. & Hurrell, J. W. (1999). Common Dynamic Structure of Canada Lynx Populations Within Three Climatic Regions. *Science* **285**, 1071–1073.

Tilman, D. (1980). Resources: a graphical-mechanistic approach to competition and predation. *The American Naturalist* **116**, 362–393.

Tilman, D. (1982). *Resource competition and community structure*, vol. 17 of *Monographs in population biology*. Princeton, New Jersey: Princeton University Press.

Tilman, D., Lehman, C. L. & Thomson, K. T. (1997). Plant diversity and ecosystem productivity: theoretical considerations. *Proc. Natl. Acad. Sci. U.S.A.* **94**, 1857–1861.

Tilman, D., May, R. M., Lehman, C. L. & Nowak, M. A. (1994). Habitat destruction and the extinction debt. *Nature* **371**, 65–66.

Veraart, A. J., Faassen, E. J., Dakos, V., Van Nes, E. H., Lurling, M. & Scheffer, M. (2012). Recovery rates reflect distance to a tipping point in a living system. *Nature* **481**, 357–359.

Volterra, V. (1926). Fluctuations in the abundance of a species considered mathematically. *Nature* **118**, 558–560.

Yodzis, P. (1978). *Competition for space and the structure of ecological communities*. Berlin: Springer-Verlag.

Yodzis, P. (1989). *Introduction to Theoretical Ecology*. New York: Harper & Row.

Yoshida, T., Jones, L. E., Ellner, S. P., Fussmann, G. F. & Hairston Nelson G, J. (2003). Rapid evolution drives ecological dynamics in a predator-prey system. *Nature* **424**, 303–306.